UNIVERSITÉ DU LUXEMBOURG

PhD-FSTM-2022-063
The Faculty of Science, Technology and Medicine

DISSERTATION

Defence held on 12/05/2022 in Esch-sur-Alzette, Luxembourg

to obtain the degree of

DOCTEUR DE L'UNIVERSITÉ DU LUXEMBOURG

EN BIOLOGIE

by

Katja BADANJAK
Born on 18 August 1992 in Rijeka (Croatia)

INVESTIGATING NEUROINFLAMMATION IN SPORADIC AND LRRK2-ASSOCIATED PARKINSON'S DISEASE

Dissertation defence committee

Prof Dr Anne Grünewald, dissertation supervisor
Université du Luxembourg / LCSB

Prof Dr Alexander Skupin, Chairman
Université du Luxembourg / LCSB

Dr Tony Heurtaux
Université du Luxembourg / Department of Life Sciences and Medicine (DLSM)

Dr Alessandro Michelucci
Luxembourg Institute of Health / Department of Oncology (DONC)

Dr habil Joanne Trinh
Universität zu Lübeck / Institut für Neurogenetik

L'UNIVERSITÉ DU LUXEMBOURG

DOCTORAL THESIS

Investigating neuroinflammation in sporadic and LRRK2-associated Parkinson's disease

---

Author:
Katja BADANJAK

Supervisor:
Prof. Dr. Anne GRÜNEWALD

A thesis submitted in fulfillment of the requirements for the degree of Doctor of Philosophy in Biology

in the

Molecular and Functional Neurobiology Group
Luxembourg Centre for Systems Biomedicine

May 12, 2022

Declaration of Authorship

I, Katja BADANJAK, declare that this thesis titled, "Investigating neuroinflammation in sporadic and LRRK2-associated Parkinson's disease" and the work presented in it are my own. I confirm that:

- This work was done wholly or mainly while in candidature for a research degree at this University.
- Where any part of this thesis has previously been submitted for a degree or any other qualification at this University or any other institution, this has been clearly stated.
- Where I have consulted the published work of others, this is always clearly attributed.
- Where I have quoted from the work of others, the source is always given. With the exception of such quotations, this thesis is entirely my own work.
- I have acknowledged all main sources of help.
- Where the thesis is based on work done by myself jointly with others, I have made clear exactly what was done by others and what I have contributed myself.

Signed:

Date:

"...it is the struggle itself that is most important. We must strive to be more than we are. It does not matter that we will never reach our ultimate goal. The effort yields its own rewards."

Lt Cmdr Data (*Star Trek: The Next Generation*)

Abstract

Investigating neuroinflammation in sporadic and LRRK2-associated Parkinson's disease

by Katja BADANJAK

Inflammatory responses are evolutionarily conserved reactions to pathogens, injury, or any form of a serious perturbation of a human organism. These mechanisms evolved together with us and, although capable of somewhat adapting, innate responses are gravely impacted by prolonged human lifespan. Better sanitary measures, health systems, food and medicine supply have prolonged human life expectancy to ~72 years. Aging is characterized by prolonged, chronic (often low-grade) inflammation. With tissue and cellular defense mechanisms becoming dysfunctional over time, this inflammation becomes detrimental and destructive to the human body.

Aging is a major risk factor for Parkinson's disease (PD), a movement disorder characterized by the loss of dopaminergic neurons. Even though the disease is predominantly idiopathic, genetic cases are contributing to a better understanding of the underlying cellular and neuropathological mechanisms. In comparison to neuronal demise, the contribution of microglia (the immune cells of the brain) to PD is relatively understudied. Initially studied in PD patient-derived post-mortem tissue, novel *in vitro* technologies, such as induced pluripotent stem cells (iPSCs), are permitting the generation of specific cell types of interest in order to study disease mechanisms.

We derived microglia cells from iPSCs of patients and healthy or isogenic controls to explore (shared) pathological immune responses in LRRK2-PD and idiopathic PD. Our findings suggest a significant involvement of microglia cells in the pathogenesis of PD and highlight potential therapeutic targets in alleviating overactive immune responses.

Acknowledgements

I would like to acknowledge people who have helped me grow as a scientist and as a person, throughout these four and a half years of my doctoral education at the University of Luxembourg. Although this PhD thesis is a result of a hard work and dedication, it would not be possible without the guidance and support of certain people.

Firstly, I would like to thank my supervisor, Prof. Dr Anne Grünewald, for giving me the opportunity to work in one of the most exciting fields of research. I will forever be grateful for the patience and trust you have put in my work, and for understanding and supporting me during my PhD journey. I sincerely thank you.

I need to acknowledge my CET committee members, Prof. Dr Alexander Skupin and Prof. Dr Rejko Krüger, for their invaluable comments and great scientific discussions during my doctoral education. Your advice and observations during my CET presentations are a part of my PhD progress, and were greatly appreciated.

Special thanks goes to my MFN group. Thank you for all the fun times, cake breaks, and for always maintaining the sweets corner full. Big thanks to the postdocs: Dr Sandro Pereira and Dr Carmen Venegas, for being patient with all of my (sometimes ridiculous) questions and theories. Time in the lab would not be the same without Dr Sylvie Delcambre and Jenny Ghelfi - thank you for helping me get around the lab when I joined the group, and for your encouraging words during the hard times. In the end, it will be ok.

I need to thank my PhD colleagues: Dr Kobi Wasner, Patrycja Mulica, Semra Smajić and Gideon Agyeah. Kobi, thank you for everything you taught me on my first year in the lab, and for always bringing the fun jokes to the office. To Patrycja – thank you for all the knowledge you so selflessly share, and for supporting me during the most challenging times. Semra – I am always grateful for our talks "na našem" and your support in everything I needed.

My deepest gratitude goes to my family. To my parents and sisters who encouraged me to undertake this journey, who were always there in the most difficult times, and never allowed me to give up, thank you. Biggest thanks to my friends in Croatia who, despite being far away, would always be there for me when I came back.

Coming to Luxembourg has changed my life in so many ways. I would not be here without the huge support I found in my "home away from home"- thank you Max for always listening to my issues and always finding the right words of encouragement.

Contents

List of Abbreviations

BBB	Blood-brain barrier
ccf-mtDNA	Circulating cell-free mtDNA
cGAS	Cyclic GMP-ATP synthase
CNS	Central nervous system
DAMP	Damage-associated molecular pattern
GPNMB	Glycoprotein non-metastatic melanoma protein B
IL1β	Interleukin beta
IL6	Interleukin 6
IFN-γ	Interferon gamma
IPD	Idiopathic Parkinson's disease
iPSCs	Induced pluripotent stem cells
LB	Lewy body
LBD	Lewy body disorder
LN	Lewy neurites
LRRK2	Leucine-rich repeat kinase 2
mtDNA	Mitochondrial DNA
MHC-II	Major histocompatibility complex 2
NLRP3	NOD-, LRR- and pyrin domain-containing protein 3
PAMP	Pathogen-associated molecular pattern
PD	Parkinson's disease
PSP	Progressive supranuclear palsy
RBD	REM sleep behavior disorder
ROS	Reactive oxygen species
RNAseq	RNA sequencing
sc-RNAseq	Single-cell RNA sequencing
sn-RNAseq	Single-nuclei RNA sequencing
SN	Substantia nigra
SND	Substantia nigra degeneration
SNpc	Substantia nigra pars compacta
TNF-α	Tumor necrosis factor alpha

1 Introduction

1.1 Parkinson's disease

Parkinson's disease (PD) is globally the fastest growing neurological disorder in terms of prevalence, disability, and deaths (GBD 2015 Neurological Disorders Collaborator Group, 2017). It is the most common type of parkinsonism, a condition resulting in a combination of movement disabilities: postural instability, muscular rigidity, bradykinesia, freezing, flexed posture, and tremor (Fahn et al., 2011).

While age is the most important risk factor, the disease is further associated with environmental factors such as exposure to pollution, heavy metals, and pesticides (GBD 2015 Neurological Disorders Collaborator Group, 2017). The expected increase in life expectancy and industrialization will further increase the incidence and duration of PD. Between 1990 and 2016, the incidence of PD has doubled: from 2.6 million to more than 6 million patients worldwide (GBD 2016 Parkinson's Disease Collaborators, 2018). If this trend continues, by 2040, the number of cases will exceed 12 million, with some estimates predicting even a staggering number of 17 million patients. The prevalence of PD is increasing so dramatically that it is considered as the pandemic of modern times (albeit of non-infectious kind), with the risk of developing PD during one's lifetime being 1 in 15 (Dorsey et al., 2018; Wanneveich et al., 2018). Continuous scientific efforts to explain the disease mechanisms are crucial in developing therapies that not only ameliorate the symptoms, but also halt the disease progression.

PD was first studied more than 200 years ago by James Parkinson, who provided initial clinical insights and described the motor symptoms of six patients (Parkinson, 2002). By now, it is known that most PD cases are suffering from an idiopathic (sporadic) form, while 10% of patients carry a mutation in one of the established PD genes.

At the cellular level, the main hallmark of PD is the progressive loss of dopaminergic neurons in the *substantia nigra pars compacta* (SNpc) of the midbrain, which consequently leads to the movement deficits outlined above. In addition, the formation of Lewy bodies (LB) and Lewy neurites (LN) are a key pathological hallmark of PD. Both are due to inclusions of α-synuclein protein aggregates found in neurons of PD patients (Baba et al., 1998; Mahul-Mellier et al., 2020; Spillantini et al., 1998). Genetic mutations in the *SNCA* gene (which encodes the α-synuclein protein) are causative of PD, while *SNCA* variants can still increase the risk of developing the disease (Krüger et al., 1998; Lill and Klein, 2017). The propagation of α-synuclein through the different brain regions was suggested as a means of classifying the stages of PD pathogenesis (Braak et al., 2003). Additionally, the aggregation of α-synuclein in the form of LBs or LNs is not a characteristic feature found in all PD cases. Thus, it still needs to be elucidated if this disease hallmark is a cause or a consequence of the complex and heterogeneous disorder (Gaig et al., 2007; Johansen et al., 2018; Schneider and Alcalay, 2017).

1.2 Clinical features of idiopathic and LRRK2-associated Parkinson's disease

Mutations in *LRRK2* are the most frequent cause of genetic PD, comprising around 5% of all autosomal dominant familial PD cases, and around 1-2% of all idiopathic PD (IPD) patients (Marras et al., 2011). While multiple genetic variants are known, G2019S is the most common mutation in *LRRK2*. Several studies show that this nucleotide change has incomplete penetrance (Kachergus et al., 2005; Latourelle et al., 2008). Furthermore, LRRK2 disease penetrance among cases in families with PD is higher than that of sporadic PD. This finding, together with the presence of LRRK2 phenocopies (PD-manifesting relatives of G2019S mutation carriers, who do not carry the mutation) in LRRK2-affected families, suggests the role of additional genetic modifiers and/or environmental factors as contributors to the disease manifestation (Latourelle et al., 2008). Interestingly, the clinical phenotypes of LRRK2-PD and IPD are similar, but with some major motor and non-motor differences. Tremor is more prominent in LRRK2-PD when compared to IPD. Although disease severity, falls, dyskinesia, and overall motor function decline are lower and more benign in LRRK2-PD. Regarding non-motor symptoms, LRRK2 individuals have better cognitive and olfactory function (although still abnormal), lower levels of depression, but worse performance on color discrimination tests (Healy et al., 2008; Marras et al., 2011; Saunders-Pullman et

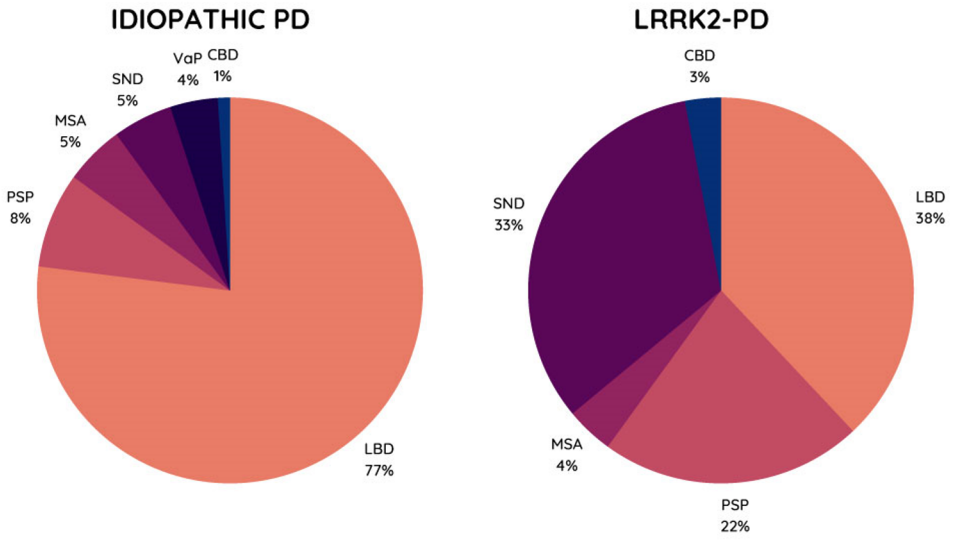

Figure 1. Frequency of neuropathological features in idiopathic and LRRK2-PD. LBD-Lewy body disorder; PSP-progressive supranuclear palsy; MSA-multiple system atrophy; SND-substantia nigra degeneration; VaP-vascular parkinsonism; CBD-corticobasal degeneration (adapted from (Chittoor-Vinod et al., 2021)).

al., 2018; Shu et al., 2018). Finally, sleep disturbances are reported to be another non-motor symptom. A study showed LRRK2-PD patients experiencing more frequent sleep onset insomnia, but more discreet REM sleep behavior disorder (RBD) compared to IPD patients (Pont-Sunyer et al., 2015). Even though the clinical features of IPD and LRRK2-PD largely overlap, upon studying post-mortem tissues, major differences with regard to pathological features were discovered. LRRK2 parkinsonism has more heterogeneous neuropathology, with Lewy body disorder (LBD), substantia nigra degeneration (SND), and progressive supranuclear palsy (PSP) being the main observed post-mortem findings (Figure 1.). On the other hand, IPD brains displayed primarily LBD tissue pathology (Chittoor-Vinod et al., 2021).

1.3 Manuscript I

The contribution of microglia to neuroinflammation in Parkinson's disease

Katja Badanjak[1], Sonja Fixemer[1,2], Semra Smajic[1], Alexander Skupin[1,3], Anne Grünewald[1,4*]

[1]Luxembourg Centre for Systems Biomedicine, University of Luxembourg, Esch-sur-Alzette, Luxembourg
[2]Luxembourg Center for Neuropathology (LCNP), Dudelange, Luxembourg
[3]Department of Neuroscience, University California San Diego, La Jolla, USA
[4]Institute of Neurogenetics, University of Lübeck, Lübeck, Germany
[*]Corresponding author

This article has been published in the *International Journal of Molecular Sciences*.

1.3.1 Preface

So far, PD research has primarily been focused on various neuronal aspects of the disease, i.e. the relevance of neuronal demise in terms of PD pathogenesis, clinical symptoms, and potential therapies. Relatively recently, microglia started to emerge as important contributors to neuronal cell death. Thus, we decided to summarize the current literature concerning the contribution of microglia to PD, hoping that such an overview would benefit the scientific community studying this disease.

In this review, we explored the role of innate immune signaling in the pathogenesis of PD. We focused on microglial function and findings from single-cell (sc) and single-nuclei (sn) RNAseq datasets. Furthermore, we discussed different animal and iPSC-derived genetic models of PD, and presented intriguing perspectives of 3D cell culture technologies. Lastly, we highlighted immunotherapies that either modulate the immune response or prevent the accumulation of α-synuclein with the aim to delay the onset of PD.

I contributed to this review by being in charge of sections 1 (Introduction), 3 ([Neuro] Inflammation in PD), and 4 (Disease Modeling: Animal Models, Patient-Derived iPSC models, and Cell-Based 3D Models and Platforms). In addition, I contributed to the writing of the abstract and the generation of all figures.

International Journal of
Molecular Sciences

MDPI

Review

The Contribution of Microglia to Neuroinflammation in Parkinson's Disease

Katja Badanjak [1], Sonja Fixemer [1,2], Semra Smajić [1], Alexander Skupin [1,3] and Anne Grünewald [1,4,*]

[1] Luxembourg Centre for Systems Biomedicine, University of Luxembourg, L-4367 Esch-sur-Alzette, Luxembourg; katja.badanjak@uni.lu (K.B.); sonja.fixemer@uni.lu (S.F.); semra.smajic@uni.lu (S.S.); alexander.skupin@uni.lu (A.S.)
[2] Luxembourg Centre for Neuropathology (LCNP), L-3555 Dudelange, Luxembourg
[3] Department of Neuroscience, University California San Diego, La Jolla, CA 92093, USA
[4] Institute of Neurogenetics, University of Lübeck, 23562 Lübeck, Germany
* Correspondence: anne.gruenewald@uni.lu

Abstract: With the world's population ageing, the incidence of Parkinson's disease (PD) is on the rise. In recent years, inflammatory processes have emerged as prominent contributors to the pathology of PD. There is great evidence that microglia have a significant neuroprotective role, and that impaired and over activated microglial phenotypes are present in brains of PD patients. Thereby, PD progression is potentially driven by a vicious cycle between dying neurons and microglia through the instigation of oxidative stress, mitophagy and autophagy dysfunctions, a-synuclein accumulation, and pro-inflammatory cytokine release. Hence, investigating the involvement of microglia is of great importance for future research and treatment of PD. The purpose of this review is to highlight recent findings concerning the microglia-neuronal interplay in PD with a focus on human postmortem immunohistochemistry and single-cell studies, their relation to animal and iPSC-derived models, newly emerging technologies, and the resulting potential of new anti-inflammatory therapies for PD.

Keywords: neuroinflammation; microglia; brain; neurodegeneration; animal models; iPSC; Parkinson's disease

Citation: Badanjak, K.; Fixemer, S.; Smajić, S.; Skupin, A.; Grünewald, A. The Contribution of Microglia to Neuroinflammation in Parkinson's Disease. *Int. J. Mol. Sci.* **2021**, *22*, 4676. https://doi.org/10.3390/ijms22094676

Academic Editor: Antonella Scorziello

Received: 31 March 2021
Accepted: 24 April 2021
Published: 28 April 2021

1. Introduction

1.1. Parkinson's Disease

Parkinson's disease (PD) is one of the most common neurodegenerative disorders with prevalence of around 1% in people aged above 65 years [1]. It is caused by a chronic and progressive loss of dopaminergic neurons in the substantia nigra (SN) pars compacta (pc) [2]. Despite great advances in research, it is still an elusive field of medical science, with around 10% of all cases being of genetic and others of idiopathic origin [3]. Genetic forms of PD include mutations in 23 loci, some of which have been studied intensely in the past two decades: *LRRK2* (*PARK8*), *SNCA* (*PARK1*), *PRKN* (*PARK2*), *PINK-1* (*PARK6*), and *DJ-1* (*PARK7*) [4,5]. Age is considered a major risk factor for the development of PD [6,7]. However, in addition, the genetic predisposition and exposure to environmental factors contribute to pathogenesis, making PD an age-related multifactorial disease. Environmental factors such as herbicides or pesticides can induce oxidative stress, DNA damage, and neuronal cell death [8]. The demise of dopaminergic neurons leads to lower levels of dopamine that is released into the striatum and thus, with progression of the disease, patients endure characteristic motor symptoms (tremor, rigidity, bradykinesia), cognitive decline (dementia) and even psychiatric signs (depression, apathy, anxiety) coupled with constipation and sleep disturbances [1,9,10].

A first clue to what might be the underlying mechanism of parkinsonism symptoms came unexpectedly in 1982 from a group of drug addicts who, after injection of a synthetic heroin, began experiencing symptoms commonly seen in PD patients. The drug was found

to be 1-methyl-4-phenyl-1,2,3,6-tetrahydropyridine (MPTP). MPTP, when transformed into its ion 1-methyl-4-phenylpyridinium (MPP+), acts as a highly potent initiator of neuronal cell death through inhibition of complex 1 of the respiratory chain machinery in mitochondria [11,12]. Besides the demise of dopaminergic neurons and mitochondrial dysfunction, other molecular pathologies have been linked to PD since the late 20th century. They include aggregation of α-synuclein, formation of α-synuclein-containing Lewy bodies and neurites, somatic mtDNA alterations, autophagy dysfunction, and activation of microglia cells [13–17].

As of today, most common therapies are purely symptomatic, and they usually include substitution of dopamine by administering the drug Levodopa. Current treatments also have their drawbacks: 1. they only relieve some of the symptoms; 2. they do not slow the progression of the disease; 3. they have limited long-term efficacy. Therefore, PD researchers have turned their focus on how to diagnose the disease during its early phases. Motor symptoms occur at a rather late stage of the disease—only after 50% of dopaminergic neurons have been lost, patients experience impaired movement [18]. Thus, there is hope that with the discovery of early-stage biomarkers, we will be able to target molecular impairments and inflammatory phenotypes during the prodromal phase of the disease, thereby preventing the worst motor symptoms [19]. Among others, promising biomarkers would be indicators of inflammation, cytokines and chemokines, released by microglia into the extracellular space.

1.2. Microglia

Microglia are immune cells of the brain, representing the neural tissue's defense system [20]. Microglia cells were first discovered more than 100 years ago by Pío Del Río Hortega, using a silver carbonate staining method which allowed identifying them in brain tissue samples. He called microglia "the true third element" in addition to neurons and astrocytes [21]. He described microglia as a heterogeneous cell type with various morphologies ranging from highly ramified to ameboid shaped cells providing a first indication for the existence of microglia sub-populations [22].

During fetal development, microglia migrate from the yolk sac as primitive macrophages to the central nervous system's (CNS) neuroepithelium. In the CNS, they constitute up to 12% of all cells, and their density changes depending on the brain region [23]. Early studies in mice showed that bone-marrow-derived hematopoietic cells move to the CNS, where they differentiate into microglia-like cells. Accordingly, microglia cannot be replenished from the internal CNS pool but peripheral cells need to be recruited to maintain a sufficient number of microglia [24]. By contrast, these studies employed whole-body irradiation techniques, which led to impaired blood-brain barrier (BBB) integrity, giving rise to peripheral cell entry. With innovative conditional cell depletion techniques, it was recently shown that microglia have the ability to self-renew, and that interleukin-1 (IL-1) signaling is enabling this process [25]. Just like the abundance of microglia is region-specific, microglial morphology varies from brain area to brain area. In a resting state, microglia survey the brain microenvironment and show ramified morphology. Surveillance encompasses multiple functions: clearance of accumulated or deteriorated neuronal and tissue elements, dynamic interaction with neurons whilst regulating the synaptic pruning process, and maintaining overall brain homeostasis [26,27]. Once activated upon brain damage and certain host or non-host stimuli, microglia are quickly undergoing a morphology change into an ameboid-like form, coupled with the release of inflammatory molecules, cytokines and chemokines. With regard to their activation, microglia are commonly divided into two classes: M1 (pro-inflammatory) or M2 (anti-inflammatory). Even though, by now, it is known that the states of activation are much more heterogeneous and diverse.

New approaches are being developed to determine sub-populations of microglia, mostly through single-cell gene expression studies and by determining fine morphological differences using computational methods [28–30]. With age, microglia tend to express more IL-1β and they become more phagocytic in nature compared to microglia from younger

brains [31–33]. These phenotypic changes over time can influence their ability to function normally and attain the neuronal homeostasis and support. Eventually, an accumulation of non-functional, senescent microglia could contribute to irreversible and progressive neurodegeneration in PD.

2. Human Post-Mortem Tissue Studies

The first neuropathological evidence suggesting an involvement of microglia in PD was published in 1988 [14]. Compared to age-matched non-neurologic cases, the authors observed an enrichment of reactive microglia in post-mortem SN samples from PD patients characterized by the activation of human major histocompatibility class II (MHC2) proteins which function in antigen presentation and inflammatory signalling. While these MHC2-positive cells covered the whole range of microglia morphologies, the reactive ameboid shape was strongly enriched indicating the association with a neuropathological activity.

A more recent study confirmed these observations in post-mortem SN tissue of PD patients and additionally described MHC2-positive microglia in the putamen, transentorhinal cortex, cingulate cortex and the temporal cortex of these individuals [34]. Further analysis in PD post-mortem brain tissue also revealed a correlation between ameboid shaped microglia appearance and α-synuclein pathology in the SN and the hippocampus (HPC), as well as a SN-specific Toll-like receptor 2 upregulation in these MHC2-positive microglia. Altogether, this work implicated a region-dependent and possibly disease stage-dependent microglia heterogeneity in PD [34].

To complement these morphology-based analyses of microglia heterogeneity on the transcriptional level, single-cell laser capture microscopy was applied to microglia in post-mortem PD brains [35]. This approach allowed exclusively collecting microglia, thereby creating an advantage over common bulk RNA analyses of brain homogenates, which are either contaminated by other cell types or exhibit sorting-induced skewed RNA profiles. The single-cell study revealed that the transcriptional profiles of microglia differ between brain regions (SN, HPC) in both control subjects and PD patients. PD samples exhibited unique active pathways compared to controls, including inflammation-related aldosterone and reactive oxygen species metabolism. A comparison of isolated microglia from the HPC or the SN in PD samples showed that biological pathways linked to behavior, regulation of transport and synaptic transmission were among the most differentially regulated ones. Thus, this study was the first to demonstrate microglia transcriptional heterogeneity when comparing different brain regions from control subjects and PD patients.

During the last decade, high-throughput techniques for single-cell RNA sequencing (scRNAseq) have been developed, which have revolutionized our capability to decipher cellular heterogeneity at the transcriptional level. Most of these high-throughput methods rely on the dissociation of the sample into individual cells and can therefore mainly be applied to cultured cells, frozen tissue from young animals or fresh tissue.

A comprehensive cross-species single-cell microglia transcriptomic analysis in brain tissue confirmed the existence of different microglia transcriptional subpopulations in animals and humans. In addition, the study revealed that human microglia heterogeneity is more complex in humans than any of the tested animal species. Especially microglia pathways suspected to be implicated in neurodegenerative diseases such as the complement system and phagocytosis, as well as PD risk factors are more profoundly expressed in humans compared to rodents as the typical animal model [36].

To circumvent dissociation issues with more mature and solid samples, the RNA sequencing methodology was adapted to single-nuclei (sn). snRNAseq does not rely on intact cells but intact individual cell nuclei. This approach is applicable to frozen human post-mortem brain tissue, the most accessible sample type provided by biobanks (in light of the general unavailability of fresh brain tissue samples from living patients).

One of the first snRNAseq studies of human cortical and nigral tissue was performed by Agarwal and colleagues [37]. They created a single-cell atlas based on healthy control tissue. Their analysis indicated an enrichment in PD risks variants in neurons. By contrast,

they reported no such association in microglia. On the one hand, the lack of PD risk association in microglia may be due to reduced sensitivity of snRNAseq compared to scRNAseq [38] that suggests that snRNAseq might not be ideal to recover microglial states in human tissue. On the other hand, it is possible that exclusively employing control brain samples may mask PD associations in certain cell types. This hypothesis is supported by our own results. Applying snRNAseq analysis to frozen post-mortem midbrain tissue from idiopathic PD patients and controls, we identified a disease-specific upregulation of microglia [39]. In PD patients, activated microglia split into two activation branches; one with GPNMB-high microglia and the other with IL-1β-high microglia. Moreover, employing immunofluorescence and quantitative imaging analyses, we showed that the increase in microglia abundance is restricted to the PD nigra. Additional morphological analyses confirmed that PD patient microglia are more amoeboid supporting cell activation in the SN [39]. Contrary to the findings by Agarwal et al., we observed a significant PD risk variant enrichment in microglia and neurons when focusing on patient midbrain sections. For example, variants in *LRRK2* were highly associated with PD in microglia, which is in accordance with previous research [40].

Overall, very few sc- or snRNAseq datasets from post-mortem brain tissue from PD patients have been published so far, certainly due to the only very recent availability of advanced RNAseq techniques (Table 1). This low number of studies, which typically include only few samples, also does not yet allow for a definitive conclusion about the exact relevance of microglia transcriptional heterogeneity but strongly suggest a functional role of microglia in PD.

Based on the above-mentioned studies, human microglia are considerably more heterogeneous in terms of morphology and transcriptomics when comparing different brain regions than rodents and possibly show disease-specific signatures. These findings highlight the need for further in-depth studies in human tissue to characterize the role of microglia heterogeneity in PD. Beyond human postmortem brain tissue, also the application of single-cell technologies to iPSC-derived patient models may be useful to further elucidate microglia functions and mechanisms in PD (see Section 4.2 for information on this topic).

Table 1. Overview of human single cell and single nuclei studies.

Reference	Condition	Samples	Brain Region	Gender	Age (Years)	Tissue State	Method	Analyzed Microglia	Major Outcomes
Mastroeni et al. 2018 [35]	Age-matched control subjects (absence of PD pathology), PD patients	Controls: $n = 6$, PD patients: $n = 6$	SN, HPC (CA1)	All M	controls: 73.6 ± 6 PD patients: 74.6 ± 15.6	Post-mortem frozen unfixed	RT-PCR of immunolabeled (LN3) laser-captured microdissected microglia	Control SN $n = 3600$ microglia cells, control CA1 $n = 3600$ microglia cells, PD SN $n = 3600$ microglia cells, PD CA1 $n = 3600$ microglia cells	Regional heterogeneity (inter- and intra-condition), PD-specific active pathways including inflammation-related aldosterone and reactive oxygen species metabolism
Geirsdottir et al. 2019 [36]	Control subjects (absence of neuropathology)	controls: $n = 6$	Various	3 F, 3 M	9–55	Fresh (surgically removed excess tissue surrounding epileptic focal)	scRNAseq (MARS-seq2.0)	$n = 1069$ microglia cells	Complex human microglia heterogeneity, Neurodegeneration-linked pathways and PD risk factors most profoundly expressed in human microglia
Agarwal et al. 2020 [37]	Age-matched control subjects (no neurological disease)	Controls: $n = 5$	Cortex (middle frontal gyrus), SN (central portion at the level of the third nerve encompassing both ventral and dorsal tiers)	Cortex: 1 F, 3 M; SN: 2 F, 4M	55–70	Post-mortem frozen unfixed	snRNAseq (10X Genomics Chromium Single Cell Kit [v2 chemistry])	Cortex $n = 500$ microglia nuclei, SN $n = 325$ microglia nuclei	PD risk variants in neurons but not in microglia
Smajic et al. 2021 [39]	Age-matched control subjects, idiopathic PD patients	Controls: $n = 6$, PD patients: $n = 5$	Midbrain	Control: 1 F, 5 M; PD: 1 F, 4 M	Controls: 65–95; PD patients: 65–85	Post-mortem frozen unfixed	snRNAseq (10X Genomics Chromium Next GEM Single Cell 3′ Kit v3.1)	$n = 3903$ microglia nuclei	Disease-specific upregulation of microglia, into two branches: GPNMB-high resp. IL-1β-high microglia PD risk variants enrichment in neurons and microglia

3. (Neuro) Inflammation in PD

With a high degree of neuroplasticity and with low capacity to self-regenerate, the brain is especially sensitive to outer stimuli and injury. In addition, being protected by a blood-brain and blood-cerebrospinal fluid barrier, the brain was considered an "immune-privileged" organ. By contrast, in the last decade, this perception has been challenged and studies have changed our understanding of the immune response in the brain.

Inflammatory processes are considered to be a "double-edged sword": on the one hand, they help to clear out toxins and unwanted pathogens, while on the other hand, they promote cytotoxicity and neurodegeneration. Several studies suggested mechanisms of immune response and how they can influence neuronal cell death in PD. Already by the end of the 20th century, cytokines and complement proteins, which are components of the innate immune system, were found to be upregulated in brain, cerebrospinal fluid (CSF) and sera of PD patients [41]. Specifically, TNFα, Il-1β and IL6 were discussed as possible PD biomarkers [42–45]. In addition, Mount and colleagues showed a rise of IFN-γ plasma levels in PD patients compared to healthy controls [46]. Interestingly, the concentration of these markers in peripheral tissues might depend on PD severity and progression. Higher levels of TNFα in serum were characteristic of PD patients with more severe clinical features of impaired cognition, depression, sleep disturbances and fatigue [47,48]. As those studies identified that some of the prodromal symptoms are coupled with an underlying inflammatory response, the question arises whether inflammation really is only a consequence, rather than an active contributor to neurodegeneration.

The adaptive immune response has also been associated with neuropathological features of PD and, initially, the importance of microglial Fcγ receptor was studied. Immunoglobulins from PD patients activated Fcγ receptor positive (Fcγ R+/+) microglia cells in mice, which further promoted dopaminergic neuron cell death, while Fcγ R-/- microglia are not activated and no neuronal loss is detected [49]. There are a number of candidates in PD pathology capable of eliciting immune response and in vitro studies are focusing on components released by dying neurons. Significantly increased levels of autoantibodies were found against neuronal cells, brain lysate, and dsDNA accompanied with significantly higher titers of all three in sera of PD patients compared to healthy individuals [50]. Corroborating this, some studies focused on investigating the amount of mitochondrial DNA (mtDNA) in serum of PD patients. MtDNA, like some other mitochondrial compounds, is considered a damage-associated molecular pattern (DAMP), triggering pro-inflammatory signalling [51,52]. Our own biomarker study revealed higher serum levels of circulating cell-free mtDNA in patients with mutations in *PRKN* or *PINK1* compared to patients with idiopathic PD (IPD) [45]. On another note, studies also showed PD patients having higher autoantibody levels against α-synuclein in blood serum. Those differences highly correlate with inheritance mode of the disease but not with other disease-associated factors, while IPD cases were not significantly different from healthy controls [53]. A different study also showed increased levels of antibodies towards monomeric α-synuclein in serum of PD patients compared to controls, but ELISA responses reduced as PD progressed [54]. Neuromelanin is another neuronal component implicated in the disease. PD patients had elevated levels of autoantibodies against melanin in sera samples. Interestingly, ELISA absorbance response was significantly and negatively correlated with disease duration [55].

With regard to the adaptive immune system, studies investigating postmortem brain samples found reactive CD4+ and CD8+ T cells in postmortem brain samples from PD patients [56,57], suggesting a "porous" BBB and an impact of additional inflammatory mechanisms on the CNS. Furthermore, in the periphery, PD patients have elevated numbers of Th17 cells, which primarily produce IL-17. Interestingly, IL-17 was also found to have a detrimental effect on dopaminergic neuron iPSC-derived autologous cultures [57]. Another study, which explored peripheral immunity in PD, found a reduction in CD4+ T cells in patients. In addition, these cells were observed to preferentially differentiate towards a Th1-reactive state [58]. Recent PD research also showed differentially expressed genes in peripheral blood mononuclear cells (PBMCs), with patients presenting an elevated

abundance of CD49d+ Treg cells, which are known to suppress inflammatory processes [59]. When investigating the interaction of microglia and peripheral immune cells in PD, a recent study in rats found an important role of infiltrating T cells. These cells induce a microglial pro-inflammatory response to α-synuclein through upregulation of microglial MHC-II. In turn, this cell-cell communication causes neuronal cell death [60]. Considering the previously mentioned phenomenon of a "leaky" BBB in PD, the above-described phenotypes might be a mere consequence of dysfunctional pathways in brain cells, which release DAMPs into the periphery, causing an ongoing inflammatory loop. It is yet to be investigated how peripheral and CNS immune regulation is achieved in PD. These studies provide insights into the early immune response in PD and highlight novel targets for immunotherapies, which are further discussed in Section 5.

4. Disease Modeling: Animal Models, Patient-Derived iPSC Models, and Cell-Based 3D Models and Platforms

Since the discovery of microglia cells more than 100 years ago, multiple models have been designed to study inflammation in PD. Some of the most widely used models are summarized in Figure 1. In next sections, we will summarize key studies performed in animal and human patient-derived microglial model systems.

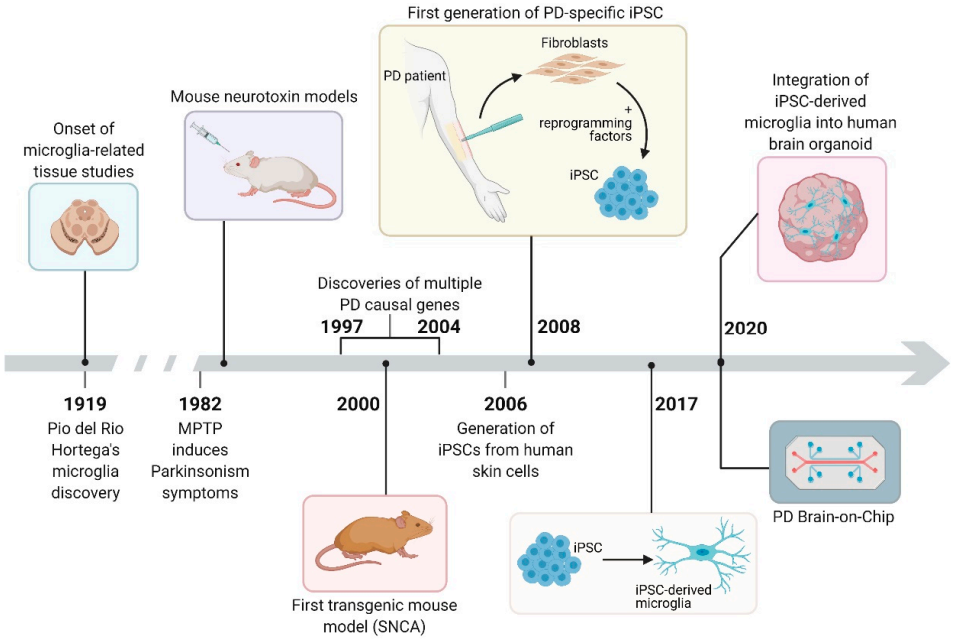

Figure 1. Historical overview of the different model systems used in PD microglia research. Figure created using BioRender.com.

4.1. Animal Models

PD animal studies may be either of genetic or neurotoxin nature. In vivo animal models are an essential part of pre-clinical trials in drug development. They are highly valuable when investigating the relevance of mutations, tissue pathology, motor symptoms and behavioral patterns in many diseases [61]. In addition, although these models cannot exhibit full neuropathological mechanisms, the progressive nature of PD and sometimes even robust neurodegeneration, they have proven to be invaluable resources of knowledge for researchers. Furthermore, in vitro models include primary microglia isolated from mice or rats, and immortalized murine microglia cell lines like BV-2, which can be greatly expanded and ultimately lead to reduction of animals used in studies. In the next section,

we will briefly summarize the inflammatory phenotypes observed in in vivo and in vitro models of PD.

4.1.1. Neurotoxin Model

Not long after the discovery that mitochondrial respiratory chain inhibition can induce parkinsonism symptoms in healthy individuals, scientists around the world studied the neurotoxic effects of such agents in invertebrate, vertebrate and non-human primates model systems and immortalized cell lines. Among the most commonly used neurotoxins is MPTP, while other studies have also investigated the impact of rotenone or paraquat.

One of the first studies performed in mice with MPTP-induced PD found a significant increase in microglia numbers and altered/activated microglia morphology in the SN early upon treatment, while dopaminergic neurons were depleted days after microglial activation [62]. Furthermore, blocking microglia activation with minocycline (a tetracycline compound with anti-inflammatory properties) after MPTP exposure not only prevented IL-1β formation but also diminished the demise of dopaminergic neurons. Minocycline treatment also reduced MPTP-induced iNOS activity, NADPH-oxidase (both enzymes known for microglia-mediated neurotoxicity), and TNF-α production [63,64]. TNF-α mRNA expression was upregulated in MPTP-treated mice compared to saline-treated animals. This increase preceded the loss of dopaminergic markers such as TH and dopamine, suggesting the involvement of inflammatory pathways prior to neurodegeneration. In addition, upon MPTP treatment, transgenic mice lacking TNF receptors did not exhibit dopamine or dopaminergic neuron loss [65]. Of note, MPTP-treated macaques had increased serum levels of IFN-γ and TNF-α compared to controls, even 5 years after neurotoxin exposure. Monkeys with severe parkinsonism (displaying symptoms of rigidity and a curved posture) showed significant dopaminergic neuronal loss, and activation of microglia and astrocytes [66].

Using knockout (KO) mouse models, molecular mechanisms of IFN-γ and TNF-α were further investigated. Upon MPTP treatment, IFN-γ KO mice had a completely rescued phenotype, while TNF-α KO mice had a minor activation of microglia, thus implying a synergistic effect of TNF-α and IFN-γ signaling pathways [66]. IFN-γ was shown to have a significant role in promoting neuronal cell loss after rotenone treatment, but only in the presence of microglia. Treatment of dopaminergic neuron-microglia co-cultures with rotenone revealed that cultures with wildtype but not IFN-γ receptor-deficient microglia had a significant loss of dopaminergic neurons [46]. In rats, rotenone together with lipopolysaccharide (LPS) is initiating neurodegeneration through microglia-mediated NADPH oxidase activation and release of ROS [67]. This NADPH activation was further found to be a direct consequence of HMGB1 (high-mobility group box 1) release from microglia and dying neurons upon ongoing LPS treatment, thereby propagating the detrimental inflammatory loop [68]. Although there have been reports that rotenone cannot directly activate microglia cells [69], additional work confirmed that the activation process is indeed mediated by p38-MAPK signaling [70].

4.1.2. SNCA

The aggregation of α-synuclein and formation of a-synuclein-containing Lewy bodies and neurites have been established as hallmarks of PD pathology since the first immunohistochemistry analysis of SNpc tissue [13]. Duplication, triplication and point mutations (A30P, A53T, E46K, H50Q, and G51D) in the *SNCA* gene cause an autosomal dominant form of PD [71–76]. SNCA mouse models include α-synuclein treatments, overexpression (OE) of human α-synuclein, and transgenic models with inserted human α-synuclein point mutations. Aggregation and neurotoxicity of a-synuclein are subsequent events of oxidative stress, genetic alterations and post-translational modifications like phosphorylation, nitration, ubiquitination and others [77]. Nitrated α-synuclein can activate not only microglia, but also peripheral leukocytes, thus accelerating neurodegeneration [78,79]. Furthermore, when released, a-synuclein can trigger microglia activation and an inflammatory

response (Figure 2). In rat midbrain neuron-microglia co-cultures, extracellular α-synuclein had a strong neurotoxic effect, which was mediated by an increase in ROS. Interestingly, neurotoxicity was abolished when microglia were depleted [80]. When priming microglia with α-synuclein injected into the SNpc, mice were more susceptible to environmental insults [81]. This finding suggests a more intricate relationship between the CNS and the peripheral immune response. In addition, both, treatment of primary mouse microglia with α-synuclein and α-synuclein OE in mice, are known to give rise to microglial ROS, TNF-α, IL-1β, COX2, iNOS [82,83]. Furthermore, α-synuclein exposure enhances the gene expression of toll-like receptors (TLRs) as well as of adapters and transcription factors such as MyD88 and NF-κB [84,85]. These results implicate α-synuclein as a damage-associated molecular pattern (DAMP). In agreement with this hypothesis, the activation of TLRs was found to be temporally and regionally induced after α-synuclein treatment, with an early response specifically in the nigrostriatal pathway [83]. Fibrils of α-synuclein but not monomers, can activate the NLR family pyrin domain containing 3 (NLRP3) inflammasome, induce the production and release of IL-1β and cleaved caspase-1, and mediate the release of ASC specks into the extracellular space. Pre-treatment of mice microglia with the small-molecule NLRP3 inhibitor MCC950, ameliorated α-synuclein-mediated inflammation [86,87]. With regard to point mutations in α-synuclein, some studies have shown their greater potential to activate microglia compared to wildtype α-synuclein [88–90]. Treatments with mutated α-synuclein triggered diverse phenotypes of microglia activation (based on cellular morphology and pro-inflammatory cytokine expression). While A53T-mutant α-synuclein has shown the strongest effect, wt and E46K had little to no effect on microglia activation. In addition, A53T-mutant α-synuclein is implicated in the NF-κB/AP-1/Nrf2 pathway, which can lead to higher cytokine expression and elevated ROS levels (Figure 2) [88]. Together, these studies suggest a molecular link between α-synuclein aggregation and neuroinflammation in PD.

Int. J. Mol. Sci. **2021**, *22*, 4676

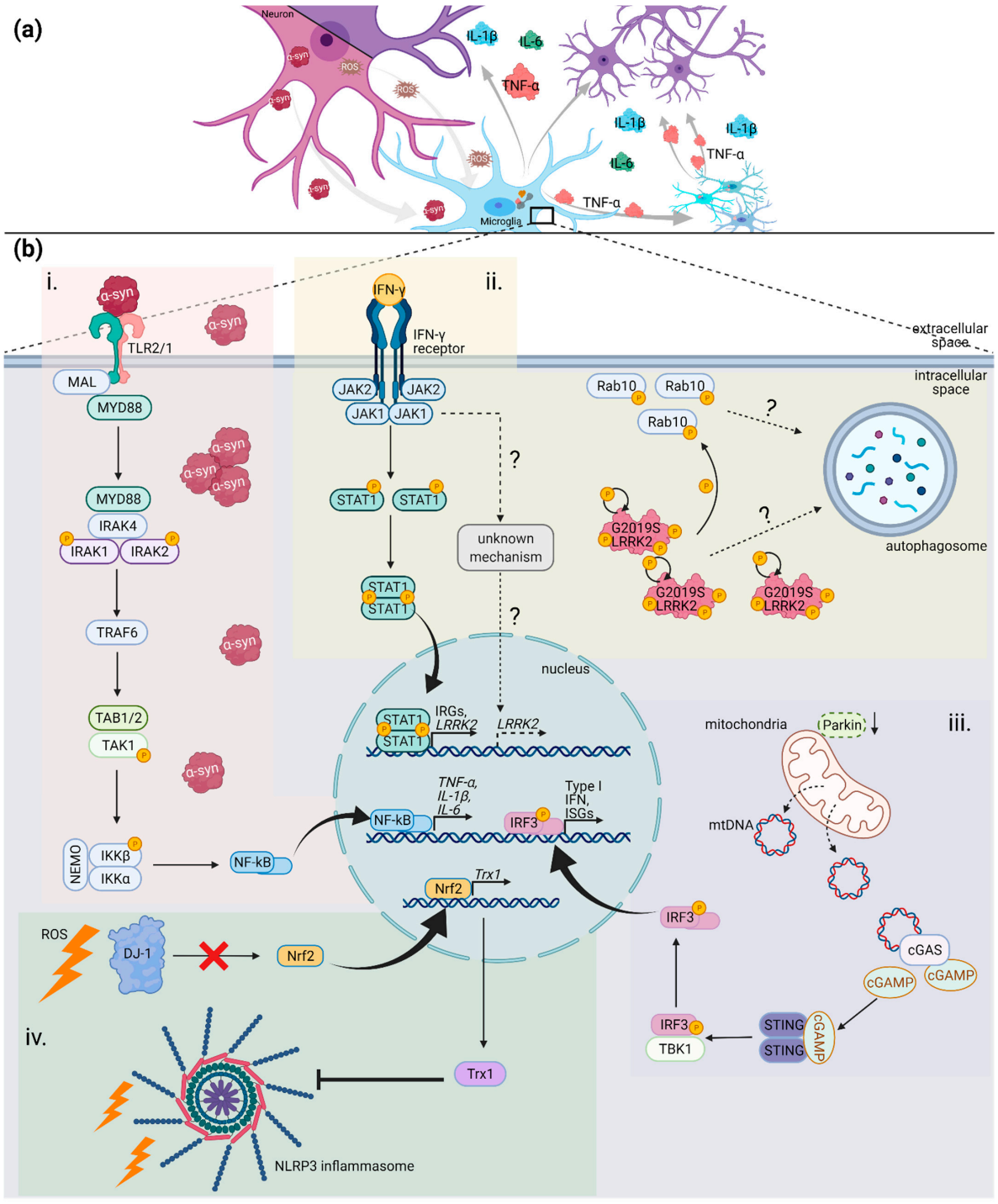

Figure 2. Neuron-microglia cross talk and selected inflammatory pathways involved in PD. (**a**) Inflammatory loop initiated by neuronal demise and propagated by microglial dysfunction. (**b**) Inflammatory pathways associated with α-synuclein (i), LRRK2 (ii), parkin (iii) or DJ-1 (iv) in the context of PD pathology. This figure was created with BioRender.com.

4.1.3. LRRK2

Mutations in the *leucine rich repeat kinase 2* (*LRRK2*) gene are the most common cause of PD, having been associated with up to 3% of idiopathic and 5–15% of all familial PD cases [91]. Pathogenic variants include R1441C and N1437H in the Ras-of-complex (ROC) domain, Y1699C in the C-terminal of ROC (COR) domain, and G2019S and I2020T in the kinase domain. Mutations in *LRRK2* are autosomal dominantly inherited. The complex structure of the protein with several active domains may be one reason why the function of LRRK2 is still not fully understood. LRRK2 is predominantly expressed in immune cells (macrophages and monocytes) of the CNS, certain peripheral tissues, and blood, which led to the hypothesis that LRRK2 has its main function in innate immunity [92–94]. In this context, it is also important to note that single nucleotide polymorphisms (SNPs) in *LRRK2* have been associated with higher susceptibility to bacterial infections and chronic inflammatory diseases such as Crohn's disease and leprosy [95–98]. Unlike other alterations in LRRK2, the most common mutation, G2019S, is not completely penetrant, meaning that not all individuals harboring the single nucleotide change will develop PD [99]. Thus, a "multiple-hit" model was suggested, where a "second-hit" is required for the onset of PD in a G2019S mutation carrier. This model is further corroborated by studies in transgenic LRRK2-mutant mice, which show little to no neurodegeneration [100,101]. Upon stimulation of LRRK2 R1441G transgenic mice with LPS, LRRK2 levels significantly increased [94]. Interestingly, although in primary microglia LRRK2 protein levels were consistently elevated upon LPS stimulation, some studies showed no upregulation at mRNA level, implicating complex post-translational modifications [102]. In addition, LPS-treated transgenic microglia released higher levels of pro-inflammatory TNF-α, IL-1β and IL-6, and lower levels of anti-inflammatory IL-10. The same results were obtained when studying the gene expression of these cytokines, indicating an upstream role of LRRK2 in cytokine modulation. When assessing the neurotoxic effect of microglia-derived molecules, conditioned medium from LPS-stimulated transgenic microglia caused more severe neurodegeneration than medium from LPS-stimulated wildtype microglia [94]. Furthermore, the knockdown of LRRK2 (LRRK2-KD) almost completely abrogated microglial pro-inflammatory phenotypes (with *TNF-α*, *IL-1β* and *IL-6* being significantly reduced) in LPS-treated microglia [103]. These findings in LRRK2-KD microglia were consistent with results obtained after exposure of wildtype microglia to a small-molecule kinase inhibitor, implicating both *LRRK2* expression and kinase activity in the induction of pro-inflammatory mechanisms (Figure 2) [102]. The activation of LRRK2 can be induced through TLR pathways in a MyD88-dependent manner [104]. This finding further illustrates the connection between the innate immune response and LRRK2 function in PD.

4.1.4. PRKN

Somatic mutations in the *PRKN* gene cause early-onset familial PD, and they are inherited in an autosomal recessive manner [105]. *PRKN* codes for parkin, an E3 ubiquitin ligase, and it is involved in the removal of damaged mitochondria, a process also known as mitophagy [106]. Parkin mutations are rare, but have a strong "mitochondrial phenotype" [107]. The frequency of *PRKN* mutation can reach up to 10–25% in early-onset PD patients, suggesting a strong genetic role in the pathology of PD [108]. Although inflammatory phenotypes in *PRKN*-associated PD have only recently became a research focus, mitochondria have the potential to enable immune responses through several of its components such as ROS, N-formyl peptides, cytochrome c, cardiolipin, and mtDNA, mutually referred to as mito-DAMPs [109]. Deficiencies in both mitophagy and autophagy pathways can lead to the release of these components into the cytosol and the activation of the NLRP3 inflammasome [110,111]. In wt mice, the treatment with rotenone upon an insult with LPS and ATP enabled mtDNA translocation into the cytosol, which, in turn, contributed to the secretion of the pro-inflammatory cytokines IL-1β and IL-18 [111]. First studies in parkin-/- mice could not conclude any differences in neurodegeneration between wt and mutants, prior or even upon acute treatment with LPS. Only upon chronic LPS administration, parkin-/- mice had SNpc dopaminergic neuron degeneration and fine-motor

function deficits [112]. The protective role of parkin in immune cells has been reported in multiple studies. Parkin-deficient macrophages had enhanced mtDNA release, mtROS levels, and IL-1β extracellular release upon NLRP3 agonist (LPS and ATP) treatment. Parkin can prevent the accumulation of damaged mitochondria. In Parkin-silenced cells, a buildup of damaged mitochondria was observed upon LPS and ATP insult. The study implicated NF-κB-p62 anti-inflammatory signaling, since parkin recruitment to mitochondria is crucial for p62 tagging within the mitophagy/autophagy process [113]. In addition, parkin is suspected to regulate the transcription of A20, an inhibitor of NF-κB-mediated cytokine expression [114]. Surprisingly, another study found that LPS-treated microglia and macrophages have reduced mRNA levels of *PRKN* and this was prevented by blocking NF-κB signaling [115]. Thus, chronic neuroinflammation can phenocopy parkin depletion, where anti-inflammatory pathways may not be enough to rescue the exacerbated inflammatory phenotype. Furthermore, mtDNA can be detected by the cyclic GMP-AMP synthase (cGAS)—stimulator of interferon genes (STING) pathway. A brief report showed higher mtDNA release in Parkin-/- mice under exhaustive exercise. Moreover, Parkin-/- mice that were crossed with mutator mice (that harbor a defective mtDNA proofreading polymerase) had higher mtDNA release and production of pro-inflammatory cytokines. This increased cytokine expression was abrogated upon STING deletion, implicating mtDNA release and cGAS-STING signalling in the observed phenotypes (Figure 2) [44]. Finally, parkin has the ability to prevent the presentation of mitochondrial antigens on the surface of immune cells by inhibiting mitochondria-derived vesicles (MDVs), linking also autoimmune mechanisms to PD [116].

4.1.5. DJ-1

Although *DJ-1* was first described as an oncogene, mutations in this gene are associated with an early-onset PD. The inheritance of *DJ-1* is autosomal recessive and mutations are rare [107]. DJ-1 is expressed in cells with high-energy demand, and it can successfully "buffer" oxidative stress through stabilization of nuclear factor erythroid-derived 2-like 2 (Nrf2) protein [117]. Its role in microglia and inflammatory pathways has not been extensively studied since the focus has primarily been on its expression in dopaminergic neurons, which are particularly energy-demanding cells. Nevertheless, together with its antioxidant activity, some studies concluded DJ-1 has a major anti-inflammatory role in the brain. DJ-1 KO mice had elevated basal levels of IFN-γ in SNpc compared to control mice and this was aggravated after LPS administration [118]. In mouse microglia, DJ-1 can prevent prolonged phosphorylation of signal-transducers and activators of transcription (STAT1) proteins upon IFN-γ treatment by enabling the interaction between Src-homology 2 domain-containing 101 protein tyrosine phosphatase-1 (SHP-1) and STAT1. DJ-1 KO microglia had elevated levels of nuclear p-STAT1, higher expression of *COX-2*, *iNOS*, and *TNF-α* [119]. In addition, DJ-1-deficient microglia had increased mitochondrial activity, which resulted in elevated ROS levels compared to control microglia and those were further exacerbated upon LPS exposure. LPS-treated DJ-1-deficient microglia had higher levels of nitric oxide (NO) and secreted cytokines but lower levels of anti-inflammatory triggering receptor expressed on myeloid cells 2 (TREM2) protein [120]. Although the same group of authors reported higher phagocytosis ability based on zymosan particle uptake, another study showed reduced uptake of soluble α-synuclein in DJ-1 KD microglial cells [121]. α-synuclein could significantly increase the secretion of IL-1β, IL-6, and NO. Also, DJ-1 KD microglia had impaired degradation of p62 and LC3-II upon activation of autophagy. Furthermore, control cells accumulated more α-synuclein upon inhibition of autophagy, while this effect was observed to a lesser extent in DJ-1 KD microglia [121]. Additionally, an extensive study found shared pathways between DJ-1 and NLRP3, which to some extent explains the upregulation of pro-inflammatory cytokines (Figure 2). After MPTP treatment, DJ-1 can suppress NLRP3 activity through upregulation of the antioxidant pathway Nrf2/Trx1, while DJ-1-deficient cells could only be partially rescued by overexpression of

Nrf2 [122]. More studies will be needed to further explore the link between DJ-1 regulation of oxidative stress and neuroinflammation.

4.2. Human Induced Pluripotent Stem Cell (iPSC) Studies

Advancements in stem cell techniques had a significant impact on the quality of research, especially in neuroscience, since patient material is hard to obtain and animal models in the majority of cases do not fully mirror PD-associated neurodegeneration. Two major classes of iPSC models can be distinguished: gene-modified (in which PD causing mutations are either inserted or corrected) and patient-derived cells. The biggest advantage of iPSC models, which also constitutes their biggest disadvantage, is the genetic background. The original genetic signature of a patient can, on the one hand, help to decipher the potentially multifaceted molecular mechanisms underlying PD in this particular case, while on the other hand, it may cause (functional) heterogeneity between different patient lines. Further information on this topic can be found in a detailed review by Volpato and colleagues [123]. Although, currently, PD studies employing iPSCs are mainly focusing on neuronal differentiation protocols, in the next few paragraphs, we will briefly summarize the available literature exploring iPSC-derived microglia and macrophages in the context of PD.

4.2.1. SNCA

To our knowledge, only one study investigating *SNCA*-mutant iPSC-derived microglia and/or macrophages has been published to date. Differences between control, A53T and *SNCA* triplication macrophages were assessed. *SNCA* triplication cells had higher intracellular levels and an increased release rate of α-synuclein compared to, both, A53T and control cells. The CXCL1, IL-18, and IL-22 cytokine levels in the supernatant of *SNCA* triplication macrophage cultures were significantly upregulated compared to all other investigated cultures. By contrast, there was no difference with regard to the levels of released CCL17, IL-4, IL-6, IL-8, IL-10, and TNF-α between healthy and *SNCA*-mutant macrophages. In addition, in *SNCA* triplication cells, the phagocytic ability was significantly reduced. Further strengthening this result, treating control cells with monomeric α-synuclein had the same impact. Accordingly, high levels of exogenous and endogenous α-synuclein severely disrupt the functionality of iPSC-derived macrophages. The authors found differences with regard to the uptake mechanisms of fibrillar and monomeric α-synuclein [124]. Finally, a very recent study investigated the effect of an α-synuclein antibody on iPSC-derived microglia. Surprisingly, misfolded α-synuclein bound to the antibody triggered inflammatory signalling through the upregulation of the NLRP3 inflammasome [125]. This finding calls into question ongoing clinical trials with antibodies against α-synuclein (see Section 5 for details).

4.2.2. LRRK2

As described in the previous sections, LRRK2 is highly abundant in immune cells. Thus, iPSC-derived microglia and macrophages are used to explore the impact of LRRK2 mutations on immune signalling in PD. First research revealed that LRRK2 is involved in the later stages of phagosome maturation. Furthermore, the localization of LRRK2 is essential for the recruitment of Rab8 and Rab10 to phagosomes, which is mediated by LRRK2 kinase activity. Moreover, it was confirmed that IFN-γ directly upregulates *LRRK2* gene expression [126]. In another study, LRRK2 G2019S microglia showed increased motility compared to healthy control and LRRK2 KO microglia. This motility reached control levels upon IFN-γ treatment. An assessment of the phagocytic ability showed that G2019S microglia have an increased capacity to engulf fluorescent beads. In addition, LRRK2 G2019S microglia had reduced levels of nuclear NF-kB, upon treatment with both LPS and IFN-γ, suggesting impaired inflammatory signaling mediated by this transcription factor. Moreover, when the supernatant from LPS-treated G2019S microglia was added to control or G2019S iPSC-derived neurons a shortening of the neurite length was ob-

served [127]. Conversely, a study investigating the motility of iPSC-derived monocytes found that G2019S knock-in cells were less motile than wild type cells [128]. In light of opposing findings in microglia, this suggests a cell-type specific impact of the G2019S mutation in LRRK2.

4.3. Human Cell-Based 3D Models and Platforms

On the one hand, the complex tissue organization in the brain makes cell-cell communication and interactions difficult to study in in vivo models. On the other hand, in vitro models do not cover the full scope of signalling between all types of brain cells. However, thanks to the development of iPSC-derived co-culture systems, it is now possible to investigate the role of non-neuronal cells in neurodegeneration at least to some degree. Excitingly, 3D cultures, such as brain organoids and brain spheres, have recently emerged as highly valuable tools to model multiple cellular interactions and the pathophysiology of numerous concurrent processes in vivo. Brain organoids have been particularly useful in the research of developmental and neurodegenerative diseases as well as brain cancers [129–136]. By contrast, only a few studies have focused on PD pathogenesis so far [137,138]. Since brain organoids consist of cells from the neuroectodermal region, microglial cells, which originate from the yolk sac, need to be "artificially" added to the 3D culture. While multiple groups have successfully integrated microglia into cortical organoids and brain sphere cultures [139–141], some researchers observed spontaneous microglia formation in cortical organoids under differentiation conditions, which do not inhibit non-neuronal lineages [142]. First results suggest that the incorporated microglia support neuronal development and maturation in cortical organoids. Moreover, the microglia appear to become more ramified and matured as the organoid grows [141]. Several research teams, including our close collaborators, are investigating microglial inflammatory signalling in midbrain-specific organoids from PD patients. Though, this work is not without its hurdles. A major challenge of microglia-midbrain organoid cultures is to obtain (and maintain) physiological ratios and distributions of different brain cell types. Significant scientific efforts are currently ongoing to configure cell culture media compositions that will facilitate the simultaneous growth of all cell types, thereby achieving a more physiological microenvironment that prevents the activation of microglia (which is, for instance, commonly observed in the dead core of organoids). Furthermore, cell-based microfluidics systems (also known as Brain-on-Chip technology) have been developed to investigate microglia interactions with astrocytes and neurons under the impact of a continuous fluid flow [143–145]. To mimic the BBB composition, some systems are designed to contain a layer of microvascular endothelial cells and pericytes. Exposing a human Brain-Chip (which mirrored the microenvironment of the substantia nigra) to α-synuclein fibrils initiated dopaminergic neuron death, mitochondrial dysfunction and neuroinflammation, while BBB was significantly compromised [145]. Due to their capacity to model the BBB, both organoids and microfluidic systems have emerged as highly promising resources for therapeutic testing in brain diseases [146,147].

5. Immunotherapies in Parkinson's Disease

5.1. Anti-Inflammatory Treatments in PD

In a number of animal PD models, the use of nonsteroidal anti-inflammatory drugs (NSAIDs) showed promising results [148]. Exemplary, in an MPTP mouse model, treatment with acetylsalicylic acid, which inhibits the cyclooxygenase isoenzymes COX-1 and COX-2, prevents neuronal loss in the substantia nigra [149]. By contrast, clinical trials exploring the neuroprotective effect of NSAIDs were less conclusive. While several studies reported that NSAIDs may be able to delay or even prevent the onset of PD [148,150], there have also been reports of no impact of NSAID intake on PD risk [148]. A recent meta-analysis that comprised 15 studies on the use of NSAIDs and PD risk found no association. Moreover, a dose-response analysis revealed that the amount and duration of NSAIDs administration did not influence the outcome [151].

In light of these results, alternative approaches that specifically target the transition of microglia from a proinflammatory (M1) to an anti-inflammatory (M2) state have been suggested [148]. Suppression of the M1 state may be achieved by acting at the level of the proinflammatory cytokines TNF-α, IL-1β and IFN-γ [148]. Supporting this hypothesis, the overexpression of dominant negative TNF (DN-TNF) in the nigra of 6-OHDA-treated rats reduced the loss of dopaminergic neurons [152]. An alternative approach may be to modify the endocannabinoid system with the aim to reduce pro-inflammatory microglial toxicity [148]. The expression of the cannabinoid receptor CB2 was found to be increased in glial cells in various conditions affecting the CNS, including AD and PD [153]. Interestingly, while the abundance of CB2 is enhanced in activated PD microglia, an immunolabeling study in human postmortem nigral tissue revealed that CB2 levels are decreased in dopaminergic neurons from PD patients. This observation coincided with diminished numbers of tyrosine hydroxylase-containing neurons in the PD tissue [153]. In line with these findings, administering the CB2 agonist β-caryophyllene to rotenone-challenged rats reduced the release of proinflammatory cytokines which, in turn, prevented dopaminergic neuron demise and the activation of glial cells [154].

Also strategies that actively promote a shift of microglia from M1 to M2 have been considered [148]. For instance, the cerebral infusion of a recombinant adeno-associated viral vector expressing human *interleukin-10* (*IL-10*) was tested in an MPTP mouse model. Enhancing the abundance of the anti-inflammatory cytokine led to an increase in striatal TH protein levels [155]. Further of interest in this regard, the multiple sclerosis drug Glatiramer acetate was shown to decrease microglial activation by promoting an M2 state [156]. As in the case of *IL-10* overexpression, treatment of MPTP mice with Glatiramer acetate rescued tyrosine hydroxylase (TH) protein levels in the striatum. Moreover, exposure to the immuno-modulatory agent reversed motor phenotypes in these animals [157]. However, none of the proposed treatments facilitating a shift from M1 to M2 has been tested in humans (for a more detailed review of immuno-modulatory treatment approaches in PD—including a study comparison in tabular form—see Subramaniam and Federoff [148]). Thus, further research in PD patient-derived cellular models will be required to understand the molecular consequences of microglial activation regulators, which will be a prerequisite to eventually use such agents in clinical trials.

5.2. Anti-α-Synuclein Immunotherapies

One of the best studied hallmarks of PD are α-synuclein aggregates. As mentioned above, the protein can act as DAMP triggering inflammatory processes. Thus, one research focus in PD is the development of immunotherapeutic approaches that reduce intra- and extracellular α-synuclein levels in the brain. Specifically, antibodies hold the promise of alleviating α-synuclein toxicity and promoting the protein's degradation [158]. Various epitopes have been tested in preclinical studies with α-synuclein transgenic mice. In two independent studies, administration of antibodies that target the C-terminus (Ab274, 1H7 or 5C1) reduced microgliosis and improved neuronal survival [159,160]. In animals that received ab274, there is even evidence that microglia block the cell-to-cell transfer of α-synuclein by enhancing the clearance of neuron-derived aggregates [160]. With regard to antibodies that are directed against the N-terminus, no improvement of microgliosis phenotypes was observed [158]. Finally, when focusing on antibodies that recognize oligomeric or fibrilar forms of α-synuclein, Syn-O1, Syn-O4 and Syn-F1 effectively reduced protein aggregation and neurodegeneration in transgenic mice [161]. Only animals treated with Syn-O4 displayed decreased microglia levels and showed reduced ramification of these cells in the hippocampus [161].

In light of the overall promising results from immunotherapeutic analyses in mice, several antibodies are being tested in phase I clinical trials, which focus primarily on the safety of treatments [162]. By contrast, only two antibodies have so far been moved forward into phase II clinical trials [162], which aim to establish the clinical efficiency of the immunotherapeutics. In the PASADENA study (ClinicalTrials.gov Identifier: NCT03100149),

Prasinezumab (PRX002) is currently being tested in patients with early PD. Initial results indicate that the primary outcome of the study was not achieved. At week 52, the MDS-UPDRS total score was not significantly different between the treatment and the placebo group. Nevertheless, some parameters suggest that the antibody delays the progression of motor symptoms in PD patients. However, whether Prasinezumab has a positive impact on microglial phenotypes in these individuals currently remains elusive. In addition, the SPARK study (ClinicalTrials.gov Identifier: NCT03318523), which aims to evaluate the clinical benefits of the α-synuclein antibody BIIB054, is currently ongoing.

6. Outlook

The complex and diverse aetiology of PD represents a major obstacle for effective therapeutic interventions. The here described recent findings highlight the importance of neuroinflammatory processes and put microglia as the immanent immune cells of the brain in the focus of novel therapeutic approaches. In particular, this immunological entry point could not only support the identification of common mechanisms underlying the different genetic and idiopathic disease developments but also allow to target disease progression not on the cellular but on the (immune) system level of the brain. While the evidence for the contribution of microglia to disease progression clearly demonstrates the large potential for alternative treatments, further detailed investigations are required to reveal underlying mechanisms and to dissect cellular heterogeneity of microglia in the disease context. Thus, scRNAseq has shown that microglia diversity goes beyond the traditional M1/M2 description and that PD-associated signatures are species- and human-specific but the impact of the microenvironment is still elusive. The recent developments in spatial transcriptomics [163,164] and the application to human iPSC model systems such as organoids [141] and the brain [165] will allow for further insights into the regulation of the complex ecosystem within the brain and how intercellular interactions contribute to PD progression. A major challenge for these studies is the lack of physiologically realistic model systems due to the general limitations of animal models and the not yet resolved issue in human organoid systems, which do not reflect the brain composition of the affected brain regions as described above. Hence, addressing these current limitations is essential to deepen our understanding of the multicellular dimension of PD development and particularly the impact of microglia and their role in neuroimmunology that will not only support the development of new therapeutic strategies in PD but may also provide a more unifying perspective on neurodegeneration given the recent indications for the involvement of microglia in Alzheimer's disease and multiple sclerosis [165,166].

Author Contributions: All authors contributed to the conception, literature review and writing of the manuscript, and reviewed the final document. All authors have read and agreed to the published version of the manuscript.

Funding: KB was supported by the Luxembourg National Research Fund (FNR) through the PRIDE15/10907093/CriTiCS grant. SF and SS received funding from the Luxembourg National Research Fund (FNR) within the PARK-QC DTU (PRIDE17/12244779/PARK-QC). AG received funding from the FNR within the framework of the ATTRACT (FNR9631103) and INTER (INTER/DFG/19/14429377) programmes. In addition, AG and AS are supported by the FNR as members of the Luxembourgish National Centre of Excellence in Research on Parkinson's Disease (NCER-PD). In addition, AG was supported by the German Research Foundation (DFG, GR 3731/5-2, FOR 2488/2).

Institutional Review Board Statement: Not applicable.

Informed Consent Statement: Not applicable.

Data Availability Statement: No new data were created or analyzed in this study. Data sharing is not applicable to this article.

Conflicts of Interest: The authors declare no conflict of interest.

References

1. Toulouse, A.; Sullivan, A.M. Progress in Parkinson's Disease-Where Do We Stand? *Prog. Neurobiol.* **2008**, *85*, 376–392. [CrossRef]
2. Forno, L.S. Neuropathology of Parkinson's Disease. *J. Neuropathol. Exp. Neurol.* **1996**, *55*, 259–272. [CrossRef]
3. Deng, H.; Dodson, M.W.; Huang, H.; Guo, M. The Parkinson's Disease Genes pink1 and Parkin Promote Mitochondrial Fission And/or Inhibit Fusion in Drosophila. *Proc. Natl. Acad. Sci. USA* **2008**, *105*, 14503–14508. [CrossRef]
4. Klein, C.; Westenberger, A. Genetics of Parkinson's Disease. *Cold Spring Harb. Perspect. Med.* **2012**, *2*, a008888. [CrossRef]
5. Del Rey, N.L.-G.; Quiroga-Varela, A.; Garbayo, E.; Carballo-Carbajal, I.; Fernández-Santiago, R.; Monje, M.H.G.; Trigo-Damas, I.; Blanco-Prieto, M.J.; Blesa, J. Advances in Parkinson's Disease: 200 Years Later. *Front. Neuroanat.* **2018**, *12*, 113. [CrossRef]
6. Hindle, J.V. Ageing, Neurodegeneration and Parkinson's Disease. *Age Ageing* **2010**, *39*, 156–161. [CrossRef]
7. Collier, T.J.; Kanaan, N.M.; Kordower, J.H. Ageing as a Primary Risk Factor for Parkinson's Disease: Evidence from Studies of Non-Human Primates. *Nat. Rev. Neurosci.* **2011**, *12*, 359–366. [CrossRef] [PubMed]
8. Chade, A.R.; Kasten, M.; Tanner, C.M. Nongenetic Causes of Parkinson's Disease. In *Parkinson's Disease and Related Disorders*; Springer: Vienna, Austria, 2006; pp. 147–151.
9. Braak, H.; Rüb, U.; Del Tredici, K. Cognitive Decline Correlates with Neuropathological Stage in Parkinson's Disease. *J. Neurol. Sci.* **2006**, *248*, 255–258. [CrossRef] [PubMed]
10. Schapira, A.H.V.; Chaudhuri, K.R.; Jenner, P. Non-Motor Features of Parkinson Disease. *Nat. Rev. Neurosci.* **2017**, *18*, 435–450. [CrossRef] [PubMed]
11. Langston, J.W.; Forno, L.S.; Tetrud, J.; Reeves, A.G.; Kaplan, J.A.; Karluk, D. Evidence of Active Nerve Cell Degeneration in the Substantia Nigra of Humans Years after 1-Methyl-4-Phenyl-1,2,3,6-Tetrahydropyridine Exposure. *Ann. Neurol.* **1999**, *46*, 598–605. [CrossRef]
12. Langston, J.W.; Ballard, P.; Tetrud, J.W.; Irwin, I. Chronic Parkinsonism in Humans due to a Product of Meperidine-Analog Synthesis. *Science* **1983**, *219*, 979–980. [CrossRef]
13. Spillantini, M.G.; Schmidt, M.L.; Lee, V.M.; Trojanowski, J.Q.; Jakes, R.; Goedert, M. Alpha-Synuclein in Lewy Bodies. *Nature* **1997**, *388*, 839–840. [CrossRef]
14. McGeer, P.L.; Itagaki, S.; Boyes, B.E.; McGeer, E.G. Reactive Microglia Are Positive for HLA-DR in the Substantia Nigra of Parkinson's and Alzheimer's Disease Brains. *Neurology* **1988**, *38*, 1285–1291. [CrossRef]
15. Grünewald, A.; Kumar, K.R.; Sue, C.M. New Insights into the Complex Role of Mitochondria in Parkinson's Disease. *Prog. Neurobiol.* **2019**, *177*, 73–93. [CrossRef]
16. Hauser, D.N.; Hastings, T.G. Mitochondrial Dysfunction and Oxidative Stress in Parkinson's Disease and Monogenic Parkinsonism. *Neurobiol. Dis.* **2013**, *51*, 35–42. [CrossRef] [PubMed]
17. Park, J.-S.; Davis, R.L.; Sue, C.M. Mitochondrial Dysfunction in Parkinson's Disease: New Mechanistic Insights and Therapeutic Perspectives. *Curr. Neurol. Neurosci. Rep.* **2018**, *18*, 21. [CrossRef]
18. Lang, A.E.; Lozano, A.M. Parkinson's Disease. First of Two Parts. *N. Engl. J. Med.* **1998**, *339*, 1044–1053. [CrossRef]
19. Gao, H.-M.; Hong, J.-S. Why Neurodegenerative Diseases Are Progressive: Uncontrolled Inflammation Drives Disease Progression. *Trends Immunol.* **2008**, *29*, 357–365. [CrossRef] [PubMed]
20. Verkhratsky, A.; Ho, M.S.; Zorec, R.; Parpura, V. (Eds.) *Neuroglia in Neurodegenerative Diseases*; Springer: Singapore, 2019.
21. Pérez-Cerdá, F.; Sánchez-Gómez, M.V.; Matute, C. Pío Del Río Hortega and the Discovery of the Oligodendrocytes. *Front. Neuroanat.* **2015**, *9*, 92. [CrossRef]
22. Sierra, A.; de Castro, F.; Del Río-Hortega, J.; Rafael Iglesias-Rozas, J.; Garrosa, M.; Kettenmann, H. The "Big-Bang" for Modern Glial Biology: Translation and Comments on Pío Del Río-Hortega 1919 Series of Papers on Microglia. *Glia* **2016**, *64*, 1801–1840. [CrossRef]
23. Hickman, S.; Izzy, S.; Sen, P.; Morsett, L.; El Khoury, J. Microglia in Neurodegeneration. *Nat. Neurosci.* **2018**, *21*, 1359–1369. [CrossRef]
24. Priller, J.; Flügel, A.; Wehner, T.; Boentert, M.; Haas, C.A.; Prinz, M.; Fernández-Klett, F.; Prass, K.; Bechmann, I.; de Boer, B.A.; et al. Targeting Gene-Modified Hematopoietic Cells to the Central Nervous System: Use of Green Fluorescent Protein Uncovers Microglial Engraftment. *Nat. Med.* **2001**, *7*, 1356–1361. [CrossRef] [PubMed]
25. Bruttger, J.; Karram, K.; Wörtge, S.; Regen, T.; Marini, F.; Hoppmann, N.; Klein, M.; Blank, T.; Yona, S.; Wolf, Y.; et al. Genetic Cell Ablation Reveals Clusters of Local Self-Renewing Microglia in the Mammalian Central Nervous System. *Immunity* **2015**, *43*, 92–106. [CrossRef]
26. Ueno, M.; Fujita, Y.; Tanaka, T.; Nakamura, Y.; Kikuta, J.; Ishii, M.; Yamashita, T. Layer V Cortical Neurons Require Microglial Support for Survival during Postnatal Development. *Nat. Neurosci.* **2013**, *16*, 543–551. [CrossRef] [PubMed]
27. Nimmerjahn, A.; Kirchhoff, F.; Helmchen, F. Resting Microglial Cells Are Highly Dynamic Surveillants of Brain Parenchyma in Vivo. *Science* **2005**, *308*, 1314–1318. [CrossRef]
28. Bennett, M.L.; Bennett, F.C.; Liddelow, S.A.; Ajami, B.; Zamanian, J.L.; Fernhoff, N.B.; Mulinyawe, S.B.; Bohlen, C.J.; Adil, A.; Tucker, A.; et al. New Tools for Studying Microglia in the Mouse and Human CNS. *Proc. Natl. Acad. Sci. USA* **2016**, *113*, E1738–E1746. [CrossRef]
29. Friedman, B.A.; Srinivasan, K.; Ayalon, G.; Meilandt, W.J.; Lin, H.; Huntley, M.A.; Cao, Y.; Lee, S.-H.; Haddick, P.C.G.; Ngu, H.; et al. Diverse Brain Myeloid Expression Profiles Reveal Distinct Microglial Activation States and Aspects of Alzheimer's Disease Not Evident in Mouse Models. *Cell Rep.* **2018**, *22*, 832–847. [CrossRef] [PubMed]

30. Walker, D.G.; Tang, T.M.; Mendsaikhan, A.; Tooyama, I.; Serrano, G.E.; Sue, L.I.; Beach, T.G.; Lue, L.-F. Patterns of Expression of Purinergic Receptor P2RY12, a Putative Marker for Non-Activated Microglia, in Aged and Alzheimer's Disease Brains. *Int. J. Mol. Sci.* **2020**, *21*, 678. [CrossRef]
31. Sheng, J.G.; Mrak, R.E.; Griffin, W.S. Enlarged and Phagocytic, but Not Primed, Interleukin-1 Alpha-Immunoreactive Microglia Increase with Age in Normal Human Brain. *Acta Neuropathol.* **1998**, *95*, 229–234. [CrossRef]
32. Conde, J.R.; Streit, W.J. Microglia in the Aging Brain. *J. Neuropathol. Exp. Neurol.* **2006**, *65*, 199–203. [CrossRef]
33. Gao, X.; Wang, X.; Xiong, W.; Chen, J. In Vivo Reprogramming Reactive Glia into iPSCs to Produce New Neurons in the Cortex Following Traumatic Brain Injury. *Sci. Rep.* **2016**, *6*, 22490. [CrossRef]
34. Imamura, K.; Hishikawa, N.; Sawada, M.; Nagatsu, T.; Yoshida, M.; Hashizume, Y. Distribution of Major Histocompatibility Complex Class II-Positive Microglia and Cytokine Profile of Parkinson's Disease Brains. *Acta Neuropathol.* **2003**, *106*, 518–526. [CrossRef]
35. Mastroeni, D.; Nolz, J.; Sekar, S.; Delvaux, E.; Serrano, G.; Cuyugan, L.; Liang, W.S.; Beach, T.G.; Rogers, J.; Coleman, P.D. Laser-Captured Microglia in the Alzheimer's and Parkinson's Brain Reveal Unique Regional Expression Profiles and Suggest a Potential Role for Hepatitis B in the Alzheimer's Brain. *Neurobiol. Aging* **2018**, *63*, 12–21. [CrossRef]
36. Geirsdottir, L.; David, E.; Keren-Shaul, H.; Weiner, A.; Bohlen, S.C.; Neuber, J.; Balic, A.; Giladi, A.; Sheban, F.; Dutertre, C.-A.; et al. Cross-Species Single-Cell Analysis Reveals Divergence of the Primate Microglia Program. *Cell* **2019**, *179*, 1609–1622.e16. [CrossRef]
37. Agarwal, D.; Sandor, C.; Volpato, V.; Caffrey, T.M.; Monzón-Sandoval, J.; Bowden, R.; Alegre-Abarrategui, J.; Wade-Martins, R.; Webber, C. A Single-Cell Atlas of the Human Substantia Nigra Reveals Cell-Specific Pathways Associated with Neurological Disorders. *Nat. Commun.* **2020**, *11*, 4183. [CrossRef] [PubMed]
38. Thrupp, N.; Sala Frigerio, C.; Wolfs, L.; Skene, N.G.; Poovathingal, S.; Fourne, Y.; Matthews, P.M.; Theys, T.; Mancuso, R.; de Strooper, B.; et al. Single Nucleus Sequencing Fails to Detect Microglial Activation in Human Tissue. *bioRxiv* **2020**. [CrossRef]
39. Smajić, S.; Prada-Medina, C.A.; Landoulsi, Z.; Dietrich, C.; Spielmann, M. Single-Cell Sequencing of the Human Midbrain Reveals Glial Activation and a Neuronal State Specific to Parkinson's Disease. *medRxiv* **2020**. [CrossRef]
40. Alessi, D.R.; Sammler, E. LRRK2 Kinase in Parkinson's Disease. *Science* **2018**, *360*, 36–37. [CrossRef] [PubMed]
41. Liu, B.; Gao, H.-M.; Hong, J.-S. Parkinson's Disease and Exposure to Infectious Agents and Pesticides and the Occurrence of Brain Injuries: Role of Neuroinflammation. *Environ. Health Perspect.* **2003**, *111*, 1065–1073. [CrossRef]
42. Dobbs, R.J.; Charlett, A.; Purkiss, A.G.; Dobbs, S.M.; Weller, C.; Peterson, D.W. Association of Circulating TNF-Alpha and IL-6 with Ageing and Parkinsonism. *Acta Neurol. Scand.* **1999**, *100*, 34–41. [CrossRef]
43. Scalzo, P.; Kümmer, A.; Cardoso, F.; Teixeira, A.L. Increased Serum Levels of Soluble Tumor Necrosis Factor-Alpha Receptor-1 in Patients with Parkinson's Disease. *J. Neuroimmunol.* **2009**, *216*, 122–125. [CrossRef]
44. Sliter, D.A.; Martinez, J.; Hao, L.; Chen, X.; Sun, N.; Fischer, T.D.; Burman, J.L.; Li, Y.; Zhang, Z.; Narendra, D.P.; et al. Parkin and PINK1 Mitigate STING-Induced Inflammation. *Nature* **2018**, *561*, 258–262. [CrossRef] [PubMed]
45. Borsche, M.; König, I.R.; Delcambre, S.; Petrucci, S.; Balck, A.; Brüggemann, N.; Zimprich, A.; Wasner, K.; Pereira, S.L.; Avenali, M.; et al. Mitochondrial Damage-Associated Inflammation Highlights Biomarkers in PRKN/PINK1 Parkinsonism. *Brain* **2020**, *143*, 3041–3051. [CrossRef]
46. Mount, M.P.; Lira, A.; Grimes, D.; Smith, P.D.; Faucher, S.; Slack, R.; Anisman, H.; Hayley, S.; Park, D.S. Involvement of Interferon-Gamma in Microglial-Mediated Loss of Dopaminergic Neurons. *J. Neurosci.* **2007**, *27*, 3328–3337. [CrossRef] [PubMed]
47. Menza, M.; Dobkin, R.D.; Marin, H.; Mark, M.H.; Gara, M.; Bienfait, K.; Dicke, A.; Kusnekov, A. The Role of Inflammatory Cytokines in Cognition and Other Non-Motor Symptoms of Parkinson's Disease. *Psychosomatics* **2010**, *51*, 474–479. [CrossRef] [PubMed]
48. Lindqvist, D.; Kaufman, E.; Brundin, L.; Hall, S.; Surova, Y.; Hansson, O. Non-Motor Symptoms in Patients with Parkinson's Disease—Correlations with Inflammatory Cytokines in Serum. *PLoS ONE* **2012**, *7*, e47387. [CrossRef]
49. He, Y.; Le, W.-D.; Appel, S.H. Role of Fcgamma Receptors in Nigral Cell Injury Induced by Parkinson Disease Immunoglobulin Injection into Mouse Substantia Nigra. *Exp. Neurol.* **2002**, *176*, 322–327. [CrossRef]
50. Benkler, M.; Agmon-Levin, N.; Hassin-Baer, S.; Cohen, O.S.; Ortega-Hernandez, O.-D.; Levy, A.; Moscavitch, S.-D.; Szyper-Kravitz, M.; Damianovich, M.; Blank, M.; et al. Immunology, Autoimmunity, and Autoantibodies in Parkinson's Disease. *Clin. Rev. Allergy Immunol.* **2012**, *42*, 164–171. [CrossRef]
51. Zhang, Q.; Raoof, M.; Chen, Y.; Sumi, Y.; Sursal, T.; Junger, W.; Brohi, K.; Itagaki, K.; Hauser, C.J. Circulating Mitochondrial DAMPs Cause Inflammatory Responses to Injury. *Nature* **2010**, *464*, 104–107. [CrossRef]
52. Grazioli, S.; Pugin, J. Mitochondrial Damage-Associated Molecular Patterns: From Inflammatory Signaling to Human Diseases. *Front. Immunol.* **2018**, *9*, 832. [CrossRef]
53. Papachroni, K.K.; Ninkina, N.; Papapanagiotou, A.; Hadjigeorgiou, G.M.; Xiromerisiou, G.; Papadimitriou, A.; Kalofoutis, A.; Buchman, V.L. Autoantibodies to Alpha-Synuclein in Inherited Parkinson's Disease. *J. Neurochem.* **2007**, *101*, 749–756. [CrossRef]
54. Yanamandra, K.; Gruden, M.A.; Casaite, V.; Meskys, R.; Forsgren, L.; Morozova-Roche, L.A. α-Synuclein Reactive Antibodies as Diagnostic Biomarkers in Blood Sera of Parkinson's Disease Patients. *PLoS ONE* **2011**, *6*, e18513. [CrossRef]
55. Double, K.L.; Rowe, D.B.; Carew-Jones, F.M.; Hayes, M.; Chan, D.K.Y.; Blackie, J.; Corbett, A.; Joffe, R.; Fung, V.S.; Morris, J.; et al. Anti-Melanin Antibodies Are Increased in Sera in Parkinson's Disease. *Exp. Neurol.* **2009**, *217*, 297–301. [CrossRef]

56. Brochard, V.; Combadière, B.; Prigent, A.; Laouar, Y.; Perrin, A.; Beray-Berthat, V.; Bonduelle, O.; Alvarez-Fischer, D.; Callebert, J.; Launay, J.-M.; et al. Infiltration of CD4+ Lymphocytes into the Brain Contributes to Neurodegeneration in a Mouse Model of Parkinson Disease. *J. Clin. Investig.* **2009**, *119*, 182–192. [CrossRef]
57. Sommer, A.; Marxreiter, F.; Krach, F.; Fadler, T.; Grosch, J.; Maroni, M.; Graef, D.; Eberhardt, E.; Riemenschneider, M.J.; Yeo, G.W.; et al. Th17 Lymphocytes Induce Neuronal Cell Death in a Human iPSC-Based Model of Parkinson's Disease. *Cell Stem Cell* **2018**, *23*, 123–131.e6. [CrossRef] [PubMed]
58. Kustrimovic, N.; Comi, C.; Magistrelli, L.; Rasini, E.; Legnaro, M.; Bombelli, R.; Aleksic, I.; Blandini, F.; Minafra, B.; Riboldazzi, G.; et al. Parkinson's Disease Patients Have a Complex Phenotypic and Functional Th1 Bias: Cross-Sectional Studies of CD4+ Th1/Th2/T17 and Treg in Drug-Naïve and Drug-Treated Patients. *J. Neuroinflammation* **2018**, *15*, 205. [CrossRef]
59. Karaaslan, Z.; Kahraman, Ö.T.; Şanlı, E.; Ergen, H.A.; Ulusoy, C.; Bilgiç, B.; Yılmaz, V.; Tüzün, E.; Hanağası, H.A.; Küçükali, C.İ. Inflammation and Regulatory T Cell Genes Are Differentially Expressed in Peripheral Blood Mononuclear Cells of Parkinson's Disease Patients. *Sci. Rep.* **2021**, *11*, 2316. [CrossRef]
60. Subbarayan, M.S.; Hudson, C.; Moss, L.D.; Nash, K.R.; Bickford, P.C. T Cell Infiltration and Upregulation of MHCII in Microglia Leads to Accelerated Neuronal Loss in an α-Synuclein Rat Model of Parkinson's Disease. *J. Neuroinflammation* **2020**, *17*, 242. [CrossRef] [PubMed]
61. Nomura, T.; Watanabe, T.; Habu, S. *Humanized Mice*; Springer: Berlin/Heidelberg, Germany, 2008; ISBN 9783540756460.
62. Członkowska, A.; Kohutnicka, M.; Kurkowska-Jastrzebska, I.; Członkowski, A. Microglial Reaction in MPTP (1-Methyl-4-Phenyl-1,2,3,6-Tetrahydropyridine) Induced Parkinson's Disease Mice Model. *Neurodegeneration* **1996**, *5*, 137–143. [CrossRef]
63. Wu, D.C.; Jackson-Lewis, V.; Vila, M.; Tieu, K.; Teismann, P.; Vadseth, C.; Choi, D.-K.; Ischiropoulos, H.; Przedborski, S. Blockade of Microglial Activation Is Neuroprotective in the 1-Methyl-4-Phenyl-1,2,3,6-Tetrahydropyridine Mouse Model of Parkinson Disease. *J. Neurosci.* **2002**, *22*, 1763–1771. [CrossRef]
64. Giuliani, F.; Hader, W.; Yong, V.W. Minocycline Attenuates T Cell and Microglia Activity to Impair Cytokine Production in T Cell-Microglia Interaction. *J. Leukoc. Biol.* **2005**, *78*, 135–143. [CrossRef] [PubMed]
65. Sriram, K.; Matheson, J.M.; Benkovic, S.A.; Miller, D.B.; Luster, M.I.; O'Callaghan, J.P. Mice Deficient in TNF Receptors Are Protected against Dopaminergic Neurotoxicity: Implications for Parkinson's Disease. *FASEB J.* **2002**, *16*, 1474–1476. [CrossRef]
66. Barcia, C.; Ros, C.M.; Annese, V.; Gómez, A.; Ros-Bernal, F.; Aguado-Yera, D.; Martínez-Pagán, M.E.; de Pablos, V.; Fernandez-Villalba, E.; Herrero, M.T. IFN-γ Signaling, with the Synergistic Contribution of TNF-α, Mediates Cell Specific Microglial and Astroglial Activation in Experimental Models of Parkinson's Disease. *Cell Death Dis.* **2011**, *2*, e142. [CrossRef]
67. Gao, H.-M.; Hong, J.-S.; Zhang, W.; Liu, B. Synergistic Dopaminergic Neurotoxicity of the Pesticide Rotenone and Inflammogen Lipopolysaccharide: Relevance to the Etiology of Parkinson's Disease. *J. Neurosci.* **2003**, *23*, 1228–1236. [CrossRef]
68. Gao, H.-M.; Zhou, H.; Zhang, F.; Wilson, B.C.; Kam, W.; Hong, J.-S. HMGB1 Acts on Microglia Mac1 to Mediate Chronic Neuroinflammation That Drives Progressive Neurodegeneration. *J. Neurosci.* **2011**, *31*, 1081–1092. [CrossRef] [PubMed]
69. Klintworth, H.; Garden, G.; Xia, Z. Rotenone and Paraquat Do Not Directly Activate Microglia or Induce Inflammatory Cytokine Release. *Neurosci. Lett.* **2009**, *462*, 1–5. [CrossRef]
70. Gao, F.; Chen, D.; Hu, Q.; Wang, G. Rotenone Directly Induces BV2 Cell Activation via the p38 MAPK Pathway. *PLoS ONE* **2013**, *8*, e72046. [CrossRef]
71. Athanassiadou, A.; Voutsinas, G.; Psiouri, L.; Leroy, E.; Polymeropoulos, M.H.; Ilias, A.; Maniatis, G.M.; Papapetropoulos, T. Genetic Analysis of Families with Parkinson Disease That Carry the Ala53Thr Mutation in the Gene Encoding Alpha-Synuclein. *Am. J. Hum. Genet.* **1999**, *65*, 555–558. [CrossRef]
72. Polymeropoulos, M.H.; Lavedan, C.; Leroy, E.; Ide, S.E.; Dehejia, A.; Dutra, A.; Pike, B.; Root, H.; Rubenstein, J.; Boyer, R.; et al. Mutation in the Alpha-Synuclein Gene Identified in Families with Parkinson's Disease. *Science* **1997**, *276*, 2045–2047. [CrossRef] [PubMed]
73. Lesage, S.; Anheim, M.; Letournel, F.; Bousset, L.; Honoré, A.; Rozas, N.; Pieri, L.; Madiona, K.; Dürr, A.; Melki, R.; et al. G51D α-Synuclein Mutation Causes a Novel Parkinsonian-Pyramidal Syndrome. *Ann. Neurol.* **2013**, *73*, 459–471. [CrossRef]
74. Ross, O.A.; Braithwaite, A.T.; Skipper, L.M.; Kachergus, J.; Hulihan, M.M.; Middleton, F.A.; Nishioka, K.; Fuchs, J.; Gasser, T.; Maraganore, D.M.; et al. Genomic Investigation of Alpha-Synuclein Multiplication and Parkinsonism. *Ann. Neurol.* **2008**, *63*, 743–750. [CrossRef]
75. Singleton, A.B.; Farrer, M.; Johnson, J.; Singleton, A.; Hague, S.; Kachergus, J.; Hulihan, M.; Peuralinna, T.; Dutra, A.; Nussbaum, R.; et al. Alpha-Synuclein Locus Triplication Causes Parkinson's Disease. *Science* **2003**, *302*, 841. [CrossRef] [PubMed]
76. Krüger, R.; Kuhn, W.; Müller, T.; Woitalla, D.; Graeber, M.; Kösel, S.; Przuntek, H.; Epplen, J.T.; Schöls, L.; Riess, O. Ala30Pro Mutation in the Gene Encoding Alpha-Synuclein in Parkinson's Disease. *Nat. Genet.* **1998**, *18*, 106–108. [CrossRef]
77. Kim, W.S.; Kågedal, K.; Halliday, G.M. Alpha-Synuclein Biology in Lewy Body Diseases. *Alzheimers. Res. Ther.* **2014**, *6*, 73. [CrossRef]
78. Reynolds, A.D.; Stone, D.K.; Mosley, R.L.; Gendelman, H.E. Nitrated {alpha}-Synuclein-Induced Alterations in Microglial Immunity Are Regulated by CD4+ T Cell Subsets. *J. Immunol.* **2009**, *182*, 4137–4149. [CrossRef]
79. Benner, E.J.; Banerjee, R.; Reynolds, A.D.; Sherman, S.; Pisarev, V.M.; Tsiperson, V.; Nemachek, C.; Ciborowski, P.; Przedborski, S.; Mosley, R.L.; et al. Nitrated Alpha-Synuclein Immunity Accelerates Degeneration of Nigral Dopaminergic Neurons. *PLoS ONE* **2008**, *3*, e1376. [CrossRef] [PubMed]

80. Zhang, W.; Wang, T.; Pei, Z.; Miller, D.S.; Wu, X.; Block, M.L.; Wilson, B.; Zhang, W.; Zhou, Y.; Hong, J.-S.; et al. Aggregated Alpha-Synuclein Activates Microglia: A Process Leading to Disease Progression in Parkinson's Disease. *FASEB J.* **2005**, *19*, 533–542. [CrossRef] [PubMed]
81. Couch, Y.; Alvarez-Erviti, L.; Sibson, N.R.; Wood, M.J.A.; Anthony, D.C. The Acute Inflammatory Response to Intranigral α-Synuclein Differs Significantly from Intranigral Lipopolysaccharide and Is Exacerbated by Peripheral Inflammation. *J. Neuroinflammation* **2011**, *8*, 166. [CrossRef]
82. Su, X.; Maguire-Zeiss, K.A.; Giuliano, R.; Prifti, L.; Venkatesh, K.; Federoff, H.J. Synuclein Activates Microglia in a Model of Parkinson's Disease. *Neurobiol. Aging* **2008**, *29*, 1690–1701. [CrossRef]
83. Watson, M.B.; Richter, F.; Lee, S.K.; Gabby, L.; Wu, J.; Masliah, E.; Effros, R.B.; Chesselet, M.-F. Regionally-Specific Microglial Activation in Young Mice over-Expressing Human Wildtype Alpha-Synuclein. *Exp. Neurol.* **2012**, *237*, 318–334. [CrossRef]
84. Béraud, D.; Twomey, M.; Bloom, B.; Mittereder, A.; Ton, V.; Neitzke, K.; Chasovskikh, S.; Mhyre, T.R.; Maguire-Zeiss, K.A. α-Synuclein Alters Toll-Like Receptor Expression. *Front. Neurosci.* **2011**, *5*, 80. [CrossRef] [PubMed]
85. Daniele, S.G.; Béraud, D.; Davenport, C.; Cheng, K.; Yin, H.; Maguire-Zeiss, K.A. Activation of MyD88-Dependent TLR1/2 Signaling by Misfolded α-Synuclein, a Protein Linked to Neurodegenerative Disorders. *Sci. Signal.* **2015**, *8*, ra45. [CrossRef]
86. Gordon, R.; Albornoz, E.A.; Christie, D.C.; Langley, M.R.; Kumar, V.; Mantovani, S.; Robertson, A.A.B.; Butler, M.S.; Rowe, D.B.; O'Neill, L.A.; et al. Inflammasome Inhibition Prevents α-Synuclein Pathology and Dopaminergic Neurodegeneration in Mice. *Sci. Transl. Med.* **2018**, *10*. [CrossRef]
87. Pike, A.F.; Varanita, T.; Herrebout, M.A.C.; Plug, B.C.; Kole, J.; Musters, R.J.P.; Teunissen, C.E.; Hoozemans, J.J.M.; Bubacco, L.; Veerhuis, R. α-Synuclein Evokes NLRP3 Inflammasome-Mediated IL-1β Secretion from Primary Human Microglia. *Glia* **2021**. [CrossRef] [PubMed]
88. Hoenen, C.; Gustin, A.; Birck, C.; Kirchmeyer, M.; Beaume, N.; Felten, P.; Grandbarbe, L.; Heuschling, P.; Heurtaux, T. Alpha-Synuclein Proteins Promote Pro-Inflammatory Cascades in Microglia: Stronger Effects of the A53T Mutant. *PLoS ONE* **2016**, *11*, e0162717. [CrossRef] [PubMed]
89. Sánchez, K.; Maguire-Zeiss, K. MMP13 Expression Is Increased Following Mutant α-Synuclein Exposure and Promotes Inflammatory Responses in Microglia. *Front. Neurosci.* **2020**, *14*, 585544. [CrossRef]
90. Zhang, W.; Dallas, S.; Zhang, D.; Guo, J.-P.; Pang, H.; Wilson, B.; Miller, D.S.; Chen, B.; Zhang, W.; McGeer, P.L.; et al. Microglial PHOX and Mac-1 Are Essential to the Enhanced Dopaminergic Neurodegeneration Elicited by A30P and A53T Mutant Alpha-Synuclein. *Glia* **2007**, *55*, 1178–1188. [CrossRef]
91. Gasser, T. Usefulness of Genetic Testing in PD and PD Trials: A Balanced Review. *J. Parkinsons. Dis.* **2015**, *5*, 209–215. [CrossRef]
92. Gardet, A.; Benita, Y.; Li, C.; Sands, B.E.; Ballester, I.; Stevens, C.; Korzenik, J.R.; Rioux, J.D.; Daly, M.J.; Xavier, R.J.; et al. LRRK2 Is Involved in the IFN-Gamma Response and Host Response to Pathogens. *J. Immunol.* **2010**, *185*, 5577–5585. [CrossRef]
93. Hakimi, M.; Selvanantham, T.; Swinton, E.; Padmore, R.F.; Tong, Y.; Kabbach, G.; Venderova, K.; Girardin, S.E.; Bulman, D.E.; Scherzer, C.R.; et al. Parkinson's Disease-Linked LRRK2 Is Expressed in Circulating and Tissue Immune Cells and Upregulated Following Recognition of Microbial Structures. *J. Neural Transm.* **2011**, *118*, 795–808. [CrossRef]
94. Gillardon, F.; Schmid, R.; Draheim, H. Parkinson's Disease-Linked Leucine-Rich Repeat Kinase 2(R1441G) Mutation Increases Proinflammatory Cytokine Release from Activated Primary Microglial Cells and Resultant Neurotoxicity. *Neuroscience* **2012**, *208*, 41–48. [CrossRef]
95. Zhang, F.-R.; Huang, W.; Chen, S.-M.; Sun, L.-D.; Liu, H.; Li, Y.; Cui, Y.; Yan, X.-X.; Yang, H.-T.; Yang, R.-D.; et al. Genomewide Association Study of Leprosy. *N. Engl. J. Med.* **2009**, *361*, 2609–2618. [CrossRef] [PubMed]
96. Umeno, J.; Asano, K.; Matsushita, T.; Matsumoto, T.; Kiyohara, Y.; Iida, M.; Nakamura, Y.; Kamatani, N.; Kubo, M. Meta-Analysis of Published Studies Identified Eight Additional Common Susceptibility Loci for Crohn's Disease and Ulcerative Colitis. *Inflamm. Bowel Dis.* **2011**, *17*, 2407–2415. [CrossRef] [PubMed]
97. Van Limbergen, J.; Wilson, D.C.; Satsangi, J. The Genetics of Crohn's Disease. *Annu. Rev. Genomics Hum. Genet.* **2009**, *10*, 89–116. [CrossRef] [PubMed]
98. Weindel, C.G.; Bell, S.L.; Huntington, T.E.; Vail, K.J.; Srinivasan, R.; Patrick, K.L.; Watson, R.O. LRRK2 Regulates Innate Immune Responses and Neuroinflammation during Mycobacterium Tuberculosis Infection. *bioRxiv* **2019**, 699066. [CrossRef]
99. Goldwurm, S.; Zini, M.; Mariani, L.; Tesei, S.; Miceli, R.; Sironi, F.; Clementi, M.; Bonifati, V.; Pezzoli, G. Evaluation of LRRK2 G2019S Penetrance: Relevance for Genetic Counseling in Parkinson Disease. *Neurology* **2007**, *68*, 1141–1143. [CrossRef] [PubMed]
100. Tong, Y.; Yamaguchi, H.; Giaime, E.; Boyle, S.; Kopan, R.; Kelleher, R.J., 3rd; Shen, J. Loss of Leucine-Rich Repeat Kinase 2 Causes Impairment of Protein Degradation Pathways, Accumulation of Alpha-Synuclein, and Apoptotic Cell Death in Aged Mice. *Proc. Natl. Acad. Sci. USA* **2010**, *107*, 9879–9884. [CrossRef] [PubMed]
101. Li, X.; Patel, J.C.; Wang, J.; Avshalumov, M.V.; Nicholson, C.; Buxbaum, J.D.; Elder, G.A.; Rice, M.E.; Yue, Z. Enhanced Striatal Dopamine Transmission and Motor Performance with LRRK2 Overexpression in Mice Is Eliminated by Familial Parkinson's Disease Mutation G2019S. *J. Neurosci.* **2010**, *30*, 1788–1797. [CrossRef]
102. Moehle, M.S.; Webber, P.J.; Tse, T.; Sukar, N.; Standaert, D.G.; DeSilva, T.M.; Cowell, R.M.; West, A.B. LRRK2 Inhibition Attenuates Microglial Inflammatory Responses. *J. Neurosci.* **2012**, *32*, 1602–1611. [CrossRef]
103. Kim, B.; Yang, M.-S.; Choi, D.; Kim, J.-H.; Kim, H.-S.; Seol, W.; Choi, S.; Jou, I.; Kim, E.-Y.; Joe, E.-H. Impaired Inflammatory Responses in Murine Lrrk2-Knockdown Brain Microglia. *PLoS ONE* **2012**, *7*, e34693. [CrossRef]

104. Dzamko, N.; Inesta-Vaquera, F.; Zhang, J.; Xie, C.; Cai, H.; Arthur, S.; Tan, L.; Choi, H.; Gray, N.; Cohen, P.; et al. The IkappaB Kinase Family Phosphorylates the Parkinson's Disease Kinase LRRK2 at Ser935 and Ser910 during Toll-like Receptor Signaling. *PLoS ONE* **2012**, *7*, e39132. [CrossRef]
105. Kitada, T.; Asakawa, S.; Hattori, N.; Matsumine, H.; Yamamura, Y.; Minoshima, S.; Yokochi, M.; Mizuno, Y.; Shimizu, N. Mutations in the Parkin Gene Cause Autosomal Recessive Juvenile Parkinsonism. *Nature* **1998**, *392*, 605–608. [CrossRef] [PubMed]
106. Pickrell, A.M.; Youle, R.J. The Roles of PINK1, Parkin, and Mitochondrial Fidelity in Parkinson's Disease. *Neuron* **2015**, *85*, 257–273. [CrossRef]
107. Larsen, S.B.; Hanss, Z.; Krüger, R. The Genetic Architecture of Mitochondrial Dysfunction in Parkinson's Disease. *Cell Tissue Res.* **2018**, *373*, 21–37. [CrossRef]
108. Klein, C.; Djarmati, A.; Hedrich, K.; Schäfer, N.; Scaglione, C.; Marchese, R.; Kock, N.; Schüle, B.; Hiller, A.; Lohnau, T.; et al. PINK1, Parkin, and DJ-1 Mutations in Italian Patients with Early-Onset Parkinsonism. *Eur. J. Hum. Genet.* **2005**, *13*, 1086–1093. [CrossRef]
109. Dela Cruz, C.S.; Kang, M.-J. Mitochondrial Dysfunction and Damage Associated Molecular Patterns (DAMPs) in Chronic Inflammatory Diseases. *Mitochondrion* **2018**, *41*, 37–44. [CrossRef] [PubMed]
110. Zhou, R.; Yazdi, A.S.; Menu, P.; Tschopp, J. A Role for Mitochondria in NLRP3 Inflammasome Activation. *Nature* **2011**, *469*, 221–225. [CrossRef] [PubMed]
111. Nakahira, K.; Haspel, J.A.; Rathinam, V.A.K.; Lee, S.-J.; Dolinay, T.; Lam, H.C.; Englert, J.A.; Rabinovitch, M.; Cernadas, M.; Kim, H.P.; et al. Autophagy Proteins Regulate Innate Immune Responses by Inhibiting the Release of Mitochondrial DNA Mediated by the NALP3 Inflammasome. *Nat. Immunol.* **2011**, *12*, 222–230. [CrossRef] [PubMed]
112. Frank-Cannon, T.C.; Tran, T.; Ruhn, K.A.; Martinez, T.N.; Hong, J.; Marvin, M.; Hartley, M.; Treviño, I.; O'Brien, D.E.; Casey, B.; et al. Parkin Deficiency Increases Vulnerability to Inflammation-Related Nigral Degeneration. *J. Neurosci.* **2008**, *28*, 10825–10834. [CrossRef]
113. Zhong, Z.; Umemura, A.; Sanchez-Lopez, E.; Liang, S.; Shalapour, S.; Wong, J.; He, F.; Boassa, D.; Perkins, G.; Ali, S.R.; et al. NF-κB Restricts Inflammasome Activation via Elimination of Damaged Mitochondria. *Cell* **2016**, *164*, 896–910. [CrossRef]
114. Mouton-Liger, F.; Rosazza, T.; Sepulveda-Diaz, J.; Ieang, A.; Hassoun, S.-M.; Claire, E.; Mangone, G.; Brice, A.; Michel, P.P.; Corvol, J.-C.; et al. Parkin Deficiency Modulates NLRP3 Inflammasome Activation by Attenuating an A20-Dependent Negative Feedback Loop. *Glia* **2018**, *66*, 1736–1751. [CrossRef]
115. Tran, T.A.; Nguyen, A.D.; Chang, J.; Goldberg, M.S.; Lee, J.-K.; Tansey, M.G. Lipopolysaccharide and Tumor Necrosis Factor Regulate Parkin Expression via Nuclear Factor-Kappa B. *PLoS ONE* **2011**, *6*, e23660. [CrossRef] [PubMed]
116. Matheoud, D.; Sugiura, A.; Bellemare-Pelletier, A.; Laplante, A.; Rondeau, C.; Chemali, M.; Fazel, A.; Bergeron, J.J.; Trudeau, L.-E.; Burelle, Y.; et al. Parkinson's Disease-Related Proteins PINK1 and Parkin Repress Mitochondrial Antigen Presentation. *Cell* **2016**, *166*, 314–327. [CrossRef] [PubMed]
117. Clements, C.M.; McNally, R.S.; Conti, B.J.; Mak, T.W.; Ting, J.P.-Y. DJ-1, a Cancer- and Parkinson's Disease-Associated Protein, Stabilizes the Antioxidant Transcriptional Master Regulator Nrf2. *Proc. Natl. Acad. Sci. USA* **2006**, *103*, 15091–15096. [CrossRef] [PubMed]
118. Chien, C.-H.; Lee, M.-J.; Liou, H.-C.; Liou, H.-H.; Fu, W.-M. Microglia-Derived Cytokines/chemokines Are Involved in the Enhancement of LPS-Induced Loss of Nigrostriatal Dopaminergic Neurons in DJ-1 Knockout Mice. *PLoS ONE* **2016**, *11*, e0151569. [CrossRef] [PubMed]
119. Kim, J.-H.; Choi, D.-J.; Jeong, H.-K.; Kim, J.; Kim, D.W.; Choi, S.Y.; Park, S.-M.; Suh, Y.H.; Jou, I.; Joe, E.-H. DJ-1 Facilitates the Interaction between STAT1 and Its Phosphatase, SHP-1, in Brain Microglia and Astrocytes: A Novel Anti-Inflammatory Function of DJ-1. *Neurobiol. Dis.* **2013**, *60*, 1–10. [CrossRef]
120. Trudler, D.; Weinreb, O.; Mandel, S.A.; Youdim, M.B.H.; Frenkel, D. DJ-1 Deficiency Triggers Microglia Sensitivity to Dopamine toward a pro-Inflammatory Phenotype That Is Attenuated by Rasagiline. *J. Neurochem.* **2014**, *129*, 434–447. [CrossRef]
121. Nash, Y.; Schmukler, E.; Trudler, D.; Pinkas-Kramarski, R.; Frenkel, D. DJ-1 Deficiency Impairs Autophagy and Reduces Alpha-Synuclein Phagocytosis by Microglia. *J. Neurochem.* **2017**, *143*, 584–594. [CrossRef] [PubMed]
122. Ji, Y.-J.; Wang, H.-L.; Yin, B.-L.; Ren, X.-Y. Down-Regulation of DJ-1 Augments Neuroinflammation via Nrf2/Trx1/NLRP3 Axis in MPTP-Induced Parkinson's Disease Mouse Model. *Neuroscience* **2020**, *442*, 253–263. [CrossRef]
123. Volpato, V.; Webber, C. Addressing Variability in iPSC-Derived Models of Human Disease: Guidelines to Promote Reproducibility. *Dis. Model. Mech.* **2020**, *13*. [CrossRef]
124. Haenseler, W.; Zambon, F.; Lee, H.; Vowles, J.; Rinaldi, F.; Duggal, G.; Houlden, H.; Gwinn, K.; Wray, S.; Luk, K.C.; et al. Excess α-Synuclein Compromises Phagocytosis in iPSC-Derived Macrophages. *Sci. Rep.* **2017**, *7*, 9003. [CrossRef] [PubMed]
125. Trudler, D.; Nazor, K.L.; Eisele, Y.S.; Grabauskas, T.; Dolatabadi, N.; Parker, J.; Sultan, A.; Zhong, Z.; Goodwin, M.S.; Levites, Y.; et al. Soluble α-Synuclein-Antibody Complexes Activate the NLRP3 Inflammasome in hiPSC-Derived Microglia. *Proc. Natl. Acad. Sci. USA* **2021**, *118*. [CrossRef] [PubMed]
126. Lee, H.; Flynn, R.; Sharma, I.; Haberman, E.; Carling, P.J.; Nicholls, F.J.; Stegmann, M.; Vowles, J.; Haenseler, W.; Wade-Martins, R.; et al. LRRK2 Is Recruited to Phagosomes and Co-Recruits RAB8 and RAB10 in Human Pluripotent Stem Cell-Derived Macrophages. *Stem Cell Rep.* **2020**, *14*, 940–955. [CrossRef] [PubMed]

127. Panagiotakopoulou, V.; Ivanyuk, D.; De Cicco, S.; Haq, W.; Arsić, A.; Yu, C.; Messelodi, D.; Oldrati, M.; Schöndorf, D.C.; Perez, M.-J.; et al. Interferon-γ Signaling Synergizes with LRRK2 in Neurons and Microglia Derived from Human Induced Pluripotent Stem Cells. *Nat. Commun.* **2020**, *11*, 5163. [CrossRef]
128. Speidel, A.; Felk, S.; Reinhardt, P.; Sterneckert, J.; Gillardon, F. Leucine-Rich Repeat Kinase 2 Influences Fate Decision of Human Monocytes Differentiated from Induced Pluripotent Stem Cells. *PLoS ONE* **2016**, *11*, e0165949. [CrossRef]
129. Lancaster, M.A.; Renner, M.; Martin, C.-A.; Wenzel, D.; Bicknell, L.S.; Hurles, M.E.; Homfray, T.; Penninger, J.M.; Jackson, A.P.; Knoblich, J.A. Cerebral Organoids Model Human Brain Development and Microcephaly. *Nature* **2013**, *501*, 373–379. [CrossRef]
130. Kadoshima, T.; Sakaguchi, H.; Nakano, T.; Soen, M.; Ando, S.; Eiraku, M.; Sasai, Y. Self-Organization of Axial Polarity, inside-out Layer Pattern, and Species-Specific Progenitor Dynamics in Human ES Cell–derived Neocortex. *Proc. Natl. Acad. Sci. USA* **2013**, *110*, 20284–20289. [CrossRef]
131. Lin, Y.-T.; Seo, J.; Gao, F.; Feldman, H.M.; Wen, H.-L.; Penney, J.; Cam, H.P.; Gjoneska, E.; Raja, W.K.; Cheng, J.; et al. APOE4 Causes Widespread Molecular and Cellular Alterations Associated with Alzheimer's Disease Phenotypes in Human iPSC-Derived Brain Cell Types. *Neuron* **2018**, *98*, 1141–1154.e7. [CrossRef]
132. Pérez, M.J.; Ivanyuk, D.; Panagiotakopoulou, V.; Di Napoli, G.; Kalb, S.; Brunetti, D.; Al-Shaana, R.; Kaeser, S.A.; Fraschka, S.A.-K.; Jucker, M.; et al. Loss of Function of the Mitochondrial Peptidase PITRM1 Induces Proteotoxic Stress and Alzheimer's Disease-like Pathology in Human Cerebral Organoids. *Mol. Psychiatry* **2020**. [CrossRef]
133. Linkous, A.; Balamatsias, D.; Snuderl, M.; Edwards, L.; Miyaguchi, K.; Milner, T.; Reich, B.; Cohen-Gould, L.; Storaska, A.; Nakayama, Y.; et al. Modeling Patient-Derived Glioblastoma with Cerebral Organoids. *Cell Rep.* **2019**, *26*, 3203–3211.e5. [CrossRef]
134. Ogawa, J.; Pao, G.M.; Shokhirev, M.N.; Verma, I.M. Glioblastoma Model Using Human Cerebral Organoids. *Cell Rep.* **2018**, *23*, 1220–1229. [CrossRef]
135. Nickels, S.L.; Modamio, J.; Mendes-Pinheiro, B.; Monzel, A.S.; Betsou, F.; Schwamborn, J.C. Reproducible Generation of Human Midbrain Organoids for in Vitro Modeling of Parkinson's Disease. *Stem Cell Res.* **2020**, *46*, 101870. [CrossRef] [PubMed]
136. Kano, M.; Takanashi, M.; Oyama, G.; Yoritaka, A.; Hatano, T.; Shiba-Fukushima, K.; Nagai, M.; Nishiyama, K.; Hasegawa, K.; Inoshita, T.; et al. Reduced Astrocytic Reactivity in Human Brains and Midbrain Organoids with PRKN Mutations. *NPJ Parkinsons Dis.* **2020**, *6*, 33. [CrossRef] [PubMed]
137. di Domenico, A.; Carola, G.; Calatayud, C.; Pons-Espinal, M.; Muñoz, J.P.; Richaud-Patin, Y.; Fernandez-Carasa, I.; Gut, M.; Faella, A.; Parameswaran, J.; et al. Patient-Specific iPSC-Derived Astrocytes Contribute to Non-Cell-Autonomous Neurodegeneration in Parkinson's Disease. *Stem Cell Rep.* **2019**, *12*, 213–229. [CrossRef]
138. Rõlova, T.; Lehtonen, Š.; Goldsteins, G.; Kettunen, P.; Koistinaho, J. Metabolic and Immune Dysfunction of Glia in Neurodegenerative Disorders: Focus on iPSC Models. *Stem Cells* **2021**, *39*, 256–265. [CrossRef]
139. Brownjohn, P.W.; Smith, J.; Solanki, R.; Lohmann, E.; Houlden, H.; Hardy, J.; Dietmann, S.; Livesey, F.J. Functional Studies of Missense TREM2 Mutations in Human Stem Cell-Derived Microglia. *Stem Cell Rep.* **2018**, *10*, 1294–1307. [CrossRef] [PubMed]
140. Abreu, C.M.; Gama, L.; Krasemann, S.; Chesnut, M.; Odwin-Dacosta, S.; Hogberg, H.T.; Hartung, T.; Pamies, D. Microglia Increase Inflammatory Responses in iPSC-Derived Human BrainSpheres. *Front. Microbiol.* **2018**, *9*, 2766. [CrossRef]
141. Fagerlund, I.; Dougalis, A.; Shakirzyanova, A.; Gómez-Budia, M.; Konttinen, H.; Ohtonen, S.; Feroze, F.; Koskuvi, M.; Kuusisto, J.; Hernández, D.; et al. Microglia Orchestrate Neuronal Activity in Brain Organoids. *bioRxiv* **2020**. [CrossRef]
142. Ormel, P.R.; Vieira de Sá, R.; van Bodegraven, E.J.; Karst, H.; Harschnitz, O.; Sneeboer, M.A.M.; Johansen, L.E.; van Dijk, R.E.; Scheefhals, N.; Berdenis van Berlekom, A.; et al. Microglia Innately Develop within Cerebral Organoids. *Nat. Commun.* **2018**, *9*, 4167. [CrossRef]
143. Hosmane, S.; Tegenge, M.A.; Rajbhandari, L.; Uapinyoying, P.; Ganesh Kumar, N.; Thakor, N.; Venkatesan, A. Toll/interleukin-1 Receptor Domain-Containing Adapter Inducing Interferon-β Mediates Microglial Phagocytosis of Degenerating Axons. *J. Neurosci.* **2012**, *32*, 7745–7757. [CrossRef]
144. Park, J.; Wetzel, I.; Marriott, I.; Dréau, D.; D'Avanzo, C.; Kim, D.Y.; Tanzi, R.E.; Cho, H. A 3D Human Triculture System Modeling Neurodegeneration and Neuroinflammation in Alzheimer's Disease. *Nat. Neurosci.* **2018**, *21*, 941–951. [CrossRef]
145. Pediaditakis, I.; Kodella, K.R.; Manatakis, D.V.; Hinojosa, C.D.; Manolakos, E.S.; Rubin, L.L.; Hamilton, G.A.; Karalis, K. Modeling Alpha-Synuclein Pathology in a Human Brain-Chip to Assess Blood-Brain Barrier Disruption in Parkinson's Disease. *bioRxiv* **2020**. [CrossRef]
146. Ribecco-Lutkiewicz, M.; Sodja, C.; Haukenfrers, J.; Haqqani, A.S.; Ly, D.; Zachar, P.; Baumann, E.; Ball, M.; Huang, J.; Rukhlova, M.; et al. A Novel Human Induced Pluripotent Stem Cell Blood-Brain Barrier Model: Applicability to Study Antibody-Triggered Receptor-Mediated Transcytosis. *Sci. Rep.* **2018**, *8*, 1873. [CrossRef]
147. Bergmann, S.; Lawler, S.E.; Qu, Y.; Fadzen, C.M.; Wolfe, J.M.; Regan, M.S.; Pentelute, B.L.; Agar, N.Y.R.; Cho, C.-F. Blood-Brain-Barrier Organoids for Investigating the Permeability of CNS Therapeutics. *Nat. Protoc.* **2018**, *13*, 2827–2843. [CrossRef]
148. Subramaniam, S.R.; Federoff, H.J. Targeting Microglial Activation States as a Therapeutic Avenue in Parkinson's Disease. *Front. Aging Neurosci.* **2017**, *9*, 176. [CrossRef]
149. Teismann, P.; Ferger, B. Inhibition of the Cyclooxygenase Isoenzymes COX-1 and COX-2 Provide Neuroprotection in the MPTP-Mouse Model of Parkinson's Disease. *Synapse* **2001**, *39*, 167–174. [CrossRef]
150. Chen, H.; Zhang, S.M.; Hernán, M.A.; Schwarzschild, M.A.; Willett, W.C.; Colditz, G.A.; Speizer, F.E.; Ascherio, A. Nonsteroidal Anti-Inflammatory Drugs and the Risk of Parkinson Disease. *Arch. Neurol.* **2003**, *60*, 1059–1064. [CrossRef]

151. Ren, L.; Yi, J.; Yang, J.; Li, P.; Cheng, X.; Mao, P. Nonsteroidal Anti-Inflammatory Drugs Use and Risk of Parkinson Disease: A Dose-Response Meta-Analysis. *Medicine* **2018**, *97*, e12172. [CrossRef] [PubMed]
152. McCoy, M.K.; Ruhn, K.A.; Martinez, T.N.; McAlpine, F.E.; Blesch, A.; Tansey, M.G. Intranigral Lentiviral Delivery of Dominant-Negative TNF Attenuates Neurodegeneration and Behavioral Deficits in Hemiparkinsonian Rats. *Mol. Ther.* **2008**, *16*, 1572–1579. [CrossRef]
153. García, M.C.; Cinquina, V.; Palomo-Garo, C.; Rábano, A.; Fernández-Ruiz, J. Identification of CB_2 Receptors in Human Nigral Neurons That Degenerate in Parkinson's Disease. *Neurosci. Lett.* **2015**, *587*, 1–4. [CrossRef]
154. Javed, H.; Azimullah, S.; Haque, M.E.; Ojha, S.K. Cannabinoid Type 2 (CB2) Receptors Activation Protects against Oxidative Stress and Neuroinflammation Associated Dopaminergic Neurodegeneration in Rotenone Model of Parkinson's Disease. *Front. Neurosci.* **2016**, *10*, 321. [CrossRef]
155. Schwenkgrub, J.; Joniec-Maciejak, I.; Sznejder-Pachołek, A.; Wawer, A.; Ciesielska, A.; Bankiewicz, K.; Członkowska, A.; Członkowski, A. Effect of Human Interleukin-10 on the Expression of Nitric Oxide Synthases in the MPTP-Based Model of Parkinson's Disease. *Pharmacol. Rep.* **2013**, *65*, 44–49. [CrossRef]
156. Wang, J.; Wang, J.; Wang, J.; Yang, B.; Weng, Q.; He, Q. Targeting Microglia and Macrophages: A Potential Treatment Strategy for Multiple Sclerosis. *Front. Pharmacol.* **2019**, *10*, 286. [CrossRef] [PubMed]
157. Churchill, M.J.; Cantu, M.A.; Kasanga, E.A.; Moore, C.; Salvatore, M.F.; Meshul, C.K. Glatiramer Acetate Reverses Motor Dysfunction and the Decrease in Tyrosine Hydroxylase Levels in a Mouse Model of Parkinson's Disease. *Neuroscience* **2019**, *414*, 8–27. [CrossRef] [PubMed]
158. Zella, M.A.S.; Metzdorf, J.; Ostendorf, F.; Maass, F.; Muhlack, S.; Gold, R.; Haghikia, A.; Tönges, L. Novel Immunotherapeutic Approaches to Target Alpha-Synuclein and Related Neuroinflammation in Parkinson's Disease. *Cells* **2019**, *8*, 105. [CrossRef] [PubMed]
159. Games, D.; Valera, E.; Spencer, B.; Rockenstein, E.; Mante, M.; Adame, A.; Patrick, C.; Ubhi, K.; Nuber, S.; Sacayon, P.; et al. Reducing C-Terminal-Truncated Alpha-Synuclein by Immunotherapy Attenuates Neurodegeneration and Propagation in Parkinson's Disease-like Models. *J. Neurosci.* **2014**, *34*, 9441–9454. [CrossRef] [PubMed]
160. Bae, E.-J.; Lee, H.-J.; Rockenstein, E.; Ho, D.-H.; Park, E.-B.; Yang, N.-Y.; Desplats, P.; Masliah, E.; Lee, S.-J. Antibody-Aided Clearance of Extracellular α-Synuclein Prevents Cell-to-Cell Aggregate Transmission. *J. Neurosci.* **2012**, *32*, 13454–13469. [CrossRef]
161. El-Agnaf, O.; Overk, C.; Rockenstein, E.; Mante, M.; Florio, J.; Adame, A.; Vaikath, N.; Majbour, N.; Lee, S.-J.; Kim, C.; et al. Differential Effects of Immunotherapy with Antibodies Targeting α-Synuclein Oligomers and Fibrils in a Transgenic Model of Synucleinopathy. *Neurobiol. Dis.* **2017**, *104*, 85–96. [CrossRef]
162. Shin, J.; Kim, H.-J.; Jeon, B. Immunotherapy Targeting Neurodegenerative Proteinopathies: α-Synucleinopathies and Tauopathies. *J. Mov. Disord.* **2020**, *13*, 11–19. [CrossRef]
163. Alon, S.; Goodwin, D.R.; Sinha, A.; Wassie, A.T.; Chen, F.; Daugharthy, E.R.; Bando, Y.; Kajita, A.; Xue, A.G.; Marrett, K.; et al. Expansion Sequencing: Spatially Precise in Situ Transcriptomics in Intact Biological Systems. *Science* **2021**, *371*. [CrossRef]
164. Vickovic, S.; Eraslan, G.; Salmén, F.; Klughammer, J.; Stenbeck, L.; Schapiro, D.; Äijö, T.; Bonneau, R.; Bergenstråhle, L.; Navarro, J.F.; et al. High-Definition Spatial Transcriptomics for in Situ Tissue Profiling. *Nat. Methods* **2019**, *16*, 987–990. [CrossRef] [PubMed]
165. Chen, W.-T.; Lu, A.; Craessaerts, K.; Pavie, B.; Sala Frigerio, C.; Corthout, N.; Qian, X.; Laláková, J.; Kühnemund, M.; Voytyuk, I.; et al. Spatial Transcriptomics and In Situ Sequencing to Study Alzheimer's Disease. *Cell* **2020**, *182*, 976–991.e19. [CrossRef]
166. Clayton, K.; Delpech, J.C.; Herron, S.; Iwahara, N.; Ericsson, M.; Saito, T.; Saido, T.C.; Ikezu, S.; Ikezu, T. Plaque Associated Microglia Hyper-Secrete Extracellular Vesicles and Accelerate Tau Propagation in a Humanized APP Mouse Model. *Mol. Neurodegener.* **2021**, *16*, 18. [CrossRef] [PubMed]

2 Aims

PD is a complex, multifactorial neurodegenerative disease. The disease onset is influenced by both genetic and environmental factors, making the modeling of PD extremely difficult. Although brain tissues from PD patients can provide insights into the cellular complexity and the involvement of the different cell types to disease pathogenesis, such tissue analyses offer merely a snapshot of the situation during late-stage PD. By contrast, the molecular mechanisms driving the disease progression cannot be studied in such a model. Thus, it was a true scientific breakthrough when Yamanaka and colleagues succeeded to generate iPSCs – patient-derived stem cells that are capable of differentiating into any cell type of interest (Takahashi and Yamanaka, 2006). Soon after, iPSC technology motivated PD and Alzheimer's disease research groups into creating multiple differentiation protocols in order to generate dopaminergic neurons, astrocytes, and macrophages/microglia (Oksanen et al., 2017; Reinhardt et al., 2013; van Wilgenburg et al., 2013).

As previously mentioned, mutations in *LRRK2* are the most common genetic form of PD, and among the pathogenic variants the G2019S substitution is the most abundant (Healy et al., 2008; Paisán-Ruíz et al., 2004; Zimprich et al., 2004). The cellular functions of LRRK2 are still not fully understood, although multiple studies implicate this protein in vesicular trafficking and autophagy lysosomal pathways in neurons. Interestingly, though, LRRK2 is mainly expressed in immune cells, suggesting that it is also crucially involved in the regulation of immune function and response. Several pathogenic forms of LRRK2 exhibit higher kinase activity - the most investigated phenotype in LRRK2-PD studies (Fraser et al., 2016; Greggio et al., 2009; Melachroinou et al., 2020).

With regard to clinical characteristics, LRRK2-PD patients are most similar to IPD cases (Aasly et al., 2005). Interestingly, genome-wide association studies revealed LRRK2 as a risk factor for IPD, while other studies detected upregulated LRRK2 kinase activity in post-mortem brain tissues of IPD patients (Di Maio et al., 2018; Sharma et al., 2012; Simón-Sánchez et al., 2009).

I had the opportunity to attend a training at Oxford University, during which I learned how to generate macrophages with a protocol that involves the formation of embryoid bodies from iPSCs. Applying this protocol to iPSCs from controls and patients, I had the chance to explore the contribution of microglia to neurodegeneration (Haenseler et al., 2017a; van Wilgenburg et al., 2013).
The similarities between IPD and LRRK2-PD compelled us to investigate iPSC-derived microglia from individuals with LRRK2 G2019S alongside cultures from IPD patients and controls, in the hopes of better understanding shared inflammatory phenotypes.

We identified several objectives that needed to be addressed:

- To generate and characterize iPSC-derived microglia cells from LRRK2 G2019S mutation carriers, gene-corrected cells, and healthy controls.
- To generate and characterize iPSC-derived microglia from an IPD patient and a healthy control.
- To investigate inflammatory phenotypes under basal conditions and upon inflammatory stimuli.
- To identify phenotypes and dysregulated pathways shared between IPD and LRRK2-PD iPSC-derived microglia.

3 Results

3.1 Manuscript II

LRRK2 G2019S as a trigger of inflammatory signaling in patient-derived microglia

Katja Badanjak[1], Patrycja Mulica[1], Paul Antony[1], Sylvie Delcambre[1], Semra Smajic[1], Carmen Venegas[1], Philip Seibler[2], Enrico Glaab[1], Anne Grünewald[1,2*]

[1]Luxembourg Centre for Systems Biomedicine, University of Luxembourg, Esch-sur-Alzette, Luxembourg
[2]Institute of Neurogenetics, University of Lübeck, Lübeck, Germany
[*]Corresponding author

This study is in preparation to be submitted to *Stem Cell Reports*.

3.1.1 Preface

Mutations in the *LRRK2* gene are causative of genetic PD, while variations in the same gene are a risk factor for IPD. The G2019S mutation, which is located in the kinase domain of the protein, is causing a pathogenic overactivation of LRRK2 kinase activity. There is evidence that inhibition of the kinase function is beneficial, and might directly influence the pathogenesis of the disease. Furthermore, the G2019S mutation is not fully penetrant. The penetrance varies between different ethnicities, increases with age, and is influenced by the collective impact of common variants in PD-linked genes (Healy et al., 2008; Iwaki et al., 2020; Latourelle et al., 2008; Lee et al., 2017; Marder et al., 2015; Squillaro et al., 2007). Moreover, at the cellular level, LRRK2 is highly expressed in immune cells and regulated by different stimuli (Ahmadi Rastegar and Dzamko, 2020; Dzamko et al., 2012; Fan et al., 2021; Lee et al., 2020; Panagiotakopoulou et al., 2020). Until now, the impact of LRRK2 G2019S on microglial innate immunity and function are not well studied.

To investigate the molecular mechanisms that may define the penetrance of LRRK2 G2019S and to identify phenotypes that distinguish cells from non-manifesting and manifesting mutation carriers, we generated iPSC-derived microglia cells from a healthy individual, an isogenic control, one non-manifesting and two manifesting LRRK2 G2019S mutation carriers. We treated the cells with IFN-γ, which was previously shown to induce *LRRK2* transcription. Furthermore, upon IFN-γ treatment, we inhibited kinase activity with MLi-2. Western blotting was used to determine the phosphorylation levels of LRRK2 and of endogenous substrates of LRRK2 kinase activity. In addition, we compared the transcriptomic profiles between different genotypes and treatment conditions. In this fashion, we identified gene targets and pathways that are genotype or disease-specific.

My contribution to this study was the maintenance and generation of iPSC- derived microglia cells and subsequent treatments, RNA and protein extraction, immunocytochemistry, and Western blotting. Furthermore, I also contributed to the analysis of the generated data. Finally, I contributed to the writing of the manuscript and have prepared (supplementary) figures, and supplementary tables.

LRRK2 G2019S as a trigger of inflammatory signaling in patient-derived microglia

Katja Badanjak[1], Patrycja Mulica[1], Paul Antony[1], Sylvie Delcambre[1], Semra Smajic[1], Carmen Venegas[1], Philip Seibler[2], Enrico Glaab[1], Anne Grünewald[1,2*]

[1]Luxembourg Centre for Systems Biomedicine, University of Luxembourg, Esch-sur-Alzette, Luxembourg
[2]Institute of Neurogenetics, University of Lübeck, Lübeck, Germany

[*]Corresponding author
Anne Grünewald, PhD
anne.gruenewald@uni.lu

Keywords: microglia, LRRK2, kinase activity, iPSC, RNA sequencing, neuroinflammation

Abstract

Mutations in *Leucine-rich repeat kinase 2* (*LRRK2*) are the most common genetic cause of Parkinson's disease (PD). The mutation with the highest prevalence in *LRRK2* is G2019S, while other variants in this gene have been identified as risk factors for idiopathic PD. The penetrance of LRRK2 G2019S is incomplete and possibly regulated by genetic modifiers and environmental factors. Moreover, elevated LRRK2 kinase activity has been a prime therapeutic target in LRRK2-linked and idiopathic PD. In the current study, we differentiated iPSC-derived microglia from a healthy individual, an isogenic control, as well as manifesting and non-manifesting LRRK2 G2019S mutation carriers. The resulting microglial models were treated with interferon gamma (IFN-γ) and subsequently with the LRRK2 kinase inhibitor MLi-2. We show that upon IFN-γ exposure, S1292 phosphorylation in LRRK2 - a readout of pathogenic kinase activity - was upregulated in a G2019S-specific manner and downregulated after MLi-2 treatment. By contrast, α-synuclein upregulation occurred exclusively in manifesting G2019S LRRK2 microglia and did not respond to MLi-2. Interestingly, RNA sequencing (RNAseq) revealed that elevated LRRK2 kinase activity and increased α-synuclein abundance disrupt Notch signaling in a PD-specific manner in LRRK2 G2019S-mutant microglia. Together, our study further implicates LRRK2 in the propagation of inflammation in PD, suggesting a role for microglia in the penetrance of the G2019S mutation.

Introduction

Parkinson's disease (PD) is a neurodegenerative disorder resulting in the demise of dopaminergic neurons. It is defined by the symptom triad tremor, rigidity and bradykinesia and other non-motor symptoms such as depression and hyposmia (Kouli et al., 2019). PD mutations in the *Leucine-rich repeat kinase 2* (*LRRK2*) gene are inherited in an autosomal dominant manner, while variants in the same gene account for 1-2% of all sporadic PD cases. The G2019S mutation in *LRRK2* is the most common cause of genetic PD and is responsible for around 5% of all familial cases (Berwick et al., 2019; Marras et al., 2011; Ren et al., 2019). Furthermore, the penetrance of this mutation is incomplete, being influenced by age, environmental and multiple inherited susceptibility factors (Latourelle et al., 2008). LRRK2-PD is clinically similar to idiopathic PD (IPD), suggestive of shared pathogenic features (Chittoor-Vinod et al., 2021; Marras et al., 2011).
LRRK2 is a large, multi-domain protein consisting of an enzymatic core, formed by a remarkable variety of enzymatic domains such as ROC/GTPase, COR (C-terminus of ROC) and serine threonine kinase domains. It has multiple interaction and binding sites such as ankyrin and leucine-rich repeat motifs, and WD40 repeats (Russo et al., 2014). This highly sophisticated and complex protein structure makes LRRK2 an important component of multiple cellular pathways, although its exact biological function currently remains elusive. The G2019S mutation is located in the kinase domain of the protein, causing a pathogenic overactivation. Frequently studied physiological substrates of LRRK2 kinase activity are Rab GTPases, regulators of vesicular trafficking, most notably Rab5, Rab8, Rab12, Rab10, and Rab29 (Lee et al., 2020; Seol et al., 2019). An evolutionary conserved phospho-site T73 on Rab10 was found to be upregulated in G2019S models of LRRK2-PD. This over-phosphorylation leads to disturbed homeostasis between membrane-bound and cytosolic Rab10 (Steger et al., 2016). Upregulation of Rab phosphorylation is considered a marker of the disease phenotype in different PD models (Jeong et al., 2018; Lara Ordóñez et al., 2021; Madero-Pérez et al., 2017; Nirujogi et al., 2021; Wang et al., 2021). Furthermore, LRRK2 is mainly regulated by other kinases and can also be phosphorylated under basal conditions. It has 74 phosphorylation sites. However, half of these are still awaiting to be confirmed (Marchand et al., 2020). The heterologous phosphorylation site at S935 has emerged as an important contributor to the physiological function of LRRK2. Similarly, phosphorylation at S1292 was described as a direct and physiological marker of overactive LRRK2 kinase activity and is an established phenotype of the G2019S mutant protein (Kluss et al., 2018). Modulating overactive kinase

activity with kinase inhibitors has become a therapeutic target in LRRK2-PD research, and one of the prime candidates for clinical trials. MLi-2 is a novel, highly potent and selective inhibitor of LRRK2 kinase activity (Scott et al., 2017). Its protective effect was demonstrated by reduced neurodegeneration upon MPTP treatment and downregulation of S935 LRRK2 in G2019S mice models (Fell et al., 2015; Kluss et al., 2021; Novello et al., 2022).
Neuroinflammation is a prominent feature of PD. Multiple studies found higher levels of proinflammatory cytokines and chemokines in cerebrospinal fluid and serum of PD patients when compared to healthy individuals (Borsche et al., 2020; Dobbs et al., 1999; Mount et al., 2007; Scalzo et al., 2009; Sliter et al., 2018). Interestingly, LRRK2 has been associated with susceptibility to bacterial infections, Crohn's disease, and leprosy, all of which are characterized by highly inflammatory phenotypes (Barrett et al., 2008; Umeno et al., 2011; Weindel et al., 2019; Zhang et al., 2009). In addition, *LRRK2* expression is elevated in immune cells, suggesting its involvement in the innate immune response (Gardet et al., 2010; Gillardon et al., 2012; Hakimi et al., 2011; Thévenet et al., 2011). Corroborating this, many studies showed that LRRK2 expression can be upregulated by interferon gamma (IFN-γ), a proinflammatory cytokine involved in the pathogenesis of PD (Gardet et al., 2010; Kuss et al., 2014; Lee et al., 2020; Mount et al., 2007; Panagiotakopoulou et al., 2020; Thévenet et al., 2011). So far, LRRK2 studies have been mostly conducted in models focusing on neuronal demise. To shed more light on glial involvement in LRRK2-PD, in this study, we employed iPSC technology to generate microglia from (isogenic) controls, manifesting and non-manifesting G2019S mutation carriers. Making use of these unique cellular models, we investigated the role of LRRK2 kinase activity in PD pathogenesis and microglia activation. Furthermore, we explored the effect of IFN-γ and MLi-2 on the phosphorylation of LRRK2 and Rab10. Lastly, we performed RNAseq in order to identify disease-relevant cellular pathways.

Results

Characterization of iPSC-derived microglia

Induced pluripotent stem cells (iPSCs) used in this study were successfully characterized by assessing the expression of the pluripotency markers Nanog, Sox-2, and Oct-4 (Figure S1). We generated microglia cells from iPSCs as previously described (van Wilgenburg et al., 2013). To ascertain their microglial identity, we stained for Iba1, an established microglial marker. The comparable abundance of Iba1 per CellMask suggested no influence of the genotype on the terminal differentiation potential (Figure S2). Furthermore, we determined whether differentiated cells had the capacity to phagocyte Zymosan particles. This analysis did not reveal any impairments in G2019S-mutant microglia when compared to (isogenic) control cells (Figure S2).

Analysis of LRRK2 kinase activity

Previous studies identified kinase activity upregulation as a characteristic feature of LRRK2-PD models. LRRK2 kinase activity can be examined by analyzing phosphorylation levels of the protein at serine 935 (S935) and serine 1292 (S1292), and phosphorylation of Rab10 on threonine 73 (T73). We sought to investigate these phospho-sites in our cells under baseline conditions. LRRK2 G2019S carriers showed a downregulation of S935 phosphorylation in LRRK2, independent of the disease status (Figure 1A). By contrast, we did not detect differences in LRRK2 phosphorylation at S1292 (Figure 1B). No difference was observed in the phosphorylation levels of Rab10 (Figure 1C). Moreover, under basal conditions, we neither detected any differences in total LRRK2 protein across all microglia cell lines, nor did we observe changes in total Rab10 protein levels (Figure 1D).

Inflammation induces S1292 LRRK2 phosphorylation in G2019S mutants

A number of studies found inflammatory stimuli capable of inducing LRRK2 expression and kinase activity (Gardet et al., 2010; Lee et al., 2020; Mount et al., 2007; Panagiotakopoulou et al., 2020). One such pro-inflammatory cytokine, IFN-γ, was shown to directly influence the expression of LRRK2, supporting the role of LRRK2 in the regulation of inflammatory responses. Furthermore, MLi-2 was identified as an efficient inhibitor of LRRK2 kinase activity. Based on previous studies, we decided to expose the microglia models to IFN-γ for 72h, followed

by MLi-2 treatment for 2h (Figure 2A). We observed a significantly higher protein abundance of LRRK2 in all microglia cells upon IFN-γ stimulation. MLi-2 treatment had no effect on the abundance of total LRRK2 protein (Figure 2B, C). Conversely, only G2019S carriers displayed significantly elevated phosphorylation levels at S1292-LRRK2 upon IFN-γ treatment, when compared to both, the healthy control and the gene-corrected microglia, and these levels were successfully downregulated by kinase inhibition (Figure 2B, D). While pRab10 levels were significantly upregulated in all IFN-γ-treated cells in comparison to their untreated counterparts, no difference between genotypes was detected. The upregulation of pRab10 levels was diminished upon MLi-2 treatment (Figure 2B, D). Interestingly, S935-LRRK2 levels behaved in a similar manner to pRab10 upon all treatments (data not shown).

IFN-γ can recapitulate S1292-LRRK2 phenotype in IPD microglia

Studies in human post-mortem IPD tissues revealed an upregulation of LRRK2 kinase activity in neurons and microglia compared to control tissues (Di Maio et al., 2018). To recapitulate this finding *in vitro*, we treated iPSC-derived IPD microglia with IFN-γ, followed by inhibition of LRRK2 kinase activity with MLi-2. Despite the limitation of a small sample size, we observed a significant upregulation of phospho-S1292-LRRK2 in IPD microglia under inflammatory conditions when compared to healthy microglia (Figure S3). Furthermore, phospho-S1292-LRRK2 levels were successfully downregulated with MLi-2. In addition, total LRRK2 protein levels were significantly lower in IPD microglia, when compared to control cells, irrespective of the treatment. Moreover, total Rab10 protein levels were significantly reduced at baseline in IPD microglia in comparison to control cells (Figure S3).

Endogenous α-synuclein as a marker of disease manifestation

α-synuclein aggregates and Lewy body inclusions (LBs) in neurons are the primary neuropathological features of PD (Spillantini et al., 1997; Steiner et al., 2018). Although the molecular mechanisms underlying the aggregation are not fully understood, it has been postulated that α-synuclein spreading drives PD pathology (Braak et al., 2003). Interestingly, LRRK2 has been shown to modulate the propagation of α-synuclein in a kinase-dependent manner (Bae et al.,

2018). Thus, we wanted to investigate the impact of LRRK2 kinase overactivation on α-synuclein in our glial models under baseline and inflammatory conditions. To determine the abundance of α-synuclein, we performed immunocytochemistry experiments (Figure 3A). Under inflammatory conditions, manifesting G2019S microglia had significantly higher levels of nuclear α-synuclein when compared to both non-manifesting and gene-corrected cells. Furthermore, this phenotype was maintained upon addition of the kinase inhibitor (Figure 3B). Although non-significant, we observed a tendency for the upregulation of cytoplasmic α-synuclein, similar to what was seen in the nuclei. Moreover, total cellular α-synuclein levels (measured as a sum of nuclear and cytoplasmic α-synuclein) were significantly upregulated in manifesting G2019S LRRK2 microglia, when compared to gene-corrected cells and non-manifesting G2019S carrier microglia (Figure 3B). To test whether this increase is due to elevated *SNCA* gene expression, we made use of our RNAseq dataset. Indeed, *SNCA* mRNA levels were significantly higher in the manifesting G2019S microglia when compared to non-manifesting cells. This phenotype was maintained upon inflammatory treatment and was not changed upon kinase inhibition (Figure 3C). Furthermore, *SNCA* was not differentially expressed in IPD iPSC-derived microglia compared to control cells, under all conditions (data not shown).

Transcriptomic analysis reveals microglial activation in LRRK2 PD microglia after IFN treatment

We recently applied single-cell RNAseq to post-mortem midbrain tissues from IPD patients and controls (Smajić et al., 2021). This analysis revealed 29 differentially expressed genes along the activation trajectory of IPD microglia (Smajić et al., 2021). In order to understand if iPSC-derived LRRK2-mutant microglia are indeed activated, we assessed the expression of selected marker genes defining the trajectory in IPD. We focused on *GPNMB*, *DPYD* and *GRAMD4*, as these genes were also shown to be upregulated in other neurodegenerative diseases with glial involvement (Castillo et al., 2017; Srinivasan et al., 2020). Under basal conditions, both G2019S carriers expressed higher levels of *GPNMB*, but under IFN-γ treatment, only the manifesting G2019S microglia presented an upregulation, when compared to healthy, gene-corrected, and non-manifesting G2019S microglia cells. Moreover, kinase inhibition did not change the levels of *GPNMB* achieved under kinase-activating conditions (Figure 4A). In line with this finding, upon IFN-γ exposure, also the expression levels of *DPYD* and *GRAMD4* were most elevated in the microglia from the manifesting LRRK2 G2019S carriers (Figure 4B, C).

Pathway analysis highlights altered Notch signaling in LRRK2 PD microglia

To further assess the transcriptomic landscape of LRRK2 G2019S and (isogenic) control microglia cells under baseline, IFN-γ- and MLi-2-treated conditions, we analyzed our RNAseq dataset in more detail. Based on the top 1000 differentially expressed genes across all conditions, microglia clustered primarily by treatment condition. However, contrary to our results from the LRRK2 phosphorylation analyses, exposure to MLi-2 did not show a rescue effect on gene expression when compared to IFN-γ-treated cells (Figure 5A).

Guided by this result and the observation that our LRRK2 phosphorylation-related analyses revealed differences only upon a proinflammatory stimulus, we next focused on transcriptional alterations in IFN-γ-treated microglia. We compared cells by (i) genotype, to identify genes and pathways driven solely by the presence of the G2019S mutation (microglia from all LRRK2 G2019S mutation carriers vs [isogenic] controls), and by (ii) disease status, to identify genes and pathways involved in the manifestation of LRRK2-PD (microglia from affected vs unaffected LRRK2 G2019S mutation carriers). Among the 50 most differentially expressed genes between LRRK2 G2019S manifesting microglia and healthy or gene-corrected control microglia, *LRRC25* and *CADM1* were identified as interesting targets. LRRC25 can regulate the IFN-γ response, while *CADM1* was found upregulated along the activation trajectory in post-mortem IPD microglia (Du et al., 2018; Smajić et al., 2021). Both genes were significantly upregulated in manifesting LRRK2 G2019S microglia compared to both healthy and gene-corrected cells under inflammatory but also basal conditions (Figure 5B, C). Moreover, in the 50 most differentially expressed genes of the second comparison, we could identify genes possibly involved in the manifestation of LRRK2-PD (Figure 5B, D). For example, under IFN-γ treatment, *IRAK4* and *SH3PXD2B* were significantly downregulated in non-manifesting when compared to manifesting LRRK2 G2019S microglia (Figure 5D). Of note, IRAK4 is crucially involved in TLR-mediated innate immune response, and *SH3PXD2B* was also identified as one of the IPD-specific genes in the microglia activation trajectory (Lin et al., 2010; Smajić et al., 2021).

Finally, in order to identify pathways that are dysregulated in our dataset when considering the aforementioned comparisons, we performed pathway enrichment analysis. Among the top 20 pathways, the majority was driven by the presence of the G2019S mutation, while only a few were primarily linked to disease manifestation (Figure 6A; Figure S4). Interestingly, the comparison by genotype identified Notch signaling and the comparison by PD status highlighted ER stress

as the most significantly dysregulated pathways, respectively (Figure 6). Furthermore, the histone demethylase PHF8 can both regulate Notch signaling and is a target of the same pathway (Iacobucci et al., 2021). Analyzing our RNAseq dataset, the expression of *PHF8* was significantly downregulated in both G2019S carriers, compared to (isogenic) control cells. We additionally validated these expressions by performing a qPCR experiment (Figure S5).

Discussion

Microglia, the resident macrophages of the brain, are involved in the maintenance of CNS homeostasis, and in a multitude of defense mechanisms. Since LRRK2 has also been associated with diseases characterized by inflammation, and is mainly expressed in immune cells, our study's aim was to further elucidate inflammatory mechanisms in LRRK2-PD microglia. To achieve this, we generated and functionally characterized iPSC-derived microglia from a healthy individual, an isogenic control, a non-manifesting LRRK2 G2019S carrier, and two LRRK2 G2019S PD patients under baseline and IFN-γ-treated conditions.

While LRRK2 is both a GTPase and a kinase, increased kinase activity in G2019S models has led LRRK2-PD research to focus on the latter property. Robust readouts of the kinase activity are phosphorylation of Rab GTPases, and phosphorylation of LRRK2 itself (Berwick et al., 2019). Although at baseline, we did not observe differences in pRab10 or phospho-S1292-LRRK2 levels, we reported reduced phosphorylation at S935-LRRK2. S935 phosphorylation levels are considered a robust readout, when testing the efficiency of kinase inhibitors (Dzamko et al., 2010; Vancraenenbroeck et al., 2014). In addition, S935 phosphorylation is crucial for LRRK2 function as it enables the binding of 14-3-3 proteins and thereby induces the translocation of LRRK2 (Lavalley et al., 2016; Manschwetus et al., 2020; Nichols et al., 2010). While previous studies reported a reduction in phospho-S935-LRRK2 levels in N1437H, R1441C/G/H, Y1699C, and I2020T LRRK2-mutant models, we observed the same behavior in G2019S iPSC-derived microglia (Doggett et al., 2012; Padmanabhan et al., 2020).

Emerging evidence implicates inflammatory signaling in the pathogenesis of PD as a consequence but also as an initiator of neurodegeneration (Barcia et al., 2011). A self-perpetuating loop of cytokine release and microglial activation has been proposed as one of the mechanisms affecting the demise of neurons (Mogi et al.,

1994; Mount et al., 2007; Nagatsu et al., 2000). Exemplarily, exposure to the cytokine IFN-γ was shown to upregulate *LRRK2* mRNA levels and to modulate its kinase activity (Gardet et al., 2010; Kuss et al., 2014; Lee et al., 2020; Panagiotakopoulou et al., 2020). Upon stimulation with IFN-γ, we indeed observed an upregulation of LRRK2, both on mRNA and protein level. Moreover, the autophosphorylation at S1292 was suggested to correlate with LRRK2 kinase activity, both *in vitro* and *in vivo* (Kluss et al., 2018; Sheng et al., 2012). To date, however, detection of this phospho-site has only been possible in murine LRRK2 overexpression models, and in exosomes of LRRK2-PD patients (Fraser et al., 2016; Kluss et al., 2018; Sheng et al., 2012). Our study is the first to show a G2019S-specific upregulation of phospho-S1292 LRRK2 in iPSC-derived LRRK2-PD microglia. By contrast, we observed an overall increase in the phosphorylation of Rab10 upon treatment but no differences between (isogenic) control and manifesting or non-manifesting G2019S-mutant microglia. This finding is in accordance with a recent study investigating phospho-Rab10 levels in human peripheral blood neutrophils, where G2019S individuals showed no differences compared to healthy controls and IPD cases (Fan et al., 2021). In addition, we found that both the phosphorylation at S1292-LRRK2 and of Rab10 could be reduced by exposure to MLi-2. By contrast, total LRRK2 protein levels were not affected by MLi-2-induced kinase inhibition. Together, this suggests that an inflammatory stimulus can affect LRRK2 kinase activity in a mutation-specific manner, as evidenced by the upregulation of phospho-S1292 LRRK2 in both G2019S carriers. Moreover, this pathogenic "gain-of-kinase-activity" can be downregulated by MLi-2, demonstrating the potency of this inhibitor in iPSC-derived microglia cells.

Since S1292-LRRK2 was found upregulated in IPD microglia in post-mortem tissues, we decided to investigate if we can model these findings *in vitro* (Di Maio et al., 2018). Our results confirm that IFN-γ can recapitulate kinase activity in IPD microglia, as seen in LRRK2 G2019S microglia. Furthermore, we found no difference in pRab10 levels in IFN-γ-treated IPD microglia, which is corroborated by a study investigating IPD peripheral blood neutrophils and brain tissue, where pRab10 was also not changed (Fan et al., 2021). Interestingly, IPD microglia had lower LRRK2 levels compared to control microglia under all conditions, a phenotype already observed in LPS-stimulated iPSC-derived IPD microglia, and in IPD brain tissue (Badanjak et al., 2021; Simunovic et al., 2009). Taken together, these results indicate that IFN-γ plays a significant role in phospho-S1292-LRRK2 upregulation in IPD and LRRK2-PD iPSC-derived microglia.

Alpha-synuclein is a highly conserved protein, predominantly found in the presynaptic nerve terminal, and its aggregation is one of the hallmarks of PD neuropathology in the form of Lewy bodies (Emamzadeh, 2016; George, 2002). Animal models showed higher aggregation of neuronal α-synuclein when the LRRK2 G2019S mutation is introduced, and this aggregation could be regulated by modulating LRRK2 kinase activity (Longo et al., 2017; Volpicelli-Daley et al., 2016a; Ysselstein et al., 2019). Although predominantly studied in neurons, α-synuclein has an important role in other cells of the CNS and periphery. Mentions of its function beyond neurons and CNS are relatively sparse but important: α-synuclein was shown to be expressed in immune cells, and to be involved in the regulation of hematopoiesis, phagocytic ability, and cytokine release (Austin et al., 2006; Bido et al., 2021; Gardai et al., 2013; Shin et al., 2000; Xiao et al., 2014). In our study, we report elevated protein levels of α-synuclein in manifesting LRRK2 G2019S microglia upon IFN-γ treatment. This suggests that inflammatory cytokines can modulate total protein levels, thereby potentially influencing the penetrance of the G2019S mutation. Furthermore, several studies revealed that neuronal α-synuclein is taken up by microglia (Choi et al., 2020; Maekawa et al., 2016; Scheiblich et al., 2021). By contrast, to our knowledge, here we show for the first time that the endogenous α-synuclein mRNA and protein levels are upregulated in microglia derived from PD patients with LRRK2 G2019S. Thus, our work highlights α-synuclein as a glial marker of LRRK2 G2019S manifestation. Of note, while there is evidence for impaired lysosomal degradation of α-synuclein in LRRK2-PD neurons, we did not explore additional cellular mechanisms underlying the observed synuclein phenotypes in iPSC-derived microglia beyond RNAseq (Bieri et al., 2019; Obergasteiger et al., 2020; Volpicelli-Daley et al., 2016b).

Inspired by our single-cell RNAseq study in post-mortem midbrain tissue (Smajić et al., 2021), we explored the expression of genes, which marked the activation trajectory of IPD microglia, in our iPSC-derived cultures. In this fashion, we aimed to elucidate possible shared phenotypes, which could contribute to microglia activation in LRRK2-PD. We showed an upregulation of *GPNMB* in LRRK2-PD microglia and of *DPYD* and *GRAMD4* in manifesting and non-manifesting LRRK2 G2019S carriers. GPNMB was recently linked to neurodegeneration with high expression in activated microglia (Saade et al., 2021). Furthermore, GPNMB has been studied in the context of AD. In a transgenic AD mouse model and brain tissue form sporadic AD patients, GPNMB was overabundant in a subset of activated microglia (Hüttenrauch et al., 2018). Demonstrating common inflammatory mechanisms across different neurodegenerative

disorders, also *DPYD* and *GRAMD4* were previously shown to be upregulated in AD microglia (Castillo et al., 2017; Srinivasan et al., 2020).
In addition, we report on the main genes and pathways differentially regulated under IFN-γ treatment in LRRK2 manifesting microglia compared to healthy and gene-corrected microglia, and compared to non-manifesting G2019S-mutant microglia. In the first comparison, we identified *LRRC25* and *CADM1*. Interestingly, *LRRC25* was shown to regulate the immune response to IFN-γ through the autophagy pathway (Tian et al., 2019). CADM1 functions as a cell adhesion molecule, shown to interact with natural killer and CD8+ cells to induce cytotoxicity (Boles et al., 2005). Thus, the overexpression of both aforementioned genes highlights the role of inflammatory propagation in LRRK2-PD microglia. Furthermore, in the second comparison, we identified a downregulation of *IRAK4* and *SH3PXD2B* in non-manifesting G2019S LRRK2 microglia compared to the manifesting G2019S cells. IRAK4 was previously described as a master initiator of the immune response, and its pharmaceutical inhibition has been a promising target in pre-clinical trials for PD and inflammatory bowel disease (Lopes, 2018) and *SH3PXD2B* codes for Tks4 – a protein involved in ROS production and the regulation of the actin cytoskeleton (Gianni et al., 2011; Lányi et al., 2011). Overall, these findings indicate inflammatory and oxidative signaling genes as potential disease biomarkers and therapeutic targets in LRRK2-associated PD.
Lastly, we performed enrichment analysis to investigate, which pathways are dysregulated in IFN-γ-treated human microglia due to (i) the presence of the G2019S mutation or (ii) the disease status. We identified the Notch pathway as being the most enriched in the first comparison. Notch signaling is an evolutionary conserved pathway, responsible for cell-cell communication, ultimately influencing cell fate and proliferation, differentiation, and cell death. It was reported that both LRRK2 and α-synuclein regulate this pathway in neuronal models, while in microglia the downregulation of Notch induces pro-inflammatory activation (Crews et al., 2008; Grandbarbe et al., 2007; Imai et al., 2015). Additionally, Notch signaling was reported to be a therapeutic target for restabilization of microtubules, a defective cellular phenotype previously observed in LRRK2-PD models (Bonini et al., 2013; Leschziner and Reck-Peterson, 2021; Panagiotakopoulou et al., 2020; Parisiadou and Cai, 2010). Moreover, we showed the downregulation of *PHF8* in the Notch pathway. A recent study found this gene implicated in the fine-tuned regulation of the IFN-γ response, while its downregulation was prompting enhanced transcription of IFN-γ stimulated genes (Asensio-Juan et al., 2017). These findings further implicate Notch signaling in the regulation of inflammatory pathways in LRRK2 G2019S-mutant microglia.

In our study, we elucidated functional phenotypes in microglia derived from manifesting and non-manifesting LRRK2 G2019S carriers as well as (isogenic) controls. While, to our knowledge, this is the first investigation of LRRK2-PD penetrance mechanisms in endogenous glial models, our work has limitations. Firstly, due to high cell culture costs, all observations were made in a small sample. Future studies will need to include more microglial cultures derived from multiple patients in order to confirm our observations. Secondly, while MLi-2 had an impact on LRRK2 autophosphorylation, we did not observe a rescue effect upon LRRK2 kinase inhibition with regard to α-synuclein abundance and inflammatory signaling. This may mean that the latter phenotypes occur independently of LRRK2 kinase overactivation in patient microglia. However, we cannot rule out at this stage that longer incubation times with MLi-2 would eventually lead to diminished α-synuclein levels and altered gene expression profiles in LRRK2 G2019S microglia.

Taken together, our study highlights possible mechanisms involved in the manifestation of LRRK2-PD. Based on our findings; it is conceivable that increased LRRK2 kinase activity in G2019S-mutant microglia causes an upregulation of α-synuclein, which in turn induces Notch-mediated pro-inflammatory signaling. The disease specificity of the α-synuclein phenotype further strengthens the notion that genetic and environmental factors can modulate the cellular consequences of LRRK2 kinase overactivation. Finally, while there are several reports in the literature demonstrating that microglia can engulf α-synuclein released from neurons, we provided further evidence that PD gene mutations suffice to trigger an upregulation of the intrinsic mRNA and protein levels of α-synuclein in pure microglial cultures (Haenseler et al., 2017). Additional functional studies to elucidate the proposed LRRK2 - α-synuclein - Notch axis in more detail are warranted. This research will pave the way for penetrance-modifying anti-inflammatory treatment strategies for carriers of LRRK2 mutations.

Materials and methods

Differentiation of human iPSCs into microglia cells

Individuals who donated skin biopsies for this study (two manifesting G2019S carriers, one non-manifesting G2019S carrier, as well as a healthy control) gave written and informed consent. Skin fibroblasts were reprogrammed into iPSCs as previously described (Table S1.) (Lee et al., 2020). iPSCs were cultured in mTeSR^{TM}1 complete medium (StemCell Technologies). Microglia cells were differentiated from iPSCs following an established protocol (van Wilgenburg et al., 2013)(Badanjak et al., 2021). For full medium compositions, please refer to Table S2. The study was approved by the Comité National d'Ethique de Recherche Luxembourg (CNER, vote 201411/05).

Microglia treatments

Harvested macrophage precursors were seeded into 6-well plates at a density of $1x10^6$ cells/well. After treatment with 100 ng/ml IFN-γ (PHC4031, ThermoFisher Scientific) for 72 hours, cells were treated with MLi-2 kinase inhibitor (5756/10, R&D Systems Europe Ltd) for 2h at a concentration of 200nM. Next, cells were subjected to either protein or RNA extraction.

To assess phagocytic ability, macrophage precursors were seeded into 96-well glass-bottom plates at a density of 25 000 cells/well. Cells underwent the aforementioned treatments, and finally, 50 000 Zymosan bioparticles (ThermoFisher Scientific) were added per well for 45 minutes. Then, cells were subjected to fixation and immunocytochemistry stainings.

RNA isolation and quantitative PCR

RNA extraction was performed following the manufacturer's instructions for direct RNA extraction from the plate using the RNeasy RNA isolation kit (Qiagen, 74106). 200ng of RNA was used to synthesize cDNA with the SuperScriptTM III Reverse Transcriptase (Invitrogen, 18080044).

Quantitative PCR (qPCR) was performed using iQ SYBR Green (Biorad, 170-8885). The expression of *PHF8* was normalized to the house-keeping genes *ACTB* and *L27*. The PCR reaction was run on a LightCycler 480.

RNAseq and data analysis

Library preparation and sequencing were performed at BGI in Copenhagen, Denmark on the BGISeq-500 platform.

The raw RNAseq reads were first quality-filtered, which included removing adaptor sequences, contamination and low-quality reads, checking the base percentage distribution and distribution of quality scores along the reads. The sequence data was then pre-processed using the software package Rsubread (Liao et al., 2019). Gene-level differential expression analysis was conducted in the R statistical programming software (Team and Others, 2018) using the software package DESeq2 (Love et al., 2014) and filtering out genes with low expression counts using the filterByExpr-function with default parameters from the package edgeR (Robinson et al., 2010). P-value significance scores for differential expression were computed using the Wald test, and were adjusted for multiple hypothesis testing according to the Benjamini and Hochberg method (Benjamini and Hochberg, 1995).
Pathway enrichment analyses were implemented in the GeneGo MetaCore™ software (https://portal.genego.com) using the gene-level differential expression analysis results obtained with DESeq2 as input for the standard enrichment analysis workflow. The pathway over-representation analysis statistics, including false-discovery rate (FDR) scores according to the method by Benjamini and Hochberg, were determined for the GeneGo collections of cellular pathway maps, process networks and Gene Ontology gene set terms.

Western blotting

Total protein from microglia cultures was extracted directly from the plate, using ice cold RIPA buffer (Pierce) supplemented with 1X Protease/phosphatase Inhibitor Cocktail (ThermoScientific). The whole well was washed multiple times, on ice, and the lysate suspension was transferred to an Eppendorf tube and vortexed for 20 seconds followed by incubation on ice for 20 minutes. The samples were centrifuged at 21130 g for 20 minutes at 4°C. The protein concentration was measured using the Pierce™ BCA protein kit (ThermoFisher Scientific) following the manufacturer's instructions.
Cell lysates were denatured in a loading buffer at 70°C for 10 minutes. Proteins were then separated on NuPAGE 4%–12% Bis-Tris gels (Invitrogen) in NuPAGE MES Running Buffer (NP0002) and transferred on a 0.2 μm nitrocellulose membrane. Membranes were blocked with 5% milk in TBS-Tween (TBST, 10 mM Tris-HCl, 150 mM NaCl, 0.1% Tween-20, pH 8.0) for 1 hour at RT. Thereafter, membranes were incubated overnight at 4°C with primary antibodies (Table S3). On the next day, membranes were washed three times in TBST and incubated with the respective secondary antibodies for 1 hour at RT. Immunoreactivity was detected by enhanced chemiluminescence (ECL select western blotting detection

reagent, GE Healthcare) or near-infrared detection (Odyssey, Li-COR).

Immunocytochemistry and image analysis

IPSCs and microglia were fixed in 4% PFA (ThermoFisher Scientific, Alfa Aesar J61899) for 15 minutes and washed twice with PBS (Westburg, LO BE17-513F). The cells were permeabilized and blocked in PBS containing 0.25% Triton X-100 and 1% BSA for 1 hour at RT followed by overnight incubation with primary antibodies (Table S3). Next, cells were washed with PBS and incubated with the corresponding secondary antibodies. Thereafter, another three washing steps with PBS were completed and Hoechst was used as a counterstain at 0.1 mg/mL for 15 minutes in PBS. CellMask Orange stain (ThermoFisher Scientific, H32713) was added in certain experiments and was used as indicated per manufacturer's protocol. To mount the cover slips onto slides, Prolong Antifade mounting media (ThermoFisher) was used. Acquisition of microglia images was performed using a Yokogawa CV8000 microscope and images of iPSCs were acquired with a Zeiss LSM 710. All images were acquired using a secondary antibody-only control, to confirm the specificity of the observed signal.
For quantitative image analysis, custom code was implemented using Matlab 2020a, and computations were hosted on the High-Performance Computing infrastructure of the University of Luxembourg (Varrette et al., 2014). Briefly, 'Iba1VolumeByCellMaskVolume' is the ratio between Iba1-positive pixels and CellMask-positive pixels per field of view. Furthermore, 'ZymosanVolumeByCellMaskVolume' is the ratio between Zymosan-positive pixels and CellMask-positive pixels per field of view. Finally, 'SNCAVolumeByNucleiVolume' is the ratio between α-synuclein-positive pixels and Hoechst-positive pixels per field of view, and 'SNCAVolumeByCytoplasm' is the ratio of α-synuclein-positive pixels and CellMask-positive pixels, without taking into account Hoechst-positive pixels, per field of view. The underlying Matlab and R codes are available upon request.

Statistics

All experiments were performed in at least three biological replicates of iPSC-derived microglia. The data was normalized by the average of values per replicate. GraphPad Prism software (version 9) was used for all statistical analyses. To determine the presence of outliers, we used the ROUT test. Two-way ANOVA was used for grouped values. Differences were considered significant (*) when p-values were below 0.05.

Author contributions

KB collected the data. KB, PM, SD, SS, PA, and EG performed the analysis. KB and AG wrote the manuscript, which was reviewed by all authors. PS contributed to the collection of fibroblasts and the generation of iPSCs. AG acquired funding for the study. AG was in charge of direction and planning of the study.

Funding

KB was supported by the Luxembourg National Research Fund (FNR) through the PRIDE15/10907093/CriTiCS grant. PM and SS received funding from the FNR within the framework of the PARK-QC DTU (PRIDE17/12244779/PARK-QC). CV was supported by the FNR through the C20/BM/14548100 CORE Junior grant. AG was supported by the FNR within the framework of the INTER (ProtectMove, INTER/DFG/19/14429377) and ATTRACT (Model-IPD, FNR9631103) programs as well as the National Centre of Excellence in Research on Parkinson's disease (NCER-PD, FNR/NCER13/BM/11264123).

Competing interests

The authors report no competing interests.

Bibliography

Asensio-Juan, E., Fueyo, R., Pappa, S., Iacobucci, S., Badosa, C., Lois, S., Balada, M., Bosch-Presegué, L., Vaquero, A., Gutiérrez, S., et al. (2017). The histone demethylase PHF8 is a molecular safeguard of the IFNγ response. Nucleic Acids Res. *45*, 3800–3811.

Austin, S.A., Floden, A.M., Murphy, E.J., and Combs, C.K. (2006). Alpha-synuclein expression modulates microglial activation phenotype. J. Neurosci. *26*, 10558 –10563.

Badanjak, K., Mulica, P., Smajic, S., Delcambre, S., Tranchevent, L.-C., Diederich, N., Rauen, T., Schwamborn, J.C., Glaab, E., Cowley, S.A., et al. (2021). iPSC-Derived Microglia as a Model to Study Inflammation in Idiopathic Parkinson's Disease. Front Cell Dev Biol *9*, 740758.

Bae, E.-J., Kim, D.-K., Kim, C., Mante, M., Adame, A., Rockenstein, E., Ulusoy, A., Klinkenberg, M., Jeong, G.R., Bae, J.R., et al. (2018). LRRK2 kinase regulates α-synuclein propagation via RAB35 phosphorylation. Nat. Commun. *9*, 3465.

Barcia, C., Ros, C.M., Annese, V., Gómez, A., Ros-Bernal, F., Aguado-Yera, D., Martínez-Pagán, M.E., de Pablos, V., Fernandez-Villalba, E., and Herrero, M.T. (2011). IFN-γ signaling, with the synergistic contribution of TNF-α, mediates cell specific microglial and astroglial activation in experimental models of Parkinson's disease. Cell Death Dis. *2*, e142.

Barrett, J.C., Hansoul, S., Nicolae, D.L., Cho, J.H., Duerr, R.H., Rioux, J.D., Brant, S.R., Silverberg, M.S., Taylor, K.D., Barmada, M.M., et al. (2008). Genome-wide association defines more than 30 distinct susceptibility loci for Crohn's disease. Nat. Genet. *40*, 955–962.

Benjamini, Y., and Hochberg, Y. (1995). Controlling the false discovery rate: A practical and powerful approach to multiple testing. J. R. Stat. Soc. *57*, 289–300.

Berwick, D.C., Heaton, G.R., Azeggagh, S., and Harvey, K. (2019). LRRK2 Biology from structure to dysfunction: research progresses, but the themes remain the same. Mol. Neurodegener. *14*, 49.

Bido, S., Muggeo, S., Massimino, L., Marzi, M.J., Giannelli, S.G., Melacini, E., Nannoni, M., Gambarè, D., Bellini, E., Ordazzo, G., et al. (2021). Microglia-specific overexpression of α-synuclein leads to severe dopaminergic neurodegeneration by phagocytic exhaustion and oxidative toxicity. Nat. Commun. *12*, 6237.

Bieri, G., Brahic, M., Bousset, L., Couthouis, J., Kramer, N.J., Ma, R., Nakayama, L., Monbureau, M., Defensor, E., Schüle, B., et al. (2019). LRRK2 modifies α-syn pathology and spread in mouse models and human neurons. Acta Neuropathol. *137*, 961–980.

Boles, K.S., Barchet, W., Diacovo, T., Cella, M., and Colonna, M. (2005). The tumor suppressor TSLC1/NECL-2 triggers NK-cell and CD8+ T-cell responses through the cell-surface receptor CRTAM. Blood *106*, 779–786.

Bonini, S.A., Ferrari-Toninelli, G., Montinaro, M., and Memo, M. (2013). Notch signalling in adult neurons: a potential target for microtubule stabilization. Ther. Adv. Neurol. Disord. *6*, 375–385.

Borsche, M., König, I.R., Delcambre, S., Petrucci, S., Balck, A., Brüggemann, N., Zimprich, A., Wasner, K., Pereira, S.L., Avenali, M., et al. (2020). Mitochondrial damage-associated inflammation highlights biomarkers in PRKN/PINK1 parkinsonism. Brain *143*, 3041–3051.

Braak, H., Del Tredici, K., Rüb, U., de Vos, R.A.I., Jansen Steur, E.N.H., and Braak, E. (2003). Staging of brain pathology related to sporadic Parkinson's disease. Neurobiol. Aging *24*, 197–211.

Castillo, E., Leon, J., Mazzei, G., Abolhassani, N., Haruyama, N., Saito, T., Saido, T., Hokama, M., Iwaki, T., Ohara, T., et al. (2017). Comparative profiling of cortical gene expression in Alzheimer's disease patients and mouse models demonstrates a link between amyloidosis and neuroinflammation. Sci. Rep. *7*, 17762.

Chittoor-Vinod, V.G., Nichols, R.J., and Schüle, B. (2021). Genetic and Environmental Factors Influence the Pleomorphy of LRRK2 Parkinsonism. Int. J. Mol. Sci. *22*.

Choi, I., Zhang, Y., Seegobin, S.P., Pruvost, M., Wang, Q., Purtell, K., Zhang, B., and Yue, Z. (2020). Microglia clear neuron-released α-synuclein via selective autophagy and prevent neurodegeneration. Nat. Commun. *11*, 1386.

Chung, J.-S., Sato, K., Dougherty, I.I., Cruz, P.D., Jr, and Ariizumi, K. (2007). DC-HIL is a negative regulator of T lymphocyte activation. Blood *109*, 4320–4327.

Crews, L., Mizuno, H., Desplats, P., Rockenstein, E., Adame, A., Patrick, C., Winner, B., Winkler, J., and Masliah, E. (2008). Alpha-synuclein alters Notch-1 expression and neurogenesis in mouse embryonic stem cells and in the hippocampus of transgenic mice. J. Neurosci. *28*, 4250–4260.

Di Maio, R., Hoffman, E.K., Rocha, E.M., Keeney, M.T., Sanders, L.H., De Miranda, B.R., Zharikov, A., Van Laar, A., Stepan, A.F., Lanz, T.A., et al. (2018). LRRK2 activation in idiopathic Parkinson's disease. Sci. Transl. Med. *10*.

Dobbs, R.J., Charlett, A., Purkiss, A.G., Dobbs, S.M., Weller, C., and Peterson, D.W. (1999). Association of circulating TNF-alpha and IL-6 with ageing and parkinsonism. Acta Neurol. Scand. *100*, 34–41.

Doggett, E.A., Zhao, J., Mork, C.N., Hu, D., and Nichols, R.J. (2012). Phosphorylation of LRRK2 serines 955 and 973 is disrupted by Parkinson's disease mutations and LRRK2 pharmacological inhibition. J. Neurochem. *120*, 37–45.

Du, Y., Duan, T., Feng, Y., Liu, Q., Lin, M., Cui, J., and Wang, R.-F. (2018). LRRC25 inhibits type I IFN signaling by targeting ISG15-associated RIG-I for autophagic degradation. EMBO J. *37*, 351–366.

Dzamko, N., Deak, M., Hentati, F., Reith, A.D., Prescott, A.R., Alessi, D.R., and Nichols, R.J. (2010). Inhibition of LRRK2 kinase activity leads to dephosphorylation of Ser(910)/Ser(935), disruption of 14-3-3 binding and altered cytoplasmic localization. Biochem. J *430*, 405–413.

Emamzadeh, F.N. (2016). Alpha-synuclein structure, functions, and interactions. J. Res. Med. Sci. *21*, 29.

Fan, Y., Nirujogi, R.S., Garrido, A., Ruiz-Martínez, J., Bergareche-Yarza, A., Mondragón-Rezola, E., Vinagre-Aragón, A., Croitoru, I., Gorostidi Pagola, A., Paternain Markinez, L., et al. (2021). R1441G but not G2019S mutation enhances LRRK2 mediated Rab10 phosphorylation in human peripheral blood neutrophils. Acta Neuropathol. *142*, 475–494.

Fell, M.J., Mirescu, C., Basu, K., Cheewatrakoolpong, B., DeMong, D.E., Ellis, J.M., Hyde, L.A., Lin, Y., Markgraf, C.G., Mei, H., et al. (2015). MLi-2, a Potent, Selective, and Centrally Active Compound for Exploring the Therapeutic Potential and Safety of LRRK2 Kinase Inhibition. J. Pharmacol. Exp. Ther. *355*, 397–409.

Fraser, K.B., Moehle, M.S., Alcalay, R.N., West, A.B., and LRRK2 Cohort Consortium (2016). Urinary LRRK2 phosphorylation predicts parkinsonian phenotypes in G2019S LRRK2 carriers. Neurology *86*, 994–999.

Gardai, S.J., Mao, W., Schüle, B., Babcock, M., Schoebel, S., Lorenzana, C., Alexander, J., Kim, S., Glick, H., Hilton, K., et al. (2013). Elevated alpha-synuclein impairs innate immune cell function and provides a potential peripheral biomarker for Parkinson's disease. PLoS One *8*, e71634.

Gardet, A., Benita, Y., Li, C., Sands, B.E., Ballester, I., Stevens, C., Korzenik, J.R., Rioux, J.D., Daly, M.J., Xavier, R.J., et al. (2010). LRRK2 is involved in the IFN-gamma response and host response to pathogens. J. Immunol. *185*, 5577–5585.

George, J.M. (2002). The synucleins. Genome Biol. *3*, REVIEWS3002.

Gianni, D., DerMardirossian, C., and Bokoch, G.M. (2011). Direct interaction between Tks proteins and the N-terminal proline-rich region (PRR) of NoxA1 mediates Nox1-dependent ROS generation. Eur. J. Cell Biol. *90*, 164–171.

Gillardon, F., Schmid, R., and Draheim, H. (2012). Parkinson's disease-linked leucine-rich repeat kinase 2(R1441G) mutation increases proinflammatory cytokine release from activated primary microglial cells and resultant neurotoxicity. Neuroscience *208*, 41–48.

Grandbarbe, L., Michelucci, A., Heurtaux, T., Hemmer, K., Morga, E., and Heuschling, P. (2007). Notch signaling modulates the activation of microglial cells. Glia *55*, 1519–1530.

Haenseler, W., Zambon, F., Lee, H., Vowles, J., Rinaldi, F., Duggal, G., Houlden, H., Gwinn, K., Wray, S., Luk, K.C., et al. (2017). Excess α-synuclein compromises phagocytosis in iPSC-derived macrophages. Sci. Rep. *7*, 9003.

Hakimi, M., Selvanantham, T., Swinton, E., Padmore, R.F., Tong, Y., Kabbach, G., Venderova, K., Girardin, S.E., Bulman, D.E., Scherzer, C.R., et al. (2011). Parkinson's disease-linked LRRK2 is expressed in circulating and tissue immune cells and upregulated following recognition of microbial structures. J. Neural Transm. *118*, 795–808.

Hüttenrauch, M., Ogorek, I., Klafki, H., Otto, M., Stadelmann, C., Weggen, S., Wiltfang, J., and Wirths, O. (2018). Glycoprotein NMB: a novel Alzheimer's disease associated marker expressed in a subset of activated microglia. Acta Neuropathologica Communications *6*.

Iacobucci, S., Padilla, N., Gabrielli, M., Navarro, C., Lombardi, M., Vicioso-Mantis, M., Verderio, C., de la Cruz, X., and Martínez-Balbás, M.A. (2021). The histone demethylase PHF8 regulates astrocyte differentiation and function. Development 148.Imai, Y., Kobayashi, Y., Inoshita, T., Meng, H., Arano, T., Uemura, K., Asano, T., Yoshimi, K., Zhang, C.-L., Matsumoto, G., et al. (2015). The Parkinson's Disease-Associated Protein Kinase LRRK2 Modulates Notch Signaling through the Endosomal Pathway. PLoS Genet. *11*, e1005503.

Jeong, G.R., Jang, E.-H., Bae, J.R., Jun, S., Kang, H.C., Park, C.-H., Shin, J.-H., Yamamoto, Y., Tanaka-Yamamoto, K., Dawson, V.L., et al. (2018). Dysregulated phosphorylation of Rab GTPases by LRRK2 induces neurodegeneration. Mol. Neurodegener. *13*, 8.

Jiang, P., Scarpa, J.R., Gao, V.D., Vitaterna, M.H., Kasarskis, A., and Turek, F.W. (2019). Parkinson's Disease is Associated with Dysregulations of a Dopamine-Modulated Gene Network Relevant to Sleep and Affective Neurobehaviors in the Striatum. Sci. Rep. *9*, 4808.

Kluss, J.H., Conti, M.M., Kaganovich, A., Beilina, A., Melrose, H.L., Cookson, M.R., and Mamais, A. (2018). Detection of endogenous S1292 LRRK2 autophosphorylation in mouse tissue as a readout for kinase activity. NPJ Parkinsons Dis *4*, 13.

Kluss, J.H., Mazza, M.C., Li, Y., Manzoni, C., Lewis, P.A., Cookson, M.R., and Mamais, A. (2021). Preclinical modeling of chronic inhibition of the Parkinson's disease associated kinase LRRK2 reveals altered function of the endolysosomal system in vivo. Mol. Neurodegener. *16*, 17.

Kouli, A., Torsney, K.M., and Kuan, W.-L. (2019). Parkinson's Disease: Etiology, Neuropathology, and Pathogenesis. In Parkinson's Disease: Pathogenesis and Clinical Aspects, T.B. Stoker, and J.C. Greenland, eds. (Brisbane (AU): Codon Publications),.

Kuss, M., Adamopoulou, E., and Kahle, P.J. (2014). Interferon-γ induces leucine-rich repeat kinase LRRK2 via extracellular signal-regulated kinase ERK5 in macrophages. J. Neurochem. *129*, 980–987.

Lányi, Á., Baráth, M., Péterfi, Z., Bogel, G., Orient, A., Simon, T., Petrovszki, E., Kis-Tóth, K., Sirokmány, G., Rajnavölgyi, É., et al. (2011). The homolog of the five SH3-domain protein (HOFI/SH3PXD2B) regulates lamellipodia formation and cell spreading. PLoS One *6*, e23653.

Lara Ordóñez, A.J., Fasiczka, R., Naaldijk, Y., and Hilfiker, S. (2021). Rab GTPases in Parkinson's disease: a primer. Essays Biochem. *65*, 961–974.

Latourelle, J.C., Sun, M., Lew, M.F., Suchowersky, O., Klein, C., Golbe, L.I., Mark, M.H., Growdon, J.H., Wooten, G.F., Watts, R.L., et al. (2008). The Gly2019Ser mutation in LRRK2 is not fully penetrant in familial Parkinson's disease: the GenePD study. BMC Med. *6*, 32.

Lavalley, N.J., Slone, S.R., Ding, H., West, A.B., and Yacoubian, T.A. (2016). 14-3-3 Proteins regulate mutant LRRK2 kinase activity and neurite shortening. Hum. Mol. Genet. *25*, 109–122.

Lee, H., Flynn, R., Sharma, I., Haberman, E., Carling, P.J., Nicholls, F.J., Stegmann, M., Vowles, J., Haenseler, W., Wade-Martins, R., et al. (2020). LRRK2 Is Recruited to Phagosomes and Co-recruits RAB8 and RAB10 in Human Pluripotent Stem Cell-Derived Macrophages. Stem Cell Reports *14*, 940–955.

Leschziner, A.E., and Reck-Peterson, S.L. (2021). Structural Biology of LRRK2 and its Interaction with Microtubules. Mov. Disord. *36*, 2494–2504.

Liao, Y., Smyth, G.K., and Shi, W. (2019). The R package Rsubread is easier, faster, cheaper and better for alignment and quantification of RNA sequencing reads. Nucleic Acids Res. *47*, e47.

Lin, S.-C., Lo, Y.-C., and Wu, H. (2010). Helical assembly in the MyD88–IRAK4–IRAK2 complex in TLR/IL-1R signalling. Nature *465*, 885–890.

Longo, F., Mercatelli, D., Novello, S., Arcuri, L., Brugnoli, A., Vincenzi, F., Russo, I., Berti, G., Mabrouk, O.S., Kennedy, R.T., et al. (2017). Age-dependent dopamine transporter dysfunction and Serine129 phospho-α-synuclein overload in G2019S LRRK2 mice. Acta Neuropathol Commun *5*, 22.

Lopes, J.M. (2018). IRAK4 protein inhibitor could lead to treatment for Parkinson's.

Love, M.I., Huber, W., and Anders, S. (2014). Moderated estimation of fold change and dispersion for RNA-seq data with DESeq2. Genome Biol. *15*, 550.

Madero-Pérez, J., Fdez, E., Fernández, B., Lara Ordóñez, A.J., Blanca Ramírez, M., Romo Lozano, M., Rivero-Ríos, P., and Hilfiker, S. (2017). Cellular effects mediated by pathogenic LRRK2: homing in on Rab-mediated processes. Biochem. Soc. Trans. *45*, 147–154.

Maekawa, T., Sasaoka, T., Azuma, S., Ichikawa, T., Melrose, H.L., Farrer, M.J., and Obata, F. (2016). Leucine-rich repeat kinase 2 (LRRK2) regulates α-synuclein clearance in microglia. BMC Neurosci. *17*, 77.

Manschwetus, J.T., Wallbott, M., Fachinger, A., Obergruber, C., Pautz, S., Bertinetti, D., Schmidt, S.H., and Herberg, F.W. (2020). Binding of the Human 14-3-3 Isoforms to Distinct Sites in the Leucine-Rich Repeat Kinase 2. Front. Neurosci. *14*, 302.

Marchand, A., Drouyer, M., Sarchione, A., Chartier-Harlin, M.-C., and Taymans, J.-M. (2020). LRRK2 Phosphorylation, More Than an Epiphenomenon. Front. Neurosci. *14*, 527.

Marras, C., Schüle, B., Munhoz, R.P., Rogaeva, E., Langston, J.W., Kasten, M., Meaney, C., Klein, C., Wadia, P.M., Lim, S.-Y., et al. (2011). Phenotype in parkinsonian and nonparkinsonian LRRK2 G2019S mutation carriers. Neurology *77*, 325–333.

Mogi, M., Harada, M., Riederer, P., Narabayashi, H., Fujita, K., and Nagatsu, T. (1994). Tumor necrosis factor-alpha (TNF-alpha) increases both in the brain and in the cerebrospinal fluid from parkinsonian patients. Neurosci. Lett. *165*, 208–210.

Moloney, E.B., Moskites, A., Ferrari, E.J., Isacson, O., and Hallett, P.J. (2018). The glycoprotein GPNMB is selectively elevated in the substantia nigra of Parkinson's disease patients and increases after lysosomal stress. Neurobiol. Dis. *120*, 1–11.

Mount, M.P., Lira, A., Grimes, D., Smith, P.D., Faucher, S., Slack, R., Anisman, H.,

Hayley, S., and Park, D.S. (2007). Involvement of Interferon-γ in Microglial-Mediated Loss of Dopaminergic Neurons. J. Neurosci. *27*, 3328–3337.

Murthy, M.N., UKBEC, Blauwendraat, C., Guelfi, S., Hardy, J., Lewis, P.A., Trabzuni, D., and IPDGC (2017). Increased brain expression of GPNMB is associated with genome wide significant risk for Parkinson's disease on chromosome 7p15.3. Neurogenetics *18*, 121–133.

Nagatsu, T., Mogi, M., Ichinose, H., and Togari, A. (2000). Cytokines in Parkinson's disease. J. Neural Transm. Suppl. 143–151.

Neal, M.L., Boyle, A.M., Budge, K.M., Safadi, F.F., and Richardson, J.R. (2018). The glycoprotein GPNMB attenuates astrocyte inflammatory responses through the CD44 receptor. J. Neuroinflammation *15*, 73.

Nichols, R.J., Dzamko, N., Morrice, N.A., Campbell, D.G., Deak, M., Ordureau, A., Macartney, T., Tong, Y., Shen, J., Prescott, A.R., et al. (2010). 14-3-3 binding to LRRK2 is disrupted by multiple Parkinson's disease-associated mutations and regulates cytoplasmic localization. Biochem. J *430*, 393–404.

Nirujogi, R.S., Tonelli, F., Taylor, M., Lis, P., Zimprich, A., Sammler, E., and Alessi, D.R. (2021). Development of a multiplexed targeted mass spectrometry assay for LRRK2-phosphorylated Rabs and Ser910/Ser935 biomarker sites. Biochem. J *478*, 299–326.

Novello, S., Mercatelli, D., Albanese, F., Domenicale, C., Brugnoli, A., D'Aversa, E., Vantaggiato, S., Dovero, S., Murtaj, V., Presotto, L., et al. (2022). *In vivo* susceptibility to energy failure parkinsonism and LRRK2 kinase activity. Neurobiol. Dis. *162*, 105579.

Obergasteiger, J., Frapporti, G., Lamonaca, G., Pizzi, S., Picard, A., Lavdas, A.A., Pischedda, F., Piccoli, G., Hilfiker, S., Lobbestael, E., et al. (2020). Kinase inhibition of G2019S-LRRK2 enhances autolysosome formation and function to reduce endogenous alpha-synuclein intracellular inclusions. Cell Death Discov *6*, 45.

Ono, Y., Tsuruma, K., Takata, M., Shimazawa, M., and Hara, H. (2016). Glycoprotein nonmetastatic melanoma protein B extracellular fragment shows neuroprotective effects and activates the PI3K/Akt and MEK/ERK pathways via the Na /K -ATPase. Scientific Reports *6*.

Padmanabhan, S., Lanz, T.A., Gorman, D., Wolfe, M., Joyce, A., Cabrera, C., Lawrence-Henderson, R., Levers, N., Joshi, N., Ma, T.C., et al. (2020). An Assessment of LRRK2 Serine 935 Phosphorylation in Human Peripheral Blood Mononuclear Cells in Idiopathic Parkinson's Disease and G2019S LRRK2 Cohorts. J. Parkinsons. Dis. *10*, 623–629.

Panagiotakopoulou, V., Ivanyuk, D., De Cicco, S., Haq, W., Arsić, A., Yu, C., Messelodi, D., Oldrati, M., Schöndorf, D.C., Perez, M.-J., et al. (2020). Interferon-γ signaling synergizes with LRRK2 in neurons and microglia derived from human induced pluripotent stem cells. Nat. Commun. *11*, 5163.

Parisiadou, L., and Cai, H. (2010). LRRK2 function on actin and microtubule dynamics in Parkinson disease. Commun. Integr. Biol. *3*, 396–400.

Ren, C., Ding, Y., Wei, S., Guan, L., Zhang, C., Ji, Y., Wang, F., Yin, S., and Yin, P. (2019). G2019S Variation in LRRK2: An Ideal Model for the Study of Parkinson's Disease? Front. Hum. Neurosci. *13*, 306.

Ripoll, V.M., Irvine, K.M., Ravasi, T., Sweet, M.J., and Hume, D.A. (2007). Gpnmb is induced in macrophages by IFN-gamma and lipopolysaccharide and acts as a feedback regulator of proinflammatory responses. J. Immunol. *178*, 6557–6566.

Robinson, M.D., McCarthy, D.J., and Smyth, G.K. (2010). edgeR: a Bioconductor package for differential expression analysis of digital gene expression data. Bioinformatics *26*, 139–140.

Russo, I., Bubacco, L., and Greggio, E. (2014). LRRK2 and neuroinflammation: partners in crime in Parkinson's disease? J. Neuroinflammation *11*, 52.

Saade, M., Araujo de Souza, G., Scavone, C., and Kinoshita, P.F. (2021). The Role of GPNMB in Inflammation. Front. Immunol. *12*, 674739.

Scalzo, P., Kümmer, A., Cardoso, F., and Teixeira, A.L. (2009). Increased serum levels of soluble tumor necrosis factor-alpha receptor-1 in patients with Parkinson's disease. J. Neuroimmunol. *216*, 122–125.

Scheiblich, H., Dansokho, C., Mercan, D., Schmidt, S.V., Bousset, L., Wischhof, L., Eikens, F., Odainic, A., Spitzer, J., Griep, A., et al. (2021). Microglia jointly degrade fibrillar alpha-synuclein cargo by distribution through tunneling nanotubes. Cell *184*, 5089–5106.e21.

Scott, J.D., DeMong, D.E., Greshock, T.J., Basu, K., Dai, X., Harris, J., Hruza, A., Li, S.W., Lin, S.-I., Liu, H., et al. (2017). Discovery of a 3-(4-Pyrimidinyl) Indazole (MLi-2), an Orally Available and Selective Leucine-Rich Repeat Kinase 2 (LRRK2) Inhibitor that Reduces Brain Kinase Activity. J. Med. Chem. *60*, 2983–2992.

Seol, W., Nam, D., and Son, I. (2019). Rab GTPases as Physiological Substrates of LRRK2 Kinase. Exp. Neurobiol. *28*, 134–145.

Seugnet, L., Suzuki, Y., Merlin, G., Gottschalk, L., Duntley, S.P., and Shaw, P.J. (2011). Notch signaling modulates sleep homeostasis and learning after sleep deprivation in Drosophila. Curr. Biol. *21*, 835–840.

Sheng, Z., Zhang, S., Bustos, D., Kleinheinz, T., Le Pichon, C.E., Dominguez, S.L., Solanoy, H.O., Drummond, J., Zhang, X., Ding, X., et al. (2012). Ser1292 autophosphorylation is an indicator of LRRK2 kinase activity and contributes to the cellular effects of PD mutations. Sci. Transl. Med. *4*, 164ra161.

Shin, E.C., Cho, S.E., Lee, D.-K., Hur, M.-W., Paik, S.R., Park, J.H., and Kim, J. (2000). Expression Patterns of α-Synuclein in Human Hematopoietic Cells and in Drosophila at Different Developmental Stages. Mol. Cells *10*, 65–70.

Simunovic, F., Yi, M., Wang, Y., Macey, L., Brown, L.T., Krichevsky, A.M., Andersen, S.L., Stephens, R.M., Benes, F.M., and Sonntag, K.C. (2009). Gene expression profiling of substantia nigra dopamine neurons: further insights into Parkinson's disease pathology. Brain *132*, 1795–1809.

Singh, K., Chao, M.Y., Somers, G.A., Komatsu, H., Corkins, M.E., Larkins-Ford, J., Tucey, T., Dionne, H.M., Walsh, M.B., Beaumont, E.K., et al. (2011). C. elegans Notch signaling regulates adult chemosensory response and larval molting quiescence. Curr. Biol. *21*, 825–834.

Sliter, D.A., Martinez, J., Hao, L., Chen, X., Sun, N., Fischer, T.D., Burman, J.L., Li, Y., Zhang, Z., Narendra, D.P., et al. (2018). Parkin and PINK1 mitigate STING-induced inflammation. Nature *561*, 258–262.

Smajić, S., Prada-Medina, C.A., Landoulsi, Z., Ghelfi, J., Delcambre, S., Dietrich, C., Jarazo, J., Henck, J., Balachandran, S., Pachchek, S., et al. (2021). Single-cell sequencing of human midbrain reveals glial activation and a Parkinson-specific neuronal state. Brain.

Spillantini, M.G., Schmidt, M.L., Lee, V.M., Trojanowski, J.Q., Jakes, R., and Goedert, M. (1997). Alpha-synuclein in Lewy bodies. Nature *388*, 839–840.

Srinivasan, K., Friedman, B.A., Etxeberria, A., Huntley, M.A., van der Brug, M.P., Foreman, O., Paw, J.S., Modrusan, Z., Beach, T.G., Serrano, G.E., et al. (2020). Alzheimer's Patient Microglia Exhibit Enhanced Aging and Unique Transcriptional Activation. Cell Rep. *31*, 107843.

Steger, M., Tonelli, F., Ito, G., Davies, P., Trost, M., Vetter, M., Wachter, S., Lorentzen, E., Duddy, G., Wilson, S., et al. (2016). Phosphoproteomics reveals that Parkinson's disease kinase LRRK2 regulates a subset of Rab GTPases. Elife *5*.

Steiner, J.A., Quansah, E., and Brundin, P. (2018). The concept of alpha-synuclein as a prion-like protein: ten years after. Cell Tissue Res. *373*, 161–173.

Tanaka, H., Shimazawa, M., Kimura, M., Takata, M., Tsuruma, K., Yamada, M., Takahashi, H., Hozumi, I., Niwa, J.-I., Iguchi, Y., et al. (2012). The potential of GPNMB as novel neuroprotective factor in amyotrophic lateral sclerosis. Sci. Rep. *2*, 573.

Team, R.C., and Others (2018). R: A language and environment for statistical computing; 2018.

Thévenet, J., Pescini Gobert, R., Hooft van Huijsduijnen, R., Wiessner, C., and Sagot, Y.J. (2011). Regulation of LRRK2 expression points to a functional role in human monocyte maturation. PLoS One *6*, e21519.

Tian, Y., Wang, M.-L., and Zhao, J. (2019). Crosstalk between Autophagy and Type I Interferon Responses in Innate Antiviral Immunity. Viruses *11*.

Toritsuka, M., Kimoto, S., Muraki, K., Kitagawa, M., Kishimoto, T., Sawa, A., and Tanigaki, K. (2017). Regulation of striatal dopamine responsiveness by Notch/RBP-J signaling. Transl. Psychiatry *7*, e1049.

Umeno, J., Asano, K., Matsushita, T., Matsumoto, T., Kiyohara, Y., Iida, M., Nakamura, Y., Kamatani, N., and Kubo, M. (2011). Meta-analysis of published studies identified eight additional common susceptibility loci for Crohn's disease and ulcerative colitis. Inflamm. Bowel Dis. *17*, 2407–2415.

Vancraenenbroeck, R., De Raeymaecker, J., Lobbestael, E., Gao, F., De Maeyer, M., Voet, A., Baekelandt, V., and Taymans, J.-M. (2014). *in silico*, *in vitro* and cellular analysis with a kinome-wide inhibitor panel correlates cellular LRRK2 dephosphorylation to inhibitor activity on LRRK2. Front. Mol. Neurosci. *7*, 51.

Varrette, S., Bouvry, P., Cartiaux, H., and Georgatos, F. (2014). Management of an academic HPC cluster: The UL experience. In 2014 International Conference on High Performance Computing Simulation (HPCS), pp. 959–967.

Volpicelli-Daley, L.A., Abdelmotilib, H., Liu, Z., Stoyka, L., Daher, J.P.L., Milnerwood, A.J., Unni, V.K., Hirst, W.D., Yue, Z., Zhao, H.T., et al. (2016a). G2019S-LRRK2 Expression Augments α-Synuclein Sequestration into Inclusions in Neurons. Journal of Neuroscience *36*, 7415–7427.

Volpicelli-Daley, L.A., Abdelmotilib, H., Liu, Z., Stoyka, L., Daher, J.P.L., Milnerwood, A.J., Unni, V.K., Hirst, W.D., Yue, Z., Zhao, H.T., et al. (2016b). G2019S-LRRK2 Expression Augments α-Synuclein Sequestration into Inclusions in Neurons. J. Neurosci. *36*, 7415–7427.

Wang, X., Negrou, E., Maloney, M.T., Bondar, V.V., Andrews, S.V., Montalban, M., Llapashtica, C., Maciuca, R., Nguyen, H., Solanoy, H., et al. (2021). Understanding LRRK2 kinase activity in preclinical models and human subjects through quantitative analysis of LRRK2 and pT73 Rab10. Sci. Rep. *11*, 12900.

Weindel, C.G., Bell, S.L., Huntington, T., Vail, K., Srinivasan, R., Patrick, K.L., and Watson, R.O. (2019). LRRK2 regulates innate immune responses and neuroinflammation during Mycobacterium tuberculosis infection.

Weissmann, R., Hüttenrauch, M., Kacprowski, T., Bouter, Y., Pradier, L., Bayer, T.A., Kuss, A.W., and Wirths, O. (2015). Gene Expression Profiling in the APP/PS1KI Mouse Model of Familial Alzheimer's Disease. Journal of Alzheimer's Disease *50*, 397–409.

van Wilgenburg, B., Browne, C., Vowles, J., and Cowley, S.A. (2013). Efficient, long term production of monocyte-derived macrophages from human pluripotent stem cells under partly-defined and fully-defined conditions. PLoS One *8*, e71098.

Xiao, W., Shameli, A., Harding, C.V., Meyerson, H.J., and Maitta, R.W. (2014). Late stages of hematopoiesis and B cell lymphopoiesis are regulated by α-synuclein, a key player in Parkinson's disease. Immunobiology *219*, 836–844.

Ysselstein, D., Nguyen, M., Young, T.J., Severino, A., Schwake, M., Merchant, K., and Krainc, D. (2019). LRRK2 kinase activity regulates lysosomal glucocerebrosidase in neurons derived from Parkinson's disease patients. Nat. Commun. *10*, 5570.

Zhang, F.-R., Huang, W., Chen, S.-M., Sun, L.-D., Liu, H., Li, Y., Cui, Y., Yan, X.-X., Yang, H.-T., Yang, R.-D., et al. (2009). Genomewide association study of leprosy. N. Engl. J. Med. *361*, 2609–2618.

Figure captions

Figure 1. Kinase activity in LRRK2 iPSC-derived microglia. **A)** Immunoblot of pS935 LRRK2, LRRK2 and β-actin, and quantification of S935 LRRK2 normalized to total LRRK2. **B)** Immunoblot of pS1292 LRRK2, LRRK2 and β-actin, and quantification of S1292 LRRK2 normalized to total LRRK2. **C)** Immunoblot of pRab10, Rab10 and β-actin, and quantification of pRab10 normalized to total Rab10. **D)** Immunoblot of LRRK2, Rab10 and β-actin, and quantification of LRRK2 and Rab10 normalized to β-actin. Data are represented as mean ± SEM. *p < 0.05; HC, healthy control; GC, gene correction of M1 LRRK2; M1 LRRK2, manifesting LRRK2; M2 LRRK2, manifesting LRRK2; NM LRRK2, non-manifesting LRRK2.

Figure 2. Inflammatory stimulus induces upregulation of kinase activity. **A)** Overview of the treatments performed during terminal differentiation of microglia cells. On day 12, cells were treated with IFN-γ (100 ng/ml) for 72h. 2h prior to the collection of the samples, a subset of cells pretreated with IFN-γ were further treated with MLi-2 kinase inhibitor. **B)** Immunoblots of pS1292 LRRK2, LRRK2, pRab10, Rab10, and β-actin. **C)** Quantification of LRRK2 protein levels, normalized for β-actin. **D)** Quantification of kinase activity readouts, phospho-S1292-LRRK2 and pRab10, normalized for total LRRK2 and Rab10 levels, respectively. Data are represented as mean ± SEM. ***p < 0.001; ****p < 0.0001; HC, healthy control; GC, gene correction of M1 LRRK2; M1 LRRK2, manifesting LRRK2; M2 LRRK2, manifesting LRRK2; NM LRRK2, non-manifesting LRRK2.

Figure 3. Endogenous levels of α-synuclein in iPSC-derived microglia. **A)** Immunocytochemistry staining for α-synuclein of microglia cells. **B)** Quantification of data from A). Volume of α-synuclein in nuclei was normalized to NucleiMask. Volume of α-synuclein in the cytoplasm was normalized to Cytoplasm volume (defined as CellMaskVolume - NucleiVolume). Total α-synuclein was calculated as a sum of nuclear (SNCAVolumebyNucleiVolume) and cytoplasmic α-synuclein volume (SNCAVolumeinCytoplasmVolume). Scale bar: 50μm. **C)** Expression of *SNCA* in iPSC-derived microglia cells, upon all conditions. Data are represented as mean ± SEM. *p < 0.05 , **p < 0.01 , ***p < 0.001; HC, healthy control; GC, gene correction of M1 LRRK2; M1 LRRK2, manifesting PD; M2 LRRK2, manifesting PD; NM LRRK2, non-manifesting LRRK2.

Figure 4. Expression of microglia-activating genes in iPSC-derived microglia. **A)** Expression of *GPNMB* in the RNAseq dataset. **B)** Expression of *DPYD* in the RNAseq dataset. **C)** Expression of *GRAMD4* in the RNAseq dataset. *p < 0.05 , **p < 0.01 , ***p < 0.001; HC, healthy control; GC, gene correction of M1 LRRK2; M1 LRRK2, manifesting LRRK2; M2 LRRK2, manifesting LRRK2; NM LRRK2, non-manifesting LRRK2.

Figure 5. Transcriptomic analysis of iPSC-derived microglia. **A)** Heatmap of 1000 DEGs across all conditions shows clustering of microglia cells. **B)** Heatmaps of 50 DEGs in IFN-γ treated microglia, between manifesting G2019S LRRK2 microglia and healthy and gene-corrected microglia, and between manifesting and non-manifesting G2019S LRRK2 microglia. **C)** Selected gene expression levels from the first comparison: *LRRC25* and *CADM1*. **D)** Selected gene expression levels from the second comparison: *IRAK4* and *SH3PXD2B*. HC, healthy control; GC, gene correction of M1 LRRK2; M1 LRRK2, manifesting LRRK2; M2 LRRK2, manifesting LRRK2; NM LRRK2, non-manifesting LRRK2.

Figure 6. Pathway analysis. **A)** First 20 enriched pathways in iPSC-derived microglia, upon IFN-γ stimulation. In orange: LRRK2-PD vs healthy and gene-corrected microglia; in blue: LRRK2-PD vs NM-LRRK2. **B)** Visualization of the most enriched pathway; the blue bars represent under-expressed genes, the red bars over-expressed genes; the numbers refer to the comparison (1 = "Lrrk2-PD vs. healthy and gene-corrected cells", 2 = "Lrrk2-PD vs. NM-LRRK2"). HC, healthy control; GC, gene correction of M1 LRRK2; M1 LRRK2, manifesting LRRK2; M2 LRRK2, manifesting LRRK2; NM LRRK2, non-manifesting LRRK2

Figures

Figure 1.

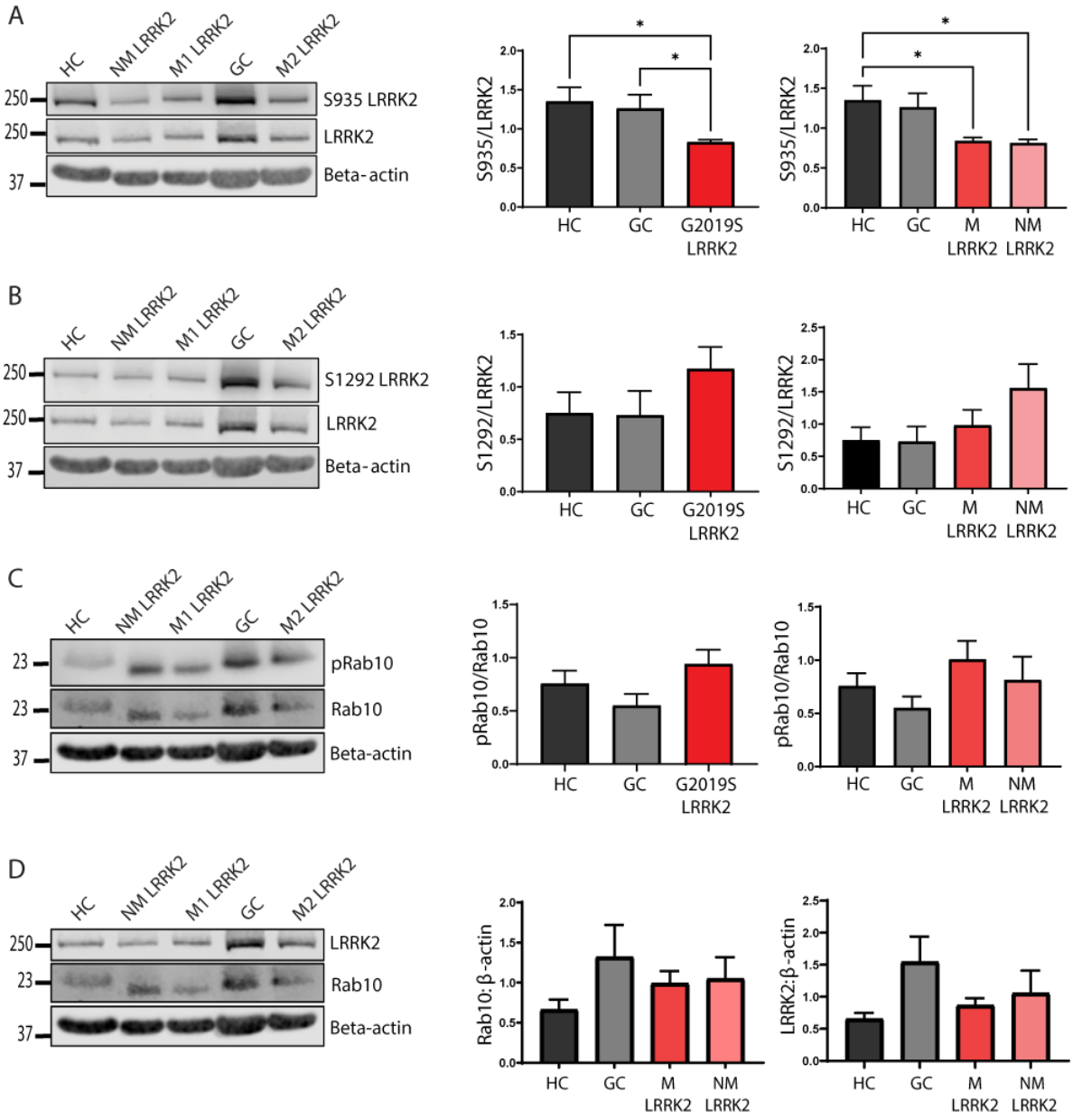

Figure 2.

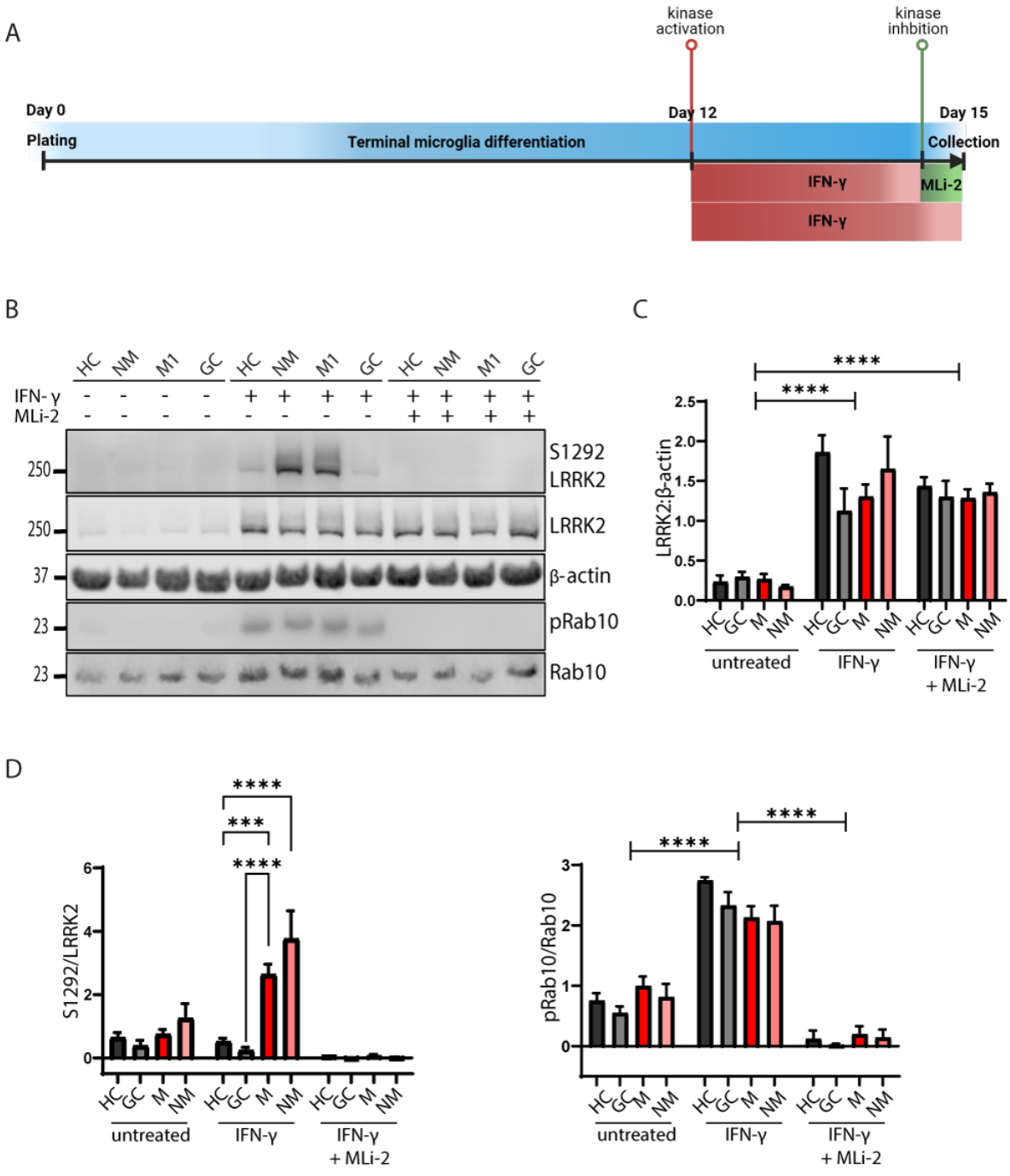
A
kinase activation
kinase inhbition
Day 0
Plating
Terminal microglia differentiation
Day 12
Day 15
Collection
IFN-γ
MLi-2
IFN-γ
B
HC NM M1 GC HC NM M1 GC HC NM M1 GC
IFN- γ
MLi-2
250
250
37
23
23
S1292 LRRK2
LRRK2
β-actin
pRab10
Rab10
C
LRRK2:β-actin
****
****
untreated
IFN-γ
IFN-γ + MLi-2
D
S1292/LRRK2
****
***
****
pRab10/Rab10
****
****
untreated
IFN-γ
IFN-γ + MLi-2

Figure 3.

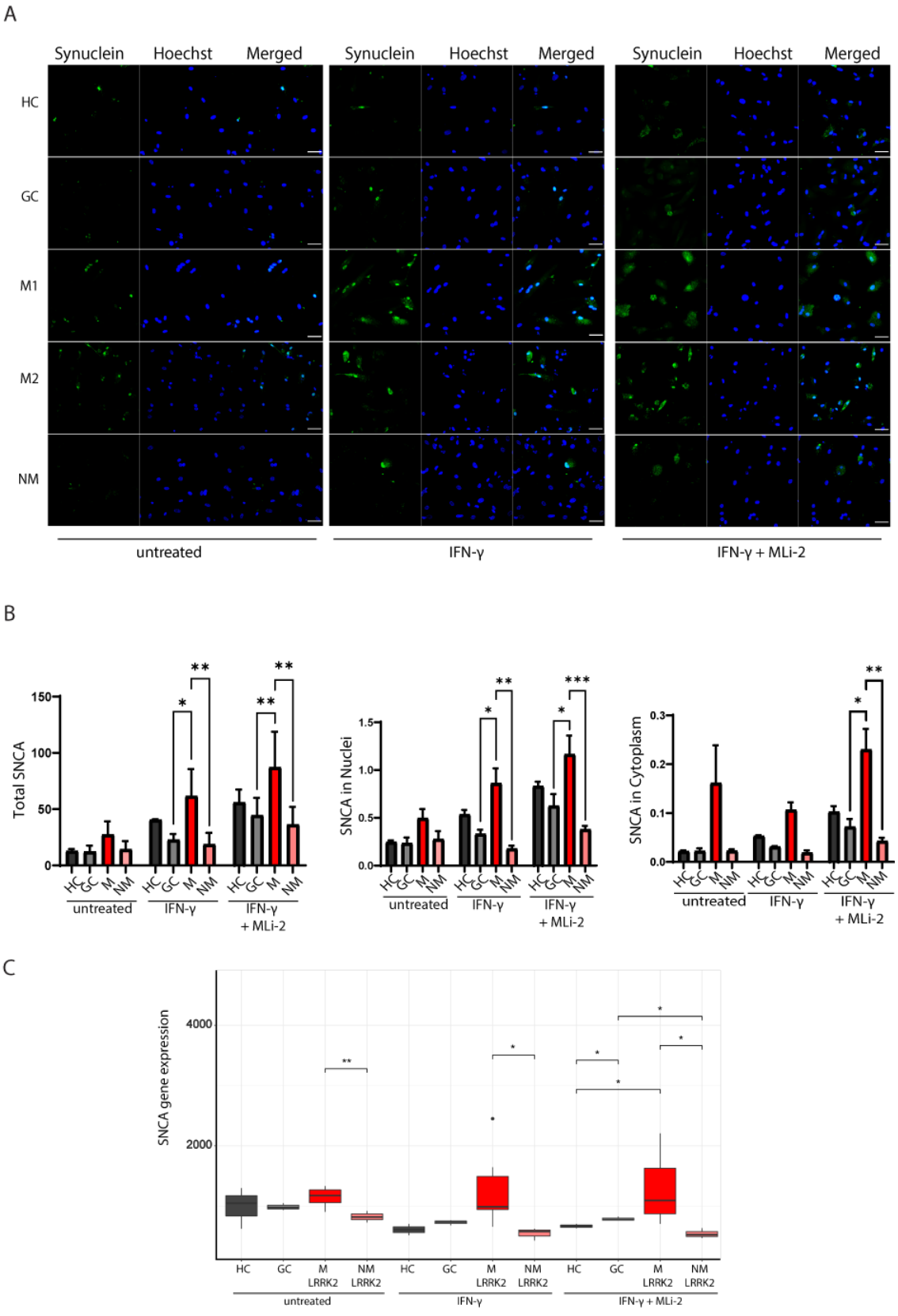
A
Synuclein
Hoechst
Merged
HC
GC
M1
M2
NM
untreated
IFN-γ
IFN-γ + MLi-2
B
Total SNCA
SNCA in Nuclei
SNCA in Cytoplasm
HC GC M NM
untreated
IFN-γ
IFN-γ + MLi-2
C
SNCA gene expression
HC
GC
M LRRK2
NM LRRK2
untreated
IFN-γ
IFN-γ + MLi-2

Figure 4.

A

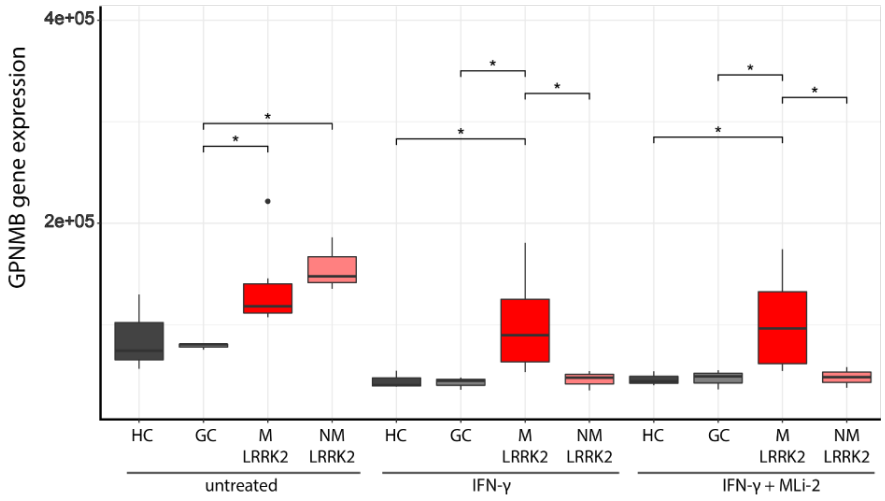
GPNMB gene expression
4e+05
2e+05
HC
GC
M LRRK2
NM LRRK2
untreated
IFN-γ
IFN-γ + MLi-2

B

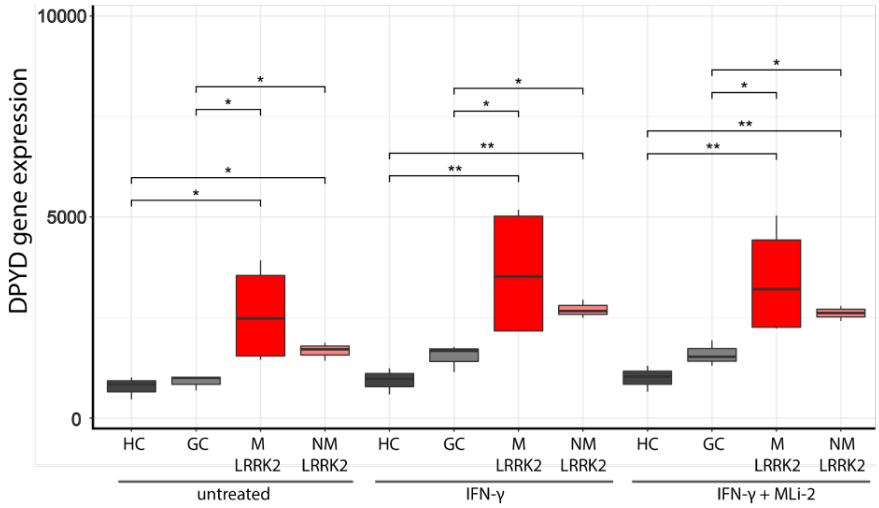
DPYD gene expression
10000
5000
0
HC
GC
M LRRK2
NM LRRK2
untreated
IFN-γ
IFN-γ + MLi-2

C

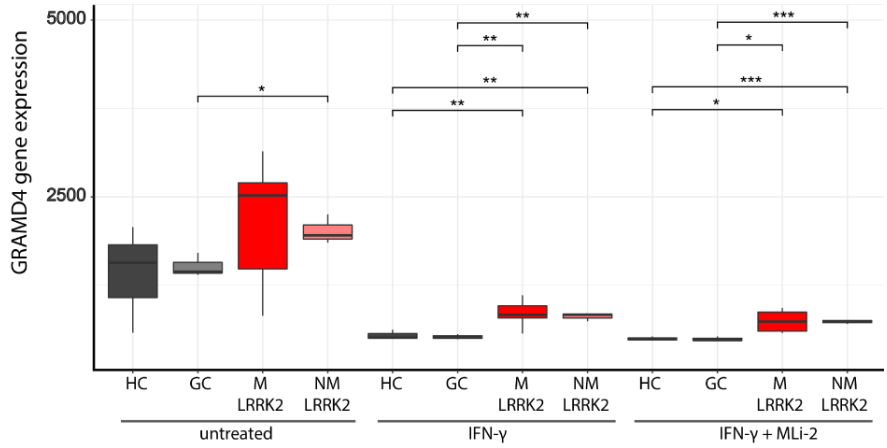
GRAMD4 gene expression
5000
2500
HC
GC
M LRRK2
NM LRRK2
untreated
IFN-γ
IFN-γ + MLi-2

Figure 5.

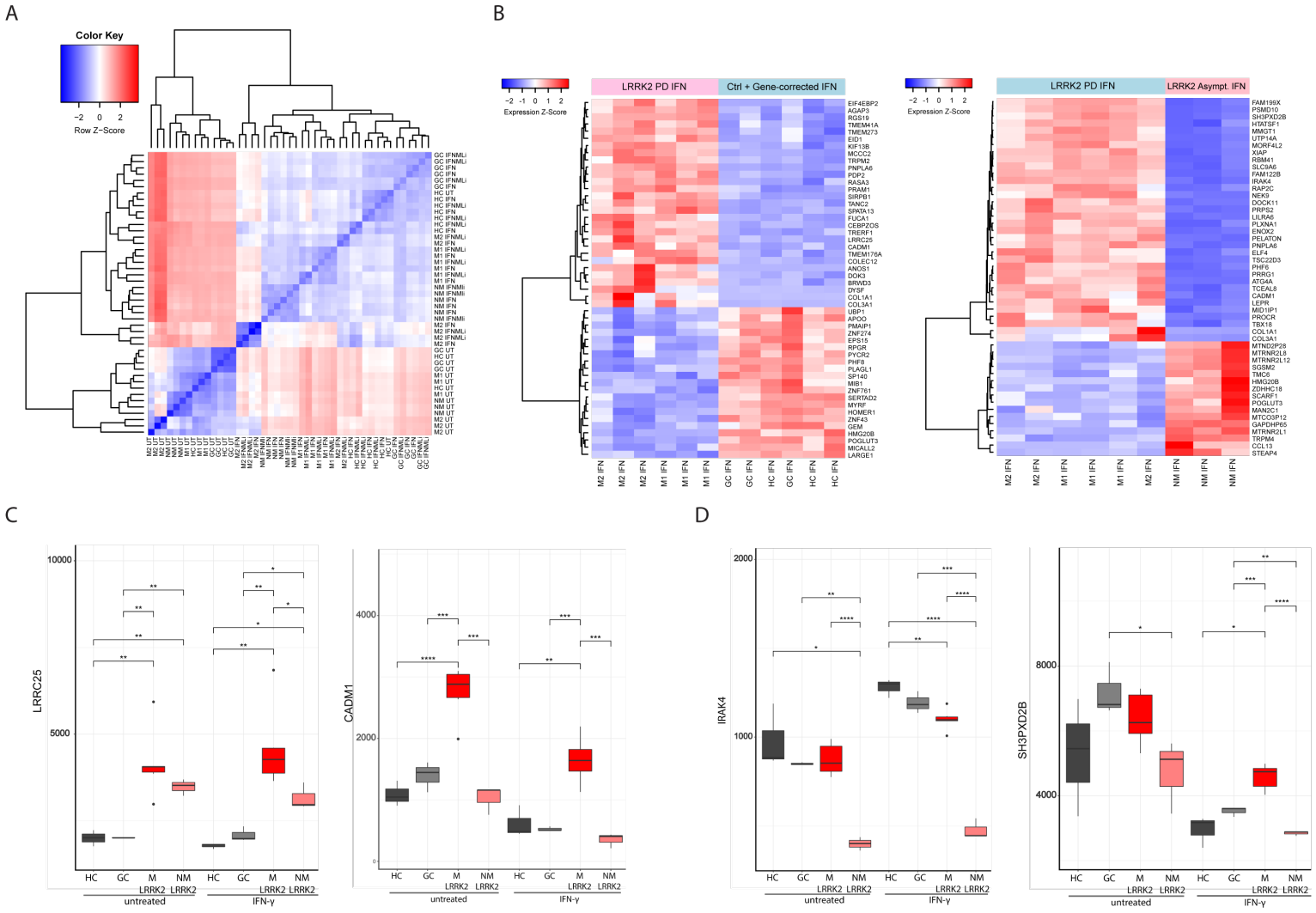
A
Color Key
Row Z-Score
B
LRRK2 PD IFN
Ctrl + Gene-corrected IFN
LRRK2 Asympt. IFN
Expression Z-Score
C
LRRC25
CADM1
D
IRAK4
SH3PXD2B
HC GC M NM HC GC M NM
LRRK2 LRRK2
untreated
IFN-γ

Figure 6.

A

#	Maps	0 1 2 3 4 5 -log(pValue)	pValue	min(pValue)	FDR	Ratio
1	Development Notch signaling activation		1.129e-7 5.505e-1	1.129e-7	7.925e-5 7.725e-1	18/82 2/82
2	Immune response IL-15 signaling via JAK-STAT and PPAR cascades		1.204e-7 2.587e-3	1.204e-7	7.925e-5 1.759e-1	13/43 5/43
3	Role of ER stress in obesity and type 2 diabetes		3.396e-4 2.664e-7	2.664e-7	1.736e-2 2.718e-4	10/54 10/54
4	Transcription_Epigenetic regulation of gene expression		6.793e-7 1.347e-1	6.793e-7	2.959e-4 6.189e-1	14/57 3/57
5	Notch signaling in oligodendrocyte precursor cell differentiation in multiple sclerosis		8.995e-7 4.813e-1	8.995e-7	2.959e-4 7.725e-1	10/29 1/29
6	Role of TGF-beta 1 in fibrosis development after myocardial infarction		9.310e-5 1.541e-6	1.541e-6	1.021e-2 7.858e-4	9/38 8/38
7	Development_NOTCH in inhibition of WNT/Beta-catenin-induced osteogenesis		1.659e-6 6.391e-1	1.659e-6	4.366e-4 7.725e-1	12/45 1/45
8	Role of SHH and Notch in SCLC		3.454e-6 5.262e-1	3.454e-6	7.576e-4 7.725e-1	10/33 1/33
9	SCAP/SREBP Transcriptional Control of Cholesterol and FA Biosynthesis		7.174e-3 5.930e-6	5.930e-6	9.937e-2 2.016e-3	7/45 8/45
10	Insulin-dependent stimulation of SREBP-1 in type 2 diabetes in liver		3.103e-4 2.357e-5	2.357e-5	1.736e-2 6.010e-3	7/27 6/27
11	Regulation of lipid metabolism_Regulation of fatty acid synthase activity in hepatocytes		2.514e-5 8.213e-3	2.514e-5	3.677e-3 2.958e-1	7/19 3/19
12	Role of stellate cells in progression of pancreatic cancer		8.349e-2 5.267e-5	5.267e-5	3.763e-1 1.074e-2	6/60 8/60
13	Transcription_Sirtuin6 regulation and functions		6.640e-5 4.910e-4	6.640e-5	8.739e-3 6.260e-2	12/63 7/63
14	Regulation of lipid metabolism_Regulation of lipid metabolism via LXR, NF-Y and SREBP		9.310e-5 9.927e-3	9.310e-5	1.021e-2 3.266e-1	9/38 4/38
15	Oxidative stress_ROS-induced cellular signaling		1.075e-4 9.450e-2	1.075e-4	1.088e-2 5.525e-1	16/108 5/108
16	Main genetic and epigenetic alterations in lung cancer		1.222e-4 2.914e-1	1.222e-4	1.113e-2 7.179e-1	10/48 2/48
17	TGF-beta signaling via kinase cascades in breast cancer		1.385e-4 4.045e-2	1.385e-4	1.113e-2 4.485e-1	11/58 4/58
18	Development_NOTCH signaling in the nervous system		1.494e-4 5.951e-1	1.494e-4	1.113e-2 7.725e-1	14/89 2/89
19	Cell adhesion_ECM remodeling		6.299e-3 2.096e-4	2.096e-4	9.053e-2 3.564e-2	8/55 7/55
20	Development_TGF-beta receptor signaling		2.461e-4 3.245e-1	2.461e-4	1.611e-2 7.339e-1	10/52 2/52

B

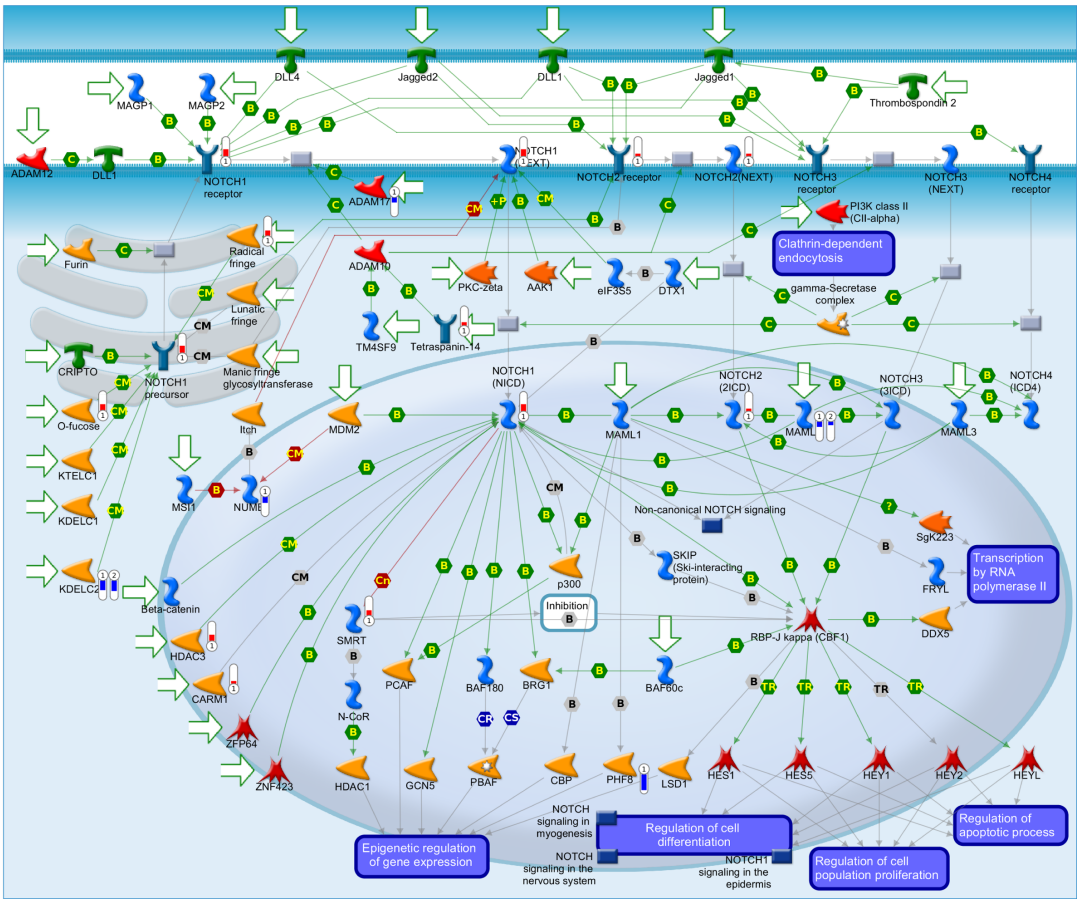

Supplemental information

LRRK2 G2019S as a trigger of inflammatory signaling in patient-derived microglia

Katja Badanjak[1], Patrycja Mulica[1], Paul Antony[1], Sylvie Delcambre[1], Semra Smajic[1], Carmen Venegas[1], Philip Seibler[2], Enrico Glaab[1], Anne Grünewald[1,2*]

Figure captions

Figure S1. Characterization of iPSC lines used in the study. A) iPSCs were characterized for the presence of Sox-2, Nanog, and Oct-4. Immunostainings were coupled with Hoechst stain, confirming the correct cell identity. Scale bar: 50μm. HC, healthy control; GC, gene correction of M1 LRRK2; M1 LRRK2, manifesting LRRK2; M2 LRRK2, manifesting LRRK2; NM LRRK2, non-manifesting LRRK2.

Figure S2. Characterization of iPSC-derived microglia. A) Immunostaining with microglia-specific marker Iba1 shows positive expression in all microglia cells. **B)** Assessment of functionality with Zymosan particles demonstrates phagocytic ability of terminally differentiated cells. **C-D)** Quantification of data from A, and B, respectively. Both Iba1 volume and Zymosan volume were normalized to the CellMask volume. Scale bar: 50μm. Data are represented as mean ± SEM. HC, healthy control; GC, gene correction of M1 LRRK2; M1 LRRK2, manifesting LRRK2; M2 LRRK2, manifesting LRRK2; NM LRRK2, non-manifesting LRRK2.

Figure S3. IFN-γ recapitulates S1292-LRRK2 phenotype in IPD iPSC-derived microglia. A) Immunoblot of pS1292 LRRK2, LRRK2, pRab10, Rab10, and β-actin. **B)** Quantifications of S1292-LRRK2 and pRab10 protein levels normalized for total LRRK2 and Rab10, respectively. **C)** Quantifications of total LRRK2 and Rab10 protein levels, normalized for β-actin. Data are represented as mean ± SEM. *p < 0.05, **p < 0.01, ****p < 0.0001; HC, healthy control; IPD, idiopathic Parkinson's disease.

Figure S4. Pathway analysis legend. Visualization taken from the website: www.portal.genego.com.

Figure S5. *PHF8* gene expression. A) RNAseq analysis of *PHF8* expression levels. **B)** Validation of *PHF8* expression levels by means of qPCR, normalized for *ACTB* and *L27*. Data are represented as mean ± SEM. *p < 0.05 , **p < 0.01 , ***p < 0.001 , ****p < 0.0001; HC, healthy control; GC, gene correction of M1 LRRK2; M1 LRRK2, manifesting PD; M2 LRRK2, manifesting PD; NM LRRK2, non-manifesting LRRK2.

Figures

Figure S1.

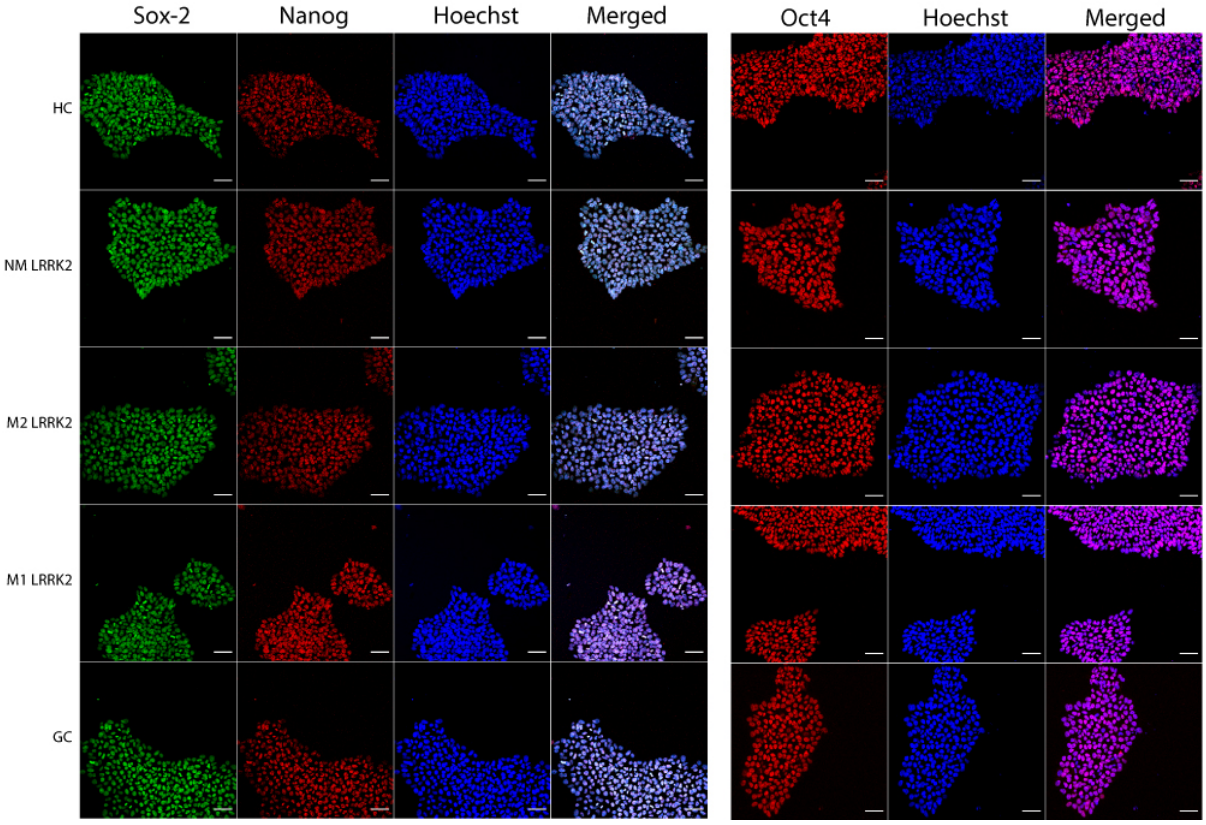

Figure S2.

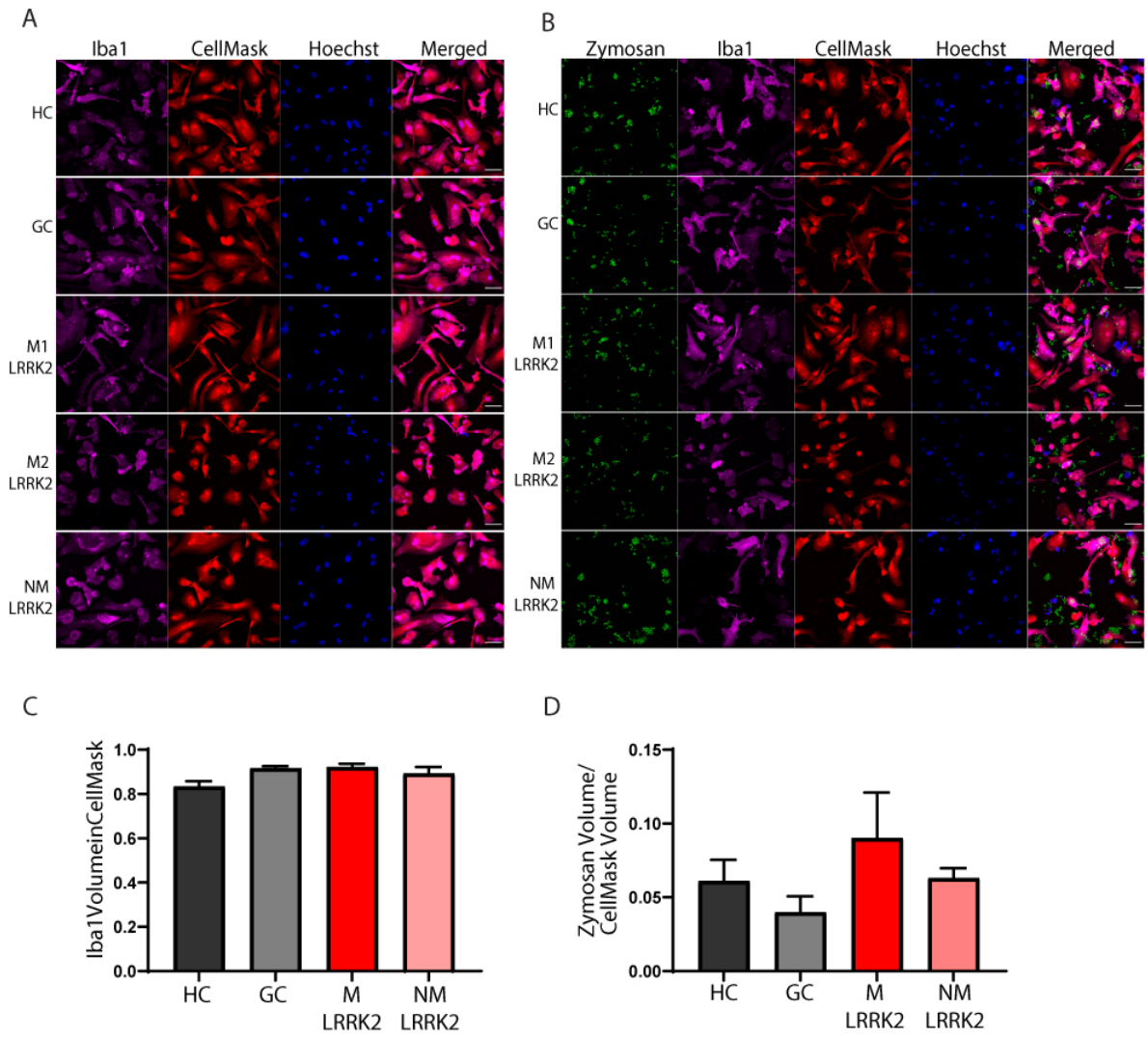
A
Iba1
CellMask
Hoechst
Merged
HC
GC
M1 LRRK2
M2 LRRK2
NM LRRK2
B
Zymosan
Iba1
CellMask
Hoechst
Merged
HC
GC
M1 LRRK2
M2 LRRK2
NM LRRK2
C
Iba1VolumeinCellMask
1.0
0.8
0.6
0.4
0.2
0.0
HC
GC
M LRRK2
NM LRRK2
D
Zymosan Volume/ CellMask Volume
0.15
0.10
0.05
0.00
HC
GC
M LRRK2
NM LRRK2

Figure S3.

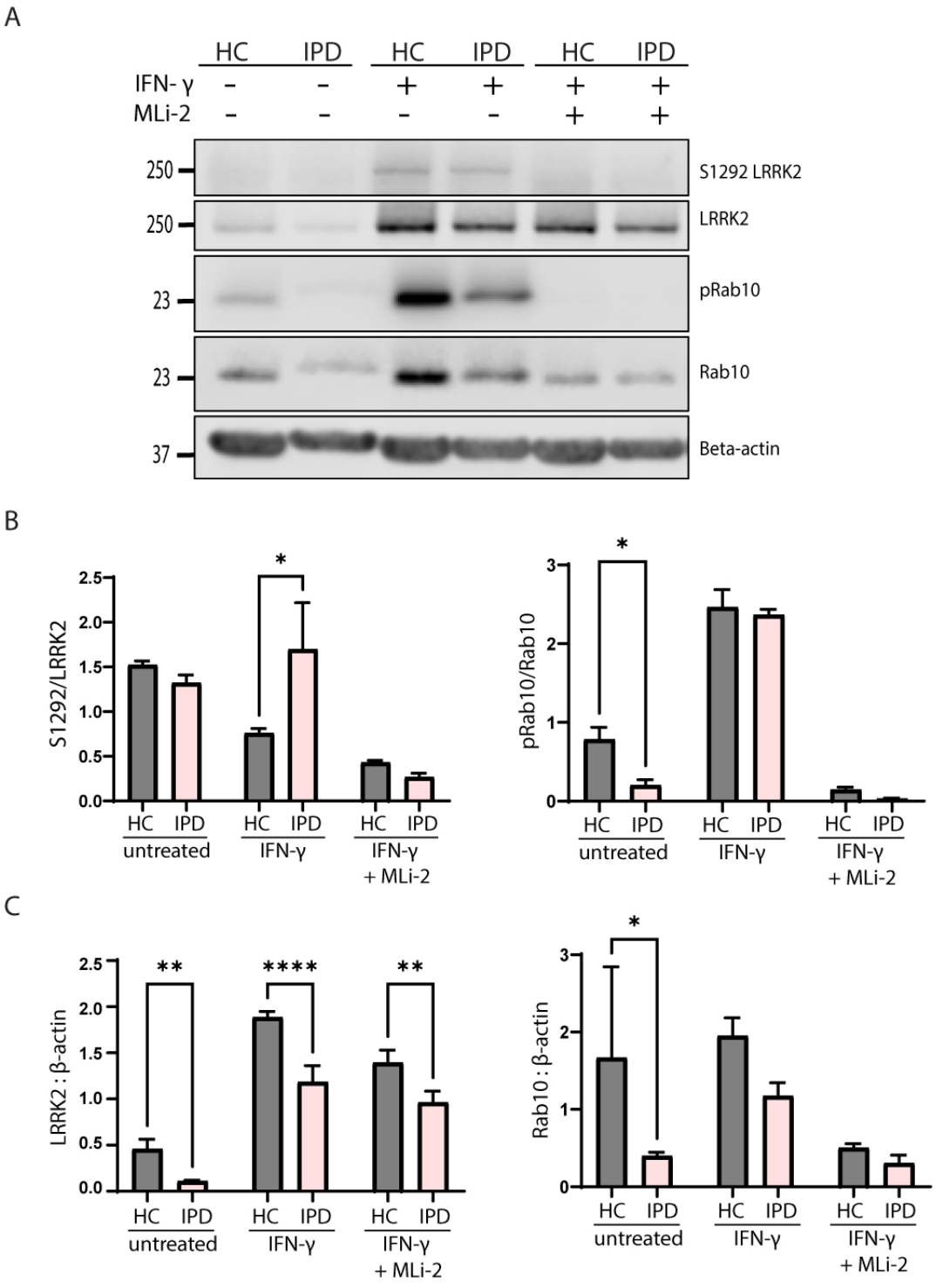
A
HC
IPD
HC
IPD
HC
IPD
IFN- γ
MLi-2
250
250
23
23
37
S1292 LRRK2
LRRK2
pRab10
Rab10
Beta-actin
B
S1292/LRRK2
pRab10/Rab10
HC
IPD
untreated
IFN-γ
IFN-γ
+ MLi-2
C
LRRK2 : β-actin
Rab10 : β-actin

Figure S4.

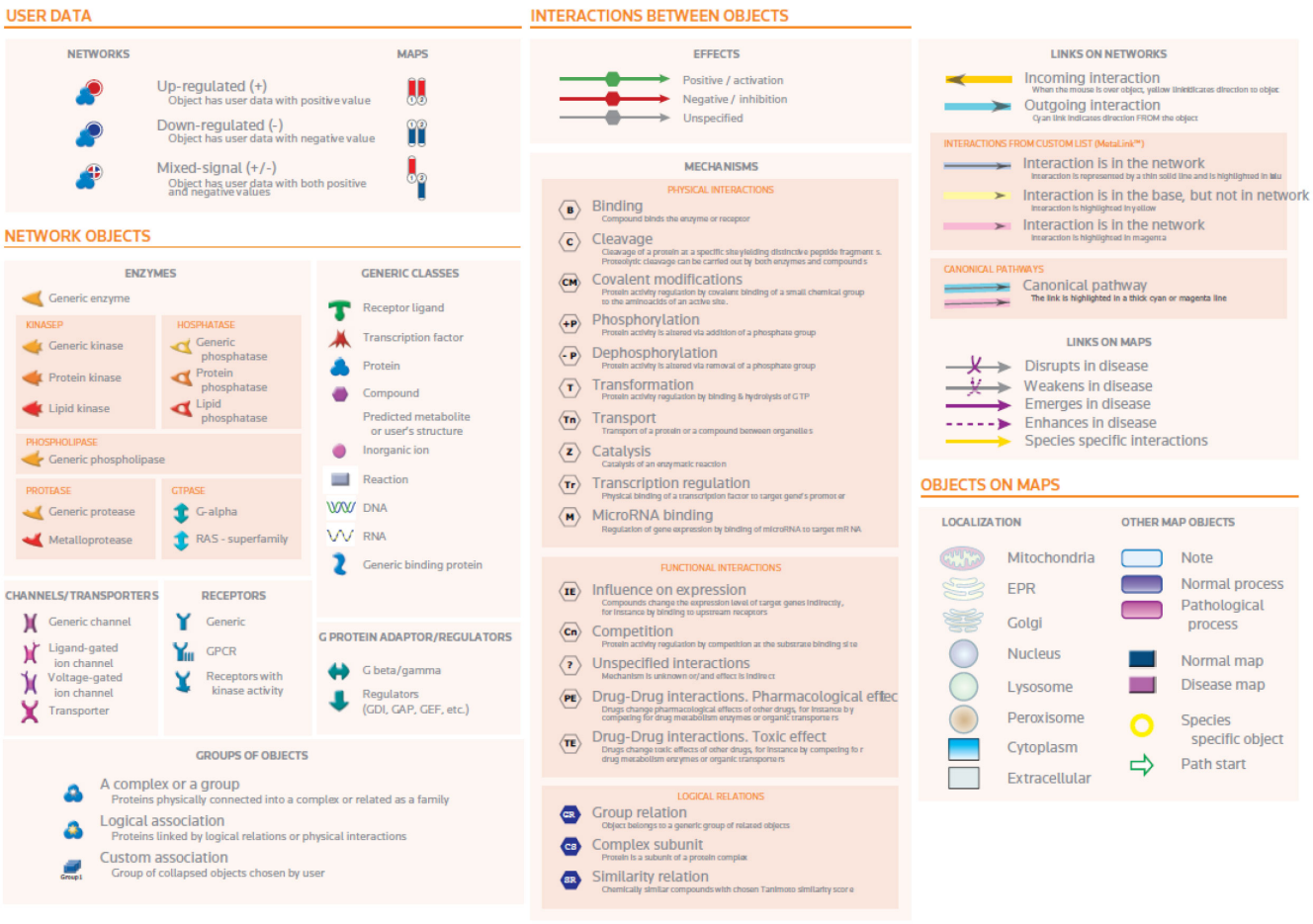
USER DATA
NETWORKS
MAPS
Up-regulated (+)
Object has user data with positive value
Down-regulated (-)
Object has user data with negative value
Mixed-signal (+/-)
Object has user data with both positive and negative values
NETWORK OBJECTS
ENZYMES
Generic enzyme
KINASE
Generic kinase
Protein kinase
Lipid kinase
HOSPHATASE
Generic phosphatase
Protein phosphatase
Lipid phosphatase
PHOSPHOLIPASE
Generic phospholipase
PROTEASE
Generic protease
Metalloprotease
GTPASE
G-alpha
RAS - superfamily
GENERIC CLASSES
Receptor ligand
Transcription factor
Protein
Compound
Predicted metabolite or user's structure
Inorganic ion
Reaction
DNA
RNA
Generic binding protein
CHANNELS/TRANSPORTERS
Generic channel
Ligand-gated ion channel
Voltage-gated ion channel
Transporter
RECEPTORS
Generic
GPCR
Receptors with kinase activity
G PROTEIN ADAPTOR/REGULATORS
G beta/gamma
Regulators (GDI, GAP, GEF, etc.)
GROUPS OF OBJECTS
A complex or a group
Proteins physically connected into a complex or related as a family
Logical association
Proteins linked by logical relations or physical interactions
Custom association
Group of collapsed objects chosen by user
INTERACTIONS BETWEEN OBJECTS
EFFECTS
Positive / activation
Negative / inhibition
Unspecified
MECHANISMS
PHYSICAL INTERACTIONS
Binding
Compound binds the enzyme or receptor
Cleavage
Covalent modifications
Phosphorylation
Dephosphorylation
Transformation
Transport
Catalysis
Transcription regulation
MicroRNA binding
FUNCTIONAL INTERACTIONS
Influence on expression
Competition
Unspecified interactions
Drug-Drug interactions. Pharmacological effec
Drug-Drug interactions. Toxic effect
LOGICAL RELATIONS
Group relation
Complex subunit
Similarity relation
LINKS ON NETWORKS
Incoming interaction
Outgoing interaction
INTERACTIONS FROM CUSTOM LIST (MetaLink™)
Interaction is in the network
Interaction is in the base, but not in network
Interaction is in the network
CANONICAL PATHWAYS
Canonical pathway
LINKS ON MAPS
Disrupts in disease
Weakens in disease
Emerges in disease
Enhances in disease
Species specific interactions
OBJECTS ON MAPS
LOCALIZATION
Mitochondria
EPR
Golgi
Nucleus
Lysosome
Peroxisome
Cytoplasm
Extracellular
OTHER MAP OBJECTS
Note
Normal process
Pathological process
Normal map
Disease map
Species specific object
Path start

Figure S5.

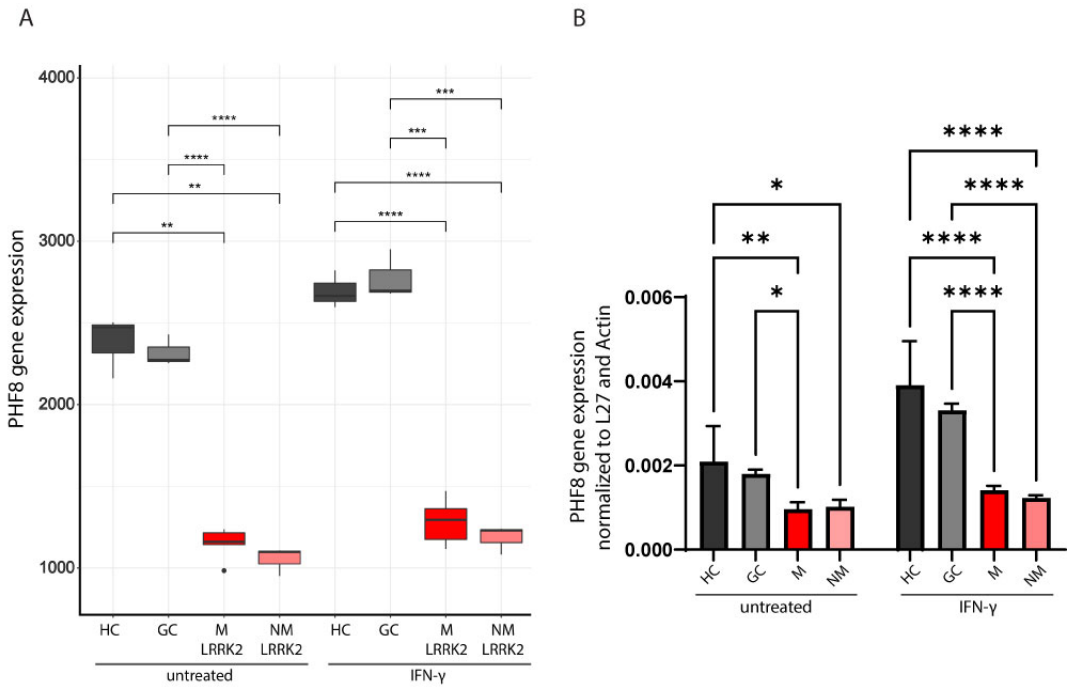
A
B
PHF8 gene expression
4000
3000
2000
1000
HC
GC
M LRRK2
NM LRRK2
untreated
IFN-γ
PHF8 gene expression normalized to L27 and Actin
0.006
0.004
0.002
0.000

Table S1. Human iPSC lines used in the study.

LABEL	ID OF IPSC	DIAGNOSIS	GENOTYPE LRRK2	GENDER	AGE AT BIOPSY
HC	#48	Healthy	WT/WT	F	63
GC	SFC832-03-06 LRRK2WT/WT	Gene correction	WT/WT	F	77
M PD1	SFC832-03-19	PD	G2019S/WT	F	77
M PD2	L-3200	PD	G2019S/WT	F	57
NM PD	L-3085	Healthy	G2019S/WT	F	55

Table S2. Differentiation media

	Basal medium	Supplements
iPSC culture	mTeSR (StemCell Technologies, 100-0276)	none
EB formation	mTeSR (StemCell Technologies, 100-0276)	50ng/ml BMP4 (Invitrogen, PHC9534), 50ng/ml VEGF (Invitrogen, PHC9394), 20ng/ml SCF (MIltenyi, 130-096-695)
Macrophage precursor factory	X-VIVO 15 (Lonza, LO BE02-060Q)	100 U/ml Pen/Strep (Gibco, 15140-122), 2mM GlutaMax (Gibco, 35050-038), 0,055 mM B-ME (Gibco, 31350-010), 100ng/ml M-CSF (Invitrogen, PHC9501), 25ng/ml IL-3 (Invitrogen, PHC0033)
Terminal microglia differentiation	Advanced DMEM (ThermoFisher, 12634010)	100 U/ml Pen/Strep (Gibco, 15140-122), 2mM GlutaMax (Gibco, 35050-038), 1 in 100 N2 (ThermoFisher, 17502001), 0,055 mM B-ME (Gibco, 31350-010), 100ng/ml GM-CSF (Peprotech, 300-03-100ug), 100ng/ml IL-34 (Peprotech, 200-34-100ug)

Table S3. Antibodies used either for Western blotting or immunocytochemistry experiments

ANTIBODY	SUPPLIER	CATEGORY NUMBER	WB	ICC
ACTIN	Sigma	A1978	1:5000	
LRRK2	UCDavis	75-188	1:1000	
PS935 LRRK2	abcam	ab133450	1:1000	
PS1292 LRRK2	abcam	ab203181	1:1000	
PAN RAB10	abcam	ab230261	1:1000	
PT73 RAB10	Nanotools	0680-100/Rab10-605B11	1:1000	
NANOG	Bioke	3580S		1:1000
SOX-2	SantaCruz	sc-365823		1:1000
OCT4	abcam	ab19857		1:1000
IBA1	Fujifilm	019-19741		1:500
A-SYNUCLEIN	Novus	NBP1-05194		1:500

3.2 Manuscript III

IPSC-derived microglia as a model to study inflammation in idiopathic Parkinson's disease

Katja Badanjak[1], Patrycja Mulica[1], Semra Smajic[1], Sylvie Delcambre[1], Leon-Charles Tranchevent[1], Nico Diederich[2], Thomas Rauen[3], Jens C. Schwamborn[1], Enrico Glaab[1], Sally A. Cowley[4], Paul Antony[1], Sandro Pereira[1], Carmen Venegas[1], Anne Grünewald[1,5*]

[1]Luxembourg Centre for Systems Biomedicine, University of Luxembourg, Esch-sur-Alzette, Luxembourg
[2]Centre Hospitalier de Luxembourg (CHL), Luxembourg, Luxembourg
[3]Max Planck Institute for Molecular Biomedicine, Department of Cell and Developmental Biology, Münster, Germany
[4]James Martin Stem Cell Facility, Sir William Dunn School of Pathology, University of Oxford, Oxford, United Kingdom
[5]Institute of Neurogenetics, University of Lübeck, Lübeck, Germany
[*]Corresponding author

This article has been published in *Frontiers in Cell and Developmental Biology*.

3.2.1 Preface

The majority of PD patients are idiopathic, meaning there is no known (genetic) cause of the disease. High clinical and molecular heterogeneity of the disease, complex environmental influences, and genetic variability between patients, make IPD the most difficult form of PD to study. Multiple analyses investigating serum and CSF levels of certain inflammatory cytokines identified an upregulation of IL-1β, IL-10, IL-18, IL-6, and TNF-α, thus defining inflammation as one of the hallmarks of IPD (Brodacki et al., 2008; Long-Smith et al., 2009; Nagatsu and Sawada, 2005; Wang et al., 2015).
In this proof-of-concept study, we made use of publicly available bulk RNAseq datasets, and identified *IL1B* and *IL10* as inflammatory targets significantly upregulated in nigral tissue of IPD patients. Furthermore, by exploring our previously generated single nuclei-RNAseq dataset, we confirmed microglia as primary cell type involved in the expression of these cytokines. To understand if we can model these observations *in vitro*, by employing iPSC technology, we derived microglia cells from IPD and control cells. Both *IL1B* and *IL10* are involved in inflammasome activation, and lipopolysaccharide (LPS) treatment is often used in cell culture models to induce the first, priming step of the NLRP3 inflammasome activation. By applying this approach to our cultures, we observed higher levels of both *IL1B* and *IL10* in IPD compared to control microglia. Furthermore, we found higher expression of NLRP3 on both mRNA and protein level in LPS-stimulated IPD microglia. Lastly, we detected a downregulation of LRRK2, on basal mRNA levels, and on both mRNA and protein levels upon LPS treatment.

My contribution to this study included the maintenance of the cell cultures, generation of iPSC-derived microglia and subsequent treatments, RNA and protein extraction, immunocytochemistry of iPSC-derived microglia cells, and Western blotting. Furthermore, I also contributed to the analysis of the generated data. Finally, I contributed to the writing of the manuscript and have prepared figures 2, 3, 4, and 5.

frontiers in Cell and Developmental Biology

ORIGINAL RESEARCH
published: 05 November 2021
doi: 10.3389/fcell.2021.740758

iPSC-Derived Microglia as a Model to Study Inflammation in Idiopathic Parkinson's Disease

*Katja Badanjak[1], Patrycja Mulica[1], Semra Smajic[1], Sylvie Delcambre[1], Leon-Charles Tranchevent[1], Nico Diederich[2], Thomas Rauen[3], Jens C. Schwamborn[1], Enrico Glaab[1], Sally A. Cowley[4], Paul M. A. Antony[1,5], Sandro L. Pereira[1], Carmen Venegas[1] and Anne Grünewald[1,6]**

[1] Luxembourg Centre for Systems Biomedicine, University of Luxembourg, Luxembourg, Luxembourg, [2] Centre Hospitalier de Luxembourg (CHL), Luxembourg, Luxembourg, [3] Department of Cell and Developmental Biology, Max Planck Institute for Molecular Biomedicine, Münster, Germany, [4] James Martin Stem Cell Facility, Sir William Dunn School of Pathology, University of Oxford, Oxford, United Kingdom, [5] Disease Modeling and Screening Platform (DMSP), Luxembourg Institute of Systems Biomedicine, University of Luxembourg and Luxembourg Institute of Health, Luxembourg, Luxembourg, [6] Institute of Neurogenetics, University of Lübeck, Lübeck, Germany

OPEN ACCESS

Edited by:
Andreas Hermann, University Hospital Rostock, Germany

Reviewed by:
Qian Chen, Warren Alpert Medical School of Brown University, United States
Björn Spittau, Bielefeld University, Germany

***Correspondence:**
Anne Grünewald
anne.gruenewald@uni.lu

Specialty section:
This article was submitted to Stem Cell Research, a section of the journal Frontiers in Cell and Developmental Biology

Received: *13 July 2021*
Accepted: *08 October 2021*
Published: *05 November 2021*

Citation:
Badanjak K, Mulica P, Smajic S, Delcambre S, Tranchevent L-C, Diederich N, Rauen T, Schwamborn JC, Glaab E, Cowley SA, Antony PMA, Pereira SL, Venegas C and Grünewald A (2021) iPSC-Derived Microglia as a Model to Study Inflammation in Idiopathic Parkinson's Disease. Front. Cell Dev. Biol. 9:740758. doi: 10.3389/fcell.2021.740758

Parkinson's disease (PD) is a neurodegenerative disease with unknown cause in the majority of patients, who are therefore considered "idiopathic" (IPD). PD predominantly affects dopaminergic neurons in the substantia nigra pars compacta (SNpc), yet the pathology is not limited to this cell type. Advancing age is considered the main risk factor for the development of IPD and greatly influences the function of microglia, the immune cells of the brain. With increasing age, microglia become dysfunctional and release pro-inflammatory factors into the extracellular space, which promote neuronal cell death. Accordingly, neuroinflammation has also been described as a feature of PD. So far, studies exploring inflammatory pathways in IPD patient samples have primarily focused on blood-derived immune cells or brain sections, but rarely investigated patient microglia *in vitro*. Accordingly, we decided to explore the contribution of microglia to IPD in a comparative manner using, both, iPSC-derived cultures and postmortem tissue. Our meta-analysis of published RNAseq datasets indicated an upregulation of *IL10* and *IL1B* in nigral tissue from IPD patients. We observed increased expression levels of these cytokines in microglia compared to neurons using our single-cell midbrain atlas. Moreover, *IL10* and *IL1B* were upregulated in IPD compared to control microglia. Next, to validate these findings *in vitro*, we generated IPD patient microglia from iPSCs using an established differentiation protocol. IPD microglia were more readily primed as indicated by elevated *IL1B* and *IL10* gene expression and higher mRNA and protein levels of NLRP3 after LPS treatment. In addition, IPD microglia had higher phagocytic capacity under basal conditions—a phenotype that was further exacerbated upon stimulation with LPS, suggesting an aberrant microglial function. Our results demonstrate the significance of microglia as the key player in the neuroinflammation process in IPD. While our study highlights the importance of microglia-mediated inflammatory signaling in IPD, further investigations will be needed to explore particular disease mechanisms in these cells.

Keywords: microglia, iPSC, neuroinflammation, idiopathic Parkinson's disease, disease modeling

INTRODUCTION

Parkinson's disease (PD) is an age-related, multifactorial disorder, resulting in the demise of dopaminergic neurons in the substantia nigra pars compacta (SNpc) of the midbrain, which subsequently leads to motor difficulties, tremor, and postural instability in affected individuals (Pang et al., 2019). While there is a genetic component to the disease, with 10% of all cases carrying a mutation in one of the causal PD genes, 90% of patients are deemed idiopathic.

The majority of studies published to date describe molecular mechanisms centered around α-synuclein aggregation, mitochondrial dysfunction, dysregulated autophagy flux, and neuroinflammation as the underlying causes of PD (Wang et al., 2015; Maiti et al., 2017). Interestingly, all of these processes are also affected by aging, which leads to functional decline, both at the physiological and molecular level. Thus, it is not surprising that aging is considered a major risk factor for the development of PD (Jin et al., 2020).

Additionally, "inflammaging" is a novel term coined to define basal, low-level inflammation during adult life that, with time, turns into a destructive, pathological process. On the one hand, lower levels of inflammation are considered to have a positive outcome on the overall cellular state. On the other hand, during prolonged inflammation, beneficial mechanisms of defense start to wear off while damaging insults increase. This phenomenon might explain why seemingly low-grade inflammatory occurrences can have a significant negative impact on health in older individuals (Calabrese et al., 2018).

Inflammation is one of the hallmarks of PD and it is propagated mostly through microglia cells, which are responsible for the innate immune defense of the brain. Early brain tissue studies showed an upregulation of microglial cells in the SNpc and higher expression of human major histocompatibility complex class II (MHC-II) molecules, while in human serum and cerebrospinal fluid (CSF), increased concentrations of cytokines such as IL-1β, IL-6, TNF-α, IL-2, IL-18, and, IL-10 were detected (Nagatsu and Sawada, 2005; Brodacki et al., 2008; Long-Smith et al., 2009; Collins et al., 2012; Wang et al., 2015; Badanjak et al., 2021). In line with these results, our own immunohistochemistry and single-nuclei transcriptomic analyses in postmortem midbrain tissue revealed an increase in abundance and a decrease in the complexity of microglia in IPD tissue, suggestive of an activated state. Moreover, patient microglia presented a disease-specific gene expression signature, indicating a significant role of these cells in the pathogenesis of the movement disorder (Smajić et al., 2020). Also, most recently, genes of the IFN-γ signaling pathway were found to be dysregulated in IPD patients (Magalhaes et al., 2021).

One of the most commonly implicated inflammatory pathways in PD is the inflammasome pathway (Chao et al., 2014; Sebastian-Valverde and Pasinetti, 2020; Yan et al., 2020). The NOD-, LRR-, and pyrin domain-containing protein 3 (NLRP3) is by far the most studied inflammasome, the main function of which is the clearance of pathogens. NLRP3 is a cytosolic sensor of intracellular and extracellular stimuli such as damage-associated and pathogen-associated molecular patterns (DAMPs and PAMPs, respectively). Two signals are necessary to fully activate this pathway, a priming signal and an activation signal. The priming signal is characterized by the upregulation of *IL1B* and *NLRP3* expression, while the secondary signal is characterized by the release of mature cytokines (Swanson et al., 2019). Underlining the relevance of the NLRP3 inflammasome, IL-1β has been associated with disease pathogenesis in multiple PD biomarker studies (Koprich et al., 2008; Su et al., 2008; Nakahira et al., 2011; Gillardon et al., 2012; Pike et al., 2021).

In our current study, we investigated inflammation markers in different models of IPD. First, we explored available RNAseq transcriptomic datasets from postmortem midbrain tissues to assess the expression of key cytokines in IPD. Next, we differentiated microglia from iPSC from IPD and control donors to test whether these cells can mirror the phenotypes observed in the brain. We detected elevated levels of *IL1B* and *IL10* in whole tissue or single cell RNAseq datasets from IPD nigral or midbrain sections. Indicative of the fidelity of iPSC-derived cellular PD models, both *IL1B* and *IL10* were also upregulated in patient microglia upon lipopolysaccharide (LPS) treatment. This coincided with increased protein abundance of NLRP3 in these cells, further implicating the inflammasome in the pathogenesis of PD.

MATERIALS AND METHODS

Bulk RNA Cytokine Expression Analysis

To profile the expression of cytokines in human SN tissue, we used a differential expression meta-analysis of publicly available case-control transcriptomics datasets, including only SN samples, as previously described (Glaab and Schneider, 2015). This provided meta-analysis Z-scores and FDR significance scores for candidate genes of interest (see **Supplementary Table 1**).

Postmortem Single-Nuclei RNA Sequencing of Human Midbrain

To analyze cytokine expression in a single-cell landscape, in this study, we used our previously published snRNAseq dataset from five IPD and six control postmortem midbrain tissues (GSE157783). The normalization, sample integration and cell clustering were performed using *Seurat* (version 3.1.5) in R 4.0.0., as described in Smajić et al. (2020).

The gene expression analysis was performed in neuronal and microglial clusters derived from our snRNAseq dataset (Smajić et al., 2020). For each of the two clusters, pseudobulk populations were created by merging all cells in the cluster from every individual in order to present the overall expression of cytokines. Then, the expression was presented as a sum of expressions of each individual cell and displayed in a bar plot using *"ggplot2"* and *"gg.gap"* packages. The cytokine expression in microglia was shown in both conditions using the *"DotPlot"* function.

Differentiation of Human iPSCs Into Microglia

An IPD patient as well as an age- and gender-matched control (both female, age: 68; IPD patient AAO: 60), who donated skin biopsies for the study, gave written and informed consent. Skin fibroblasts were reprogrammed into iPSCs as previously described (Arias-Fuenzalida et al., 2017). The study was approved by the Comité National d'Ethique de Recherche Luxembourg (CNER, vote 201411/05 V1.3). iPSCs were maintained in mTeSR^{TM}1 complete medium (StemCell Technologies). Microglia were differentiated from iPSCs following an established protocol (van Wilgenburg et al., 2013; Haenseler et al., 2017). In brief, embryoid bodies (EBs) were generated from iPSCs in mTeSR Plus (STEMCELL Technologies) supplemented with 50 ng/ml BMP-4 (Invitrogen), 50 ng/ml VEGF (Invitrogen) and 20 ng/ml SCF (Miltenyi). On day 4, EBs were transferred to a low attachment 6-well plate and were replenished with fresh EB media. On day 7, the medium was changed to X-VIVO 15 (Lonza) supplemented with 25 ng/ml IL-3 (Invitrogen), 100 ng/ml M-CSF (Invitrogen), 2 mM Glutamax (Gibco), 1% P/S (Gibco) and 0.055 mM β-mercaptoethanol (Gibco) and the EBs were transferred to T75 flasks (factories). These conditions promoted the generation of macrophage precursors. The factories were kept in culture for up to 6–8 months and macrophage precursors were harvested regularly. Terminal differentiation was achieved by culturing macrophage precursors in advanced DMEM/F12 supplemented with N2, Glutamax, P/S, β-mercaptoethanol, 100 ng/ml IL-34 (Peprotech) and 10 ng/ml GM-CSF (Peprotech). During all steps of the differentiation, cells were incubated at 37°C, 5% CO_2.

Microglia Treatments

Microglia were seeded into 6-well plates at a density of 1 × 10^6 cells/well. Upon treatment with 100 ng/ml LPS (Thermo Fisher Scientific 00-4976-93) for 3 h, cells were subjected to protein and RNA extractions. For functional analyses, microglia were seeded into 96-well glass-bottom plates at a density of 25,000 cells/well. Cells were treated with 50,000 Zymosan bioparticles (Thermo Fisher Scientific) per well for 45 min. After, cells were subjected to fixation (described in more detail below).

RNA Isolation and Quantitative PCR

RNA was isolated from microglia using the RNeasy RNA isolation kit (Qiagen, 74106) following the manufacturer's instructions for direct RNA extraction from the plate. cDNA was synthesized from 200 ng of RNA using the SuperScript^{TM} III Reverse Transcriptase (Invitrogen, 18080044). Quantitative PCR (qPCR) was performed using iQ SYBR Green (Biorad, 170-8885). The PCR reaction was run on a LightCycler 480 (Roche). The samples were denatured for 5 min at 95°C. Amplification ran over 45 cycles with a denaturation step of 10 s at 95°C, primer annealing of 10 s at 60°C, and elongation of 10 s at 75°C. The expression of *IL1B*, *IL10, LRRK2*, and *NLRP3* was normalized to the expression of the housekeeping gene *ACTB*.

Western Blotting

Total protein from microglia cultures were extracted directly from the plate, using ice cold RIPA buffer (Pierce) supplemented with 1X Protease/phosphatase Inhibitor Cocktail (Thermo Fisher Scientific). The whole well was washed multiple times, on ice, and the lysate suspension was transferred to an Eppendorf tube and vortexed for 20 s followed by incubation on ice for 20 min. The samples were centrifuged at 21,130 g for 20 min at 4°C. The protein concentration of the cell lysates was measured using a bicinchoninic acid assay using Pierce^{TM} BCA protein kit (Thermo Fisher Scientific) following the manufacturer's instructions.

Cell lysates were denatured in a loading buffer at 95°C for 5 min prior to loading on the gels. Proteins were then separated on NuPAGE 4–12% Bis-Tris gels (Invitrogen) in NuPAGE MES Running Buffer (NP0002) and transferred on a 0.2 μm nitrocellulose membrane. Membranes were blocked with 5% milk in TBS supplemented with Tween-20 (TBST, 10 mM Tris-HCl, 150 mM NaCl, 0.1% Tween-20, pH 8.0) for 1 h at RT. Thereafter, membranes were incubated overnight at 4°C with the following primary antibodies: 1:1,000 anti-NLRP3 (D4D8T, Cell Signaling), 1:500 anti-LRRK2 (75–188, UC Davis), 1:10,000 anti-β-actin (A1978, Sigma). On the next day, membranes were washed three times in TBST and incubated with the respective secondary antibodies for 1 h at RT. Immunoreactivity was detected by enhanced chemiluminescence reaction (ECL select Western blotting detection reagent, GE Healthcare) or near-infrared detection (Odyssey, Li-COR).

Immunocytochemistry and Image Analysis

IPSCs and microglia were fixed in 4% PFA (Thermo Fisher Scientific, Alfa Aesar J61899) for 15 min and washed twice with PBS (Westburg, LO BE17-513F). The cells were permeabilized and blocked in PBS containing 0.25% Triton X-100 and 1% BSA for 1 h at RT followed by overnight incubation with primary antibodies: anti-Nanog (3580S, Bioke), anti-Sox2 (sc-365823, Santa Cruz), anti-Oct4 (ab19857, Abcam), anti-Iba1 (ab5076, Abcam), anti-P2RY12 (APR-020-F, Alomone labs). On the next day, cells were washed and incubated with the corresponding secondary antibodies. Thereafter, another three washing steps with PBS were completed and Hoechst was used as a counterstain at 0.1 mg/ml for 15 min in PBS. To mount the cover slips onto slides, Prolong Antifade mounting media (Thermo Fisher Scientific) was used. Acquisition of microglia images was performed using a Zeiss LSM 710 and Yokogawa CV8000 microscope, and images of iPSC were acquired with a Zeiss Axio Imager M2. All acquired images were normalized for secondary-only antibody control, to confirm specificity of the signal observed.

For quantitative image analysis, custom code was implemented using MATLAB 2020a, and computations were performed using the High-Performance Computing (HPC) infrastructure of the University of Luxembourg (Varrette et al., 2014). Briefly, the "ZymosanAreaByIba1Area" is the ratio between Zymosan positive pixels and Iba1 positive pixels per

field of view. Furthermore, the mean abundance of Iba1 has been quantified as ratio of Iba1 area per nuclei count. The underlying MATLAB code is available upon request.

Statistics

All experiments carried out using iPSC-derived microglia were performed with 3–4 biological replicates. The data was normalized by the average of values per replicate. For statistical analyses, GraphPad Prism software (version 9) was used. To evaluate the presence of outliers, we used the ROUT test. Two-way ANOVA was used for grouped values. Differences were considered significant (*) when p-values were below 0.05.

RESULTS

Idiopathic Postmortem Midbrain Tissue Is Exhibiting Increased Cytokine Gene Expression

Studies implicating inflammatory cytokines in PD have been mostly conducted on neurotoxin and genetic animal models, or by analyzing peripheral blood samples and CSF from PD patients (Badanjak et al., 2021). To further confirm if these findings are indeed occurring in the brain of IPD patients, we analyzed available transcriptomic datasets. The transcriptomics data of human IPD and control SN revealed a significant increase in *IL1B* and *IL10* expression in the patient tissue ($FDR = 0.023$; $FDR = 0.0067$, respectively) (**Figure 1A** and **Supplementary Table 1**). A recent study showed that inflammation is not only mediated by microglia but can also be observed in neurons from an IPD mouse model (Panicker et al., 2020). In order to understand whether the detected immune signatures in the human SN are also cell-type specific, we examined our midbrain snRNAseq dataset to obtain an insight into transcriptional changes with single-cell resolution. We confirmed that the expression of cytokines is specific to microglia (**Figure 1B**). Further analysis of the microglia population revealed higher expression and a larger percentage of expressing cells in IPD compared to control tissue (**Figure 1C** and **Supplementary Table 2**).

Characterization of iPSC-Derived Microglia Model

IPD patient and control microglia were generated using an established protocol (van Wilgenburg et al., 2013; Haenseler et al., 2017; **Figure 2A**). The available iPSC lines were characterized by immunostaining with the stem cell markers Nanog, Sox2 and Oct4 (**Figure 2B**). Differentiation of iPSCs into microglia was achieved with the addition of multiple factors throughout the differentiation process (**Figure 2A**) to mimic microglia development in the human embryo. The microglial identity of cells was confirmed by positive expression of Iba1 and purinergic receptor (P2RY12) (**Figure 2C**). Comparable Iba1 areas per nuclei suggest that the disease status of the investigated lines did not have an impact on the differentiation procedure (**Figure 2D**). Additionally, we wanted to functionally characterize microglia cells by treating them with Zymosan bioparticles and assessing their phagocytic ability. While both control and IPD microglia were able to phagocyte the bioparticles, IPD microglia had a higher capacity (mean: 0.02493, $SD = 0.02472$) compared to control microglia (mean: 0.01606, $SD = 0.01304$; ANOVA: $^{***}p = 0.0004$). Furthermore, although the mean phagocytic capacity after LPS treatment was not significantly different between untreated and treated cells, IPD microglia had a significantly higher uptake of Zymosan particles compared to control cells upon addition of LPS (CTR/LPS mean: 0.01897, $SD = 0.01695$; IPD/LPS mean: 0.02683, $SD = 0.02835$; ANOVA: $^{**}p = 0.0070$) (**Figure 3**).

Upregulation of NOD-, LRR- and Pyrin Domain-Containing Protein 3 Inflammasome Components in Idiopathic Microglia

To test the transferability of our findings from postmortem single-nuclei transcriptomics to live cells, we investigated the gene expression of *IL1B* and *IL10* in iPSC-derived IPD microglia. Moreover, we quantified the mRNA and protein levels of the NLRP3 inflammasome, the inflammatory pathway most associated with chronic inflammation in PD. The priming step in inflammasome assembly is frequently mimicked by LPS

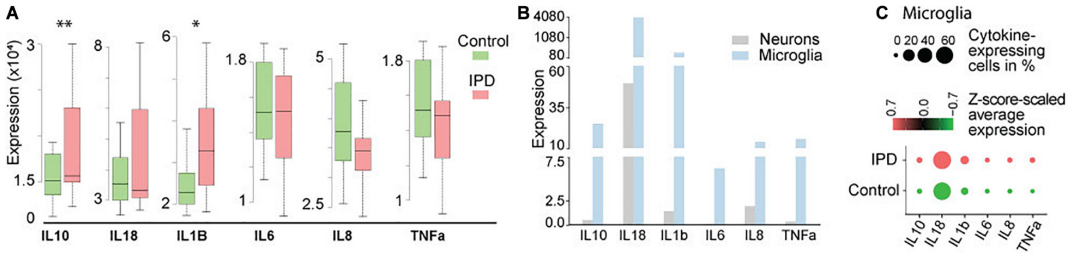

FIGURE 1 | Cytokine expression in bulk RNA-seq and single-nuclei RNA-seq datasets. **(A)** Bulk analysis of SN tissue displays higher expression of *IL1B* and *IL10* in IPD ($FDR = 0.023$; $FDR = 0.0067$). **(B)** Single-nuclei analysis of the human midbrain shows that the overall expression of cytokines is higher in microglia (3903 cells) than in neurons (5314 cells). **(C)** Cytokines are expressed in a large number of IPD and control microglia. Z-score-scaled average expression per cluster shows higher levels in IPD compared to control microglia. "*DotPlot*" function (Seurat package) was used to visualize expression and percentage of cytokine-expressing cells. $^{*}p < 0.05$; $^{**}p < 0.01$; IPD, idiopathic PD.

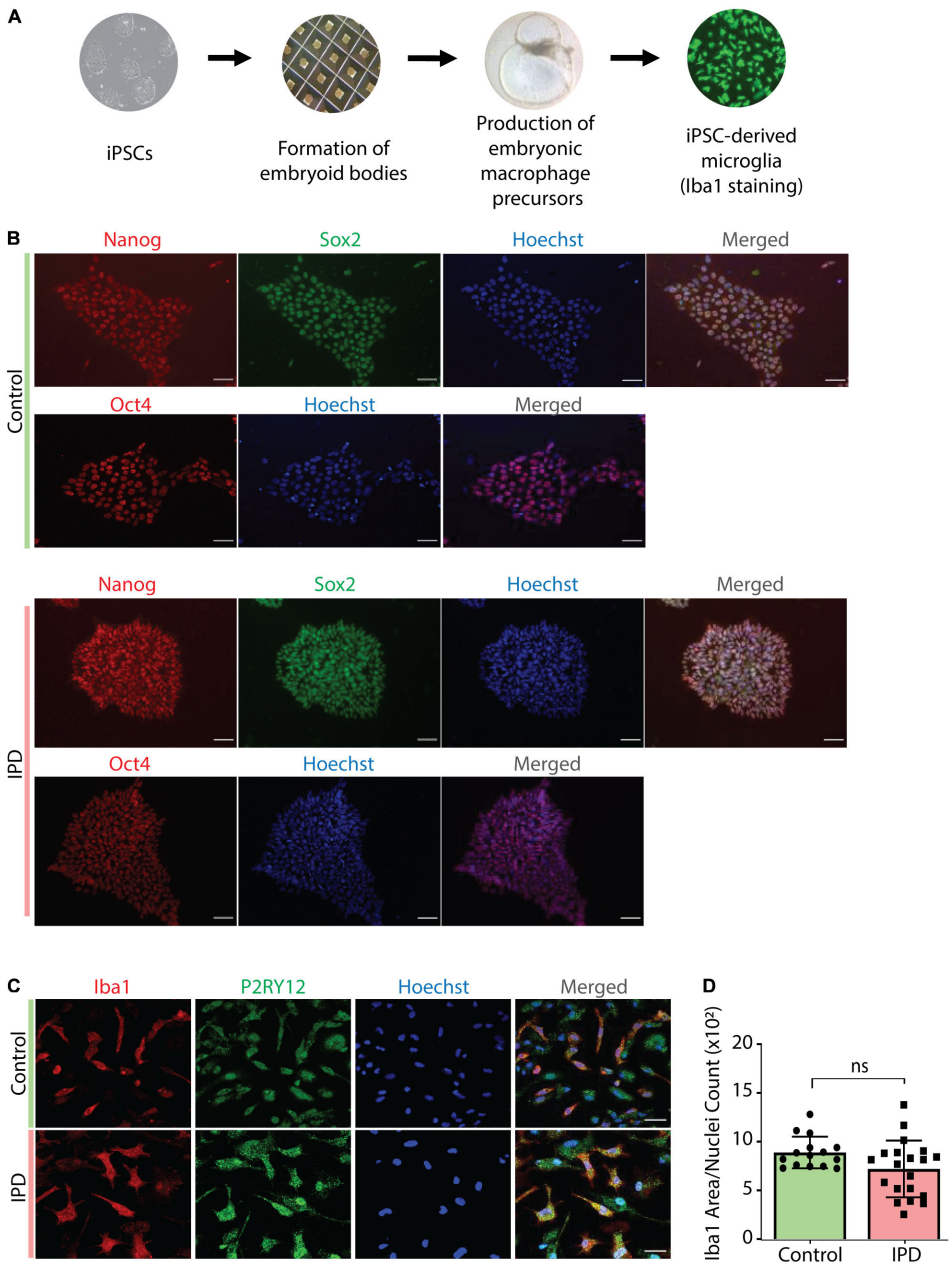

FIGURE 2 | Characterization of cellular models used in the study. **(A)** Overview of the protocol used to derive microglia from iPSCs. **(B)** Immunostaining with Nanog, Sox-2 and Oct-4, coupled with nuclear staining with Hoechst, confirmed the iPSC identity of our cells. Scale bar, 50 μm. **(C)** Terminally differentiated microglia were confirmed to express the microglia-specific markers Iba1 and P2RY12. Scale bar, 30 μm. **(D)** Quantification of data from **(C)**; no difference in Iba1 protein levels (Iba1 area was normalized for nuclei count); IPD, idiopathic PD; CTR, healthy control.

treatment (McKee and Coll, 2020). At baseline, IPD and control microglia did not show significant differences (data not shown). However, upon LPS treatment, the expression levels of *IL1B* and *IL10* increased significantly in both conditions compared to the respective untreated cells (*IL1B* CTR/LPS fold mean: 1.558, $SD = 0.117$; ANOVA: $^{**}p = 0.0098$; IPD/LPS fold mean: 3.880, $SD = 0.323$; ANOVA: $^{****}p < 0.0001$; *IL10* CTR/LPS fold mean: 3.409, $SD = 0.342$, ANOVA: $^{****}p < 0.0001$; IPD/LPS

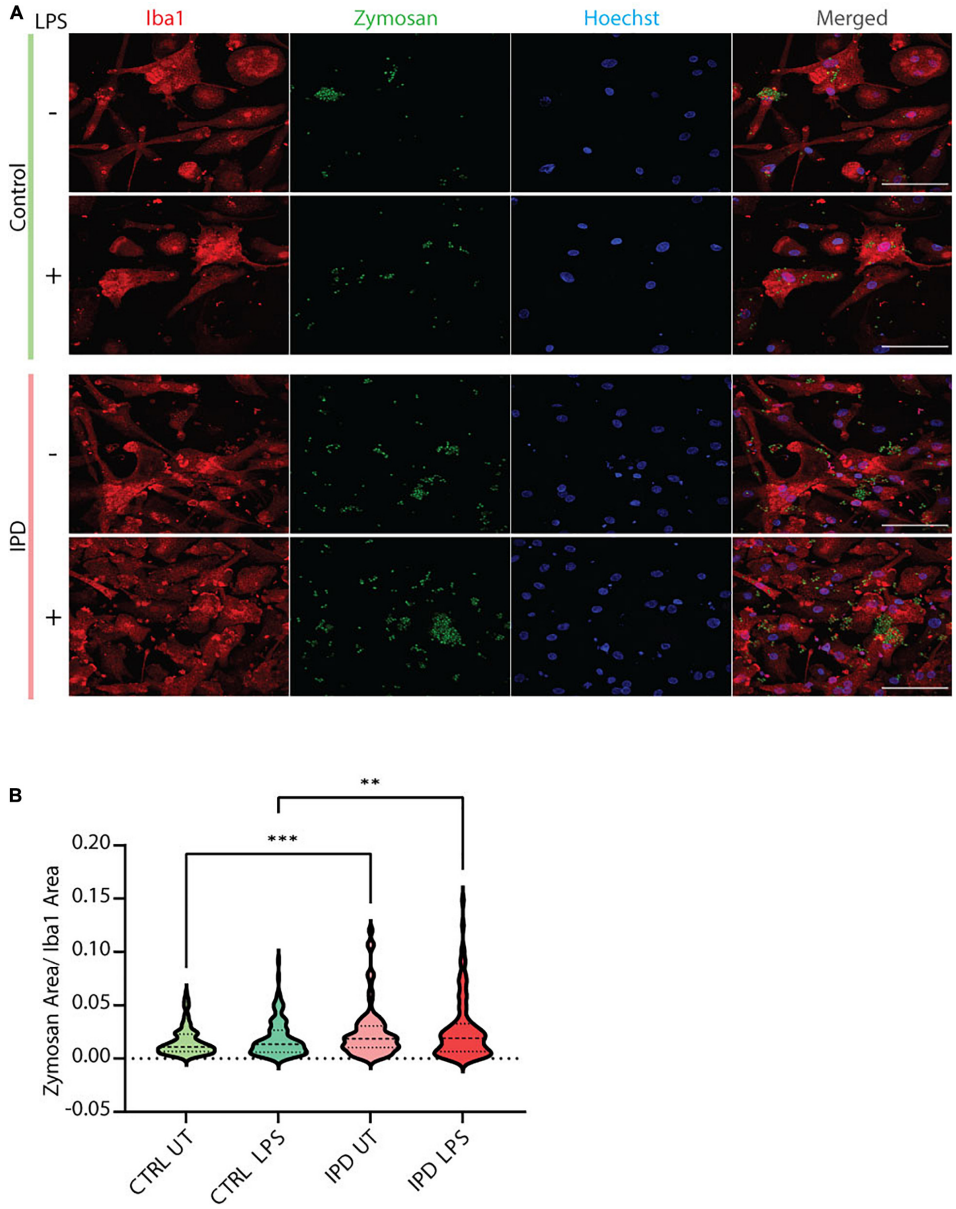

FIGURE 3 | Functional assessment of iPSC-derived microglia. **(A)** Representative immunostaining showing the functional ability of cultured control and IPD microglia treated with Zymosan bioparticles. Scale bar, 50 μm. **(B)** Quantification of data from **(A)**; IPD microglia have higher phagocytic capacity (Zymosan area was normalized for Iba1 area) compared to control cells. $^{**}p < 0.01$; $^{***}p < 0.001$; IPD, idiopathic PD; CTRL, healthy control.

fold mean: 7.717, $SD = 0.530$, ANOVA: $^{****}p < 0.0001$). When comparing the treatment response between both conditions, IPD microglia showed significantly higher *IL1B* and *IL10* expressions fold changes compared to control cells (*IL1B* LPS mean: 2.719, $SD = 1.642$; ANOVA: $^{****}p < 0.0001$; *IL10* LPS mean: 5.563, $SD = 3.047$, ANOVA: $^{****}p < 0.0001$). Additionally, when investigating *NLRP3* expression, only IPD microglia showed a significant upregulation upon LPS treatment, compared to both untreated IPD cells (*NLRP3* IPD/LPS fold mean: 3.984, $SD = 0.250$; ANOVA: $^{****}p < 0.0001$) and to LPS-treated healthy microglia (*NLRP3* LPS mean: 2.627, $SD = 1.918$; ANOVA: $^{****}p < 0.0001$) (**Figure 4A**).

Furthermore, NLRP3 protein levels corroborated the gene expression results. Again, both control and IPD microglia had significantly higher NLRP3 protein levels upon LPS addition compared to their respective basal levels (CTR/LPS fold mean:

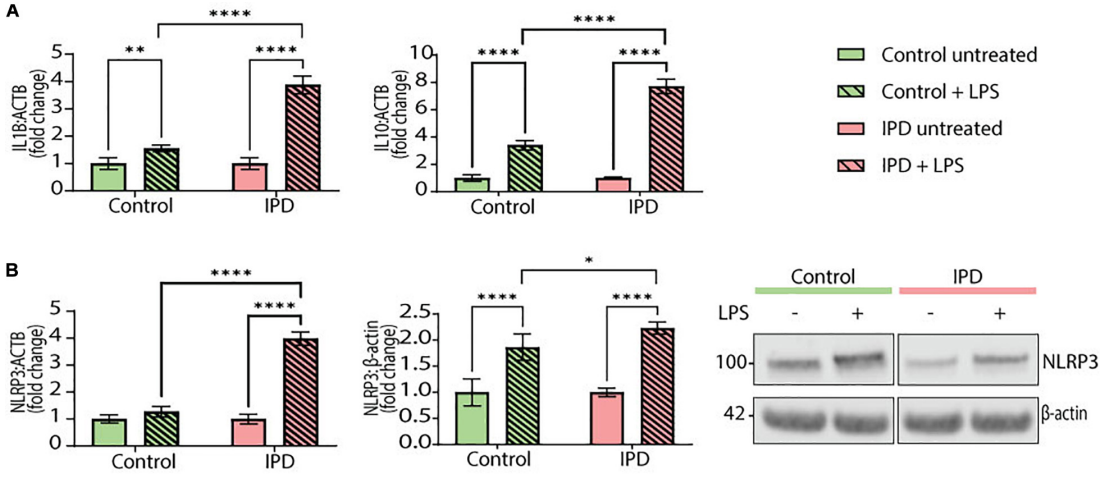

FIGURE 4 | Inflammatory phenotype and LRRK2 levels in iPSC-derived microglia. **(A)** *IL1B* and *IL10* gene expression (normalized to *ACTB*) in control and IPD microglia; a quantitative PCR showed higher gene expressions of *IL1B* and *IL10* in IPD compared to control cells upon priming with LPS (100 ng/ml). Values are represented as fold changes of untreated cells. **(B)** NLRP3 mRNA and protein levels (normalized to *ACTB* and β-actin, respectively) are increased in IPD microglia compared to control cells upon priming with LPS (100 ng/ml). Values are represented as fold change of untreated cells. $^{*}p < 0.05$; $^{**}p < 0.01$; $^{****}p < 0.0001$; IPD, idiopathic PD, NLRP3, NOD-, LRR-, and pyrin domain-containing protein 3.

1.866, $SD = 0.254$; IPD/LPS fold mean: 2.231, SD = 0.115; ANOVA: $^{****}p < 0.0001$). However, when comparing across conditions, IPD microglia showed a significant upregulation compared to treated control glia (LPS mean: 2.048, $SD = 0.2585$; ANOVA: $^{*}p = 0.0416$) (**Figure 4B**).

Downregulation of Leucine-Rich Repeat Kinase 2 Upon Lipopolysaccharide Treatment in Idiopathic Microglia

Leucine-rich repeat kinase 2 (LRRK2) is a protein implicated in both the idiopathic and genetic forms of PD. It is highly expressed in cells of the immune system and associated with immune disorders (Van Limbergen et al., 2009; Umeno et al., 2011) as well as infectious diseases (Zhang et al., 2009; Weindel et al., 2020). Its pathogenic effects have been extensively studied in the context of LRRK2-PD and in some instances in IPD. Basal levels of *LRRK2* expression were significantly downregulated in IPD microglia (CTR mean: 1.355, $SD = 0.136$; IPD mean: 0.929, $SD = 0.244$; ANOVA: $^{*}p = 0.0226$), while control cells had significantly lower expression upon LPS treatment (CTR mean: 1.355, $SD = 0.136$; CTR/LPS mean: 0.915, $SD = 0.178$; ANOVA: $^{*}p = 0.0186$) (**Figure 5A**). Furthermore, we investigated LRRK2 protein levels in our iPSC-derived microglia and saw a non-significant downregulation in untreated IPD microglia compared to controls (CTR mean: 1.332, $SD = 0.257$; IPD mean: 0.615, $SD = 0.425$; ANOVA: $p = 0.0593$). Moreover, after stimulating the cells with LPS, IPD microglia had significantly less LRRK2 protein compared to LPS-treated control glia (CTR/LPS mean: 1.649, $SD = 0.391$; IPD/LPS mean: 0.402, $SD = 0.215$; ANOVA: $^{**}p = 0.0036$) (**Figure 5B**).

DISCUSSION

Although the majority of PD cases suffer from the idiopathic form of the movement disorder, the cause of neurodegeneration in these individuals has not been extensively investigated. Genome wide association studies (GWAS) identified over 40 PD risk loci, the majority of which overlaps with known autosomal dominant PD genes, most notably *SNCA* and *LRRK2*, while other studies revealed the presence of heterozygous variants in autosomal recessively inherited PD genes (Simón-Sánchez et al., 2009; Nalls et al., 2014; Zeng et al., 2018; Germer et al., 2019; Lai et al., 2020). The main difficulty scientists are facing when studying IPD is the heterogeneous nature of the disease, which is further exacerbated by a plethora of environmental and epigenetic influences.

Inflammation has been considered a hallmark of PD since the late 1980's, when an upregulation of reactive microglia was first seen in patient brain tissue samples (McGeer et al., 1988). Positron emission tomography (PET) imaging dyes, which allow visualizing activated microglia *in vivo* over time, have been tested as biomarkers for disease progression (Gerhard et al., 2006; Terada et al., 2016; Roussakis and Piccini, 2018). Unfortunately, however, the findings from PET studies have not been successfully transferred to the clinic and the exact molecular mechanisms triggering neuroinflammation in PD currently remain elusive.

Thus, in this study, we investigated patient-derived microglia to explore the inflammatory component of IPD. First, we made use of publicly available transcriptomic data from nigral postmortem tissue to assess the expression of different cytokines in IPD patients compared to age-matched controls. Previous reports established certain secreted cytokines as reliable biomarkers in serum and plasma of PD patients, among them

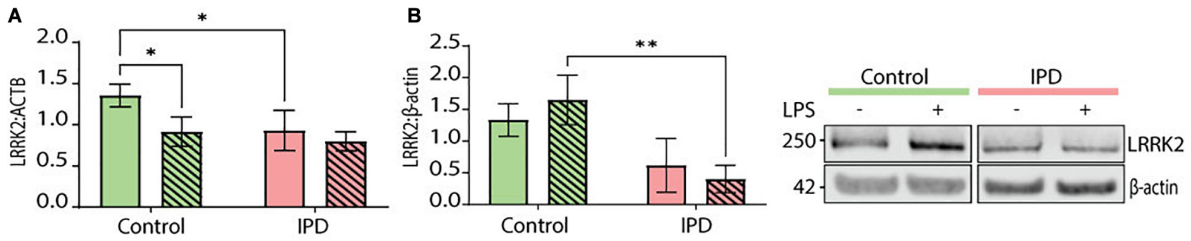

FIGURE 5 | LRRK2 levels in iPSC-derived microglia. **(A)** IPD microglia have a significant decrease of *LRRK2* expression at basal level (normalized to *ACTB*). **(B)** IPD microglia show a significant downregulation of total LRRK2 protein levels (normalized to β-actin) compared to control cells upon LPS treatment only. $*p < 0.05$; $**p < 0.01$; IPD, idiopathic PD; LRRK2, Leucine-rich repeat kinase 2.

IL-1β, IL-18, IL-6, IL-10, IL-8, TNF-α (Nagatsu et al., 2000; Brodacki et al., 2008; Qin et al., 2016). In line with these studies, our meta-analysis of published brain SNpc case-control transcriptomics datasets indicated elevated levels of *IL10* and *IL1B* in IPD patients.

To explore the cellular origin of this upregulation in IPD, we made use of our previously generated snRNAseq dataset from midbrain IPD and control tissue. Multiple cytokines, including *IL10* and *IL1B*, were predominantly expressed in microglia. This is in accordance with microglia acting as the main player of the immune system in the CNS. Moreover, in the same published dataset, we observed an increase in the microglia number as well as morphological alterations, indicative of an activated state, in IPD patients (Smajić et al., 2020). Next, to corroborate our findings from homogenized SN tissue, we investigated whether any of the aforementioned cytokines show an IPD-specific expression pattern in microglia. While we observed an increase in the expression of all investigated candidates in the patient compared to control cells, the levels of *IL10*, *IL18*, and *IL1B* were the most abundant.

Albeit informative, these postmortem results may be confounded by the fact that they only represent the molecular situation during the latest stage of the disease. Thus, to study inflammatory phenotypes and pathways in an *in vitro* IPD model, we differentiated microglia from control and patient-derived iPSCs using a published protocol (van Wilgenburg et al., 2013; Haenseler et al., 2017). While cultured IPD microglia did not show altered morphology (data not shown), we observed elevated phagocytosis in these cells indicative of overactive immune function. Phagocytosis is an integral part of microglial homeostatic function, and is not only involved in the recognition of self and non-self threats, but also in the engulfment of synaptic elements and the pruning process. Furthermore, enhanced and uncontrolled clearance is contributing to synaptic degeneration. Indeed, multiple PD studies showed loss of presynaptic terminals and synaptic changes in PD patient compared to control brains (Delva et al., 2020; Matuskey et al., 2020). It is also worth noting that disrupting the phagocytic ability of mouse glia was sufficient to rescue the neuronal degeneration phenotype observed in these animals after LPS injection (Bodea et al., 2014). Since we observed the differences in phagocytosis already at basal level, one may speculate that the genetic background in IPD glia contributes to the development of the disease. However, it is still unclear whether overactive, defective or perturbed uptake triggers PD pathogenesis (Janda et al., 2018).

To further validate our findings from postmortem tissue, we analyzed different inflammasome components in the iPSC-derived microglia cultures. IPD microglia were more reactive after priming with LPS, as indicated by enhanced expressions of *IL1B* and *IL10*, and higher mRNA and protein levels of NLRP3 compared to treated control cells. Higher levels of *IL1B* and NLRP3 in IPD microglia indicate a stronger priming step, which is necessary for downstream inflammasome activation and immune response. While we are the first to show NLRP3 dysregulation in iPSC-derived IPD microglia, our results are in agreement with findings from genetic PD models. Specifically, α-synuclein fibrils were shown to induce NLRP3 activation, and loss of the PD-associated protein Parkin triggered the release of mitoDAMPs into the cytosol, which in turn activated the NLRP3 inflammasome in mice (Zhong et al., 2016; Gordon et al., 2018; Ji et al., 2020; Pike et al., 2021). Moreover, NLRP3 was shown to regulate *IL10* levels in mice macrophages, with *IL10* production being decreased in NLRP3$^{-/-}$ mice (Gurung et al., 2015; Kobayashi et al., 2016). This is consistent with our observation of *IL10* and *NLRP3* co-regulation. In line with a biomarker study in serum, IPD patients had higher levels of IL-10 compared to healthy individuals (Rentzos et al., 2009). Furthermore, while the relationship of IL-1β and IL-10 has not been extensively studied in the context of PD, there are reports showing that, under inflammatory conditions, IL-10 selectively inhibits the release of IL-1β (Sun et al., 2019). Patient-derived microglia will be a useful model to explore the molecular mechanisms linking IL-10 and IL-1β in PD in more detail.

Further of interest with regard to inflammation in genetic but also IPD is the kinase LRRK2. Affected individuals harboring mutations in LRRK2 closely mirror the clinical picture of IPD patients (Tolosa et al., 2020) with kinase activity dysregulation being a shared feature of both forms of the disease. Due to its high abundance in immune cells, researchers have speculated that LRRK2 may be crucially involved in the regulation of neuroinflammatory processes (Gardet et al., 2010; Di Maio et al., 2018; Fyfe, 2018). Studies investigating *LRRK2* expression in IPD brain tissue showed a significant downregulation in dopaminergic neurons, which may contribute to the pathology

of the movement disorder (Simunovic et al., 2009; Sharma et al., 2011; Yılmazer et al., 2021). In agreement with these reports, we detected significantly reduced *LRRK2* expression and a trend toward lower LRRK2 protein abundance in IPD patient microglia at baseline. Inflammatory insults exacerbated this phenotype, leading to a further reduction in LRRK2 protein levels in the IPD patient-derived cells. However, the exact pathways connecting LRRK2 downregulation to microglia dysfunction in IPD warrant further investigation.

Taken together, inspired by published biomarker studies, we investigated inflammatory phenotypes in different models of IPD. In both, nigral and midbrain RNAseq datasets, we observed a disease-specific upregulation of *IL10* and *IL1B*. Furthermore, from our postmortem single-cell results, we derived that this overexpression predominantly stems from microglia. Next, to test whether we could reproduce this phenotype in a dish, we generated iPSC-derived IPD microglia. Further implicating *IL10* and *IL1B*, in IPD, the expression of these cytokines was also enhanced in patient microglia upon LPS treatment. Finally, we identified an upregulation of NLRP3 on RNA and protein level, corroborating our findings concerning *IL10* and *IL1B*. However, in light of the variability of sporadic PD, our results from a small sample may only be representative for a subset of IPD cases, warranting validation studies in larger cohorts. Moreover, while our study highlights the relevance of microglia in IPD, further experiments will be needed to decipher the exact pathways triggering neuroinflammation in sporadic PD patients.

DATA AVAILABILITY STATEMENT

The datasets presented in this study can be found in online repositories. The names of the repository/repositories and accession number(s) can be found below: https://www.ncbi.nlm.nih.gov/geo/, GSE157783; https://www.ncbi.nlm.nih.gov/geo/, GSE8397.

ETHICS STATEMENT

Patients gave written and informed consent. The study was approved by the Comité National d'Ethique de Recherche Luxembourg (CNER, vote 201411/05 V1.3).

AUTHOR CONTRIBUTIONS

SAC provided training in iPSC-derived microglia. KB, PM, SD, and SLP collected the data. KB, PM, SS, L-CT, PMAA, and EG performed the analysis. KB, PM, SS, PMAA, CV, and AG wrote the manuscript, which was reviewed by all authors. CV and AG conceived the study. ND, TR, and JCS contributed to the establishment of fibroblast cultures and iPSC generation from patient and control cells. AG acquired funding for the study and was in charge of direction and planning of the study.

FUNDING

KB was supported by the Luxembourg National Research Fund (FNR) through the PRIDE15/10907093/CriTiCS grant. SS and PM received funding from the FNR within the framework of the PARK-QC DTU (PRIDE17/12244779/PARK-QC). TR was supported by the EU Joint Programme—Neurodegenerative Disease Research (JPND) project 3DPD. CV was supported by the FNR through the C20/BM/14548100 CORE Junior grant. AG was awarded an FNR ATTRACT career development grant (Model IPD, FNR9631103). Moreover, AG and JCS were supported by the FNR as part of the National Centre of Excellence in Research on Parkinson's disease (NCER-PD, FNR/NCER13/BM/11264123).

ACKNOWLEDGMENTS

We would like to thank Jane Vowles and Cathy Browne from the University of Oxford for sharing their expertise and giving us valuable in-person training on iPSC-derived microglia protocol. In addition, we would like to express our gratitude to Anna-Lena Hallmann and Hans R. Schöler from the Max Planck Institute for Molecular Biomedicine for reprogramming fibroblasts into iPSCs.

SUPPLEMENTARY MATERIAL

The Supplementary Material for this article can be found online at: https://www.frontiersin.org/articles/10.3389/fcell.2021.740758/full#supplementary-material

REFERENCES

Arias-Fuenzalida, J., Jarazo, J., Qing, X., Walter, J., Gomez-Giro, G., Nickels, S. L., et al. (2017). FACS-Assisted CRISPR-Cas9 Genome Editing Facilitates Parkinson's Disease Modeling. *Stem Cell Rep.* 9, 1423–1431. doi: 10.1016/j.stemcr.2017.08.026

Badanjak, K., Fixemer, S., Smajić, S., Skupin, A., and Grünewald, A. (2021). The Contribution of Microglia to Neuroinflammation in Parkinson's Disease. *Int. J. Mol. Sci.* 22:ijms22094676. doi: 10.3390/ijms22094676

Bodea, L.-G., Wang, Y., Linnartz-Gerlach, B., Kopatz, J., Sinkkonen, L., Musgrove, R., et al. (2014). Neurodegeneration by activation of the microglial complement-phagosome pathway. *J. Neurosci.* 34, 8546–8556. doi: 10.1523/JNEUROSCI.5002-13.2014

Brodacki, B., Staszewski, J., Toczyłowska, B., Kozłowska, E., Drela, N., Chalimoniuk, M., et al. (2008). Serum interleukin (IL-2, IL-10, IL-6, IL-4), TNFalpha, and INFgamma concentrations are elevated in patients with atypical and idiopathic parkinsonism. *Neurosci. Lett.* 441, 158–162. doi: 10.1016/j.neulet.2008.06.040

Calabrese, V., Santoro, A., Monti, D., Crupi, R., Di Paola, R., Latteri, S., et al. (2018). Aging and Parkinson's Disease: Inflammaging, neuroinflammation and biological remodeling as key factors in pathogenesis. *Free Radic. Biol. Med.* 115, 80–91. doi: 10.1016/j.freeradbiomed.2017.10.379

Chao, Y., Wong, S. C., and Tan, E. K. (2014). Evidence of inflammatory system involvement in Parkinson's disease. *Biomed Res. Int.* 2014:308654.

Collins, L. M., Toulouse, A., Connor, T. J., and Nolan, Y. M. (2012). Contributions of central and systemic inflammation to the pathophysiology of Parkinson's

disease. *Neuropharmacology* 62, 2154–2168. doi: 10.1016/j.neuropharm.2012.01.028

Delva, A., Van Weehaeghe, D., Koole, M., Van Laere, K., and Vandenberghe, W. (2020). Loss of Presynaptic Terminal Integrity in the Substantia Nigra in Early Parkinson's Disease. *Mov. Disord.* 35, 1977–1986.

Di Maio, R., Hoffman, E. K., Rocha, E. M., Keeney, M. T., Sanders, L. H., De Miranda, B. R., et al. (2018). LRRK2 activation in idiopathic Parkinson's disease. *Sci. Transl. Med.* 10:aar5429. doi: 10.1126/scitranslmed.aar5429

Fyfe, I. (2018). Familial PD gene involved in idiopathic disease. *Nat. Rev. Neurol.* 14:508.

Gardet, A., Benita, Y., Li, C., Sands, B. E., Ballester, I., Stevens, C., et al. (2010). LRRK2 is involved in the IFN-gamma response and host response to pathogens. *J. Immunol.* 185, 5577–5585. doi: 10.4049/jimmunol.1000548

Gerhard, A., Pavese, N., Hotton, G., Turkheimer, F., Es, M., Hammers, A., et al. (2006). In vivo imaging of microglial activation with [11C](R)-PK11195 PET in idiopathic Parkinson's disease. *Neurobiol. Dis.* 21, 404–412. doi: 10.1016/j.nbd.2005.08.002

Germer, E. L., Imhoff, S., Vilariño-Güell, C., Kasten, M., Seibler, P., Brüggemann, N., et al. (2019). The Role of Rare Coding Variants in Parkinson's Disease GWAS Loci. *Front. Neurol.* 10:1284. doi: 10.3389/fneur.2019.01284

Gillardon, F., Schmid, R., and Draheim, H. (2012). Parkinson's disease-linked leucine-rich repeat kinase 2(R1441G) mutation increases proinflammatory cytokine release from activated primary microglial cells and resultant neurotoxicity. *Neuroscience* 208, 41–48. doi: 10.1016/j.neuroscience.2012.02.001

Glaab, E., and Schneider, R. (2015). Comparative pathway and network analysis of brain transcriptome changes during adult aging and in Parkinson's disease. *Neurobiol. Dis.* 74, 1–13. doi: 10.1016/j.nbd.2014.11.002

Gordon, R., Albornoz, E. A., Christie, D. C., Langley, M. R., Kumar, V., Mantovani, S., et al. (2018). Inflammasome inhibition prevents α-synuclein pathology and dopaminergic neurodegeneration in mice. *Sci. Transl. Med.* 10:aah4066. doi: 10.1126/scitranslmed.aah4066

Gurung, P., Li, B., Subbarao Malireddi, R. K., Lamkanfi, M., Geiger, T. L., and Kanneganti, T.-D. (2015). Chronic TLR Stimulation Controls NLRP3 Inflammasome Activation through IL-10 Mediated Regulation of NLRP3 Expression and Caspase-8 Activation. *Sci. Rep.* 5:14488. doi: 10.1038/srep14488

Haenseler, W., Sansom, S. N., Buchrieser, J., Newey, S. E., Moore, C. S., Nicholls, F. J., et al. (2017). A Highly Efficient Human Pluripotent Stem Cell Microglia Model Displays a Neuronal-Co-culture-Specific Expression Profile and Inflammatory Response. *Stem Cell Rep.* 8, 1727–1742. doi: 10.1016/j.stemcr.2017.05.017

Janda, E., Boi, L., and Carta, A. R. (2018). Microglial Phagocytosis and Its Regulation: A Therapeutic Target in Parkinson's Disease? *Front. Mol. Neurosci.* 11:144. doi: 10.3389/fnmol.2018.00144

Ji, Y.-J., Wang, H.-L., Yin, B.-L., and Ren, X.-Y. (2020). Down-regulation of DJ-1 Augments Neuroinflammation via Nrf2/Trx1/NLRP3 Axis in MPTP-induced Parkinson's Disease Mouse Model. *Neuroscience* 442, 253–263. doi: 10.1016/j.neuroscience.2020.06.001

Jin, H., Gu, H.-Y., Mao, C.-J., Chen, J., and Liu, C.-F. (2020). Association of inflammatory factors and aging in Parkinson's disease. *Neurosci. Lett.* 736:135259. doi: 10.1016/j.neulet.2020.135259

Kobayashi, M., Usui, F., Karasawa, T., Kawashima, A., Kimura, H., Mizushina, Y., et al. (2016). NLRP3 Deficiency Reduces Macrophage Interleukin-10 Production and Enhances the Susceptibility to Doxorubicin-induced Cardiotoxicity. *Sci. Rep.* 6:26489. doi: 10.1038/srep26489

Koprich, J. B., Reske-Nielsen, C., Mithal, P., and Isacson, O. (2008). Neuroinflammation mediated by IL-1beta increases susceptibility of dopamine neurons to degeneration in an animal model of Parkinson's disease. *J. Neuroinflamm.* 5:8. doi: 10.1186/1742-2094-5-8

Lai, D., PhD, Alipanahi, B., PhD, Fontanillas, P., PhD, et al. (2020). Genome-wide association studies of LRRK2 modifiers of Parkinson's disease. *Ann. Neurol.* 90, 76–88. doi: 10.1101/2020.12.14.20224378

Long-Smith, C. M., Sullivan, A. M., and Nolan, Y. M. (2009). The influence of microglia on the pathogenesis of Parkinson's disease. *Prog. Neurobiol.* 89, 277–287. doi: 10.1016/j.pneurobio.2009.08.001

Magalhaes, J., Tresse, E., Ejlerskov, P., Hu, E., Liu, Y., Marin, A., et al. (2021). PIAS2-mediated blockade of IFN-β signaling: a basis for sporadic Parkinson disease dementia. *Mol. Psychiatry* 2021:01207–w. doi: 10.1038/s41380-021-01207-w

Maiti, P., Manna, J., and Dunbar, G. L. (2017). Current understanding of the molecular mechanisms in Parkinson's disease: Targets for potential treatments. *Transl. Neurodegener.* 6:28.

Matuskey, D., Tinaz, S., Wilcox, K. C., Naganawa, M., Toyonaga, T., Dias, M., et al. (2020). Synaptic Changes in Parkinson Disease Assessed with in vivo Imaging. *Ann. Neurol.* 87, 329–338. doi: 10.1002/ana.25682

McGeer, P. L., Itagaki, S., Boyes, B. E., and McGeer, E. G. (1988). Reactive microglia are positive for HLA-DR in the substantia nigra of Parkinson's and Alzheimer's disease brains. *Neurology* 38, 1285–1291. doi: 10.1212/wnl.38.8.1285

McKee, C. M., and Coll, R. C. (2020). NLRP3 inflammasome priming: A riddle wrapped in a mystery inside an enigma. *J. Leukoc. Biol.* 108, 937–952. doi: 10.1002/JLB.3MR0720-513R

Nagatsu, T., and Sawada, M. (2005). Inflammatory process in Parkinson's disease: role for cytokines. *Curr. Pharm. Des.* 11, 999–1016. doi: 10.2174/1381612053381620

Nagatsu, T., Mogi, M., Ichinose, H., and Togari, A. (2000). Cytokines in Parkinson's disease. *J. Neural Transm. Suppl.* 2000, 143–151.

Nakahira, K., Haspel, J. A., Rathinam, V. A. K., Lee, S.-J., Dolinay, T., Lam, H. C., et al. (2011). Autophagy proteins regulate innate immune responses by inhibiting the release of mitochondrial DNA mediated by the NALP3 inflammasome. *Nat. Immunol.* 12, 222–230. doi: 10.1038/ni.1980

Nalls, M. A., Pankratz, N., Lill, C. M., Do, C. B., Hernandez, D. G., Saad, M., et al. (2014). Large-scale meta-analysis of genome-wide association data identifies six new risk loci for Parkinson's disease. *Nat. Genet.* 46, 989–993.

Pang, S. Y.-Y., Ho, P. W.-L., Liu, H.-F., Leung, C.-T., Li, L., Chang, E. E. S., et al. (2019). The interplay of aging, genetics and environmental factors in the pathogenesis of Parkinson's disease. *Transl. Neurodegener.* 8:23.

Panicker, N., Kam, T.-I., Neifert, S., Hinkle, J., Mao, X., Karuppagounder, S., et al. (2020). NLRP3 inflammasome activation in dopamine neurons contributes to neurodegeneration in Parkinson's Disease. *FASEB J.* 34, 1–1.

Pike, A. F., Varanita, T., Herrebout, M. A. C., Plug, B. C., Kole, J., Musters, R. J. P., et al. (2021). α-Synuclein evokes NLRP3 inflammasome-mediated IL-1β secretion from primary human microglia. *Glia* 69, 1413–1428. doi: 10.1002/glia.23970

Qin, X.-Y., Zhang, S.-P., Cao, C., Loh, Y. P., and Cheng, Y. (2016). Aberrations in Peripheral Inflammatory Cytokine Levels in Parkinson Disease: A Systematic Review and Meta-analysis. *JAMA Neurol.* 73, 1316–1324. doi: 10.1001/jamaneurol.2016.2742

Rentzos, M., Nikolaou, C., Andreadou, E., Paraskevas, G. P., Rombos, A., Zoga, M., et al. (2009). Circulating interleukin-10 and interleukin-12 in Parkinson's disease. *Acta Neurol. Scand.* 119, 332–337. doi: 10.1111/j.1600-0404.2008.01103.x

Roussakis, A.-A., and Piccini, P. (2018). Molecular Imaging of Neuroinflammation in Idiopathic Parkinson's Disease. *Int. Rev. Neurobiol.* 141, 347–363. doi: 10.1016/bs.irn.2018.08.009

Sebastian-Valverde, M., and Pasinetti, G. M. (2020). The NLRP3 Inflammasome as a Critical Actor in the Inflammaging Process. *Cells* 9:cells9061552. doi: 10.3390/cells9061552

Sharma, S., Bandopadhyay, R., Lashley, T., Renton, A. E. M., Kingsbury, A. E., Kumaran, R., et al. (2011). LRRK2 expression in idiopathic and G2019S positive Parkinson's disease subjects: a morphological and quantitative study. *Neuropathol. Appl. Neurobiol.* 37, 777–790. doi: 10.1111/j.1365-2990.2011.01187.x

Simón-Sánchez, J., Schulte, C., Bras, J. M., Sharma, M., Gibbs, J. R., Berg, D., et al. (2009). Genome-wide association study reveals genetic risk underlying Parkinson's disease. *Nat. Genet.* 41, 1308–1312.

Simunovic, F., Yi, M., Wang, Y., Macey, L., Brown, L. T., Krichevsky, A. M., et al. (2009). Gene expression profiling of substantia nigra dopamine neurons: further insights into Parkinson's disease pathology. *Brain* 132, 1795–1809. doi: 10.1093/brain/awn323

Smajić, S., Prada-Medina, C. A., Landoulsi, Z., Dietrich, C., Jarazo, J., Henck, J., et al. (2020). Single-cell sequencing of the human midbrain reveals glial activation and a neuronal state specific to Parkinson's disease. *bioRxiv* [Preprint]. doi: 10.1101/2020.09.28.20202812

Su, X., Maguire-Zeiss, K. A., Giuliano, R., Prifti, L., Venkatesh, K., and Federoff, H. J. (2008). Synuclein activates microglia in a model of Parkinson's

disease. *Neurobiol. Aging* 29, 1690–1701. doi: 10.1016/j.neurobiolaging.2007.04.006

Sun, Y., Ma, J., Li, D., Li, P., Zhou, X., Li, Y., et al. (2019). Interleukin-10 inhibits interleukin-1β production and inflammasome activation of microglia in epileptic seizures. *J. Neuroinflamm.* 16:66. doi: 10.1186/s12974-019-1452-1

Swanson, K. V., Deng, M., and Ting, J. P.-Y. (2019). The NLRP3 inflammasome: molecular activation and regulation to therapeutics. *Nat. Rev. Immunol.* 19, 477–489. doi: 10.1038/s41577-019-0165-0

Terada, T., Yokokura, M., Yoshikawa, E., Futatsubashi, M., Kono, S., Konishi, T., et al. (2016). Extrastriatal spreading of microglial activation in Parkinson's disease: a positron emission tomography study. *Ann. Nucl. Med.* 30, 579–587. doi: 10.1007/s12149-016-1099-2

Tolosa, E., Vila, M., Klein, C., and Rascol, O. (2020). LRRK2 in Parkinson disease: challenges of clinical trials. *Nat. Rev. Neurol.* 16, 97–107.

Umeno, J., Asano, K., Matsushita, T., Matsumoto, T., Kiyohara, Y., Iida, M., et al. (2011). Meta-analysis of published studies identified eight additional common susceptibility loci for Crohn's disease and ulcerative colitis. *Inflamm. Bowel Dis.* 17, 2407–2415. doi: 10.1002/ibd.21651

Van Limbergen, J., Wilson, D. C., and Satsangi, J. (2009). The genetics of Crohn's disease. *Annu. Rev. Genomics Hum. Genet.* 10, 89–116.

van Wilgenburg, B., Browne, C., Vowles, J., and Cowley, S. A. (2013). Efficient, long term production of monocyte-derived macrophages from human pluripotent stem cells under partly-defined and fully-defined conditions. *PLoS One* 8:e71098. doi: 10.1371/journal.pone.0071098

Varrette, S., Bouvry, P., Cartiaux, H., and Georgatos, F. (2014). "Management of an academic HPC cluster: The UL experience," in *2014 International Conference on High Performance Computing Simulation (HPCS)*, (Bologna: HPCS), 959–967.

Wang, Q., Liu, Y., and Zhou, J. (2015). Neuroinflammation in Parkinson's disease and its potential as therapeutic target. *Transl. Neurodegener.* 4:19.

Weindel, C. G., Bell, S. L., Vail, K. J., West, K. O., Patrick, K. L., and Watson, R. O. (2020). LRRK2 maintains mitochondrial homeostasis and regulates innate immune responses to Mycobacterium tuberculosis. *Elife* 9:51071. doi: 10.7554/eLife.51071

Yan, Y.-Q., Fang, Y., Zheng, R., Pu, J.-L., and Zhang, B.-R. (2020). NLRP3 Inflammasomes in Parkinson's disease and their Regulation by Parkin. *Neuroscience* 446, 323–334. doi: 10.1016/j.neuroscience.2020.08.004

Yılmazer, S., Candaş, E., Genç, G., Alaylıoğlu, M., Şengül, B., Gündüz, A., et al. (2021). Low Levels of LRRK2 Gene Expression are Associated with LRRK2 SNPs and Contribute to Parkinson's Disease Progression. *Neuromol. Med.* 23, 292–304. doi: 10.1007/s12017-020-08619-x

Zeng, X.-S., Geng, W.-S., Jia, J.-J., Chen, L., and Zhang, P.-P. (2018). Cellular and Molecular Basis of Neurodegeneration in Parkinson Disease. *Front. Aging Neurosci.* 10:109. doi: 10.3389/fnagi.2018.00109

Zhang, F.-R., Huang, W., Chen, S.-M., Sun, L.-D., Liu, H., Li, Y., et al. (2009). Genomewide association study of leprosy. *N. Engl. J. Med.* 361, 2609–2618.

Zhong, Z., Umemura, A., Sanchez-Lopez, E., Liang, S., Shalapour, S., Wong, J., et al. (2016). NF-κB Restricts Inflammasome Activation via Elimination of Damaged Mitochondria. *Cell* 164, 896–910. doi: 10.1016/j.cell.2015.12.057

Conflict of Interest: The authors declare that the research was conducted in the absence of any commercial or financial relationships that could be construed as a potential conflict of interest.

Publisher's Note: All claims expressed in this article are solely those of the authors and do not necessarily represent those of their affiliated organizations, or those of the publisher, the editors and the reviewers. Any product that may be evaluated in this article, or claim that may be made by its manufacturer, is not guaranteed or endorsed by the publisher.

Supplemental information

IPSC-derived microglia as a model to study inflammation in idiopathic Parkinson's disease

Katja Badanjak[1], Patrycja Mulica[1], Semra Smajic[1], Sylvie Delcambre[1], Leon-Charles Tranchevent[1], Nico Diederich[2], Thomas Rauen[3], Jens C. Schwamborn[1], Enrico Glaab[1], Sally A. Cowley[4], Paul Antony[1], Sandro Pereira[1], Carmen Venegas[1], Anne Grünewald[1,5*]

Supplementary Table 1. Gene expression analysis of human IPD and control SN transcriptome.

Gene symbol	Z-score	FDR
IL1B	2.273739646	0.022981645
IL6	-0.293008563	0.769515607
IL10	2.710259928	0.00672305
IL18	1.512416069	0.13042805
IL8	1.290107048	0.197013493
TNF	-0.37382918	0.708531408

Supplementary Table 2. Gene expression analysis in IPD and control microglia of the human midbrain single-cell transcriptome.

Gene symbol	Average expression	Percent expressed	cluster_id
IL1B	0.325002368	5.55967383	Microglia_IPD
IL6	0.003882633	0.11119348	Microglia_IPD
IL18	3.170897328	63.45441067	Microglia_IPD
TNF	0.011861339	0.48183840	Microglia_IPD
IL10	0.015103408	0.70422535	Microglia_IPD
IL8	0.014423550	0.29651594	Microglia_IPD
IL1B	0.306312685	2.98755187	Microglia_Control
IL6	0.002964900	0.08298755	Microglia_Control
IL18	3.089786862	59.33609959	Microglia_Control
TNF	0.000000000	0.00000000	Microglia_Control
IL10	0.007378525	0.24896266	Microglia_Control
IL8	0.002578054	0.08298755	Microglia_Control

3.3 Manuscript IV

Mitochondrial damage-associated inflammation highlights biomarkers in PRKN/PINK1 parkinsonism

Max Borsche[1,2], Inke R. König[3,*], Sylvie Delcambre[4,*], Simona Petrucci[5,6], Alexander Balck[1,2], Norbert Brüggemann[1,2], Alexander Zimprich[7], Kobi Wasner[4], Sandro L. Pereira[4], Micol Avenali[8], Christian Deuschle[9,10], Katja Badanjak[4], Jenny Ghelfi[4], Thomas Gasser[9,10],Meike Kasten[1,11], Philip Rosenstiel[12], Katja Lohmann[1], Kathrin Brockmann[9,10], Enza Maria Valente[8,13], Richard J. Youle[14], Anne Grünewald[1,4*], and Christine Klein[1,*]

[*]Equal contribution

[1]Institute of Neurogenetics, University of Lübeck, Lübeck, Germany
[2]Department of Neurology, University of Lübeck, Lübeck, Germany
[3]Institute of Medical Biometry and Statistics, University of Lübeck, Lübeck, Germany
[4]Luxembourg Centre for Systems Biomedicine, University of Luxembourg, Esch-sur-Alzette, Luxembourg
[5]Department of Clinical and Molecular Medicine, Sapienza University of Rome, Rome, Italy
[6]Division of Medical Genetics, IRCCS-Casa Sollievo della Sofferenza, San Giovanni Rotondo, Italy
[7]Department of Neurology, Medical University of Vienna, Vienna, Austria
[8]IRCCS Mondino Foundation, Pavia, Italy
[9]Department of Neurodegenerative Diseases, Hertie Institute for Clinical Brain Research, University of Tübingen, Tübingen, Germany
[10]German Center for Neurodegenerative Diseases (DZNE), University of Tübingen, Tübingen, Germany
[11]Department of Psychiatry, University of Lübeck, Lübeck, Germany
[12]Institute for Clinical Molecular Biology, Christian-Albrechts-University Kiel, Kiel, Germany
[13]Department of Molecular Medicine, University of Pavia, Pavia, Italy
[14]Biochemistry Section, Surgical Neurology Branch, National Institute of Neurological Disorders and Stroke, National Institutes of Health, Bethesda, Maryland, USA

This article has been published in *Brain: A Journal of Neurology*.

3.3.1 Preface

Certain innate immune responses can be a direct consequence of mitochondrial dysfunction. The PD-linked protein PINK1 and Parkin are regulating the process of mitophagy and are known as suppressors of inflammation (Litwiniuk et al., 2021). Disruptive mitophagy can lead to the release of mitochondrial damage–associated molecular patterns (mtDAMPs) such as mtROS, mtDNA, and cytochrome c. Furthermore, the release of mtDNA was shown to induce the cGAS/ STING and/or NLRP3 inflammasome pathways, and subsequently the transcription/ cleavage of pro-inflammatory cytokines (Haque et al., 2020; Mishra et al., 2021; Sliter et al., 2018; West et al., 2015).
In the following study, inflammatory biomarkers were assessed in serum samples from individuals with heterozygous or biallelic mutations in *PRKN* and *PINK1* as well as from IPD patients and controls. Interestingly, *PRKN* or *PINK1*-mutant patients had higher serum levels of IL6 and C-reactive protein (CRP) compared to healthy individuals. Furthermore, IL6 was positively correlated with the disease duration in PD patients, suggestive of a cumulative and progressive effect of *PRKN* and *PINK1* mutations to cytokine release. The upregulation of IL6 and CRP was accompanied by higher levels of circulating cell-free (ccf) mtDNA in the serum, implicating mitochondrial dysfunction as primary mechanism of inflammation in *PRKN/PINK1* patients.

My contribution to this study was the extraction of DNA from serum samples, and final revision of the manuscript.

doi:10.1093/brain/awaa246 BRAIN 2020: 143; 3041–3051 | 3041

BRAIN
A JOURNAL OF NEUROLOGY

Mitochondrial damage-associated inflammation highlights biomarkers in *PRKN/PINK1* parkinsonism

Max Borsche,[1,2] Inke R. König,[3,*] Sylvie Delcambre,[4,*] Simona Petrucci,[5,6] Alexander Balck,[1,2] Norbert Brüggemann,[1,2] Alexander Zimprich,[7] Kobi Wasner,[4] Sandro L. Pereira,[4] Micol Avenali,[8] Christian Deuschle,[9,10] Katja Badanjak,[4] Jenny Ghelfi,[4] Thomas Gasser,[9,10] Meike Kasten,[1,11] Philip Rosenstiel,[12] Katja Lohmann,[1] Kathrin Brockmann,[9,10] Enza Maria Valente,[8,13] Richard J. Youle,[14] Anne Grünewald[1,4,*] and Christine Klein[1,*]

*These authors contributed equally to this work.

There is increasing evidence for a role of inflammation in Parkinson's disease. Recent research in murine models suggests that parkin and PINK1 deficiency leads to impaired mitophagy, which causes the release of mitochondrial DNA (mtDNA), thereby triggering inflammation. Specifically, the CGAS (cyclic GMP-AMP synthase)-STING (stimulator of interferon genes) pathway mitigates activation of the innate immune system, quantifiable as increased interleukin-6 (IL6) levels. However, the role of IL6 and circulating cell-free mtDNA in unaffected and affected individuals harbouring mutations in *PRKN/PINK1* and idiopathic Parkinson's disease patients remain elusive. We investigated IL6, C-reactive protein, and circulating cell-free mtDNA in serum of 245 participants in two cohorts from tertiary movement disorder centres. We performed a hypothesis-driven rank-based statistical approach adjusting for multiple testing. We detected (i) elevated IL6 levels in patients with biallelic *PRKN/PINK1* mutations compared to healthy control subjects in a German cohort, supporting the concept of a role for inflammation in *PRKN/PINK1*-linked Parkinson's disease. In addition, the comparison of patients with biallelic and heterozygous mutations in *PRKN/PINK1* suggests a gene dosage effect. The differences in IL6 levels were validated in a second independent Italian cohort; (ii) a correlation between IL6 levels and disease duration in carriers of *PRKN/PINK1* mutations, while no such association was observed for idiopathic Parkinson's disease patients. These results highlight the potential of IL6 as progression marker in Parkinson's disease due to *PRKN/PINK1* mutations; (iii) increased circulating cell-free mtDNA serum levels in both patients with biallelic or with heterozygous *PRKN/PINK1* mutations compared to idiopathic Parkinson's disease, which is in line with previous findings in murine models. By contrast, circulating cell-free mtDNA concentrations in unaffected heterozygous carriers of *PRKN/PINK1* mutations were comparable to control levels; and (iv) that circulating cell-free mtDNA levels have good predictive potential to discriminate between idiopathic Parkinson's disease and Parkinson's disease linked to heterozygous *PRKN/PINK1* mutations, providing functional evidence for a role of heterozygous mutations in *PRKN* or *PINK1* as Parkinson's disease risk factor. Taken together, our study further implicates inflammation due to impaired mitophagy and subsequent mtDNA release in the pathogenesis of *PRKN/PINK1*-linked Parkinson's disease. In individuals carrying mutations in *PRKN/PINK1*, IL6 and circulating cell-free mtDNA levels may serve as markers of Parkinson's disease state and progression, respectively. Finally, our study suggests that targeting the immune system with anti-inflammatory medication holds the potential to influence the disease course of Parkinson's disease, at least in this subset of patients.

1 Institute of Neurogenetics, University of Lübeck, Lübeck, Germany
2 Department of Neurology, University of Lübeck, Lübeck, Germany

Received December 17, 2019. Revised May 14, 2020. Accepted June 17, 2020. Advance access publication October 8, 2020

3042 | BRAIN 2020: 143; 3041–3051 M. Borsche et al.

3 Institute of Medical Biometry and Statistics, University of Lübeck, Lübeck, Germany
4 Luxembourg Centre for Systems Biomedicine, University of Luxembourg, Esch-sur-Alzette, Luxembourg
5 Department of Clinical and Molecular Medicine, Sapienza University of Rome, Rome, Italy
6 Division of Medical Genetics, IRCCS-Casa Sollievo della Sofferenza, San Giovanni Rotondo, Italy
7 Department of Neurology, Medical University of Vienna, Vienna, Austria
8 IRCCS Mondino Foundation, Pavia, Italy
9 Department of Neurodegenerative Diseases, Hertie Institute for Clinical Brain Research, University of Tübingen, Tübingen, Germany
10 German Center for Neurodegenerative Diseases (DZNE), University of Tübingen, Tübingen, Germany
11 Department of Psychiatry, University of Lübeck, Lübeck, Germany
12 Institute for Clinical Molecular Biology, Christian-Albrechts-University Kiel, Kiel, Germany
13 Department of Molecular Medicine, University of Pavia, Pavia, Italy
14 Biochemistry Section, Surgical Neurology Branch, National Institute of Neurological Disorders and Stroke, National Institutes of Health, Bethesda, Maryland, USA

Correspondence to: Christine Klein, MD
Institute of Neurogenetics, University of Lübeck, Maria-Goeppert-Str. 1, 23562 Lübeck
Germany
E-mail: christine.klein@neuro.uni-luebeck.de

Keywords: Parkinson's disease; parkin; PINK1; IL6; ccf-mtDNA

Abbreviations: ccf-mtDNA = circulating cell-free mitochondrial DNA; STING = stimulator of interferon genes

Introduction

Multiple lines of evidence support an association between Parkinson's disease and inflammatory processes (Hirsch and Hunot, 2009). In particular, pro-inflammatory cytokines are elevated in serum and CSF samples from patients with Parkinson's disease (Dzamko *et al.*, 2015). These studies are in keeping with the epidemiological observation that intake of anti-inflammatory drugs lowers the risk of developing Parkinson's disease (Noyce *et al.*, 2012). However, it remains unclear if inflammation originates from peripheral tissue or the CNS. If the latter is true, additional studies are required to clarify if the observed inflammation triggers the loss of dopaminergic neurons as a primary event or whether it is a secondary consequence of neurodegeneration. Either way, there is evidence that cytokines, such as interleukin-6 (IL6), overcome the blood–brain barrier and are transported from brain tissue to the blood and vice versa (Banks, 2015). Despite more than two decades of intense research, the molecular pathways connecting interleukin release and anti-inflammatory treatment with Parkinson's disease remain largely elusive.

Biallelic mutations in parkin (encoded by *PRKN*) and *PINK1* cause Parkinson's disease with typical clinical features, albeit with an earlier age of onset (Kasten *et al.*, 2018). The role of heterozygous mutations as a risk factor for Parkinson's disease is still under debate as epidemiological analyses provided controversial results (Reed *et al.*, 2019). Moreover, data on the occurrence of Lewy bodies as a hallmark of Parkinson's disease is limited and must be interpreted with caution in the context of monogenic Parkinson's disease (Schneider and Alcalay, 2017). However, there is evidence that heterozygous mutations increase the risk of developing Parkinson's disease with an age of onset falling between that of biallelic mutation carriers and idiopathic Parkinson's disease patients (Klein *et al.*, 2007; Grünewald *et al.*, 2013; Huttenlocher *et al.*, 2015). Parkin and PINK1 are part of the molecular pathway that controls mitophagy (Narendra *et al.*, 2012). Intriguingly, parkin or PINK1 deficiency leads to CGAS (cyclic GMPD-AMP synthase)/STING (stimulator of interferon genes)-dependent activation of a type I interferon response, associated with increased IL6 levels in biallelic *PRKN*/*PINK1* knockout mice (Sliter *et al.*, 2018).

IL6 is a pro-inflammatory cytokine, which acts in the initiation of innate immune responses, induces the release of C-reactive protein (CRP) (Tanaka *et al.*, 2014), and is elevated in serum samples from patients with Parkinson's disease (Qin *et al.*, 2016). While the particular role of IL6 and CRP in inflammation is controversial (Del Giudice and Gangestad, 2018), there is convincing evidence that IL6 increases with age (Puzianowska-Kuźnicka *et al.*, 2016). Circulating cell-free mitochondrial DNA (ccf-mtDNA) plays a role in the aetiology of various (systemic) diseases including immune responses (West and Shadel, 2017). Connecting impaired mitochondrial clearance and inflammation, the release of ccf-mtDNA into the cytosol triggers innate immunity activation (West and Shadel, 2017) through CGAS/STING (Lood *et al.*, 2016), TLR9 (Toll-like receptor 9) or inflammasomes such as NLRP3 (nucleotide-binding oligomerization domain-like receptor family, pyrin domain-containing-3) (Zhong *et al.*, 2018). In idiopathic Parkinson's disease, reduced mtDNA levels have been observed in the CSF in early-stage idiopathic Parkinson's disease (Pyle *et al.*, 2015). However, no reports have indicated an association between serum ccf-mtDNA levels and neurodegeneration in general and with Parkinson's disease in particular.

With the aim to decipher the role of the cGAS-STING pathway in neuroinflammatory processes in monogenic Parkinson's disease, we have previously analysed IL6 levels in a small pilot sample of *PRKN* and *PINK1* mutation carriers, idiopathic Parkinson's disease patients, and healthy control subjects, demonstrating increased IL6 levels in patients with biallelic *PRKN* mutations (Sliter *et al.*, 2018). In light of the molecular mechanism identified in mice, in the current study, we hypothesized that STING signalling is triggered by ccf-mtDNA as a consequence of impaired mitophagy and results in IL6 elevation in human *PRKN* and *PINK1* mutation carriers. Using a hypothesis-driven statistical approach, we investigated, for the first time, ccf-mtDNA along with IL6 and CRP levels in sera from a large sample of patients with monogenic or idiopathic Parkinson's disease and control subjects.

Materials and methods

Patient recruitment and collection of samples

In the context of the present cross-sectional study, participants were recruited at tertiary movement disorder referral centres in Lübeck, Tübingen (Germany), and Pavia/Rome (Italy). Samples from the University of Lübeck were collected within the SysMedPD study, the EPIPARK cohort (Kasten *et al.*, 2012), and the Transregional Collaborative Research Center 134. All participants gave written informed consent, and the local ethics committees approved the study. Patients were neurologically examined by a movement disorder specialist. Demographic and clinical data, such as sex, age at examination, and regarding patients with Parkinson's disease, age at onset and disease duration were assessed. For a subset of patients, more detailed phenotypic information was obtainable including data referring to the disease state [Hoehn and Yahr stage, Movement Disorder Society Unified Parkinson's Disease Rating Scale part III (MDS-UPDRS III)], and olfactory impairment. Results from patients examined using the previous version of the UPDRS III were transformed into MDS-UPDRS III values as described (Goetz *et al.*, 2012). Olfactory impairment was assessed using the Brief Smell Identification Test (BSIT) or via TDI scores from the Sniffin' Sticks test, respectively, and age-adjusted.

Mutation carriers were identified by Sanger or gene panel sequencing, multiplex ligation-dependent probe amplification (MLPA) analysis, or real-time PCR analysis. We identified *PRKN* variants in 57 study participants and *PINK1* variants in 25 participants. Unaffected individuals harbouring nucleotide changes, which were classified as variants of unknown significance according to ACMG recommendations (Richards *et al.*, 2015), were excluded from the study.

Venous blood was obtained for preparation of serum and DNA extraction. Blood draw and clinical examination took place between 2004 and 2019. In total, samples from 245 participants were analysed. Samples from Lübeck and Tübingen were combined to form the 'German cohort' including 15 biallelic *PRKN/PINK1*, 19 affected heterozygous *PRKN/PINK1*, 15 unaffected heterozygous *PRKN/PINK1* mutation carriers, 59 idiopathic Parkinson's disease patients and 90 healthy, mutation-free control subjects. We aimed to replicate the results of the German cohort in an independent cohort from another centre. Therefore, we additionally investigated the so-called 'Italian cohort' consisting of 19 *PRKN/PINK1* biallelic, five affected heterozygous, nine unaffected heterozygous mutation carriers, as well as five idiopathic Parkinson's disease patients and nine healthy control subjects.

IL6 values from 45 individuals already reported previously (Sliter *et al.*, 2018) were included in the present study, but their serum samples were re-measured in a different laboratory (Supplementary Table 1). Since on rare occasions selected measurements (IL6, CRP or ccf-mtDNA) failed for individual study participants, sample numbers differ between analyses and are therefore indicated for each experiment.

Sample processing

At all study centres, venous blood was collected in serum tubes. Samples were centrifuged at 4°C for 10 min at 2000–4000*g* dependent on the centre within 2 h after blood collection. After centrifugation, samples were immediately frozen at −80°C.

IL6 and CRP measurements

IL6 was measured using an ELISA (Cobas Elecsys IL6 assay). High-sensitive CRP was investigated using particle-enhanced immunonephelometry (Cobas CRPHS assay). Both analyses were performed at the certified diagnostic laboratory LADR Centrallab Dr Kramer and Colleagues, Geesthacht, Germany. Samples from Lübeck and Tübingen (German cohort) were measured together in one run, those of the Italian cohort in a second run. Possibly due to batch effects, the Italian samples exhibited considerably lower IL6 levels (Italian cohort: 2.9 ± 2.9 pg/ml, $n = 47$; German cohort: 5.90 ± 1.90 pg/ml, $n = 181$). Because of these batch-dependent differences in IL6 levels, correlation analyses included only samples from the German cohort. As rank-based statistics were used throughout, values below the detection limit (IL6: 1.5 pg/ml; CRP: 0.3 mg/l) were set to arbitrarily small values of 1.4 pg/ml and 0.2 mg/l, respectively. IL6 and CRP levels were measured in a blinded fashion.

Quantification of serum circulating ccf-mtDNA levels

Levels of ccf-mtDNA in the serum samples from the German cohort were analysed in an equally blinded fashion at the Luxembourg Centre for Systems Biomedicine, University of Luxembourg.

DNA from serum of the German cohort was extracted using the QIAamp 96 DNA blood extraction kit (Qiagen) according to the manufacturer's instructions. Digital PCR (dPCR) was used to quantify ccf-mtDNA. The dPCR assay was performed using TaqMan™ technology. Primers and probes coupled with non-fluorescent quenchers were used to quantify fragments within the mitochondrial gene *MT-ND1* and the nuclear single-copy gene *B2M* (Phillips *et al.*, 2014; Rygiel *et al.*, 2015). Digital PCR was performed using the QuantStudio™ 3D Digital PCR System (Applied Biosystems), and samples were prepared following the manufacturer's instructions. Samples were loaded on a QuantStudio™ 3D digital PCR Chip v2 using

the QuantStudio™ 3D Digital PCR Chip loader. The PCR was then performed on the ProFlex™ 2X Flat PCR System using a previously published programme (Rygiel *et al.*, 2015). The chips were read using the QuantStudio™ 3D Digital PCR Instrument and the data were analysed using the QuantStudio™ 3D AnalysisSuite, version 3.1.6-PRC-build2. Samples with a *B2M* copy number >200 copies/µl were considered as contaminated with nuclear DNA and were not considered for further analysis.

Statistical analysis

The phenotypic characteristics of the study cohort, correlation analyses, and differences in CRP levels are presented at a descriptive level.

In one individual, the IL6 value was implausibly elevated [>10 standard deviations (SD) above the mean] and thus set to missing. The following group differences were tested in the German cohort: (i) IL6 between *PRKN/PINK1* biallelic, *PRKN/PINK1* heterozygous affected, *PRKN/PINK1* heterozygous unaffected, and healthy mutation-negative controls; (ii) IL6 between *PRKN/PINK1* biallelic, idiopathic Parkinson's disease, and healthy controls; and (iii) ccf-mtDNA between *PRKN/PINK1* biallelic, *PRKN/PINK1* heterozygous affected, *PRKN/PINK1* heterozygous unaffected, idiopathic Parkinson's disease, and healthy controls. For the first two comparisons, an ordered effect was assumed and Jonckheere-Terpstra tests performed; for the latter, no specific order was assumed, so that a Kruskal-Wallis test was performed. When significant, results were followed-up with pairwise Wilcoxon rank sum tests. To account for multiple testing (Harrington *et al.*, 2019) of three hypotheses, the overall significance level of 0.05 was adjusted to 0.0167. To evaluate whether the observed effects might be confounded by different ages at examination of the probands, we performed a sensitivity analysis taking age at examination into account. Specifically, we first performed linear regressions to predict log(IL6) and log(ccf-mtDNA), respectively, from age at examination and saved the residuals. Second, we tested for differences in the resulting residuals between groups as before. Moreover, we analysed the utility of ccf-mtDNA levels to discriminate between idiopathic Parkinson's disease and Parkinson's disease associated with heterozygous *PRKN/PINK1* mutations using a receiving operating characteristic (ROC) curve. Finally, we investigated a possible dependency of IL6 on disease duration in idiopathic and parkin/PINK1-associated Parkinson's disease patients after adjusting for age at examination. Thus, we performed a linear regression to predict disease duration from age and saved the residuals. The latter were then used in a correlation analysis with IL6. Data from the Italian cohort were used for replication purposes only and thus required no additional adjustment. Analyses were performed using R version 3.5 (R Core Team, 2018). Figures were created with GraphPad Prism 8.

Data availability

The data used in this study are available from the corresponding author, upon reasonable request.

Results

The following three hypotheses were addressed in this paper. First, we aimed to re-evaluate serum IL6 levels in *PRKN* mutation carriers in a larger study cohort and to extend our analysis to *PINK1* mutation carriers. Second, we investigated if a gene dosage effect for IL6 exists when comparing biallelic with heterozygous *PRKN/PINK1* mutation carriers and idiopathic Parkinson's disease patients. Third, to explore a possible link between impaired mitophagy, the CGAS-STING pathway, and inflammatory signalling in Parkinson's disease, we quantified the abundance of ccf-mtDNA in serum in our cohort.

Phenotypic characterization of the study cohort

Table 1 shows demographic data for the five study groups investigated here. For patients with Parkinson's disease, mean age at onset, disease duration, MDS-UPDRS III, Hoehn and Yahr stage, and the frequency of olfactory dysfunction were additionally provided. The essential study groups, namely *PRKN/PINK1* biallelic, affected heterozygous, and healthy control subjects, were age-matched. By contrast, as idiopathic Parkinson's disease occurs at a later age than recessively inherited monogenic Parkinson's disease (Kasten *et al.*, 2018), patients with idiopathic Parkinson's disease were older at the time of examination and sampling of biomaterials.

In our cohorts, Parkinson's disease associated with biallelic mutations in *PRKN/PINK1* was characterized by an earlier age of onset, a longer disease duration, and reduced olfactory impairment, while affected heterozygotes exhibited similar clinical features as idiopathic Parkinson's disease patients. Accordingly, the clinical phenotypes of participants included in our study agreed with previously described characteristics (Alcalay *et al.*, 2011; Kasten *et al.*, 2018), indicating that we investigated a representative group of monogenic and idiopathic Parkinson's disease patients.

IL6 is elevated in the serum of Parkinson's disease patients with biallelic mutations in *PRKN* or *PINK1*

As a first step, we tested the distribution of serum IL6 levels in the German cohort (Table 2 and Fig. 1A and C). We hypothesized that patients with Parkinson's disease, due to biallelic mutations in *PRKN* or *PINK1*, exhibit higher IL6 levels compared to healthy control subjects and higher levels compared to affected and unaffected heterozygous mutation carriers, while heterozygous mutation carriers were expected to show higher IL6 levels than healthy control subjects. We confirmed the assumed order ($P = 0.0018$, Fig. 1A). Moreover, pairwise analyses of *PRKN/PINK1* biallelic patients compared to healthy controls showed a significant

Table 1 Demographics and clinical characteristics of study participants

	PRKN/PINK1 mutation carrier	Sex, females (%)	Age at onset, years (*n*)	Age at examination, years (*n*)	Disease duration, years (*n*)	MDS-UPDRS III (*n*)	Hoehn and Yahr stage (*n*)	Olfactory impairment (%)
PRKN/PINK1 biallelic	23/11	21/34 (61.8)	33.2 ± 8.1 (34)	51.3 ± 11.7 (34)	18.1 ± 8.8 (34)	32.2 ± 16.9 (11)	2.6 ± 1.0 (11)	9/19 (47.4)
PRKN/PINK1 affected heterozygous	19/5	13/24 (54.2)	44.4 ± 11.8 (22)	53.8 ± 13.0 (24)	8.9 ± 8.9 (22)	24.8 ± 14.7 (6)	2.2 ± 0.41 (6)	9/13 (69.2)
PRKN/PINK1 unaffected heterozygous	15/11	10/24 (41.7)	NA	50.7 ± 13.4 (24)	NA	NA	NA	5/20 (25.0)
Idiopathic Parkinson's disease	NA	29/64 (45.3)	53.1 ± 11.9 (64)	61.6 ± 11.9 (64)	8.4 ± 6.1 (64)	31.7 ± 15.1 (40)	2.4 ± 0.6 (40)	32/39 (82.1)
Healthy controls	NA	57/99 (57.6)	NA	55.1 ± 10.9 (98)	NA	NA	NA	14/38 (36.8)

Sex and olfactory impairment are presented as part of the whole group with percentages in parentheses. Age at onset, age at examination, disease duration, Movement Disorder Society Unified Parkinson's Disease Rating Scale part III (MDS-UPDRS III), and Hoehn and Yahr stage are presented as mean ± standard deviation. NA = not applicable.

Table 2 IL6, CRP and mtDNA levels in the different study groups

	Cohort	IL6, pg/ml (*n*)	CRP, mg/l (*n*)	ccf-mtDNA, copy number (*n*)
PRKN/PINK1 biallelic	German	6.8 [5.6–8.5] (15)	2.7 [1.1–7.1] (15)	2774 [1315–5647] (13)
	Italian	3.0 [2.1–4.5] (19)	2.5 [0.8–4.3] (19)	NA
PRKN/PINK1 affected heterozygous	German	5.4 [4.7–6.5] (18)	1.1 [0.6–3.6] (18)	3608 [1724–5471] (17)
	Italian	2.3 [1.8–2.7] (5)	0.7 [0.3–6.9] (5)	NA
PRKN/PINK1 unaffected heterozygous	German	5.5 [4.6–6.4] (13)	0.9 [0.5–2.3] (13)	1487 [830–2194] (14)
	Italian	1.4 [1.4–2.2] (9)	1.0 [0.8–1.8] (9)	NA
Idiopathic Parkinson's disease	German	5.5 [4.7–7.1] (51)	1.2 [0.4–2.2] (51)	1226 [655–2015] (57)
	Italian	1.6 [1.5–2.5] (5)	1.0 [0.9–4.2] (5)	NA
Healthy controls	German	5.0 [4.5–6.0] (84)	1.0 [0.4–2.1] (85)	1434 [715–2688] (55)
	Italian	1.4 [1.4–1.7] (9)	0.7 [0.2–2.8] (9)	NA
All participants	German	5.3 [4.7–6.5] (181)	1.1 [0.5–2.4] (182)	1467 [752–3051] (156)
	Italian	2.1 [1.4–2.9] (47)	1.3 [0.7–3.0] (47)	NA

Distribution of IL6, CRP and ccf-mtDNA in the different study groups separated into the German and the Italian cohorts. Results are presented as median [IQR]. Statistics are shown in Figs 1 and 2 and Supplementary Fig. 3. NA = not applicable.

IL6 elevation in patients with Parkinson's disease due to biallelic *PRKN/PINK1* mutations ($P = 0.0006$, Fig. 1A). Investigating IL6 levels in the Italian cohort (Table 2 and Fig. 1B) showed similar differences (*PRKN/PINK1* biallelic > affected/unaffected heterozygotes > healthy controls; $P = 0.00008$). Pairwise analyses revealed significantly higher IL6 values in *PRKN/PINK1* biallelic patients ($P = 0.007$) and a trend towards elevated IL6 levels in affected heterozygous mutation carriers ($P = 0.065$) compared to healthy control subjects (Fig. 1B). By contrast, unaffected heterozygotes did not show an increase. Moreover, we found increased IL6 levels comparing *PRKN/PINK1* biallelic with unaffected heterozygous mutation carriers ($P = 0.0062$). A similar trend was also present in the German cohort ($P = 0.0302$, Fig. 1A).

Moreover, we hypothesized that *PRKN/PINK1* biallelic mutation carriers exhibit higher IL6 levels than patients with idiopathic Parkinson's disease, while we expected individuals in the idiopathic Parkinson's disease group to present with higher serum IL6 than healthy control subjects. Indeed, we confirmed the expected order (*PRKN/PINK1* biallelic > idiopathic Parkinson's disease > healthy controls; $P = 0.0005$, Fig. 1C). Performing pairwise analyses, we detected a trend towards higher IL6 levels in idiopathic Parkinson's disease patients than in healthy controls ($P = 0.0559$). As significance levels were adjusted to $P < 0.0167$ to account for multiple testing, differences in IL6 values between *PRKN/PINK1* biallelic mutation carriers and patients with idiopathic Parkinson's disease did not reach significance ($P = 0.0259$, Fig. 1C).

Analysing *PRKN* and *PINK1* mutation carriers separately, we did not detect any difference between IL6 levels, neither in biallelic nor in heterozygous mutation carriers (Supplementary Fig. 2). This was true for both the German (Supplementary Fig. 2A and C) and the Italian cohorts (Supplementary Fig. 2B and D).

IL6 triggers the release of CRP, which was also found to be upregulated in Parkinson's disease (Qiu *et al.*, 2019). Therefore, we investigated CRP levels (Table 2) exploring the same order as previously assumed for IL6. Investigating group differences in general, we saw no relevant differences (Supplementary Fig. 3A). However, we observed a trend

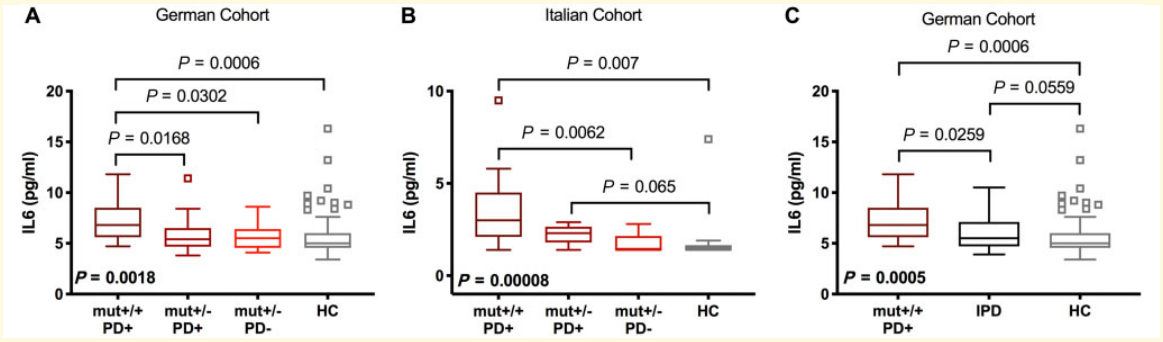

Figure 1 Interleukin 6 (IL6) is increased in serum from biallelic *PRKN/PINK1* mutation carriers compared to healthy controls. IL6 levels in serum samples from Parkinson's disease (PD) patients with mutations in *PRKN/PINK1*, unaffected mutation carriers, idiopathic Parkinson's disease (IPD) patients, and healthy control subjects (HC). (**A**) Patients with Parkinson's disease due to biallelic *PRKN/PINK1* mutations (mut+/+ PD+, $n = 15$) exhibited higher IL6 levels compared to healthy controls ($n = 84$). Unaffected heterozygous mutation carriers (mut+/– PD–, $n = 13$) showed similar IL6 levels compared to affected heterozygous mutation carriers (mut+/– PD+, $n = 18$). (**B**) Investigating an independent cohort from Italy yielded similar group differences as presented in **A**, while the total amount of IL6 among all participants was lower compared to the German cohort due to a batch effect (mut+/+ PD+, $n = 19$; mut+/– PD+, $n = 5$; mut+/– PD–, $n = 9$; HC, $n = 9$). Regarding the Italian cohort, biallelic *PRKN/PINK1* mutation carriers exhibited increased IL6 levels compared to unaffected heterozygotes. Moreover, there was a trend towards elevated IL6 levels in *PRKN/PINK1* affected heterozygotes compared to healthy control subjects. (**C**) In the German cohort, *PRKN/PINK1* biallelic patients showed a trend towards higher IL6 levels compared to patients with idiopathic Parkinson's disease ($n = 51$), while idiopathic Parkinson's disease patients exhibited a trend towards elevated IL6 release compared to healthy control subjects. As multiple testing was performed, the significance level was adjusted to $\alpha = 0.0167$. The assumed order among the different groups was tested with the Jonckheere-Terpstra test (bold, *lower left corner*). Pairwise differences between two groups were assessed using the Wilcoxon rank sum test. Data are presented as box and whisker plots. The box extends from the 25th to the 75th percentile. The line in the middle of the box represents the median. Tukey whiskers are used.

towards increased CRP levels in individuals with Parkinson's disease due to mutations in *PRKN/PINK1* compared to patients with idiopathic Parkinson's disease (exploratory $P = 0.0319$) and an elevation compared to healthy control subjects (exploratory $P = 0.0122$, Supplementary Fig. 3A). Moreover, CRP levels correlated with IL6 levels in affected biallelic and heterozygous *PRKN/PINK1* mutation carriers (Supplementary Fig. 3B), idiopathic Parkinson's disease patients (Supplementary Fig. 3C) and healthy control subjects (Supplementary Fig. 3D).

Circulating cell-free mtDNA is increased in Parkinson's disease patients with mutations in *PRKN* or *PINK1*

We expected affected heterozygous and biallelic *PRKN/PINK1* mutation carriers to exhibit higher serum levels of ccf-mtDNA compared to idiopathic Parkinson's disease patients and healthy controls. Statistical testing revealed group differences in general ($P = 0.0006$). Compared to patients with idiopathic Parkinson's disease, pairwise analyses showed increased ccf-mtDNA release in *PRKN/PINK1* biallelic mutation carriers ($P = 0.0094$) and affected heterozygous mutation carriers ($P = 0.0002$). Compared to healthy control subjects, we observed a trend towards elevated ccf-mtDNA levels in biallelic *PRKN/PINK1* mutation carriers ($P = 0.0459$) and an increase in affected heterozygous individuals ($P = 0.0019$). Furthermore, we found elevated ccf-mtDNA levels in affected compared to unaffected *PRKN/PINK1* heterozygotes ($P = 0.0058$, Table 2 and Fig. 2A). Moreover, assessing the utility of ccf-mtDNA levels to discriminate between idiopathic Parkinson's disease and Parkinson's disease associated with heterozygous *PRKN/PINK1* mutations, we found an area under the ROC curve of 0.81 (Fig. 2B).

IL6 levels are associated with disease duration in patients with *PRKN* or *PINK1* mutations

Focusing on idiopathic Parkinson's disease, we found a trend towards a positive correlation between IL6 levels and age (Fig. 3A). A similar association was absent in individuals with biallelic *PRKN/PINK1* mutations ($r = 0.018$, exploratory $P = 0.949$, $n = 15$) and in healthy control subjects ($r = 0.076$, exploratory $P = 0.490$, $n = 84$). Moreover, while in patients with Parkinson's disease due to *PRKN* or *PINK1* mutations IL6 levels correlated with disease duration (Fig. 3B), we found no such association in patients with idiopathic Parkinson's disease ($r = 0.065$, exploratory $P = 0.65$, $n = 51$).

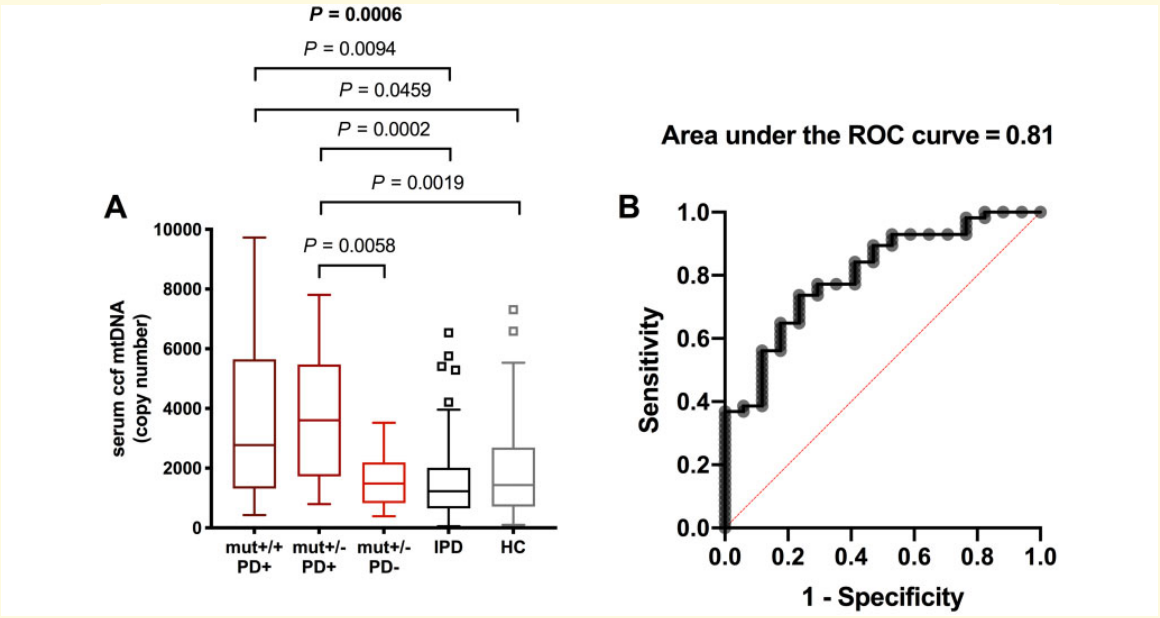

Figure 2 Serum ccf-mtDNA is increased in *PRKN*/*PINK1* mutation carriers and discriminates between affected heterozygotes and idiopathic Parkinson's disease patients. (**A**) Patients with Parkinson's disease (PD) due to biallelic *PRKN*/*PINK1* mutations (mut+/+ PD+, *n* = 13) and affected heterozygous individuals (mut+/– PD+, *n* = 17) exhibited elevated serum ccf-mtDNA levels compared to idiopathic Parkinson's disease patients (IPD, *n* = 57). Additionally, affected heterozygous patients showed higher ccf-mtDNA levels than healthy control subjects (HC, *n* = 55). Unaffected heterozygous mutation carriers (mut+/– PD–, *n* = 14) exhibited ccf-mtDNA levels between those of affected mutation carriers and idiopathic Parkinson's disease patients. As multiple testing was performed, the significance level was adjusted to $\alpha = 0.0167$. Group differences in general were tested via Kruskal-Wallis test (bold). Pairwise differences between two groups were analysed using the Wilcoxon rank sum test. Data are presented as box and whisker plots. The box extends from the 25th to the 75th percentile. The line in the middle of the box represents the median. Tukey whiskers are used. (**B**) Assessment of the utility of ccf-mtDNA levels to discriminate between idiopathic Parkinson's disease patients (*n* = 57) and affected heterozygous *PRKN*/*PINK1* mutation carriers (*n* = 17) investigated by a receiver operator characteristic (ROC) curve.

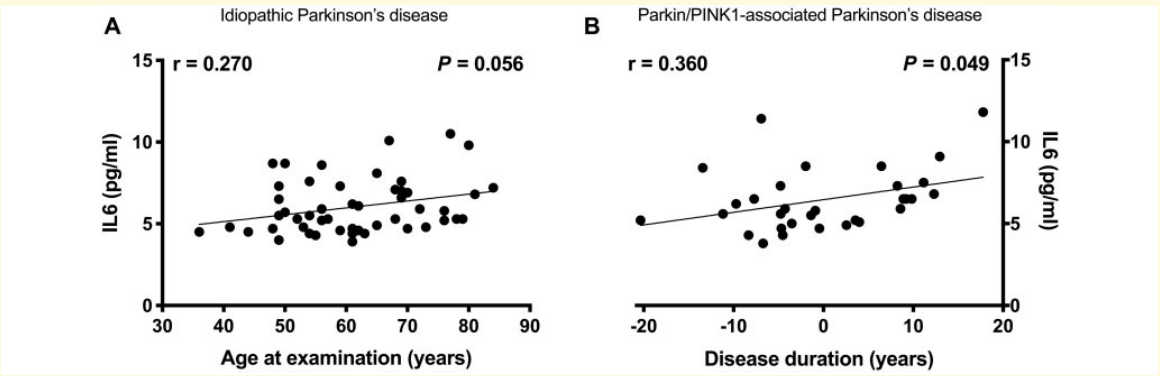

Figure 3 Association between age at examination, disease duration and IL6 release. (**A**) In patients with idiopathic Parkinson's disease (*n* = 51), we observed elevated IL6 levels with increasing age when determining the Spearman's correlation of both variables. (**B**) In *PRKN*/*PINK1* biallelic and heterozygous patients (*n* = 31), there was a positive correlation between disease duration and IL6 levels. The Spearman's correlation was calculated after adjusting for age at examination. Correlation coefficient is shown in the *top left*, exploratory *P*-values are presented in the *top right* corner. Lines represent linear regression.

As a sensitivity analysis, we additionally performed a linear regression analysis to predict the influence of age at examination on IL6 and ccf-mtDNA levels and used the resulting residuals to test for differences between study groups while taking age into account. Thereby, group- and pairwise differences in ccf-mtDNA levels remained unchanged. In the context of IL6 levels, the assumed order was still present after the adjustment for age ($P = 0.0008$). However, this adjustment led to differences regarding pairwise analyses between *PRKN/PINK1* biallelic mutation carriers and affected heterozygotes ($P = 0.0133$), supporting the assumed gene dosage effect of *PRKN* and *PINK1* mutated alleles in the context of IL6. Furthermore, this regression analysis revealed a difference in IL6 levels between *PRKN/PINK1* biallelic mutation carriers and idiopathic Parkinson's disease patients ($P = 0.0129$).

Discussion

Our study further implicates inflammation due to impaired mitophagy and subsequent mtDNA release in the pathogenesis of *PRKN/PINK1*-associated Parkinson's disease. We extended our previous findings in a small group of biallelic *PRKN* mutation carriers to an additional 18 biallelic *PRKN*, and—for the first time—11 biallelic *PINK1* mutation carriers. By this, we showed that *PRKN* and *PINK1* mutation carriers exhibit similar IL6 levels when investigated separately. As only IL6 elevation in biallelic *PRKN* mutation carriers was previously described, our study provides first-time evidence that IL6 is similarly increased in patients with Parkinson's disease due to biallelic *PINK1* mutations in line with the notion of both proteins being involved in a common pathway during mitophagy (Narendra *et al.*, 2012).

PRKN/PINK1 biallelic mutation carriers showed higher IL6 levels compared to heterozygous mutation carriers, suggesting a gene dosage effect regarding IL6 release. However, this interpretation is limited. Although we confirmed the presence of the assumed order *PRKN/PINK1* biallelic > *PRKN/PINK1* heterozygous > healthy controls, pairwise analysis between heterozygotes and healthy controls did not reach significance, which would have been necessary to show a complete gene dosage effect.

In accordance with previous reports (Qin *et al.*, 2016), we also found a trend towards elevated IL6 levels in idiopathic Parkinson's disease compared to healthy controls. In addition, we detected a positive correlation between IL6 levels and disease duration in affected *PRKN/PINK1* mutation carriers that was absent in patients with idiopathic Parkinson's disease, indicating a specific influence of the genetic alterations on IL6 levels. Moreover, although *PRKN* and *PINK1* mutation carriers included in our study were younger than idiopathic Parkinson's disease patients, they exhibited higher IL6 values, arguing for an age-independent IL6 elevation in *PRKN/PINK1* mutation carriers. Our findings appear robust, as samples from two independent cohorts revealed similar results.

In line with previous research (Tanaka *et al.*, 2014), CRP levels increased with higher IL6 serum concentrations in *PRKN/PINK1* mutation carriers, as well as in patients with idiopathic Parkinson's disease and healthy control subjects. However, as we found no significant group differences when investigating CRP levels, our data support IL6 as a more specific marker in the context of (monogenic) Parkinson's disease.

Release of ccf-mtDNA represents a common feature in various systemic diseases (West and Shadel, 2017). However, an association between ccf-mtDNA accumulation and IL6 elevation has, so far, only been established in murine models in the context of Parkinson's disease (Sliter *et al.*, 2018). We observed increased ccf-mtDNA levels in the serum of *PRKN/PINK1* biallelic mutation carriers and affected heterozygotes compared to patients with idiopathic Parkinson's disease. In line with our previous experiments in *Prkn* knockout mice (Sliter *et al.*, 2018), this finding indicates that the release of damage-associated molecular patterns (DAMPs), such as mtDNA from mitochondria, is a consequence of impaired mitophagy in *PRKN/PINK1*-associated Parkinson's disease.

The question to what extent heterozygous mutations in autosomal recessively inherited Parkinson's disease may act in a dominant manner with highly reduced penetrance is still discussed controversially (Klein *et al.*, 2007; Reed *et al.*, 2019). However, a dominant-negative mechanism in the context of affected heterozygous *PINK1* mutation carriers has been reported recently, providing insights into how heterozygous mutations might increase the probability of developing Parkinson's disease (Puschmann *et al.*, 2017). In our study, we provide evidence that ccf-mtDNA serum levels are useful to discriminate affected heterozygous *PRKN/PINK1* mutation carriers from idiopathic Parkinson's disease patients with high accuracy. Thus, our observations support the idea of a role for heterozygous variants at least as a strong risk factor for Parkinson's disease. However, while we did not find an increase in ccf-mtDNA concentrations in unaffected heterozygous mutation carriers compared to healthy control subjects or patients with idiopathic Parkinson's disease, affected heterozygous mutation carriers exhibited higher ccf-mtDNA levels than unaffected heterozygotes. This difference might indicate that in unaffected carriers, mitochondrial clearance is operating effectively until currently unknown factors trigger a breakdown of the genetically vulnerable mitophagy machinery. Subsequent to this tipping point, clinical symptoms, as well as an increase in ccf-mtDNA (and IL6) levels occur. Accordingly, investigating serum ccf-mtDNA levels in *PRKN/PINK1*-assocciated Parkinson's disease may contribute to the elucidation of mechanisms mediating penetrance and may have the potential to serve as a marker of affection status for heterozygous *PRKN/PINK1* mutation carriers. A previous study quantifying ccf-mtDNA in CSF from idiopathic Parkinson's disease cases found decreased levels in early-stage patients (Pyle *et al.*, 2015). Contrary to this report, in our study, we investigated idiopathic Parkinson's disease patients in an

advanced disease state and did not observe differences in serum ccf-mtDNA levels compared to healthy control subjects. Assuming that mtDNA levels differ over the course of the disease and vary between tissues, it will be necessary to investigate ccf-mtDNA levels in a longitudinal fashion using different patient-derived biomaterials.

Furthermore, the idiopathic Parkinson's disease group exhibited elevated serum IL6 despite low ccf-mtDNA levels. This finding can be interpreted in line with previous research providing evidence for inflammation due to impaired mitochondrial function and clearance independent of the mtDNA-cGAS-STING pathway. For example, neuromelanin-triggered NFκB (nuclear factor kappa-light-chain-enhancer of activated B cells) signalling (Wilms *et al.*, 2003) and autophagy-mediated NLRP3 inflammasome activation (Zhong *et al.*, 2018) are established molecular mechanisms in Parkinson's disease. Moreover, mtDNA variants were recently described to act as immunogenic neoepitopes (Deuse *et al.*, 2019). Thus, somatic mtDNA mutations, which have been previously documented in idiopathic Parkinson's disease (Bender *et al.*, 2006), might constitute an additional parameter modulating cGAS-STING signalling and, in turn, IL6 levels. Together, these findings highlight the potential of patient stratification attempts in personalized medicine approaches for idiopathic Parkinson's disease.

In our previous study (Sliter *et al.*, 2018), we showed that mtDNA mutator mice genetically lacking parkin accumulate ccf-mtDNA in serum and display neurodegenerative features and motor impairment. Interestingly, both of these phenotypes could be rescued by genetic inactivation of STING. Thereby, a direct contribution of neuroinflammation to the Parkinson's disease-like phenotype associated with *PRKN* and *PINK1* mutations has been observed in murine models. In light of these findings, the presence of increased ccf-mtDNA in patients with *PRKN/PINK1* mutations also implicates cGAS-STING signalling in the human disease process. Assuming that neuroinflammation causes neurodegeneration in patients with *PRKN* or *PINK1* mutations, targeted anti-inflammatory treatment may present a strategy to slow disease progression specifically in this group of individuals, who are estimated to make up 12.3% of early-onset (<45 years) Parkinson's disease cases (Kilarski *et al.*, 2012). Several approaches to influence the ccf-mtDNA-CGAS-STING-IL6 pathway that could now be applied to Parkinson's disease have already been established in the past. For instance, a protective effect of acetylsalicylic acid has been discussed in STING-mediated disease (Elkon, 2019). This finding is in accordance with epidemiological results, indicating that non-steroid-anti-inflammatory-drugs (NSAIDs) might have a positive effect on Parkinson's disease in general (Noyce *et al.*, 2012). More specific, anti-IL6 (Emery *et al.*, 2008) and anti-JAK antibodies (Lee *et al.*, 2014) represent an established treatment approach in different inflammatory conditions such as for instance, rheumatoid arthritis, and might have therapeutic potential in monogenic Parkinson's disease.

Several limitations of our study should be mentioned. First, we performed a retrospective analysis that did not allow us to correct for influencing factors. In particular, inflammatory cytokines like IL6 (Tanaka *et al.*, 2014), but also ccf-mtDNA (Grazioli and Pugin, 2018) have previously been reported to be increased in a number of inflammatory and cardiovascular diseases as well as in cancer. Thus, the specificity of the markers investigated in this study might be reduced if applied in clinical testing. Second, 45 samples, which had already been analysed for IL6 serum levels in our pilot analysis (Sliter *et al.*, 2018), were reassessed in the current study to validate the original IL6 results in an independent laboratory and to additionally obtain data on CRP and ccf-mtDNA serum levels from these individuals. Statistical testing revealed that the key findings from our study hold up, whether or not these samples are included in the analysis (Supplementary Fig. 1). Third, despite measuring IL6 levels in a certified diagnostic laboratory, the concentrations differed between the two tested cohorts. This variability may be explained by batch effects or varying pre-analytic treatment of the blood samples. However, such experimental limitations can be addressed in further studies by implementing standardized sample processing and prospective study design, as well as by increasing the number of enrolled mutation carriers. Furthermore, the role of cGAS-STING signalling in the transition from health to disease state in heterozygous mutation carriers warrants further investigation in the context of reduced penetrance. Finally, additional molecular studies in patient-derived neurons and glia will be required to fully decipher the upstream processes and downstream targets of the ccf-mtDNA-cGAS-STING-IL6 pathway in Parkinson's disease.

In conclusion, we demonstrated for the first time an association between a *PRKN* or *PINK1*-mutant genotype, increased ccf-mtDNA release, and neuroinflammation in Parkinson's disease patients. Together, the combination of elevated ccf-mtDNA and IL6 levels in serum of *PRKN* or *PINK1* mutation carriers supports the concept of impaired mitophagy triggering IL6 release (most likely via cGAS-STING signalling) that was, thus far, only demonstrated in mouse models. Our study has significant translational impact as especially serum ccf-mtDNA levels could serve as a biomarker of disease state, directing therapeutic approaches, which target the innate immune response in *PRKN/PINK1*-associated Parkinson's disease in the near future.

Acknowledgements

We thank the participants at the three study sites for generously donating their time and biomaterials, allowing us to analyse a large sample of participants with rare mutations. This project was supported by the high throughput/high content screening platform at the Luxembourg Centre for Systems Biomedicine. Moreover, we thank the LADR Centrallab Dr Kramer and Colleagues, Geesthacht, Germany, and especially Dr Bätz, for technical advice and support.

Funding

C.K. was supported by SysMedPD (European Union's Horizon 2020 research and innovation program under grant agreement 668738). C.K., I.R.K., N.B., M.K., K.L. and A.G. were supported by the German Research Foundation (FOR2488, GR 3731/5-1, KO 2250/7-1). A.G. received funding from the Luxembourg National Research Fund (ATTRACT career development grant, FNR9631103; INTER grant, FNR11250962). R.J.Y. was supported by the Intramural Program of the National Institute of Neurological Disorders and Stroke, NIH. E.M.V. received funding from the Fondazione Mondino (5 per mille grant year 2016), CARIPLO Foundation (grant 2017-0575) and MEFOPA FP7.

Competing interests

The authors report no competing interests. R.J.Y. did not supply patient materials and does not have a clinical protocol to report.

Supplementary material

Supplementary material is available at *Brain* online.

References

Alcalay RN, Siderowf A, Ottman R, Caccappolo E, Mejia-Santana H, Tang M-X, et al. Olfaction in Parkin heterozygotes and compound heterozygotes: the CORE-PD study. Neurology 2011; 76: 319–26.

Banks WA. The blood-brain barrier in neuroimmunology: tales of separation and assimilation. Brain Behav Immun 2015; 44: 1–8.

Bender A, Krishnan KJ, Morris CM, Taylor GA, Reeve AK, Perry RH, et al. High levels of mitochondrial DNA deletions in substantia nigra neurons in aging and Parkinson disease. Nat Genet 2006; 38: 515–7.

Del Giudice M, Gangestad SW. Rethinking IL-6 and CRP: why they are more than inflammatory biomarkers, and why it matters. Brain Behav Immun 2018; 70: 61–75.

Deuse T, Hu X, Agbor-Enoh S, Koch M, Spitzer MH, Gravina A, et al. De novo mutations in mitochondrial DNA of iPSCs produce immunogenic neoepitopes in mice and humans. Nat Biotechnol 2019; 37: 1137–44.

Dzamko N, Geczy CL, Halliday GM. Inflammation is genetically implicated in Parkinson's disease. Neuroscience 2015; 302: 89–102.

Elkon KB. Aspirin meets cGAS. Nat Rev Rheumatol 2019; 447: 1.

Emery P, Keystone E, Tony HP, Cantagrel A, van Vollenhoven R, Sanchez A, et al. IL-6 receptor inhibition with tocilizumab improves treatment outcomes in patients with rheumatoid arthritis refractory to anti-tumour necrosis factor biologicals: results from a 24-week multicentre randomised placebo-controlled trial. Ann Rheum Dis 2008; 67: 1516–23.

Goetz CG, Stebbins GT, Tilley BC. Calibration of unified Parkinson's disease rating scale scores to Movement Disorder Society-unified Parkinson's disease rating scale scores. Mov Disord 2012; 27: 1239–42.

Grazioli S, Pugin J. Mitochondrial damage-associated molecular patterns: from inflammatory signaling to human diseases. Front Immunol 2018; 9: 301–17.

Grünewald A, Kasten M, Ziegler A, Klein C. Next-generation phenotyping using the parkin example: time to catch up with genetics. JAMA Neurol 2013; 70: 1186–91.

Harrington D, D'Agostino RB, Gatsonis C, Hogan JW, Hunter DJ, Normand S-L, et al. New guidelines for statistical reporting in the journal. N Engl J Med 2019; 381: 285–6.

Hirsch EC, Hunot S. Neuroinflammation in Parkinson's disease: a target for neuroprotection? Lancet Neurol 2009; 8: 382–97.

Huttenlocher J, Stefánsson H, Steinberg S, Helgadottir HT, Sveinbjörnsdóttir S, Riess O, et al. Heterozygote carriers for CNVs in PARK2 are at increased risk of Parkinson's disease. Hum Mol Genet 2015; 24: 5637–43.

Kasten M, Hagenah J, Graf J, Lorwin A, Vollstedt E-J, Peters E, et al. Cohort Profile: a population-based cohort to study non-motor symptoms in Parkinsonism (EPIPARK). Int J Epidemiol 2012; 42: 128–128k.

Kasten M, Hartmann C, Hampf J, Schaake S, Westenberger A, Vollstedt E-J, et al. Genotype-phenotype relations for the Parkinson's disease genes parkin, PINK1, DJ1: MDSGene systematic review. Mov Disord 2018; 33: 730–41.

Kilarski LL, Pearson JP, Newsway V, Majounie E, Knipe MDW, Misbahuddin A, et al. Systematic review and UK-based study of PARK2 (parkin), PINK1, PARK7 (DJ-1) and LRRK2 in early-onset Parkinson's disease. Mov Disord 2012; 27: 1522–9.

Klein C, Lohmann-Hedrich K, Rogaeva E. Deciphering the role of heterozygous mutations in genes associated with Parkinsonism. Lancet Neurol 2007; 6: 652–62.

Lee EB, Fleischmann R, Hall S, Wilkinson B, Bradley JD, Gruben D, et al. Tofacitinib versus methotrexate in rheumatoid arthritis. N Engl J Med 2014; 370: 2377–86.

Lood C, Blanco LP, Purmalek MM, Carmona-Rivera C, De Ravin SS, Smith CK, et al. Neutrophil extracellular traps enriched in oxidized mitochondrial DNA are interferogenic and contribute to lupus-like disease. Nat Med 2016; 22: 146–53.

Narendra D, Walker JE, Youle R. Mitochondrial quality control mediated by PINK1 and Parkin: links to Parkinsonism. Cold Spring Harb Perspect Biol 2012; 4: a011338.

Noyce AJ, Bestwick JP, Silveira-Moriyama L, Hawkes CH, Giovannoni G, Lees AJ, et al. Meta-analysis of early nonmotor features and risk factors for Parkinson disease. Ann Neurol 2012; 72: 893–901.

Phillips NR, Sprouse ML, Roby RK. Simultaneous quantification of mitochondrial DNA copy number and deletion ratio: a multiplex real-time PCR assay. Sci Rep 2014; 4: 3887.

Puschmann A, Fiesel FC, Caulfield TR, Hudec R, Ando M, Truban D, et al. Heterozygous PINK1 p.G411S increases risk of Parkinson's disease via a dominant-negative mechanism. Brain 2017; 140: 98–117.

Puzianowska-Kuźnicka M, Owczarz M, Wieczorowska-Tobis K, Nadrowski P, Chudek J, Slusarczyk P, et al. Interleukin-6 and C-reactive protein, successful aging, and mortality: the PolSenior study. Immun Ageing 2016; 13: 21.

Pyle A, Brennan R, Kurzawa-Akanbi M, Yarnall A, Thouin A, Mollenhauer B, et al. Reduced cerebrospinal fluid mitochondrial DNA is a biomarker for early-stage Parkinson's disease. Ann Neurol 2015; 78: 1000–4.

Qin X-Y, Zhang S-P, Cao C, Loh YP, Cheng Y. Aberrations in peripheral inflammatory cytokine levels in Parkinson disease: a systematic review and meta-analysis. JAMA Neurol 2016; 73: 1316–24.

Qiu X, Xiao Y, Wu J, Gan L, Huang Y, Wang J. C-Reactive protein and risk of Parkinson's disease: a systematic review and meta-analysis. Front Neurol 2019; 10: 384.

R Core Team. R: A language and environment for statistical computing. Vienna, Austria: R Foundation for Statistical Computing; 2018. http://www.R-project.org/.

Reed X, Bandrés-Ciga S, Blauwendraat C, Cookson MR. The role of monogenic genes in idiopathic Parkinson's disease. Neurobiol Dis 2019; 124: 230–9.

Richards S, Aziz N, Bale S, Bick D, Das S, Gastier-Foster J, et al. Standards and guidelines for the interpretation of sequence variants: a joint consensus recommendation of the American College of Medical Genetics and Genomics and the Association for Molecular Pathology. Genet Med 2015; 17: 405–24.

Rygiel KA, Grady JP, Taylor RW, Tuppen HAL, Turnbull DM. Triplex real-time PCR—an improved method to detect a wide spectrum of mitochondrial DNA deletions in single cells. Sci Rep 2015; 5: 9906.

Schneider SA, Alcalay RN. Neuropathology of genetic synucleinopathies with Parkinsonism: review of the literature. Mov Disord 2017; 32: 1504–23.

Sliter DA, Martinez J, Hao L, Chen X, Sun N, Fischer TD, et al. Parkin and PINK1 mitigate STING-induced inflammation. Nature 2018; 561: 258–62.

Tanaka T, Narazaki M, Kishimoto T. IL-6 in inflammation, immunity, and disease. Cold Spring Harb Perspect Biol 2014; 6: a016295.

West AP, Shadel GS. Mitochondrial DNA in innate immune responses and inflammatory pathology. Nat Rev Immunol 2017; 17: 363–75.

Wilms H, Rosenstiel P, Sievers J, Deuschl G, Zecca L, Lucius R. Activation of microglia by human neuromelanin is NF-kappaB dependent and involves p38 mitogen-activated protein kinase: implications for Parkinson's disease. FASEB J 2003; 17: 500–2.

Zhong Z, Liang S, Sanchez-Lopez E, He F, Shalapour S, Lin X-J, et al. New mitochondrial DNA synthesis enables NLRP3 inflammasome activation. Nature 2018; 560: 198–203.

Supplemental information

Mitochondrial damage-associated inflammation highlights biomarkers in PRKN/PINK1 parkinsonism

Max Borsche[1,2], Inke R. König[3,*], Sylvie Delcambre[4,*], Simona Petrucci[5,6], Alexander Balck[1,2], Norbert Brüggemann[1,2], Alexander Zimprich[7], Kobi Wasner[4], Sandro L. Pereira[4], Micol Avenali[8], Christian Deuschle[9,10], Katja Badanjak[4], Jenny Ghelfi[4], Thomas Gasser[9,10],Meike Kasten[1,11], Philip Rosenstiel[12], Katja Lohmann[1], Kathrin Brockmann[9,10], Enza Maria Valente[8,13], Richard J. Youle[14], Anne Grünewald[1,4*], and Christine Klein[1,*]

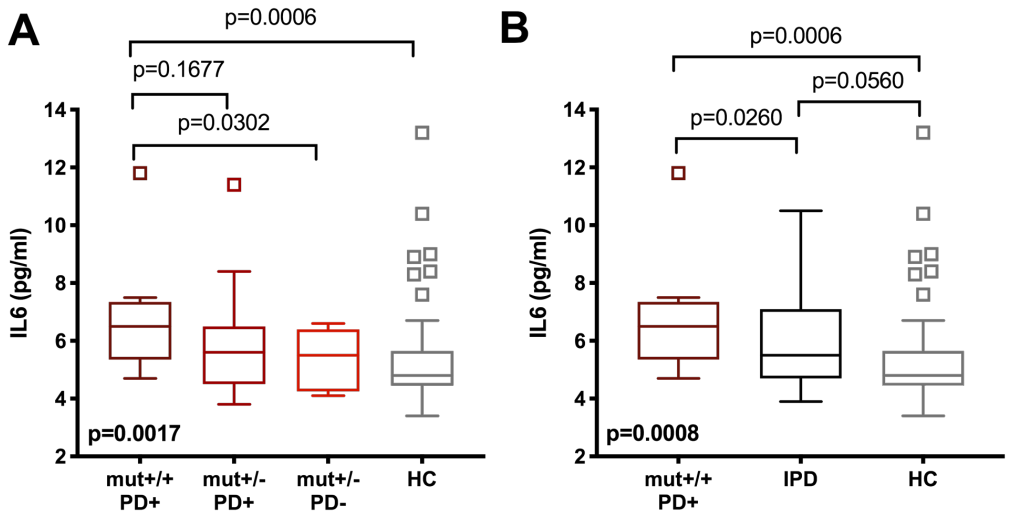

Supplementary Figure 1: Interleukin 6 (IL6) levels in newly included individuals. Serum IL6 levels in participants from the German Cohort that have not been previously assessed (Sliter et al., 2018). **A.** Investigating the hypothesized assumed order (*Parkin/PINK1* biallelic (mut+/+ PD+, n=10) > *Parkin/PINK1* affected (mut+/- PD+, n=13) and unaffected (mut+/- PD-, n=5) heterozygotes > healthy controls (HC, n=57), *Parkin/PINK1* biallelic individuals exhibit elevated IL6 level compared to healthy controls. Moreover, there was a trend towards elevated IL6 levels in patients with PD due to biallelic *Parkin/PINK* mutations compared to unaffected heterozygotes. **B.** *Parkin/PINK1* biallelic individuals exhibited a trend towards elevated IL6 levels compared to IPD patients, while IPD patients showed a trend towards higher IL6 levels than HC. Together, analyzing only the newly included individuals led to very similar results compared to the whole German Cohort. The assumed order among the different groups was tested with the Jonckheere-Terpstra test (exploratory p-value in bold, lower left corner). Pairwise differences between two groups were assessed using the Wilcoxon rank sum test (exploratory p-values, parentheses). Data is presented as box and whisker plots. The box extends from the 25th to the 75th percentile. The line in the middle of the box represents the median. Tukey whiskers are used.

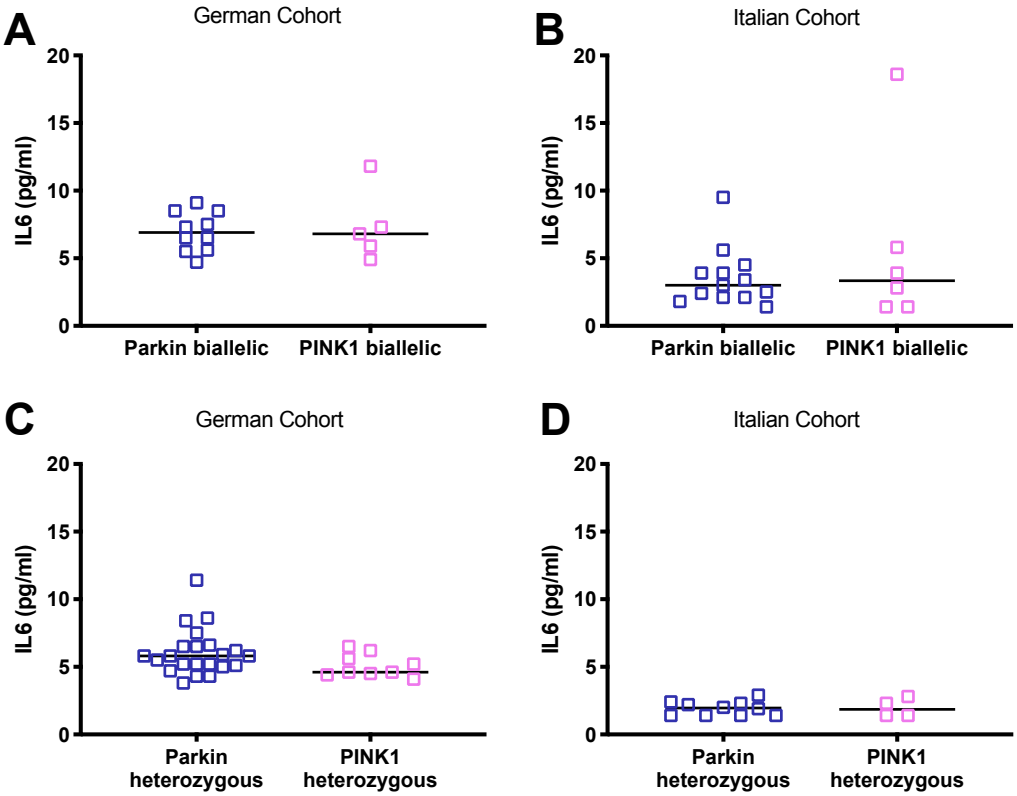

Supplementary Figure 2: *Parkin* and *PINK1* mutation carriers exhibit similar Interleukin 6 (IL6) levels. A. IL6 levels in patients with PD due to biallelic *Parkin* (n=10) and *PINK1* (n=5) mutations from the German Cohort. **B.** IL6 levels in biallelic *Parkin* (n=13) and *PINK1* (n=6) mutations carriers from the Italian Cohort. **C.** IL6 levels in heterozygous *Parkin* (n=22) and *PINK1* (n=9) mutation carriers (affected and unaffected) from the German Cohort. **D.** IL6 levels in symptomatic and asymptomatic heterozygous *Parkin* (n=10) and *PINK1* (n=4) mutation carriers from the Italian Cohort. Together, IL6 levels are similar if investigating *Parkin* and *PINK1* mutation carriers separately among all groups and cohorts. Lines represent the median.

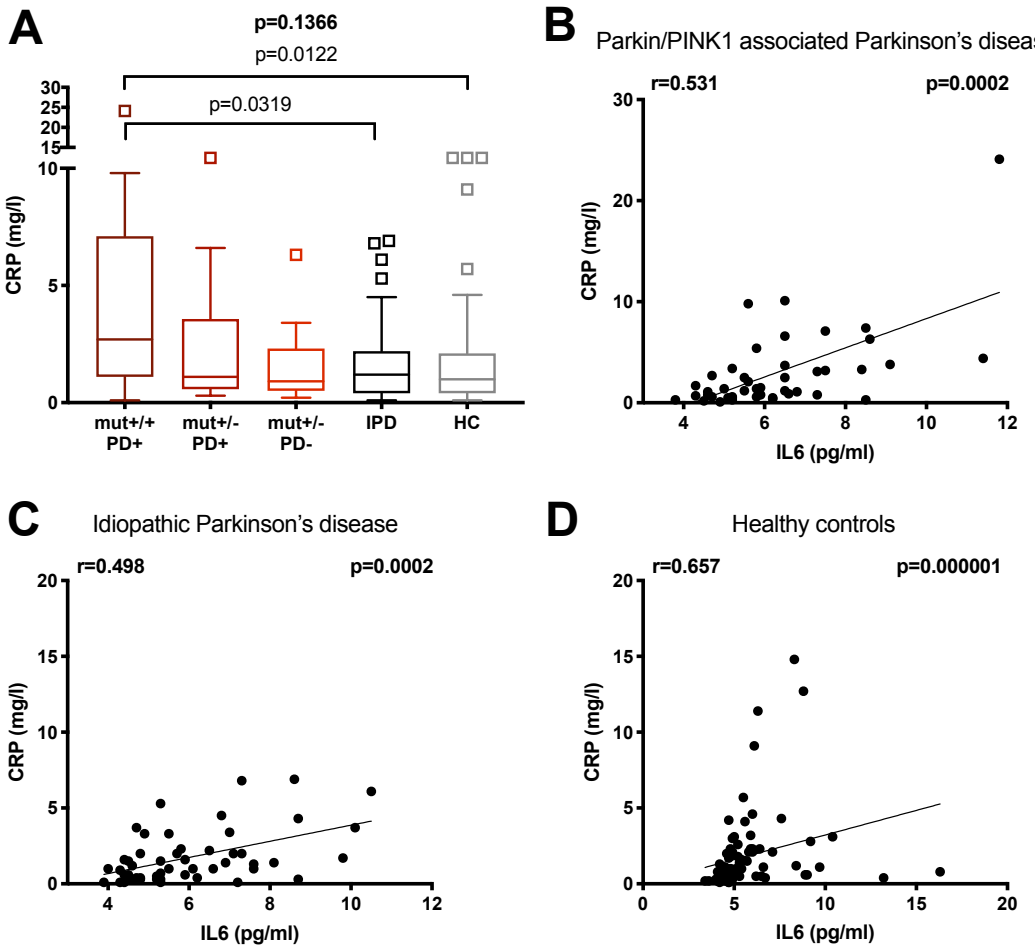

Supplementary Figure 3: C-reactive protein (CRP) levels show a trend to be elevated in biallelic *Parkin/PINK1* mutation carriers and correlate with Interleukin 6 (IL6) levels. CRP levels in monogenic and idiopathic Parkinson's disease (IPD) patients and healthy controls (HC); **A.** There is a trend towards elevated CRP levels in biallelic *Parkin/PINK1* mutation carriers (mut+/+ PD+, n=15) compared to IPD patients (n=51) and a significant difference compared to healthy controls (n=85). *Parkin/PINK1* affected heterozygotes (mut+/- PD+, n=18); *Parkin/PINK1* unaffected heterozygotes (mut+/- PD-, n=13). Results from the German Cohort are shown. A similar distribution was observed in the Italian Cohort (Table 2). CRP levels correlate with IL6 levels in **B.** *Parkin/PINK1* biallelic and heterozygous mutation carriers (n=44), in **C.** IPD patients (n=51), as well as in **D.** Healthy controls. In A, group differences in general were explored via Kruskal-Wallis test (bold). Although the overall test was not significant, exploratory p-values regarding pairwise analysis, assessed by Wilcoxon rank sum test, are shown (parentheses). Data is presented as box and whisker plots. The box extends from the 25th to the 75th percentile. The line in the middle of the box represents the median. Tukey whiskers are used. In B, C, and D, a Spearman's correlation was calculated. The correlation coefficient is shown in the upper left, exploratory p-values are presented in the upper right corner.

Supplementary Table 1: Samples from study participants already included in the pilot study.

	German Cohort	**All samples**
***Parkin/PINK1* biallelic**	5/15 (33%)	5/34 (15%)
***Parkin/PINK1* heterozygous affected**	5/19 (26%)	5/24 (21%)
***Parkin/PINK1* heterozygous unaffected**	8/15 (53%)	8/24 (33%)
Idiopathic Parkinson's disease	0/59 (0%)	0/64 (0%)
Healthy controls	27/90 (30%)	27/99 (27%)
All participants	45/198 (23%)	45/245 (18%)

A subset of the participants investigated in the recent study was already included in a pilot IL6 analysis in the context of Sliter *et al.*, 2018. In the former study, just samples from the Lübeck study site were included. For the recent study, the analysis took place in a different laboratory then in the pilot study.

4 Discussion

With the advancing age of the world population, the incidence of neurodegenerative disorders is also on the rise. The number of PD cases is growing each year and is estimated to reach 12 million people by the year 2040 (Dorsey et al., 2018). The total economic burden of PD in the USA alone was estimated at 50 billion USD in the year 2017. Furthermore, the cause of this growth is suspected not to be advanced aging of the population alone, but a complex interaction between genetic predisposition, lifestyle choices, and other factors that vary across countries, by gender, and with age (Rocca, 2018).
Given the fact that PD cases are mostly sporadic, with a spectrum of pathologies, different ages of disease onset, and possible multiple genetic modifiers, modeling the disease has proven to be extremely difficult. Animal models have given many valuable mechanistic insights into neurotoxin-induced and genetic forms of PD. However, animal models cannot fully reconstitute PD pathologies observed in patients. In order to reduce the use of animals in research, and to better mirror patient-specific phenotypes, iPSC-derived cultures have proven to be a valuable substitute.
Although primarily studied in neurons, PD pathology is covering multiple cell types of the brain. We summarized the available literature concerning the role of microglia in PD, and their importance in maintaining CNS homeostasis, in both animal and iPSC-derived model systems (Manuscript I). The result section of this thesis describes the experimental work performed in iPSC-derived microglia (Manuscript II and III) and the investigation of inflammatory phenotypes and biomarkers in blood samples from PD patients (Manuscript IV).

4.1 iPSC-derived microglia

Microglia are the resident macrophages of the brain, which are responsible for immune responses to extracellular stimuli and danger signals, and maintaining CNS homeostasis throughout the human lifetime. Human microglia originate

from the yolk sac at around 4.5 weeks of gestational age, and will colonize the midbrain area upon 22 weeks (Alliot et al., 1999; Ginhoux et al., 2010; Monier et al., 2007; Tavian and Péault, 2005). Of note, mice studies were crucial in understanding if microglia are yolk sac-derived cells or cells which develop during postnatal hematopoiesis. Yolk sac-derived macrophages are distinct from blood monocyte-derived macrophages, which are dependent on Myb (Ginhoux et al., 2010; Schulz et al., 2012). Additionally, early colonization from the yolk sac to the brain parenchyma happens prior to neurogenesis, suggestive of a role for microglia in maintaining the correct homeostatic conditions, which favor neurodevelopmental events (Alliot et al., 1991). In turn, microglia are maturing to their fully functional and ramified form in the presence of neurons (Haenseler et al., 2017b).

As described in Manuscript I, studies on microglia involving human tissue and animal models have their own drawbacks. Firstly, human tissue is extremely rare and not readily available. While it is possible to isolate microglia cells from human fetal and adult brains, the microglial transcriptomic signature upon culturing those cells *ex vivo* is lost (Butovsky et al., 2014). Secondly, mice microglia are more readily available, but they often showcase significant differences in the expression of disease risk genes, and the expression and regulation of immune pathways involved in human diseases (Booth et al., 2017; Kodamullil et al., 2017). In order to create a patient-derived model and to achieve *in vitro* cultures of near 100% microglial purity, we applied an established microglial differentiation protocol to iPSCs.

Multiple protocols for the generation of microglia-like cells were described previously (Abud et al., 2017; Haenseler et al., 2017b; Muffat et al., 2016; Pandya et al., 2017). Since most of them require additional steps of sorting, purification or co-culturing with astrocytes, we opted for a protocol devised by Haenseler *et al*. It efficiently reconstitutes the microglial journey from the yolk sac to the brain, through the formation of embryoid bodies, and establishment of macrophage precursor-producing factories, with addition of growth factors, which direct the cells to become Myb-independent macrophages. Even though this protocol aims to obtain neuron-microglia co-cultures as the final step to achieve terminally differentiated microglia, we cultured our macrophage precursors as a monoculture, by adding the factors IL-34 and GM-CSF. Both ligands are able to stimulate the activation of the IL-34 receptor, a signaling molecule that is crucial to achieve a microglia-specific signature (Haenseler et al., 2017b; Kempthorne et al., 2020).

In Manuscript II and III, we successfully differentiated iPSC–derived microglia

and confirmed their microglial identity by immunostaining for the microglia-specific markers Iba1 and P2RY12. Microglia cells are responsible for phagocyting necrotic and apoptotic brain cells and cellular debris, and modeling this function *in vitro* is part of the (functional) characterization of these cells (Janda et al., 2018). Indeed, we were able to show that both LRRK2-PD and IPD microglia are capable of phagocyting Zymosan bioparticles (Manuscript II and III). Our characterization experiments highlighted that iPSC-derived microglia are a great tool to study inflammatory processes in the CNS, *in vitro*.

4.2 Modeling LRRK2-associated PD and LRRK2 kinase activity

Modeling LRRK2-PD in animal and *in vitro* cell culture models usually consists of either LRRK2 overexpression or insertion of PD-associated LRRK2 mutations (Seegobin et al., 2020). Unfortunately, neither of these genetic modifications could prompt degeneration of dopaminergic neurons, or even obvious changes in the brain pathology (Arranz et al., 2015; Baptista et al., 2013; Garcia-Miralles et al., 2015; Herzig et al., 2012; Hinkle et al., 2012; Liu et al., 2015). These findings, together with the incomplete penetrance of LRRK2 G2019S, led to the assumption that LRRK2-PD is a result of multiple hits. According to the "multiple-hit hypothesis", a genetic insult brings a system (an organism) to the edge of perturbation, while a second (environmental) hit is needed to fully manifest the scope of the disease (Cannon and Greenamyre, 2013; Johnson et al., 2019; Sulzer, 2007). In LRRK2-PD, the second hit was assumed to be of inflammatory nature. Indeed, the LRRK2 protein is highly abundant in immune cells of both the adaptive and innate immunity (Cook et al., 2017; Gardet et al., 2010; Hakimi et al., 2011). The importance of LRRK2 in the innate immune response was corroborated when LRRK2 KO animals were shown to be less sensitive to LPS-induced neuroinflammation and neurodegeneration (Daher et al., 2014). In addition, *in vitro* studies found that inhibition of LRRK2 kinase activity can successfully lower levels of pro-inflammatory cytokines, while treatment with IFN-γ can upregulate both *LRRK2* levels and kinase activity (Gardet et al., 2010; Lee et al., 2020; Moehle et al., 2012; Panagiotakopoulou et al., 2020; Russo et al., 2016).
The main cellular sources of IFN-γ are natural killer (NK) cells, and CD8+ and CD4+ T lymphocytes. Taking into consideration that LRRK2 is highly expressed

in peripheral organs, like spleen, liver and lungs, and peripheral cells of the immune system, impact of tissue-specific macrophages, monocytes and T lymphocytes has been reported in PD patients (Konstantin Nissen et al., 2022; Wallings et al., 2020). A shift towards higher numbers of CD8+ cells, and cells producing higher amounts of IFN-γ was seen in PD patients, while naïve CD4+ cells tend to differentiate preferentially towards the Th1 lineage signature with increased IFN-γ production (Baba et al., 2005; Kustrimovic et al., 2018). T and B lymphocytes, and monocytes from PD patients showed higher expression of LRRK2 and exhibited a pro-inflammatory phenotype (Bliederhaeuser et al., 2016a; Cook et al., 2017; Kuss et al., 2014; Thévenet et al., 2011). Furthermore, a groundbreaking study in mice lymphocytes found that the presence of LRRK2 mutations alone is sufficient to prompt the LPS-induced demise of dopaminergic neurons, establishing peripheral immunity as a key trigger of neurodegeneration in this LRRK2 model (Kozina et al., 2022).

Since CNS microglia are not the main source of IFN-γ, we treated our cultures with the cytokine to mimic the "second hit" that would otherwise be caused by an inflammatory insult from the peripheral immune system. In Manuscript II, we report elevated LRRK2 protein levels in iPSC-derived microglia, upon IFN-γ exposure. While LRRK2 levels did not significantly differ between different microglia cells, phospho-S1292 LRRK2 was upregulated solely in LRRK2 G2019S carriers, after IFN-γ treatment. By including gene-corrected cells in our study, we determined that these results are primarily caused by the G2019S mutation and do not result from the genetic background of the patient.

LRRK2 phosphorylates a large group of substrates. In a recent study, changes in cellular phosphorylation events highlighted the differences between manifesting and non-manifesting LRRK2 G2019S patients (Garrido et al., 2022). Furthermore, phosphorylated levels of Rab10 protein were considered a robust readout of LRRK2 kinase activity in animal and *in vitro* models (Iannotta et al., 2020; Ito et al., 2016; Wang et al., 2021). Conversely, in a recent study in PD patient neutrophils and PBMCs, pRab10 was not different between control and patients, and pRab10 levels were not correlated to total LRRK2, indicative of a complex regulation between LRRK2 and its substrates (Atashrazm et al., 2019). In Manuscript II, we could induce phosphorylation of Rab10 upon IFN-γ treatment, indicative of higher kinase activity upon an inflammatory stimulus. However, we did not observe a mutation-specific upregulation of pRab10, as was seen in the analysis of phospho-S1292 LRRK2 levels. Furthermore, these results are in line with a recent study that found no significant influence of LRRK2 G2019S on pRab10 levels in human neutrophils. Instead, the R1441G mutation in LRRK2 induced elevated

pRab10 (Fan et al., 2021). Of note, the authors could not detect S1292 levels in their experimental setup. This might be due to a cell type-specific regulation of LRRK2 phosphorylation - an aspect of LRRK2-PD not yet fully understood.
Reducing augmented LRRK2 kinase activity is currently the main therapeutic target for LRRK2-PD patients. In Manuscript II, we successfully decreased the levels of both S1292 LRRK2 and pRab10 upon MLi-2 treatment. Our results indicate S1292 LRRK2 as the primary readout of mutation-specific kinase activity in iPSC-derived microglia cells, and highlight the importance of IFN-γ signaling in this cascade.

4.3 Alpha-synuclein and LRRK2

Alpha-synuclein is a protein primarily expressed in neurons. Its aggregation is one of the hallmarks of PD and one of the prime subjects of PD research (Bendor et al., 2013; Bernal-Conde et al., 2019). Microglia readily uptake extracellular α-synuclein, helping in clearance and degradation, which is usually disrupted in PD models (Bliederhaeuser et al., 2016b; Choi et al., 2020; George et al., 2019; Guo et al., 2020; Haenseler et al., 2017a; Mavroeidi and Xilouri, 2021). Strictly defining the intricate interplay between LRRK2 and α-synuclein has not yet been achieved (O'Hara et al., 2020). By contrast, multiple studies showed that LRRK2 G2019S plays a role in the accumulation and aggregation of α-synuclein in neurons and defective clearance of α-synuclein in astrocytes (Longo et al., 2017; Novello et al., 2018; Volpicelli-Daley et al., 2016). Interestingly, LRRK2 was found to regulate the levels of toxic accumulation of α-synuclein in a kinase-dependent manner (Daher et al., 2015; Ho et al., 2020; Obergasteiger et al., 2020; Volpicelli-Daley et al., 2016; Zhao et al., 2020). Moreover, LRRK2 G2019S microglia were shown to exchange the synuclein load through a nanotubular network (Scheiblich et al., 2021).
Beyond the above-mentioned functional studies, little is known about the significance of endogenous α-synuclein expression in immune cells. α-synuclein was found to be of importance in microglial development and function, while increased levels in peripheral immune cells were considered a biomarker of PD (Austin et al., 2006; Bido et al., 2021; Gardai et al., 2013; Shin et al., 2000; Xiao et al., 2014). An immunocytochemistry experiment allowed us to study the localization and protein levels of α-synuclein. In Manuscript II, we found elevated levels of total and nuclear α-synuclein in manifesting LRRK2 G2019S microglia, exacerbated upon IFN-γ treatment, but seemingly not dependent on kinase activity. Interestingly, a recent study found no correlation between *SNCA* expression and IFN-regulated genes in aging post-mortem brains. Only in the brains of

PD patients, *SNCA* was positively co-expressed with IFN-regulated genes (Liscovitch and French, 2014). Together with our data, these findings would signify a detrimental loop between α-synuclein and IFN-γ, and a potential role of *SNCA* in directly modulating the immune response and affecting the penetrance of LRRK2-PD. Furthermore, a recent study in LRRK2 G2019S mice found that α-synuclein fibrils trigger the recruitment of infiltrating LRRK2-expressing peripheral monocytes with a distinct pro-inflammatory signature (Xu et al., 2022). Additionally, infiltrating monocytes were found to be crucial in synuclein-driven neurodegeneration (Harms et al., 2018). These findings are indicative of a substantial involvement of α-synuclein in propagating inflammation in LRRK2-PD, beyond the CNS.

4.4 Transcriptomics of LRRK2-PD iPSC-derived microglia

In order to further assess the involvement of LRRK2 G2019S in PD pathogenesis, we performed RNA sequencing on our samples. Given that we observed major changes between different microglia mainly upon IFN-γ treatment, we decided to focus our transcriptomic analysis on microglia under inflammatory conditions only. When analyzing differentially expressed genes that define the disease status in IFN-γ-stimulated LRRK2 G2019S microglia, we identified several genes involved in inflammation. The expressions of *GPNMB*, *DPYD*, *GRAMD4*, *CADM1* and *SH3PXD2B* were specifically upregulated in LRRK2 G2019S patient microglia. This set of genes was also linked to the activation trajectories of IPD microglia, suggestive of shared microglial activation features between LRRK2-PD and IPD (Smajić et al., 2021). GPNMB is associated with activated microglia and its expression was found to be upregulated upon excessive proinflammatory signaling (Ripoll et al., 2007; Saade et al., 2021). Moreover, CADM1 is a cell-adhesion protein shown to have a major role in interaction with CD8+ T lymphocytes, and is consequently further inducing IFN-γ production (Faraji et al., 2012). Interestingly, we also identified *IRAK4* upregulation in the manifesting G2019S microglia compared to the non-manifesting G2019S microglia. Multiple studies suggested that inhibition of IRAK4 is a suitable therapeutic strategy for neurodegenerative disorders since this protein is involved in the overactivation of innate immune signaling (Giménez et al., 2020; Mullard, 2020; Ngwa et al., 2021). More work will be needed to confirm its therapeutic potential in LRRK2-PD.

Pathway enrichment analysis revealed the importance of Notch signaling in LRRK2 G2019S microglia. Notch signaling is a conserved pathway regulating development, cell fate, differentiation, and immune response by receiving cell-to-cell information (Brandstadter and Maillard, 2019; Keewan and Naser, 2020; Radtke et al., 2010; Shang et al., 2016; Wongchana et al., 2018). While there are only few publications dealing with Notch signaling in PD, it has been implicated in neuronal dysfunction in LRRK2 and α-synuclein models, and was shown to control the microglial activation state (Desplats et al., 2012; Grandbarbe et al., 2007; Imai et al., 2015). Moreover, *PHF8*, a central gene of the Notch pathway, was downregulated in LRRK2 G2019S carriers. PHF8 was previously shown to control the extent of IFN-γ signaling (Asensio-Juan et al., 2017). These findings will be the basis for further experiments exploring the role of Notch signaling in LRRK2-PD.

4.5 LRRK2 and IPD

Clinical similarities between IPD and LRRK2-PD compelled us to investigate shared phenotypes in iPSC-derived microglia from these two PD forms. LRRK2 kinase activity was recently found enhanced in IPD patient post-mortem tissues (Di Maio et al., 2018). In Manuscript II, we observed that IFN-γ treatments can elicit a similar response in IPD iPSC-derived microglia. Phospho-S1292 LRRK2 was upregulated upon IFN-γ exposure in IPD microglia compared to control cells. By contrast, pRab10 levels were comparable between the groups upon IFN-γ treatment. Even though we investigated a small sample size, we could recapitulate the S1292 phenotype as observed in post-mortem tissues.
Results in both LRRK2 and IPD microglia suggest that IFN-γ signaling mediates LRRK2 kinase overactivation. Additionally, our pRab10 data confirm the results of another study in brain tissue samples and neutrophils from IPD patients, where no differences between patients and healthy individuals were detected (Fan et al., 2021). Furthermore, LRRK2 expression was downregulated in IPD microglia compared to control cells, irrespective of the treatment, an observation already seen in our published study on IPD microglia (Manuscript III), and in IPD post-mortem tissue (Badanjak et al., 2021; Simunovic et al., 2009).
While we observe shared microglial phenotypes between the IPD and LRRK2-PD with respect to LRRK2 kinase activity, most other assessed features differed between the two forms. This discrepancy is not surprising, and is possibly a consequence of differential downstream mechanisms under IFN-γ treatment. However, in light of the number of samples investigated, future studies will be crucial to validate our findings.

4.6 Studying inflammation in IPD

Studies on inflammatory mechanisms in the CNS of IPD patients are relatively sparse. The majority of studies carried out so far, explore peripheral blood-derived immune cells and tissue samples. In addition, the high heterogeneity of cases makes IPD extremely hard to model *in vitro*. Having multiple published RNAseq datasets from IPD tissues at our disposal, we decided to explore the contribution of microglia cells in IPD in a comparative manner and to model those findings in our iPSC-derived microglia (Manuscript III).

Cytokines are inflammatory intercellular mediators responsible for the propagation of the inflammatory response and are crucially involved in defense mechanisms of the CNS. We analyzed cytokine expressions in published RNAseq datasets from postmortem tissues and observed an upregulation of *IL10* and *IL1B* in IPD nigral tissues compared to controls. In order to obtain higher cellular resolution and confirm that these expressions are indeed microglia-driven, we made use of our previously published IPD single-cell midbrain atlas. Not surprisingly, these cytokine expressions were specifically upregulated in microglia cells from IPD patients, highlighting microglia as the main drivers of neuroinflammation in IPD. Furthermore, we wanted to validate this data *in vitro*, using iPSC-derived microglia technology. In order to mount an effective inflammatory response, LPS is often used in experimental setups. LPS is a component of the highly antigenic outer membrane of Gram-negative bacteria (Qin et al., 2007). In Manuscript III, we found that iPSC-derived microglia from IPD patients have elevated *IL1B* and *IL10* levels upon LPS insult, confirming the cytokine expression findings from the public RNAseq and sn-RNAseq datasets. Furthermore, LPS was shown to stimulate *NLRP3* expression in other cellular models of neurodegeneration (Hulse and Bhaskar, 2022; Liang et al., 2022), which motivated us to explore the inflammasome in our cells. Indeed, we observed higher mRNA and protein levels of NLRP3 upon LPS exposure, highlighting the relevance of this pathway in the pathogenesis of PD.

As previously stated, LRRK2 is also implicated in IPD. Although, upon IFN-γ treatment, we observed higher phospho-S1292 LRRK2 levels in IPD microglia, LPS exposure did not have the same effect. This suggests that LRRK2 kinase activity is tightly regulated by specific inflammatory insults. Furthermore, other studies demonstrated higher total LRRK2 levels after LPS treatment, a phenotype, which we did not observe in our iPSC-derived microglia, indicative of differential responses between various microglia model systems (Moehle et al., 2012).

An important aspect of PD research is the identification of reliable blood biomarkers, which would provide insight into the susceptibility, diagnosis, and potential disease progression of an individual. In a recent study, defective mitophagy in PRKN-PD mice prompted the release of mtDNA, activation of inflammatory cGAS-STING pathway, and increased IL6 production (Sliter et al., 2018). Translating this exciting study to patients, we identified an upregulation of mtDNA, IL6, and C-reactive protein in manifesting carriers of *PRKN* and *PINK1* mutations (Manuscript IV). Interestingly, these pro-inflammatory components were not upregulated in the serum of IPD patients. Thus, we might speculate that the peripheral response in IPD patients is a low-grade chronic inflammation. While in early-onset PRKN-PD, mitochondrial dysfunction and the release of mitochondrial components (which have antigenic potential) induce even peripheral inflammatory phenotypes.

4.7 Anti-inflammatory therapies

The range of anti-inflammatory therapies tested in the treatment of PD were summarized in Manuscript I. This included the use of non-steroid anti-inflammatory drugs (NSAIDs), and antibody therapies against α-synuclein. Additionally, enhanced LRRK2 kinase activity has encouraged the development of multiple LRRK2 kinase inhibitors. Initial inhibitors (the so-called generation 0) were not very potent and selective for LRRK2, and had no ability to cross the mouse BBB. Further development saw two generations of more potent and selective kinase inhibitors, although penetration to the brain was still low (Anand et al., 2009; Choi et al., 2012; Covy and Giasson, 2009; Estrada et al., 2014; Hatcher et al., 2015; Nichols et al., 2009). The third generation is characterized by two extremely potent LRRK2 kinase inhibitors: MLi-2 and PF-06685360 (Andersen et al., 2018; Fell et al., 2015; Scott et al., 2017). Multiple studies, including our own, have shown downregulation of phospho-S935 LRRK2 and pRab10 levels upon MLi-2 treatment (Daher et al., 2015; Wang et al., 2021). While effective and useful for *in vitro* modeling of LRRK2-PD, adverse effects of these inhibitors have been reported in pre-clinical trials (Wojewska and Kortholt, 2021). Thus, we turn our focus to therapies widely available to the general population, which have an anti-inflammatory potential - NSAIDs.

NSAIDs exhibit their effect through inhibition of cyclooxygenase COX-1 and COX-2, consequently reducing the production of prostaglandins (Ghlichloo and Gerriets, 2021). Higher levels of COX enzymes and prostaglandins were associated with neurodegenerative disorders (Minghetti, 2004). It is still under debate whether there is any association between NSAIDs uptake and PD incidence (Brakedal et al., 2021; Samii et al., 2009). Interestingly, two independent studies found that the intake of aspirin and ibuprofen was associated with later age-at-onset of LRRK2-PD and IPD (Gabbert et al., 2022; San et al., 2020).

5 Outlook

In my doctoral thesis, I have provided findings on inflammatory processes in LRRK2-associated and idiopathic PD. The generation of iPSC-derived microglia was crucial in order to decipher the molecular mechanisms in endogenous patient microglia - cells that are exclusive to the CNS, and thus not readily available. Our experimental setup allowed us to investigate mutation-specific phenotypes in both manifesting and non-manifesting LRRK2 G2019S microglia. While both G2019S carriers were characterized by an upregulation of kinase activity, only LRRK2-PD microglia were additionally shown to have higher α-synuclein levels and *GPNMB* expression, upon IFN-γ treatment. Furthermore, our transcriptomic analysis identified Notch signaling as a potential pathway mediating inflammation in LRRK2-PD microglia.

Further experiments are needed to strengthen our study on LRRK-PD microglia. Firstly, taking into account the propensity of α-synuclein and GPNMB to achieve an inflammatory effect on surrounding cells and tissue, we plan to perform ELISA experiments. Furthermore, it would be interesting to investigate if the release of both is dependent on LRRK2 kinase activity.

Moreover, a study by Smajic *et al.* found several genes specific to the GPNMB^{high} cluster in IPD microglia. In order to find additional shared phenotypes in microglia activation, we plan to investigate those genes specifically in our LRRK2 microglia RNAseq dataset.

Finally, we intend to validate multiple targets identified in the RNAseq dataset, together with exploring the regulation of Notch signaling in iPSC-derived microglia cells.

Bibliography

Aasly, J.O., Toft, M., Fernandez-Mata, I., Kachergus, J., Hulihan, M., White, L.R., and Farrer, M. (2005). Clinical features ofLRRK2-associated Parkinson's disease in central Norway. *Annals of Neurology* 57, 762–765.

Abud, E.M., Ramirez, R.N., Martinez, E.S., Healy, L.M., Nguyen, C.H.H., Newman, S.A., Yeromin, A.V., Scarfone, V.M., Marsh, S.E., Fimbres, C., et al. (2017). iPSC-Derived Human Microglia-like Cells to Study Neurological Diseases. *Neuron* 94, 278–293.e9.

Ahmadi Rastegar, D., and Dzamko, N. (2020). Leucine Rich Repeat Kinase 2 and Innate Immunity. *Front. Neurosci.* 14, 193.

Alliot, F., Lecain, E., Grima, B., and Pessac, B. (1991). Microglial progenitors with a high proliferative potential in the embryonic and adult mouse brain. *Proc. Natl. Acad. Sci. U. S. A.* 88, 1541–1545.

Alliot, F., Godin, I., and Pessac, B. (1999). Microglia derive from progenitors, originating from the yolk sac, and which proliferate in the brain. *Brain Res. Dev. Brain Res.* 117, 145–152.

Anand, V.S., Reichling, L.J., Lipinski, K., Stochaj, W., Duan, W., Kelleher, K., Pungaliya, P., Brown, E.L., Reinhart, P.H., Somberg, R., et al. (2009). Investigation of leucine-rich repeat kinase 2. *FEBS Journal* 276, 466–478.

Andersen, M.A., Wegener, K.M., Larsen, S., Badolo, L., Smith, G.P., Jeggo, R., Jensen, P.H., Sotty, F., Christensen, K.V., and Thougaard, A. (2018). PFE-360-induced LRRK2 inhibition induces reversible, non-adverse renal changes in rats. *Toxicology* 395, 15–22.

Arranz, A.M., Delbroek, L., Van Kolen, K., Guimarães, M.R., Mandemakers, W., Daneels, G., Matta, S., Calafate, S., Shaban, H., Baatsen, P., et al. (2015). LRRK2 functions in synaptic vesicle endocytosis through a kinase-dependent mechanism. *J. Cell Sci.* 128, 541–552.

Asensio-Juan, E., Fueyo, R., Pappa, S., Iacobucci, S., Badosa, C., Lois, S., Balada, M., Bosch-Presegué, L., Vaquero, A., Gutiérrez, S., et al. (2017). The histone

demethylase PHF8 is a molecular safeguard of the IFNγ response. *Nucleic Acids Res.* 45, 3800.

Atashrazm, F., Hammond, D., Perera, G., Bolliger, M.F., Matar, E., Halliday, G.M., Schüle, B., Lewis, S.J.G., Nichols, R.J., and Dzamko, N. (2019). LRRK2-mediated Rab10 phosphorylation in immune cells from Parkinson's disease patients. *Mov. Disord.* 34, 406–415.

Austin, S.A., Floden, A.M., Murphy, E.J., and Combs, C.K. (2006). Alpha-synuclein expression modulates microglial activation phenotype. *J. Neurosci.* 26, 10558-10563.

Baba, M., Nakajo, S., Tu, P.H., Tomita, T., Nakaya, K., Lee, V.M., Trojanowski, J.Q., and Iwatsubo, T. (1998). Aggregation of alpha-synuclein in Lewy bodies of sporadic Parkinson's disease and dementia with Lewy bodies. *Am. J. Pathol.* 152, 879–884.

Baba, Y., Kuroiwa, A., Uitti, R.J., Wszolek, Z.K., and Yamada, T. (2005). Alterations of T-lymphocyte populations in Parkinson disease. *Parkinsonism & Related Disorders* 11, 493–498.

Badanjak, K., Mulica, P., Smajic, S., Delcambre, S., Tranchevent, L.-C., Diederich, N., Rauen, T., Schwamborn, J.C., Glaab, E., Cowley, S.A., et al. (2021). iPSC-Derived Microglia as a Model to Study Inflammation in Idiopathic Parkinson's Disease. *Front Cell Dev Biol* 9, 740758.

Baptista, M.A.S., Dave, K.D., Frasier, M.A., Sherer, T.B., Greeley, M., Beck, M.J., Varsho, J.S., Parker, G.A., Moore, C., Churchill, M.J., et al. (2013). Loss of leucine-rich repeat kinase 2 (LRRK2) in rats leads to progressive abnormal phenotypes in peripheral organs. *PLoS One* 8, e80705.

Bendor, J.T., Logan, T.P., and Edwards, R.H. (2013). The function of α-synuclein. *Neuron* 79, 1044–1066.

Bernal-Conde, L.D., Ramos-Acevedo, R., Reyes-Hernández, M.A., Balbuena-Olvera, A.J., Morales-Moreno, I.D., Argüero-Sánchez, R., Schüle, B., and Guerra-Crespo, M. (2019). Alpha-Synuclein Physiology and Pathology: A Perspective on Cellular Structures and Organelles. *Front. Neurosci.* 13, 1399.

Bido, S., Muggeo, S., Massimino, L., Marzi, M.J., Giannelli, S.G., Melacini, E., Nannoni, M., Gambarè, D., Bellini, E., Ordazzo, G., et al. (2021). Microglia-specific overexpression of α-synuclein leads to severe dopaminergic neurodegeneration by phagocytic exhaustion and oxidative toxicity. *Nat. Commun.* 12, 6237.

Bliederhaeuser, C., Zondler, L., Grozdanov, V., Ruf, W.P., Brenner, D., Melrose, H.L., Bauer, P., Ludolph, A.C., Gillardon, F., Kassubek, J., et al. (2016a).

LRRK2 contributes to monocyte dysregulation in Parkinson's disease. *Acta Neuropathologica Communications* 4.

Bliederhaeuser, C., Grozdanov, V., Speidel, A., Zondler, L., Ruf, W.P., Bayer, H., Kiechle, M., Feiler, M.S., Freischmidt, A., Brenner, D., et al. (2016b). Age-dependent defects of alpha-synuclein oligomer uptake in microglia and monocytes. *Acta Neuropathol.* 131, 379–391.

Booth, H.D.E., Hirst, W.D., and Wade-Martins, R. (2017). The Role of Astrocyte Dysfunction in Parkinson's Disease Pathogenesis. *Trends Neurosci.* 40, 358–370.

Braak, H., Del Tredici, K., Rüb, U., de Vos, R.A.I., Jansen Steur, E.N.H., and Braak, E. (2003). Staging of brain pathology related to sporadic Parkinson's disease. *Neurobiol. Aging* 24, 197–211.

Brakedal, B., Tzoulis, C., Tysnes, O.-B., and Haugarvoll, K. (2021). NSAID use is not associated with Parkinson's disease incidence: A Norwegian Prescription Database study. *PLoS One* 16, e0256602.

Brandstadter, J.D., and Maillard, I. (2019). Notch signalling in T cell homeostasis and differentiation. *Open Biol.* 9, 190187.

Brodacki, B., Staszewski, J., Toczyłowska, B., Kozłowska, E., Drela, N., Chalimoniuk, M., and Stępien, A. (2008). Serum interleukin (IL-2, IL-10, IL-6, IL-4), TNFα, and INFγ concentrations are elevated in patients with atypical and idiopathic parkinsonism. *Neurosci. Lett.* 441, 158–162.

Butovsky, O., Jedrychowski, M.P., Moore, C.S., Cialic, R., Lanser, A.J., Gabriely, G., Koeglsperger, T., Dake, B., Wu, P.M., Doykan, C.E., et al. (2014). Identification of a unique TGF-β-dependent molecular and functional signature in microglia. *Nat. Neurosci.* 17, 131–143.

Cannon, J.R., and Greenamyre, J.T. (2013). Gene–environment interactions in Parkinson's disease: Specific evidence in humans and mammalian models. *Neurobiol. Dis.* 57, 38–46.

Chittoor-Vinod, V.G., Nichols, R.J., and Schüle, B. (2021). Genetic and Environmental Factors Influence the Pleomorphy of LRRK2 Parkinsonism. *Int. J. Mol. Sci.* 22.

Choi, H.G., Zhang, J., Deng, X., Hatcher, J.M., Patricelli, M.P., Zhao, Z., Alessi, D.R., and Gray, N.S. (2012). Brain Penetrant LRRK2 Inhibitor. *ACS Medicinal Chemistry Letters* 3, 658–662.

Choi, I., Zhang, Y., Seegobin, S.P., Pruvost, M., Wang, Q., Purtell, K., Zhang, B., and Yue, Z. (2020). Microglia clear neuron-released α-synuclein via selective autophagy and prevent neurodegeneration. *Nat. Commun.* 11, 1386.

Cook, D.A., Kannarkat, G.T., Cintron, A.F., Butkovich, L.M., Fraser, K.B., Chang, J., Grigoryan, N., Factor, S.A., West, A.B., Boss, J.M., et al. (2017). LRRK2 levels in immune cells are increased in Parkinson's disease. *NPJ Parkinsons Dis* 3, 11.

Covy, J.P., and Giasson, B.I. (2009). Identification of compounds that inhibit the kinase activity of leucine-rich repeat kinase 2. *Biochemical and Biophysical Research Communications* 378, 473–477.

Daher, J.P.L., Volpicelli-Daley, L.A., Blackburn, J.P., Moehle, M.S., and West, A.B. (2014). Abrogation of α-synuclein–mediated dopaminergic neurodegeneration in LRRK2-deficient rats. *Proceedings of the National Academy of Sciences* 111, 9289–9294.

Daher, J.P.L., Abdelmotilib, H.A., Hu, X., Volpicelli-Daley, L.A., Moehle, M.S., Fraser, K.B., Needle, E., Chen, Y., Steyn, S.J., Galatsis, P., et al. (2015). Leucine-rich Repeat Kinase 2 (LRRK2) Pharmacological Inhibition Abates α-Synuclein Gene-induced Neurodegeneration. *J. Biol. Chem.* 290, 19433–19444.

Desplats, P., Spencer, B., Crews, L., Pathel, P., Morvinski-Friedmann, D., Kosberg, K., Roberts, S., Patrick, C., Winner, B., Winkler, J., et al. (2012). α-Synuclein induces alterations in adult neurogenesis in Parkinson disease models via p53-mediated repression of Notch1. *J. Biol. Chem.* 287, 31691–31702.

Di Maio, R., Hoffman, E.K., Rocha, E.M., Keeney, M.T., Sanders, L.H., De Miranda, B.R., Zharikov, A., Van Laar, A., Stepan, A.F., Lanz, T.A., et al. (2018). LRRK2 activation in idiopathic Parkinson's disease. *Sci. Transl. Med.* 10.

Dorsey, E.R., Sherer, T., Okun, M.S., and Bloem, B.R. (2018). The Emerging Evidence of the Parkinson Pandemic. *J. Parkinsons. Dis.* 8, S3–S8.

Dzamko, N., Inesta-Vaquera, F., Zhang, J., Xie, C., Cai, H., Arthur, S., Tan, L., Choi, H., Gray, N., Cohen, P., et al. (2012). The IkappaB kinase family phosphorylates the Parkinson's disease kinase LRRK2 at Ser935 and Ser910 during Toll-like receptor signaling. *PLoS One* 7, e39132.

Estrada, A.A., Chan, B.K., Baker-Glenn, C., Beresford, A., Burdick, D.J., Chambers, M., Chen, H., Dominguez, S.L., Dotson, J., Drummond, J., et al. (2014). Discovery of Highly Potent, Selective, and Brain-Penetrant Aminopyrazole Leucine-Rich Repeat Kinase 2 (LRRK2) Small Molecule Inhibitors. *Journal of Medicinal Chemistry* 57, 921–936.

Fahn, S., Jankovic, J., and Hallett, M. (2011). Chapter 4 - Parkinsonism: Clinical features and differential diagnosis. In Principles and Practice of Movement Disorders (Second Edition), S. Fahn, J. Jankovic, and M. Hallett, eds. (Edinburgh: W.B. Saunders), pp. 66–92.

Fan, Y., Nirujogi, R.S., Garrido, A., Ruiz-Martínez, J., Bergareche-Yarza, A., Mondragón-Rezola, E., Vinagre-Aragón, A., Croitoru, I., Gorostidi Pagola, A., Paternain Markinez, L., et al. (2021). R1441G but not G2019S mutation enhances LRRK2 mediated Rab10 phosphorylation in human peripheral blood neutrophils. *Acta Neuropathol.* 142, 475–494.

Faraji, F., Pang, Y., Walker, R.C., Nieves Borges, R., Yang, L., and Hunter, K.W. (2012). Cadm1 is a metastasis susceptibility gene that suppresses metastasis by modifying tumor interaction with the cell-mediated immunity. *PLoS Genet.* 8, e1002926.

Fell, M.J., Mirescu, C., Basu, K., Cheewatrakoolpong, B., DeMong, D.E., Michael Ellis, J., Hyde, L.A., Lin, Y., Markgraf, C.G., Mei, H., et al. (2015). MLi-2, a Potent, Selective, and Centrally Active Compound for Exploring the Therapeutic Potential and Safety of LRRK2 Kinase Inhibition. *Journal of Pharmacology and Experimental Therapeutics* 355, 397–409.

Fraser, K.B., Moehle, M.S., Alcalay, R.N., West, A.B., and LRRK2 Cohort Consortium (2016). Urinary LRRK2 phosphorylation predicts parkinsonian phenotypes in G2019S LRRK2 carriers. *Neurology* 86, 994–999.

Gabbert, C., König, I.R., Lüth, T., Kolms, B., Kasten, M., Vollstedt, E.J., Balck, A., Grünewald, A., Klein, C., and Trinh, J. (2022). Coffee, smoking and aspirin are associated with age at onset in idiopathic Parkinson's disease. *J. Neurol.*

Gaig, C., Martí, M.J., Ezquerra, M., Rey, M.J., Cardozo, A., and Tolosa, E. (2007). G2019S LRRK2 mutation causing Parkinson's disease without Lewy bodies. *J. Neurol. Neurosurg. Psychiatry* 78, 626–628.

Garcia-Miralles, M., Coomaraswamy, J., Häbig, K., Herzig, M.C., Funk, N., Gillardon, F., Maisel, M., Jucker, M., Gasser, T., Galter, D., et al. (2015). No dopamine cell loss or changes in cytoskeleton function in transgenic mice expressing physiological levels of wild type or G2019S mutant LRRK2 and in human fibroblasts. *PLoS One* 10, e0118947.

Gardai, S.J., Mao, W., Schüle, B., Babcock, M., Schoebel, S., Lorenzana, C., Alexander, J., Kim, S., Glick, H., Hilton, K., et al. (2013). Elevated alpha-synuclein impairs innate immune cell function and provides a potential peripheral biomarker for Parkinson's disease. *PLoS One* 8, e71634.

Gardet, A., Benita, Y., Li, C., Sands, B.E., Ballester, I., Stevens, C., Korzenik, J.R., Rioux, J.D., Daly, M.J., Xavier, R.J., et al. (2010). LRRK2 Is Involved in the IFN-γ Response and Host Response to Pathogens. *The Journal of Immunology* 185, 5577–5585.

Garrido, A., Santamaría, E., Fernández-Irigoyen, J., Soto, M., Simonet, C., Fernández, M., Obiang, D., Tolosa, E., Martí, M.-J., Padmanabhan, S., et al. (2022).

Differential phospho-signatures in blood cells identify LRRK2 G2019S carriers in Parkinson's disease. *Mov. Disord.*

GBD 2015 Neurological Disorders Collaborator Group (2017). Global, regional, and national burden of neurological disorders during 1990-2015: a systematic analysis for the Global Burden of Disease Study 2015. *Lancet Neurol.* 16, 877–897.

GBD 2016 Parkinson's Disease Collaborators (2018). Global, regional, and national burden of Parkinson's disease, 1990-2016: a systematic analysis for the Global Burden of Disease Study 2016. *Lancet Neurol.* 17, 939–953.

George, S., Rey, N.L., Tyson, T., Esquibel, C., Meyerdirk, L., Schulz, E., Pierce, S., Burmeister, A.R., Madaj, Z., Steiner, J.A., et al. (2019). Microglia affect α-synuclein cell-to-cell transfer in a mouse model of Parkinson's disease. *Molecular Neurodegeneration* 14.

Ghlichloo, I., and Gerriets, V. (2021). Nonsteroidal Anti-inflammatory Drugs (NSAIDs). In StatPearls [Internet], (StatPearls Publishing),.

Giménez, N., Schulz, R., Higashi, M., Aymerich, M., Villamor, N., Delgado, J., Juan, M., López-Guerra, M., Campo, E., Rosich, L., et al. (2020). Targeting IRAK4 disrupts inflammatory pathways and delays tumor development in chronic lymphocytic leukemia. *Leukemia* 34, 100–114.

Ginhoux, F., Greter, M., Leboeuf, M., Nandi, S., See, P., Gokhan, S., Mehler, M.F., Conway, S.J., Ng, L.G., Stanley, E.R., et al. (2010). Fate mapping analysis reveals that adult microglia derive from primitive macrophages. *Science* 330, 841–845.

Grandbarbe, L., Michelucci, A., Heurtaux, T., Hemmer, K., Morga, E., and Heuschling, P. (2007). Notch signaling modulates the activation of microglial cells. *Glia* 55, 1519–1530.

Greggio, E., Taymans, J.-M., Zhen, E.Y., Ryder, J., Vancraenenbroeck, R., Beilina, A., Sun, P., Deng, J., Jaffe, H., Baekelandt, V., et al. (2009). The Parkinson's disease kinase LRRK2 autophosphorylates its GTPase domain at multiple sites. *Biochemical and Biophysical Research Communications* 389, 449–454.

Guo, M., Wang, J., Zhao, Y., Feng, Y., Han, S., Dong, Q., Cui, M., and Tieu, K. (2020). Microglial exosomes facilitate α-synuclein transmission in Parkinson's disease. *Brain* 143, 1476–1497.

Haenseler, W., Zambon, F., Lee, H., Vowles, J., Rinaldi, F., Duggal, G., Houlden, H., Gwinn, K., Wray, S., Luk, K.C., et al. (2017a). Excess α-synuclein compromises phagocytosis in iPSC-derived macrophages. *Sci. Rep.* 7, 9003.

Haenseler, W., Sansom, S.N., Buchrieser, J., Newey, S.E., Moore, C.S., Nicholls, F.J., Chintawar, S., Schnell, C., Antel, J.P., Allen, N.D., et al. (2017b). A

Highly Efficient Human Pluripotent Stem Cell Microglia Model Displays a Neuronal-Co-culture-Specific Expression Profile and Inflammatory Response. *Stem Cell Reports* 8, 1727–1742.

Hakimi, M., Selvanantham, T., Swinton, E., Padmore, R.F., Tong, Y., Kabbach, G., Venderova, K., Girardin, S.E., Bulman, D.E., Scherzer, C.R., et al. (2011). Parkinson's disease-linked LRRK2 is expressed in circulating and tissue immune cells and upregulated following recognition of microbial structures. *J. Neural Transm.* 118, 795–808.

Haque, M.E., Akther, M., Jakaria, M., Kim, I.-S., Azam, S., and Choi, D.-K. (2020). Targeting the microglial NLRP3 inflammasome and its role in Parkinson's disease. *Mov. Disord.* 35, 20–33.

Harms, A.S., Thome, A.D., Yan, Z., Schonhoff, A.M., Williams, G.P., Li, X., Liu, Y., Qin, H., Benveniste, E.N., and Standaert, D.G. (2018). Peripheral monocyte entry is required for alpha-Synuclein induced inflammation and Neurodegeneration in a model of Parkinson disease. *Exp. Neurol.* 300, 179–187.

Hatcher, J.M., Zhang, J., Choi, H.G., Ito, G., Alessi, D.R., and Gray, N.S. (2015). Discovery of a Pyrrolopyrimidine (JH-II-127), a Highly Potent, Selective, and Brain Penetrant LRRK2 Inhibitor. *ACS Medicinal Chemistry Letters* 6, 584–589.

Healy, D.G., Falchi, M., O'Sullivan, S.S., Bonifati, V., Durr, A., Bressman, S., Brice, A., Aasly, J., Zabetian, C.P., Goldwurm, S., et al. (2008). Phenotype, genotype, and worldwide genetic penetrance of LRRK2-associated Parkinson's disease: a case-control study. *Lancet Neurol.* 7, 583–590.

Herzig, M.C., Bidinosti, M., Tatjana Schweizer, Hafner, T., Stemmelen, C., Weiss, A., Danner, S., Vidotto, N., Stauffer, D., Barske, C., et al. (2012). High LRRK2 Levels Fail to Induce or Exacerbate Neuronal Alpha-Synucleinopathy in Mouse Brain. *PLoS ONE* 7, e36581.

Hinkle, K.M., Yue, M., Behrouz, B., Dächsel, J.C., Lincoln, S.J., Bowles, E.E., Beevers, J.E., Dugger, B., Winner, B., Prots, I., et al. (2012). LRRK2 knockout mice have an intact dopaminergic system but display alterations in exploratory and motor co-ordination behaviors. *Mol. Neurodegener.* 7, 25.

Ho, P.W.-L., Leung, C.-T., Liu, H., Pang, S.Y.-Y., Lam, C.S.-C., Xian, J., Li, L., Kung, M.H.-W., Ramsden, D.B., and Ho, S.-L. (2020). Age-dependent accumulation of oligomeric SNCA/α-synuclein from impaired degradation in mutant LRRK2 knockin mouse model of Parkinson disease: role for therapeutic activation of chaperone-mediated autophagy (CMA). *Autophagy* 16, 347–370.

Hulse, J., and Bhaskar, K. (2022). Crosstalk Between the NLRP3 Inflammasome/ASC Speck and Amyloid Protein Aggregates Drives Disease Progression in Alzheimer's and Parkinson's Disease. *Front. Mol. Neurosci.* 0.

Iannotta, L., Biosa, A., Kluss, J.H., Tombesi, G., Kaganovich, A., Cogo, S., Plotegher, N., Civiero, L., Lobbestael, E., Baekelandt, V., et al. (2020). Divergent Effects of G2019S and R1441C LRRK2 Mutations on LRRK2 and Rab10 Phosphorylations in Mouse Tissues. *Cells* 9.

Imai, Y., Kobayashi, Y., Inoshita, T., Meng, H., Arano, T., Uemura, K., Asano, T., Yoshimi, K., Zhang, C.-L., Matsumoto, G., et al. (2015). The Parkinson's Disease-Associated Protein Kinase LRRK2 Modulates Notch Signaling through the Endosomal Pathway. *PLoS Genet.* 11, e1005503.

Ito, G., Katsemonova, K., Tonelli, F., Lis, P., Baptista, M.A.S., Shpiro, N., Duddy, G., Wilson, S., Ho, P.W.-L., Ho, S.-L., et al. (2016). Phos-tag analysis of Rab10 phosphorylation by LRRK2: a powerful assay for assessing kinase function and inhibitors. *Biochem. J* 473, 2671–2685.

Iwaki, H., Blauwendraat, C., Makarious, M.B., Bandrés-Ciga, S., Leonard, H.L., Gibbs, J.R., Hernandez, D.G., Scholz, S.W., Faghri, F., International Parkinson's Disease Genomics Consortium (IPDGC), et al. (2020). Penetrance of Parkinson's Disease in LRRK2 p.G2019S Carriers Is Modified by a Polygenic Risk Score. *Mov. Disord.* 35, 774–780.

Janda, E., Boi, L., and Carta, A.R. (2018). Microglial Phagocytosis and Its Regulation: A Therapeutic Target in Parkinson's Disease? *Front. Mol. Neurosci.* 11, 144.

Johansen, K.K., Torp, S.H., Farrer, M.J., Gustavsson, E.K., and Aasly, J.O. (2018). A Case of Parkinson's Disease with No Lewy Body Pathology due to a Homozygous Exon Deletion in Parkin. *Case Rep. Neurol. Med.* 2018, 6838965.

Johnson, M.E., Stecher, B., Labrie, V., Brundin, L., and Brundin, P. (2019). Triggers, Facilitators, and Aggravators: Redefining Parkinson's Disease Pathogenesis. *Trends in Neurosciences* 42, 4–13.

Kachergus, J., Mata, I.F., Hulihan, M., Taylor, J.P., Lincoln, S., Aasly, J., Gibson, J.M., Ross, O.A., Lynch, T., Wiley, J., et al. (2005). Identification of a novel LRRK2 mutation linked to autosomal dominant parkinsonism: evidence of a common founder across European populations. *Am. J. Hum. Genet.* 76, 672–680.

Keewan, E., and Naser, S.A. (2020). The Role of Notch Signaling in Macrophages during Inflammation and Infection: Implication in Rheumatoid Arthritis? *Cells* 9.

Kempthorne, L., Yoon, H., Madore, C., Smith, S., Wszolek, Z.K., Rademakers, R., Kim, J., Butovsky, O., and Dickson, D.W. (2020). Loss of homeostatic microglial phenotype in CSF1R-related Leukoencephalopathy. *Acta Neuropathol Commun* 8, 72.

Kodamullil, A.T., Iyappan, A., Karki, R., Madan, S., Younesi, E., and Hofmann-Apitius, M. (2017). Of Mice and Men: Comparative Analysis of Neuro-Inflammatory Mechanisms in Human and Mouse Using Cause-and-Effect Models. *Journal of Alzheimer's Disease* 59, 1045–1055.

Konstantin Nissen, S., Farmen, K., Carstensen, M., Schulte, C., Goldeck, D., Brockmann, K., and Romero-Ramos, M. (2022). Changes in CD163+, CD11b+, and CCR2+ peripheral monocytes relate to Parkinson's disease and cognition. *Brain Behav. Immun.* 101, 182–193.

Kozina, E., Byrne, M., and Smeyne, R.J. (2022). Mutant LRRK2 in lymphocytes regulates neurodegeneration via IL-6 in an inflammatory model of Parkinson's disease. *NPJ Parkinsons Dis* 8, 24.

Krüger, R., Kuhn, W., Müller, T., Woitalla, D., Graeber, M., Kösel, S., Przuntek, H., Epplen, J.T., Schöls, L., and Riess, O. (1998). Ala30Pro mutation in the gene encoding alpha-synuclein in Parkinson's disease. *Nat. Genet.* 18, 106–108.

Kuss, M., Adamopoulou, E., and Kahle, P.J. (2014). Interferon-γ induces leucine-rich repeat kinase LRRK2 via extracellular signal-regulated kinase ERK5 in macrophages. *Journal of Neurochemistry* 129, 980–987.

Kustrimovic, N., Comi, C., Magistrelli, L., Rasini, E., Legnaro, M., Bombelli, R., Aleksic, I., Blandini, F., Minafra, B., Riboldazzi, G., et al. (2018). Parkinson's disease patients have a complex phenotypic and functional Th1 bias: cross-sectional studies of CD4+ Th1/Th2/T17 and Treg in drug-naïve and drug-treated patients. *J. Neuroinflammation* 15, 205.

Latourelle, J.C., Sun, M., Lew, M.F., Suchowersky, O., Klein, C., Golbe, L.I., Mark, M.H., Growdon, J.H., Wooten, G.F., Watts, R.L., et al. (2008). The Gly2019Ser mutation in LRRK2 is not fully penetrant in familial Parkinson's disease: the GenePD study. *BMC Med.* 6, 32.

Lee, A.J., Wang, Y., Alcalay, R.N., Mejia-Santana, H., Saunders-Pullman, R., Bressman, S., Corvol, J.-C., Brice, A., Lesage, S., Mangone, G., et al. (2017). Penetrance estimate of LRRK2 p.G2019S mutation in individuals of non-Ashkenazi Jewish ancestry. *Mov. Disord.* 32, 1432–1438.

Lee, H., Flynn, R., Sharma, I., Haberman, E., Carling, P.J., Nicholls, F.J., Stegmann, M., Vowles, J., Haenseler, W., Wade-Martins, R., et al. (2020). LRRK2 Is Recruited to Phagosomes and Co-recruits RAB8 and RAB10 in Human Pluripotent Stem Cell-Derived Macrophages. *Stem Cell Reports* 14, 940–955.

Liang, T., Zhang, Y., Wu, S., Chen, Q., and Wang, L. (2022). The Role of NLRP3 Inflammasome in Alzheimer's Disease and Potential Therapeutic Targets. *Front. Pharmacol.* 0.

Lill, C.M., and Klein, C. (2017). What would Dr. James Parkinson think today? The role of genetics in Parkinson's disease. *Mov. Disord.* 32, 1115–1116.

Liscovitch, N., and French, L. (2014). Differential Co-Expression between α-Synuclein and IFN-γ Signaling Genes across Development and in Parkinson's Disease. *PLoS One* 9, e115029.

Litwiniuk, A., Baranowska-Bik, A., Domańska, A., Kalisz, M., and Bik, W. (2021). Contribution of Mitochondrial Dysfunction Combined with NLRP3 Inflammasome Activation in Selected Neurodegenerative Diseases. *Pharmaceuticals* 14.

Liu, G., Sgobio, C., Gu, X., Sun, L., Lin, X., Yu, J., Parisiadou, L., Xie, C., Sastry, N., Ding, J., et al. (2015). Selective expression of Parkinson's disease-related Leucine-rich repeat kinase 2 G2019S missense mutation in midbrain dopaminergic neurons impairs dopamine release and dopaminergic gene expression. *Hum. Mol. Genet.* 24, 5299–5312.

Longo, F., Mercatelli, D., Novello, S., Arcuri, L., Brugnoli, A., Vincenzi, F., Russo, I., Berti, G., Mabrouk, O.S., Kennedy, R.T., et al. (2017). Age-dependent dopamine transporter dysfunction and Serine129 phospho-α-synuclein overload in G2019S LRRK2 mice. *Acta Neuropathol Commun* 5, 22.

Long-Smith, C.M., Sullivan, A.M., and Nolan, Y.M. (2009). The influence of microglia on the pathogenesis of Parkinson's disease. *Prog. Neurobiol.* 89, 277–287.

Mahul-Mellier, A.-L., Burtscher, J., Maharjan, N., Weerens, L., Croisier, M., Kuttler, F., Leleu, M., Knott, G.W., and Lashuel, H.A. (2020). The process of Lewy body formation, rather than simply α-synuclein fibrillization, is one of the major drivers of neurodegeneration. *Proc. Natl. Acad. Sci. U. S. A.* 117, 4971–4982.

Marder, K., Wang, Y., Alcalay, R.N., Mejia-Santana, H., Tang, M.-X., Lee, A., Raymond, D., Mirelman, A., Saunders-Pullman, R., Clark, L., et al. (2015). Age-specific penetrance of LRRK2 G2019S in the Michael J. Fox Ashkenazi Jewish LRRK2 Consortium. *Neurology* 85, 89–95.

Marras, C., Schüle, B., Munhoz, R.P., Rogaeva, E., Langston, J.W., Kasten, M., Meaney, C., Klein, C., Wadia, P.M., Lim, S.-Y., et al. (2011). Phenotype in parkinsonian and nonparkinsonian LRRK2 G2019S mutation carriers. *Neurology* 77, 325–333.

Mavroeidi, P., and Xilouri, M. (2021). Neurons and Glia Interplay in α-Synucleinopathies. *Int. J. Mol. Sci.* 22.

Melachroinou, K., Kang, M.S., Liong, C., Narayan, S., Levers, N., Joshi, N., Kopil, K., Hutten, S.J., Baptista, M.A.S., Padmanabhan, S., et al. (2020). Elevated In

Vitro Kinase Activity in Peripheral Blood Mononuclear Cells of Leucine-Rich Repeat Kinase 2 G2019S Carriers: A Novel Enzyme-Linked Immunosorbent Assay-Based Method. *Mov. Disord.* 35, 2095–2100.

Minghetti, L. (2004). Cyclooxygenase-2 (COX-2) in Inflammatory and Degenerative Brain Diseases. *Journal of Neuropathology & Experimental Neurology* 63, 901–910.

Mishra, S.R., Mahapatra, K.K., Behera, B.P., Patra, S., Bhol, C.S., Panigrahi, D.P., Praharaj, P.P., Singh, A., Patil, S., Dhiman, R., et al. (2021). Mitochondrial dysfunction as a driver of NLRP3 inflammasome activation and its modulation through mitophagy for potential therapeutics. *Int. J. Biochem. Cell Biol.* 136, 106013.

Moehle, M.S., Webber, P.J., Tse, T., Sukar, N., Standaert, D.G., DeSilva, T.M., Cowell, R.M., and West, A.B. (2012). LRRK2 inhibition attenuates microglial inflammatory responses. *J. Neurosci.* 32, 1602–1611.

Monier, A., Adle-Biassette, H., Delezoide, A.-L., Evrard, P., Gressens, P., and Verney, C. (2007). Entry and distribution of microglial cells in human embryonic and fetal cerebral cortex. *J. Neuropathol. Exp. Neurol.* 66, 372–382.

Muffat, J., Li, Y., Yuan, B., Mitalipova, M., Omer, A., Corcoran, S., Bakiasi, G., Tsai, L.-H., Aubourg, P., Ransohoff, R.M., et al. (2016). Efficient derivation of microglia-like cells from human pluripotent stem cells. *Nat. Med.* 22, 1358–1367.

Mullard, A. (2020). IRAK4 degrader to take on innate immunity. *Nat. Biotechnol.* 38, 1221–1223.

Nagatsu, T., and Sawada, M. (2005). Inflammatory process in Parkinson's disease: role for cytokines. *Curr. Pharm. Des.* 11, 999–1016.

Ngwa, C., Mamun, A.A., Xu, Y., Sharmeen, R., and Liu, F. (2021). Phosphorylation of Microglial IRF5 and IRF4 by IRAK4 Regulates Inflammatory Responses to Ischemia. *Cells* 10.

Nichols, R.J., Jeremy Nichols, R., Dzamko, N., Hutti, J.E., Cantley, L.C., Deak, M., Moran, J., Bamborough, P., Reith, A.D., and Alessi, D.R. (2009). Substrate specificity and inhibitors of LRRK2, a protein kinase mutated in Parkinson's disease. *Biochemical Journal* 424, 47–60.

Novello, S., Arcuri, L., Dovero, S., Dutheil, N., Shimshek, D.R., Bezard, E., and Morari, M. (2018). G2019S LRRK2 mutation facilitates α-synuclein neuropathology in aged mice. *Neurobiol. Dis.* 120, 21–33.

Obergasteiger, J., Frapporti, G., Lamonaca, G., Pizzi, S., Picard, A., Lavdas, A.A., Pischedda, F., Piccoli, G., Hilfiker, S., Lobbestael, E., et al. (2020). Kinase inhibition of G2019S-LRRK2 enhances autolysosome formation and function

to reduce endogenous alpha-synuclein intracellular inclusions. *Cell Death Discov* 6, 45.

O'Hara, D.M., Pawar, G., Kalia, S.K., and Kalia, L.V. (2020). LRRK2 and α-synuclein: Distinct or synergistic players in Parkinson's disease? *Front. Neurosci.* 14, 577.

Oksanen, M., Petersen, A.J., Naumenko, N., Puttonen, K., Lehtonen, Š., Gubert Olivé, M., Shakirzyanova, A., Leskelä, S., Sarajärvi, T., Viitanen, M., et al. (2017). PSEN1 Mutant iPSC-Derived Model Reveals Severe Astrocyte Pathology in Alzheimer's Disease. *Stem Cell Reports* 9, 1885–1897.

Paisán-Ruíz, C., Jain, S., Evans, E.W., Gilks, W.P., Simón, J., van der Brug, M., López de Munain, A., Aparicio, S., Gil, A.M., Khan, N., et al. (2004). Cloning of the gene containing mutations that cause PARK8-linked Parkinson's disease. *Neuron* 44, 595–600.

Panagiotakopoulou, V., Ivanyuk, D., De Cicco, S., Haq, W., Arsić, A., Yu, C., Messelodi, D., Oldrati, M., Schöndorf, D.C., Perez, M.-J., et al. (2020). Interferon-γ signaling synergizes with LRRK2 in neurons and microglia derived from human induced pluripotent stem cells. *Nat. Commun.* 11, 5163.

Pandya, H., Shen, M.J., Ichikawa, D.M., Sedlock, A.B., Choi, Y., Johnson, K.R., Kim, G., Brown, M.A., Elkahloun, A.G., Maric, D., et al. (2017). Differentiation of human and murine induced pluripotent stem cells to microglia-like cells. *Nat. Neurosci.* 20, 753–759.

Parkinson, J. (2002). An essay on the shaking palsy. 1817. *J. Neuropsychiatry Clin. Neurosci.* 14, 223–236; discussion 222.

Pont-Sunyer, C., Iranzo, A., Gaig, C., Fernández-Arcos, A., Vilas, D., Valldeoriola, F., Compta, Y., Fernández-Santiago, R., Fernández, M., Bayés, A., et al. (2015). Sleep Disorders in Parkinsonian and Nonparkinsonian LRRK2 Mutation Carriers. *PLoS One* 10, e0132368.

Qin, L., Wu, X., Block, M.L., Liu, Y., Breese, G.R., Hong, J.-S., Knapp, D.J., and Crews, F.T. (2007). Systemic LPS causes chronic neuroinflammation and progressive neurodegeneration. *Glia* 55, 453–462.

Radtke, F., Fasnacht, N., and Macdonald, H.R. (2010). Notch signaling in the immune system. *Immunity* 32, 14–27.

Reinhardt, P., Glatza, M., Hemmer, K., Tsytsyura, Y., Thiel, C.S., Höing, S., Moritz, S., Parga, J.A., Wagner, L., Bruder, J.M., et al. (2013). Derivation and expansion using only small molecules of human neural progenitors for neurodegenerative disease modeling. *PLoS One* 8, e59252.

Ripoll, V.M., Irvine, K.M., Ravasi, T., Sweet, M.J., and Hume, D.A. (2007). Gpnmb is induced in macrophages by IFN-gamma and lipopolysaccharide and

acts as a feedback regulator of proinflammatory responses. *J. Immunol.* 178, 6557–6566.

Rocca, W.A. (2018). The future burden of Parkinson's disease. *Mov. Disord.* 33, 8–9.

Russo, I., Berti, G., Plotegher, N., Bernardo, G., Filograna, R., Bubacco, L., and Greggio, E. (2016). Erratum to: Leucine-rich repeat kinase 2 positively regulates inflammation and down-regulates NF-κB p50 signaling in cultured microglia cells. *Journal of Neuroinflammation* 13.

Saade, M., Araujo de Souza, G., Scavone, C., and Kinoshita, P.F. (2021). The Role of GPNMB in Inflammation. *Front. Immunol.* 12, 674739.

Samii, A., Etminan, M., Wiens, M.O., and Jafari, S. (2009). NSAID use and the risk of Parkinson's disease: systematic review and meta-analysis of observational studies. *Drugs Aging* 26.

San, L.M., Tanner, C.M., Meng, C., Marras, C., Goldman, S.M., Lang, A.E., Tolosa, E., Schüle, B., Langston, J.W., Brice, A., et al. (2020). Nonsteroidal Anti-inflammatory Use and LRRK2 Parkinson's Disease Penetrance. *Mov. Disord.* 35.

Saunders-Pullman, R., Mirelman, A., Alcalay, R.N., Wang, C., Ortega, R.A., Raymond, D., Mejia-Santana, H., Orbe-Reilly, M., Johannes, B.A., Thaler, A., et al. (2018). Progression in the LRRK2-Asssociated Parkinson Disease Population. *JAMA Neurol.* 75, 312–319.

Scheiblich, H., Dansokho, C., Mercan, D., Schmidt, S.V., Bousset, L., Wischhof, L., Eikens, F., Odainic, A., Spitzer, J., Griep, A., et al. (2021). Microglia jointly degrade fibrillar alpha-synuclein cargo by distribution through tunneling nanotubes. *Cell* 184, 5089–5106.e21.

Schneider, S.A., and Alcalay, R.N. (2017). Neuropathology of genetic synucleinopathies with parkinsonism: Review of the literature. *Mov. Disord.* 32, 1504–1523.

Schulz, C., Gomez Perdiguero, E., Chorro, L., Szabo-Rogers, H., Cagnard, N., Kierdorf, K., Prinz, M., Wu, B., Jacobsen, S.E.W., Pollard, J.W., et al. (2012). A lineage of myeloid cells independent of Myb and hematopoietic stem cells. *Science* 336, 86–90.

Scott, J.D., DeMong, D.E., Greshock, T.J., Basu, K., Dai, X., Harris, J., Hruza, A., Li, S.W., Lin, S.-I., Liu, H., et al. (2017). Discovery of a 3-(4-Pyrimidinyl) Indazole (MLi-2), an Orally Available and Selective Leucine-Rich Repeat Kinase 2 (LRRK2) Inhibitor that Reduces Brain Kinase Activity. *Journal of Medicinal Chemistry* 60, 2983–2992.

Seegobin, S.P., Heaton, G.R., Liang, D., Choi, I., Blanca Ramirez, M., Tang, B., and Yue, Z. (2020). Progress in LRRK2-Associated Parkinson's Disease Animal Models. *Front. Neurosci.* 14, 674.

Shang, Y., Smith, S., and Hu, X. (2016). Role of Notch signaling in regulating innate immunity and inflammation in health and disease. *Protein Cell* 7, 159–174.

Sharma, M., Ioannidis, J.P.A., Aasly, J.O., Annesi, G., Brice, A., Van Broeckhoven, C., Bertram, L., Bozi, M., Crosiers, D., Clarke, C., et al. (2012). Large-scale replication and heterogeneity in Parkinson disease genetic loci. *Neurology* 79, 659–667.

Shin, E.C., Cho, S.E., Lee, D.K., Hur, M.W., Paik, S.R., Park, J.H., and Kim, J. (2000). Expression patterns of alpha-synuclein in human hematopoietic cells and in Drosophila at different developmental stages. *Mol. Cells* 10, 65–70.

Shu, L., Zhang, Y., Pan, H., Xu, Q., Guo, J., Tang, B., and Sun, Q. (2018). Clinical Heterogeneity Among LRRK2 Variants in Parkinson's Disease: A Meta-Analysis. *Front. Aging Neurosci.* 10, 283.

Simón-Sánchez, J., Schulte, C., Bras, J.M., Sharma, M., Gibbs, J.R., Berg, D., Paisan-Ruiz, C., Lichtner, P., Scholz, S.W., Hernandez, D.G., et al. (2009). Genome-wide association study reveals genetic risk underlying Parkinson's disease. *Nat. Genet.* 41, 1308–1312.

Simunovic, F., Yi, M., Wang, Y., Macey, L., Brown, L.T., Krichevsky, A.M., Andersen, S.L., Stephens, R.M., Benes, F.M., and Sonntag, K.C. (2009). Gene expression profiling of substantia nigra dopamine neurons: further insights into Parkinson's disease pathology. *Brain* 132, 1795–1809.

Sliter, D.A., Martinez, J., Hao, L., Chen, X., Sun, N., Fischer, T.D., Burman, J.L., Li, Y., Zhang, Z., Narendra, D.P., et al. (2018). Parkin and PINK1 mitigate STING-induced inflammation. *Nature* 561, 258–262.

Smajić, S., Prada-Medina, C.A., Landoulsi, Z., Ghelfi, J., Delcambre, S., Dietrich, C., Jarazo, J., Henck, J., Balachandran, S., Pachchek, S., et al. (2021). Single-cell sequencing of human midbrain reveals glial activation and a Parkinson-specific neuronal state. *Brain.*

Spillantini, M.G., Crowther, R.A., Jakes, R., Hasegawa, M., and Goedert, M. (1998). alpha-Synuclein in filamentous inclusions of Lewy bodies from Parkinson's disease and dementia with lewy bodies. *Proc. Natl. Acad. Sci. U. S. A.* 95, 6469–6473.

Squillaro, T., Cambi, F., Ciacci, G., Rossi, S., Ulivelli, M., Malandrini, A., Mencarelli, M.A., Mari, F., Renieri, A., and Ariani, F. (2007). Frequency of the LRRK2

G2019S mutation in Italian patients affected by Parkinson's disease. *J. Hum. Genet.* 52, 201–204.

Sulzer, D. (2007). Multiple hit hypotheses for dopamine neuron loss in Parkinson's disease. *Trends Neurosci.* 30, 244–250.

Takahashi, K., and Yamanaka, S. (2006). Induction of pluripotent stem cells from mouse embryonic and adult fibroblast cultures by defined factors. *Cell* 126, 663–676.

Tavian, M., and Péault, B. (2005). Embryonic development of the human hematopoietic system. *Int. J. Dev. Biol.* 49, 243–250.

Thévenet, J., Pescini Gobert, R., Hooft van Huijsduijnen, R., Wiessner, C., and Sagot, Y.J. (2011). Regulation of LRRK2 expression points to a functional role in human monocyte maturation. *PLoS One* 6, e21519.

Volpicelli-Daley, L.A., Abdelmotilib, H., Liu, Z., Stoyka, L., Daher, J.P.L., Milnerwood, A.J., Unni, V.K., Hirst, W.D., Yue, Z., Zhao, H.T., et al. (2016). G2019S-LRRK2 Expression Augments α-Synuclein Sequestration into Inclusions in Neurons. J. Neurosci. 36, 7415–7427.

Wallings, R.L., Herrick, M.K., and Tansey, M.G. (2020). LRRK2 at the Interface Between Peripheral and Central Immune Function in Parkinson's. *Front. Neurosci.* 14, 443.

Wang, Q., Liu, Y., and Zhou, J. (2015). Neuroinflammation in Parkinson's disease and its potential as therapeutic target. *Transl. Neurodegener.* 4, 19.

Wang, X., Negrou, E., Maloney, M.T., Bondar, V.V., Andrews, S.V., Montalban, M., Llapashtica, C., Maciuca, R., Nguyen, H., Solanoy, H., et al. (2021). Understanding LRRK2 kinase activity in preclinical models and human subjects through quantitative analysis of LRRK2 and pT73 Rab10. *Sci. Rep.* 11, 12900.

Wanneveich, M., Moisan, F., Jacqmin-Gadda, H., Elbaz, A., and Joly, P. (2018). Projections of prevalence, lifetime risk, and life expectancy of Parkinson's disease (2010-2030) in France. *Mov. Disord.* 33, 1449–1455.

West, A.P., Khoury-Hanold, W., Staron, M., Tal, M.C., Pineda, C.M., Lang, S.M., Bestwick, M., Duguay, B.A., Raimundo, N., MacDuff, D.A., et al. (2015). Mitochondrial DNA stress primes the antiviral innate immune response. *Nature* 520, 553–557.

van Wilgenburg, B., Browne, C., Vowles, J., and Cowley, S.A. (2013). Efficient, long term production of monocyte-derived macrophages from human pluripotent stem cells under partly-defined and fully-defined conditions. *PLoS One* 8, e71098.

Wojewska, D.N., and Kortholt, A. (2021). LRRK2 Targeting Strategies as Potential Treatment of Parkinson's Disease. *Biomolecules* 11, 1101.

Wongchana, W., Kongkavitoon, P., Tangtanatakul, P., Sittplangkoon, C., Butta, P., Chawalitpong, S., Pattarakankul, T., Osborne, B.A., and Palaga, T. (2018). Notch signaling regulates the responses of lipopolysaccharide-stimulated macrophages in the presence of immune complexes. *PLoS One* 13, e0198609.

Xiao, W., Shameli, A., Harding, C.V., Meyerson, H.J., and Maitta, R.W. (2014). Late stages of hematopoiesis and B cell lymphopoiesis are regulated by α-synuclein, a key player in Parkinson's disease. *Immunobiology* 219, 836–844.

Xu, E., Boddu, R., Abdelmotilib, H.A., Sokratian, A., Kelly, K., Liu, Z., Bryant, N., Chandra, S., Carlisle, S.M., Lefkowitz, E.J., et al. (2022). Pathological α-synuclein recruits LRRK2 expressing pro-inflammatory monocytes to the brain. *Mol. Neurodegener.* 17, 7.

Zhao, Y., Keshiya, S., Perera, G., Schramko, L., Halliday, G.M., and Dzamko, N. (2020). LRRK2 kinase inhibitors reduce alpha-synuclein in human neuronal cell lines with the G2019S mutation. *Neurobiol. Dis.* 144, 105049.

Zimprich, A., Biskup, S., Leitner, P., Lichtner, P., Farrer, M., Lincoln, S., Kachergus, J., Hulihan, M., Uitti, R.J., Calne, D.B., et al. (2004). Mutations in LRRK2 cause autosomal-dominant parkinsonism with pleomorphic pathology. *Neuron* 44, 601–607.

Appendix

Additional publication

Parkin Deficiency Impairs Mitochondrial DNA Dynamics and Propagates Inflammation

RESEARCH ARTICLE

Parkin Deficiency Impairs Mitochondrial DNA Dynamics and Propagates Inflammation

Kobi Wasner, PhD,[1] Semra Smajic, MSc,[1] Jenny Ghelfi, BSc,[1] Sylvie Delcambre, PhD,[1] Cesar A. Prada-Medina, PhD,[2] Evelyn Knappe, MSc,[3] Giuseppe Arena, PhD,[1] Patrycja Mulica, MSc,[1] Gideon Agyeah, MSc,[1] Aleksandar Rakovic, PhD,[3] Ibrahim Boussaad, PhD,[1,4] Katja Badanjak, MSc,[1] Jochen Ohnmacht, PhD,[1,5] Jean-Jacques Gérardy, BSc,[6] Masashi Takanashi, MD,[7] Joanne Trinh, PhD,[3] Michel Mittelbronn, MD,[1,6,8,9] Nobutaka Hattori, MD, PhD,[7] Christine Klein, MD,[3] Paul Antony, PhD,[1,4] Philip Seibler, PhD,[3] Malte Spielmann, MD,[2,10] Sandro L. Pereira, PhD,[1,7] and Anne Grünewald, PhD[1,3*]

[1]*Luxembourg Centre for Systems Biomedicine, University of Luxembourg, Esch-sur-Alzette*
[2]*Max Planck Institute for Molecular Genetics, Berlin, Germany*
[3]*Institute of Neurogenetics, University of Lübeck, Lübeck, Germany*
[4]*Disease Modeling and Screening Platform, Luxembourg Centre of Systems Biomedicine, University of Luxembourg & Luxembourg Institute of Health, Luxembourg*
[5]*Department of Life Science and Medicine, University of Luxembourg, Esch-sur-Alzette, Luxembourg*
[6]*National Center of Pathology, Laboratoire National de Santé, Dudelange, Luxembourg*
[7]*Department of Neurology, Juntendo University, Tokyo, Japan*
[8]*Luxembourg Center of Neuropathology, Dudelange, Luxembourg*
[9]*Department of Cancer Research, Luxembourg Institute of Health, Luxembourg, Luxembourg*
[10]*Institute of Human Genetics, University of Lübeck, Lübeck, Germany*

ABSTRACT: Background: Mutations in the E3 ubiquitin ligase parkin cause autosomal recessive Parkinson's disease (PD). Together with PTEN-induced kinase 1 (*PINK1*), parkin regulates the clearance of dysfunctional mitochondria. New mitochondria are generated through an interplay of nuclear- and mitochondrial-encoded proteins, and recent studies suggest that parkin influences this process at both levels. In addition, parkin was shown to prevent mitochondrial membrane permeability, impeding mitochondrial DNA (mtDNA) escape and subsequent neuroinflammation. However, parkin's regulatory roles independent of mitophagy are not well described in patient-derived neurons.

Objectives: We sought to investigate parkin's role in preventing neuronal mtDNA dyshomeostasis, release, and glial activation at the endogenous level.

Methods: We generated induced pluripotent stem cell (iPSC)–derived midbrain neurons from PD patients with parkin (*PRKN*) mutations and healthy controls. Live-cell imaging, proteomic, mtDNA integrity, and gene expression analyses were employed to investigate mitochondrial biogenesis and genome maintenance. To assess neuroinflammation, we performed single-nuclei RNA sequencing in postmortem tissue and quantified interleukin expression in mtDNA/lipopolysaccharides (LPS)-treated iPSC-derived neuron–microglia co-cultures.

Results: Neurons from patients with *PRKN* mutations revealed deficits in the mitochondrial biogenesis pathway, resulting in mtDNA dyshomeostasis. Moreover, the energy sensor sirtuin 1, which controls mitochondrial biogenesis and clearance, was downregulated in parkin-deficient cells. Linking mtDNA disintegration to neuroinflammation, in postmortem midbrain with *PRKN* mutations, we confirmed mtDNA dyshomeostasis and detected an upregulation of microglia overexpressing proinflammatory cytokines. Finally, parkin-deficient neuron–microglia co-cultures elicited an enhanced immune response when exposed to mtDNA/LPS.

Conclusions: Our findings suggest that parkin coregulates mitophagy, mitochondrial biogenesis, and mtDNA maintenance pathways, thereby protecting midbrain neurons from neuroinflammation and degeneration.

Key Words: Parkinson's disease; mitochondrial DNA; induced pluripotent stem cells; parkin; neuroinflammation

***Correspondence to:** Dr. Anne Grünewald, Luxembourg Centre for Systems Biomedicine, University of Luxembourg, 6 Avenue du Swing, L-4367 Belvaux. E-mail: anne.gruenewald@uni.lu

Semra Smajic and Jenny Ghelfi contributed equally.

Relevant conflicts of interest/financial disclosures: The authors report no conflicts of interest.

Received: 22 December 2021; **Revised:** 7 March 2022; **Accepted:** 27 March 2022

Published online in Wiley Online Library (wileyonlinelibrary.com). DOI: 10.1002/mds.29025

Introduction

Dopaminergic neurons (DANs) of the substantia nigra pars compacta (SNpc) in the midbrain are critically involved in the regulation of movement.[1] Loss of DANs results in clinical motor disturbances of patients with Parkinson's disease (PD)—the second most common neurodegenerative disorder.[2] Although the underlying biological mechanisms causing neuronal loss are still under investigation, mitochondrial dysfunction has been well implicated in PD pathology.[3]

The majority of patients with PD are sporadic, with individuals manifesting the disease at ≥65 years of age. The remainder are caused by genetic mutations, of which many are linked to mitochondrial dysfunction. Roughly 50% of patients with early-onset PD harbor mutations in parkin (*PRKN*).[2,4]

PRKN encodes the E3 ubiquitin ligase parkin—an established regulator of mitochondrial clearance.[5] However, parkin's substrates are involved in several fundamental cellular processes. For instance, parkin targets parkin-interacting substrate (PARIS)—an inhibitor of the mitochondrial biogenesis regulator peroxisome gamma coactivator 1-alpha (PGC1-α).[6] Moreover, *PRKN* overexpression in cell models revealed an association with the mitochondrial genome and a direct interaction with mitochondral transcription factor A (TFAM)—the main transcription factor of mitochondrial DNA (mtDNA).

mtDNA has gained recent interest as a determinant of aging and age-associated diseases, including PD.[7] Improper mtDNA maintenance has been shown to allow its escape from the mitochondrial compartment, triggering an immune response.[8,9] This phenomenon was furthermore demonstrated in parkin-knockout (KO) "mutator" mice, which harbor an error-prone version of DNA polymerase γ (POLG). These animals show elevated extracellular mtDNA levels and cyclic GMP-AMP synthase (cGAS)-stimulator of interferon genes (STING) signaling under stress conditions.[10] However, parkin's involvement in these cellular processes has yet to be investigated in patient-derived neurons.

To explore the role of parkin in mtDNA maintenance endogenously, we generated induced pluripotent stem cell (iPSC)–derived midbrain neurons from patients with PD with biallelic *PRKN* mutations. We found that parkin-deficient neurons exhibit impaired mitochondrial biogenesis, mtDNA dynamics, and increased cytosolic mtDNA levels. Parkin knockdown during mutagenic stress mirrored these phenotypes and evidenced upregulations of the cGAS protein and extracellular mtDNA. Moreover, treatment with lipopolysaccharides (LPS) and mtDNA elicited a stronger inflammatory response in *PRKN*-mutant compared with control neuron–microglia co-cultures. Finally, single-nuclei RNA sequencing (snRNAseq) of postmortem midbrain sections from a patient with *PRKN*-PD revealed microgliosis and proinflammatory signaling. Our findings elucidate novel parkin-regulated mitophagy-independent mechanisms contributing toward mitochondrial quality control. We show that parkin coordinates mitochondrial biogenesis and mtDNA maintenance and is essential to prevent neuroinflammation and neurodegeneration.

Materials and Methods

Generation of iPSCs was performed as described,[11] and DANs and microglia were derived using established protocols.[12-14] To isolate tyrosine hydroxylase (TH)–positive cells, iPSC-derived neurons were subjected to fluorescence-activated cell sorting (FACS) using an adapted protocol.[15] Production of lentiviral vectors expressing short hairpin RNA (shRNA) against human *PRKN* or a control plasmid was performed as described.[16] SH-SY5Y neuroblastoma cells were treated with 200 μM cobalt chloride ($CoCl_2$).[17] Nicotinamide adenine dinucleotide:nicotinamide adenine dinucleotide hydrogen (NAD^+:NADH) ratios were determined using a kit (Sigma, St. Louis, MO). Respiratory chain complex I (CI) and citrate synthase activities were assessed in mitochondrial fractions by means of spectrophotometry.[18,19] Isolated extracellular mtDNA was quantified using a Digital PCR System (Applied Biosystems, Waltham, MA) and TaqMan probes specific for mitochondrially encoded NADH:ubiquinone oxidoreductase core subunit 1 (*MT-ND1*) and beta-2-microglobulin (*B2M*).[20,21] Polar metabolites from 30 day-old neurons were extracted and then derivatized and measured as published.[22] All experiments using iPSC-derived neurons and SH-SY5Y cells were performed with at least three biological replicates. Unpaired two-tailed Student's *t* tests or one-way analysis of variance followed by post hoc Tukey tests were used to determine statistical significance ($P < 0.05$).

Midbrain sections were immunostained, and TH-positive neurons were isolated through laser capture microdissection (LCM) using the PALM MicroBeam (Zeiss, Oberkochen, Germany).[20] Nuclei isolation, snRNAseq, and data analysis of the *PRKN*-mutant midbrain was carried out as described.[23]

A detailed description of the materials and methods can be found in the supplement.

Results

Parkin Deficiency Impairs Mitochondrial Biogenesis in the Neurons of Patients with PD

We generated iPSC-derived midbrain neurons from healthy controls and *PRKN* mutation carriers (Fig. S1A, B), which lack the parkin protein (Fig. S1C). Furthermore, we employed SH-SY5Y wild-type (WT) and

isogenic parkin-KO cells, which were generated using clustered regularly interspaced short palindromic repeats and CRISPR-associated protein 9 (CRISPR/Cas9) technology (Fig. S1D).

Parkin targets a plethora of proteins,[24] with mounting evidence supporting regulatory roles in diverse cellular mechanisms beyond mitophagy. Given that mitophagy and mitochondrial biogenesis are tightly linked to preserve bioenergetic homeostasis,[25] we sought to investigate possible alterations in mitochondrial biogenesis in our models. Previous research demonstrated that parkin overexpression enhances mitochondrial biogenesis through PGC1-α, either directly or via PARIS, its transcriptional repressor.[6,26,27] We found significantly lower levels of PGC1-α protein in parkin-deficient neurons and SH-SY5Y cells compared with controls (Fig. 1A,B). Interestingly, neither cell model showed differences in the PARIS protein under basal conditions (Fig. 1A,C).

Conversely, parkin deficiency substantially reduced sirtuin 1 (SIRT1) levels (Fig. 1A,D), an NAD^+-dependent energy sensor acting on mitochondrial biogenesis through regulation of PGC1-α gene expression and protein deacetylation.[28,29] Moreover, in parkin-deficient neurons, we detected higher lactate:pyruvate ratios (Fig. 1E), which suggests a lack of free NAD^+ based on the chemical equilibrium principle.[30]

PGC1-α regulates the transcription of nuclear respiratory factors (NRFs), which in turn mediates gene expressions of mtDNA transcription factors and replication activators TFAM and mitochondrial transcription factor B2 (TFB2M).[31] In agreement with reduced PGC1-α abundance, we found that parkin deficiency resulted in decreased NRF1 protein levels (Fig. 1A,F) and reduced *TFAM* and *TFB2M* expression (Fig. 1G, H). In addition, we detected significantly downregulated mRNA levels of twinkle mtDNA helicase (*TWNK*), a factor mainly involved in mtDNA replication (Fig. 1I).

Parkin Influences mtDNA Dynamics and Respiratory Chain Function

Mitochondrial biogenesis may be defined as the division and growth of preexisting mitochondria and is accomplished by the import of nuclear-encoded proteins and transcription and replication of the mitochondrial genome, which contains genes encoding subunits

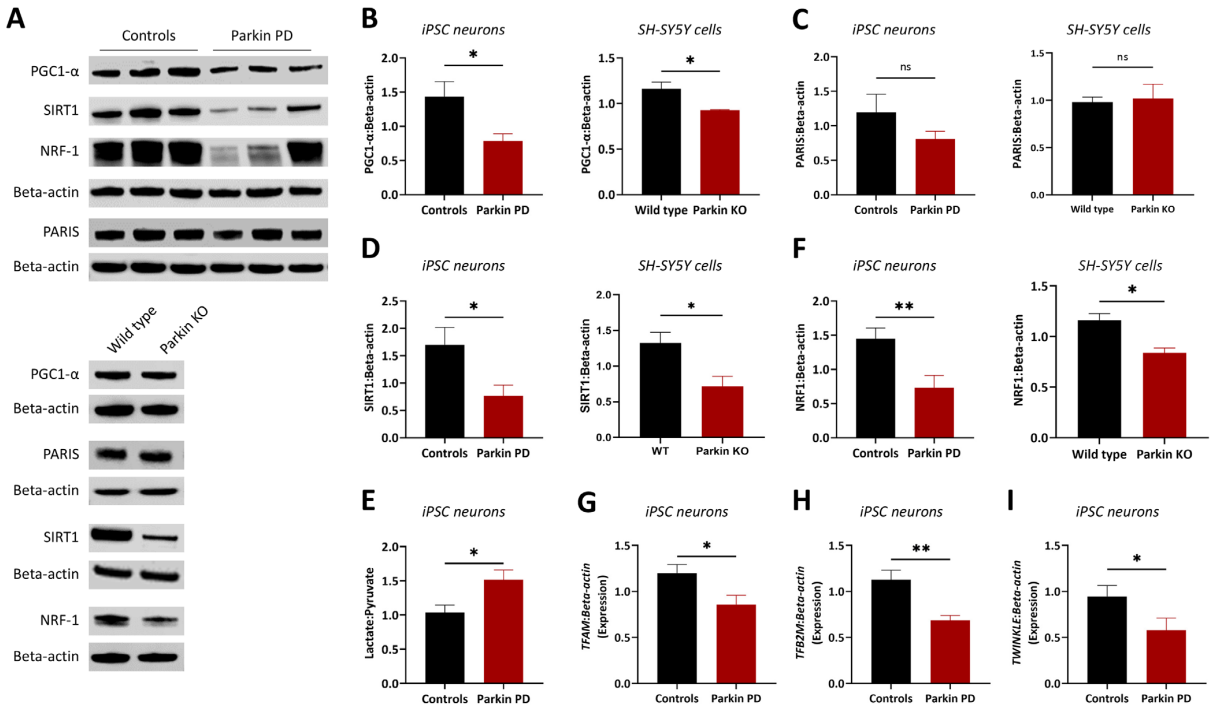

FIG. 1. Mitochondrial biogenesis is impaired in parkin-deficient cells. (**A**) Representative cropped Western blot images of total cell lysates from induced pluripotent stem cell (iPSC)–derived neurons from controls and patients with parkin-associated Parkinson's disease (Parkin PD) as well as wild-type and parkin-knockout (KO) SH-SY5Y neuroblastoma cells. (**B**-**E**) Quantifications from (**A**) peroxisome gamma coactivator 1-alpha (PGC1-α) (**B**), parkin-interacting substrate (PARIS) (**C**), sirtuin 1 (SIRT1) (**D**) and nuclear respiratory factor 1 (NRF1) (**F**) protein levels normalized to beta-actin. (**E**) Lactate-to-pyruvate ratios served as a proxy measure for free nicotinamide adenine dinucleotide:nicotinamide adenine dinucleotide hydrogen (NAD^+/NADH) ratios. (**G**-**I**) Quantitative polymerase chain reaction (qPCR) was used to quantify gene expression of mitochondrial transcription factor A (*TFAM*) (**G**), mitochondrial transcription factor B2 (*TFB2M*) (**H**) and twinkle mtDNA helicase (*TWNK*) (**I**) in iPSC-derived neurons from controls and patients with parkin-associated PD normalized to beta-actin. Data are presented as the mean ± SEM. SEM = standard error of the mean, $^*P < 0.05$, $^{**}P < 0.01$; ns = not significant as determined by Student's *t* test.

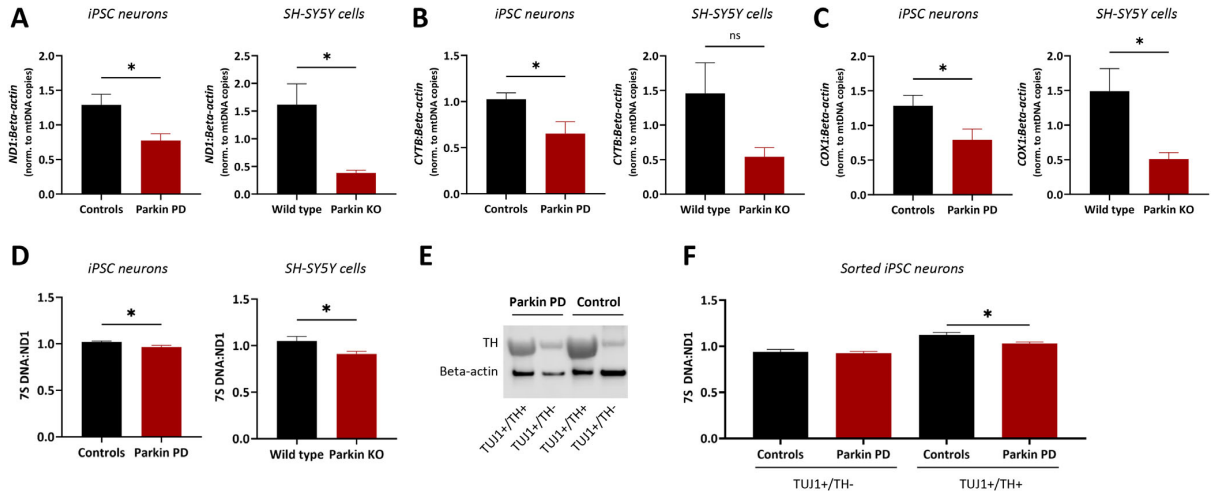

FIG. 2. Parkin influences mitochondrial DNA (mtDNA) dynamics. (**A**-**C**) Quantitative polymerase chain reaction (qPCR) was used to measure expression of mtDNA-encoded genes NADH:ubiquinone oxidoreductase core subunit 1 (*ND1*) (**A**), cytochrome B (*CYTB*) (**B**), and (**C**) cytochrome C oxidase I *(COX1)* in induced pluripotent stem cell (iPSC)–derived neurons from controls and Parkinson's disease patients with mutations in parkin (Parkin PD) and wild-type and parkin-knockout (KO) SH-SY5Y neuroblastoma cells. Gene expression was normalized to beta-actin and mtDNA copy number. (**D**) A multiplex real-time polymerase chain reaction (RT-PCR) assay was used to quantify transcription-associated 7S DNA per mtDNA molecule (with probes targeting *ND1*) in iPSC-derived neurons and SH-SY5Y cells. (**E, F**) Neuronal cultures from three controls and three *PRKN* mutation carriers were sorted using the pan-neuronal marker β-Tubulin 3 (TUJ1) and the dopaminergic neuron (DAN) marker tyrosine hydroxylase (TH) and subjected to Western blotting and RT-PCR analyses. (**E**) Representative cropped Western blotting images of TH and TUJ1 protein abundances in sorted control and patient neurons. (**F**) TUJ1/TH double-positive iPSC-derived neurons were separated from TUJ1-positive/TH-negative neurons derived from controls and patients with *PRKN* mutations. The resulting cell populations underwent multiplex RT-PCR to quantify the abundance of 7S DNA per mtDNA molecule (with a probe targeting *ND1*). RT-PCR results are from two technical replicates. n = 3 biological replicates; data are presented as the mean ± SEM; SEM = standard error of the mean, $^*P < 0.05$, ns = not significant as determined by Student's *t* test.

of the electron transport chain (ETC).[32] Our experiments suggest decreases in nuclear-encoded factors controlling mitochondrial biogenesis. We next sought to assess mtDNA dynamics by measuring the expression of mtDNA-encoded genes. The expression of mitochondrially encoded NADH:ubiquinone oxidoreductase core subunit 1 (*MT-ND1*), mitochondrially encoded cythochrome B (*MT-CYTB*), and mitochondrially encoded cytochrome C oxidase I (*MT-COX1*) (encoding subunits of complexes I, III, and IV, respectively) per mtDNA molecule was significantly downregulated in our parkin-deficient models (Fig. 2A–C). In line with this, both parkin-deficient iPSC-derived neurons and SH-SY5Y cells showed diminished 7S DNA: *MT-ND1* ratios, suggestive of fewer transcription initiation events (Fig. 2D).[20] Moreover, we used FACS to isolate TH-positive neurons and found that the 7S DNA phenotype is specific to DANs (Fig. 2E,F).

Because parkin overexpression was reported to enhance the selective removal of mitochondria harboring deleterious mtDNA mutations,[33] we explored the abundance of somatic major arc deletions. By contrast, we did not find differences between groups (data not shown). We further evaluated the mtDNA copy number and detected significantly higher mtDNA levels in parkin-deficient cells using both real-time polymerase chain reaction (RT-PCR) (Fig. 3A) and immunocytochemistry (Fig. 3B). Finally, we assessed respiratory chain function in SH-SY5Y cells and found that parkin-KO cells exhibited significantly reduced CI activity compared with WT cells (Fig. 3C). These results suggest that although parkin deficiency leads to an accumulation of mtDNA molecules, it also hinders the mtDNA transcription process, which likely contributes to ETC dysfunction.

Parkin Mitigates Cytosolic mtDNA Infiltration

Consistent with its evolutionary bacterial origin, mtDNA has been identified as a damage-associated molecular pattern (DAMP). Cytosolic mtDNA molecules can activate the innate immune system via the cGAS-STING pathway.[8] Implicating mtDNA release in the pathogenesis of *PRKN*-PD, our previous research showed increased levels of circulating cell-free mtDNA (ccf-mtDNA) and inflammatory cytokines in serum from *PRKN* mutation carriers.[34] Several mechanisms have been proposed to facilitate mtDNA release into the cytosol, including TFAM depletion.[8] We next confirmed that reduced *TFAM* gene expression detected in parkin-deficient neurons resulted in diminished TFAM (protein):mtDNA ratios (Fig. 3D, Fig. S2A). TFAM also acts as a packaging factor compacting the mtDNA molecule to form the mitochondrial nucleoid, and disruption of this process is associated with mtDNA extrusion from mitochondria. To investigate if impaired TFAM:mtDNA ratios coupled to disrupted mtDNA

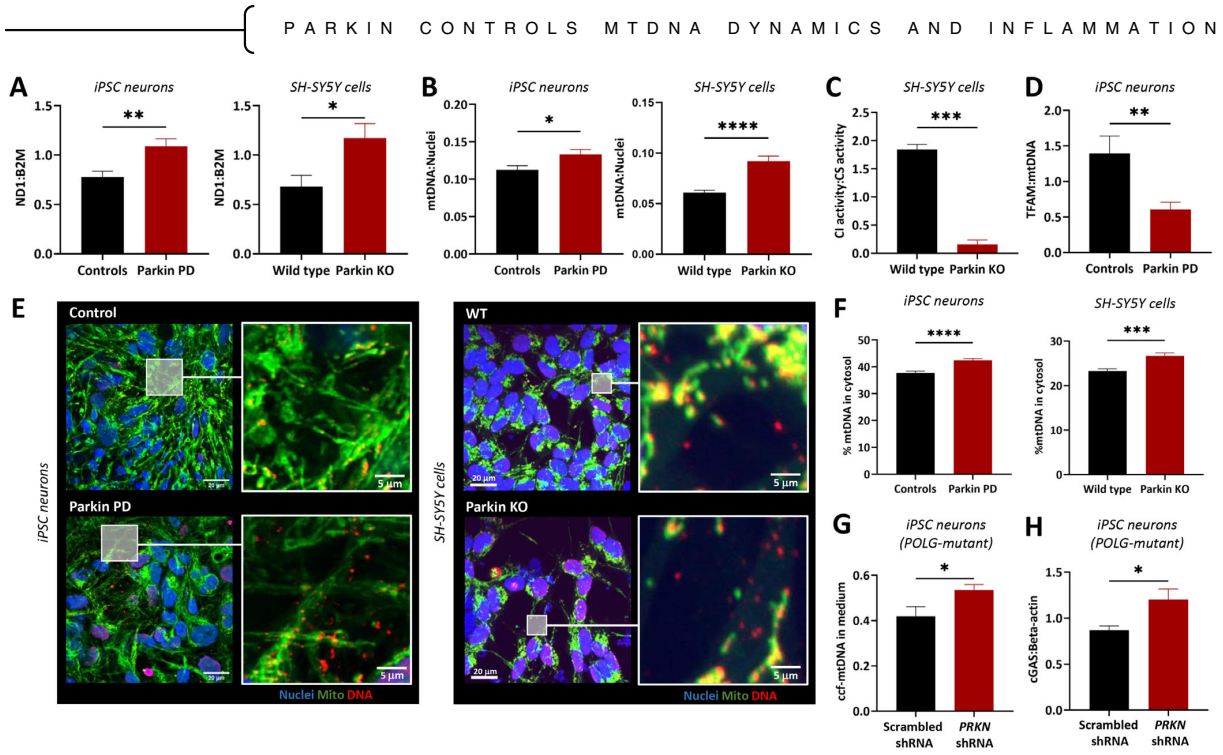

FIG. 3. Parkin attenuates cytosolic mitochondrial DNA (mtDNA) infiltration at baseline and extracellular mtDNA release during mutagenic stress. (**A**) A real-time polymerase chain reaction (RT-PCR) assay was used to quantify mtDNA copy number (with a probe targeting NADH:ubiquinone oxidoreductase core subunit 1 [*ND1*]) relative to the nuclear single copy gene beta-1-microglobulin (*B2M*) in induced pluripotent stem cell (iPSC)–derived neurons and SH-SY5Y neuroblastoma cells in healthy controls and patients with parkin-associated Parkinson's disease (Parkin PD) as well as wild-type (WT) and parkin-knockout (KO) SH-SY5Y cells. (**B**) Immunocytochemistry analysis of mtDNA copy number in iPSC-derived neurons and SH-SY5Y cells. Copy number was determined by mtDNA volume:nuclei volume. (**C**) Quantification of mitochondrial complex I activity normalized to citrate synthase activity in SH-SY5Y cells. (**D**) Quantification of mitochondrial transcription factor A (TFAM) protein abundance normalized to mtDNA copy number in iPSC-derived neurons. (**E**) Representative cropped immunocytochemistry images used to assess mtDNA subcellular location by targeting mtDNA, nuclei (Hoechst 33342), the mitochondrial marker translocase of outer mitochondrial membrane 20 (TOM20) and cytosol (high content screening CellMask Orange Stain [ThermoFisher Scientific, Waltham, MA]). (**F**) Analysis of mtDNA localization in iPSC-derived neurons and SH-SY5Y cells from (**E**). Percentage of mtDNA in cytosol was calculated by dividing the mtDNA volume outside mitochondria by total mtDNA volume. (**G**) Extracellular circulating cell-free mtDNA (ccf-mtDNA) in medium from polymerase γ (POLG)–mutant iPSC-derived neurons transduced with scrambled or *PRKN* short hairpin RNA (shRNA). Quantification by means of multiplex digital PCR (dPCR) targeting the mtDNA fragment *ND1* and the nuclear single-copy gene *B2M*. ccf-mtDNA was calculated as the ratio of extracellular *ND1* normalized to extracellular *B2M* copies to the sum of intra- and extracellular *ND1* normalized by their respective intra- and extracellular *B2M* copies. (**H**) cyclic GMP-AMP synthase (cGAS)-stimulator of interferon genes (STING) signaling in *POLG*-mutant iPSC-derived neurons transduced with scrambled or *PRKN* shRNA. Quantification of cGAS protein levels relative to beta-actin from Figure S2E. n = 3 or 5 biological replicates; data are presented as the mean ± SEM; SEM = standard error of the mean, $^{*}P < 0.05$, $^{**}P < 0.01$, $^{***}P < 0.001$, $^{****}P < 0.0001$ as determined by Student's *t* test.

dynamics could result in elevated mtDNA release, we assessed the subcellular localization of mtDNA molecules with an imaging approach. Indeed, patient neurons and parkin-KO SH-SY5Y cells harbored significantly more mtDNA molecules in the cytosol compared with controls (Fig. 3E,F). This mtDNA shift from mitochondria to the cytosol was independently validated by applying an RT-PCR approach to cellular fractions from control and parkin-KO SH-SY5Y cells (Fig. S2B).

Hypoxic Conditions Mirror mtDNA Phenotypes Observed in Parkin-Deficient Cells

To test our hypothesis of metabolic remodeling as the underlying cause of mtDNA dyshomeostasis in *PRKN*-PD, we exposed WT SH-SY5Y cells to the hypoxia-inducing agent $CoCl_2$.[17] $CoCl_2$ treatment triggered an upregulation of the hypoxia-inducible factor 1-α (Fig. 4A) and a shift from oxidative phosphorylation to glycolysis as indicated by increased NAD^+:NADH ratios (Fig. 4B). In line with the cellular function of SIRT1, the protein was less abundant under hypoxic conditions (Fig. 4A,C). We then investigated the SIRT1 target PGC1-α, which was also downregulated in $CoCl_2$-treated cells (Fig. 4A,D). To explore the impact of PGC1-α depletion on mtDNA maintenance, we next determined the protein levels of NRF1 and TFAM, which were both downregulated in response to $CoCl_2$ exposure (Fig. 4A,E,F). In addition, the treatment reduced the 7S DNA:*MT-ND1* ratio (Fig. 4G) and *MT-ND1* mRNA levels (Fig. 4H).

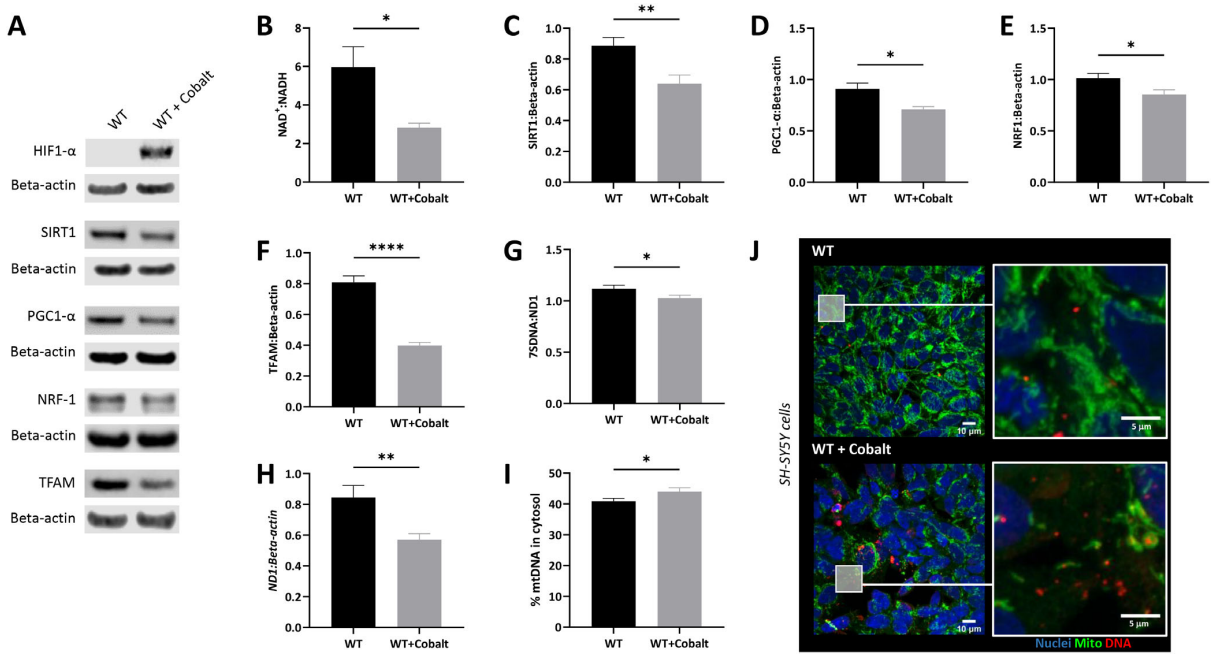

FIG. 4. Hypoxia-mediated metabolic alterations induce mitochondrial DNA (mtDNA) dyshomeostasis. (**A**) Representative cropped Western blot images of total cell lysates from untreated and cobalt chloride ($CoCl_2$)-treated wild-type (WT) SH-SY5Y neuroblastoma cells. (**B**) Nicotinamide adenine dinucleotide:nicotinamide adenine dinucleotide hydrogen (NAD^+/NADH) ratios measured in cellular extracts from untreated and $CoCl_2$-treated WT SH-SY5Y cells. Quantifications from (**A**) sirtuin 1 (SIRT1) (**C**), peroxisome gamma coactivator 1-alpha (PGC1-α) (**D**), nuclear respiratory factor 1 (NRF1) (**E**), mitochondrial transcription factor A (TFAM) (**F**) protein levels normalized to Beta-actin. (**G**) Real-time polymerase chain reaction quantification of transcription-associated 7S DNA per mtDNA molecule. (**H**) qPCR was used to quantify gene expression of the mtDNA gene NADH:ubiquinone oxidoreductase core subunit 1(*ND1*). (**I**) Analysis of mtDNA localization in untreated and $CoCl_2$-treated WT SH-SY5Y cells (**J**). Percentage of mtDNA in cytosol was calculated by dividing the mtDNA volume outside mitochondria by total mtDNA volume. (**J**) Representative cropped immunocytochemistry images used to assess mtDNA subcellular location by targeting mtDNA, nuclei (Hoechst 33342), the mitochondrial marker translocase of outer mitochondrial membrane 20 (TOM20), and cytosol (high content screening CellMask Orange Stain [ThermoFisher Scientific, Waltham, MA]). n ≤ 3 biological replicates; data are presented as the mean ± SEM; SEM = standard error of the mean, $^*P < 0.05$, $^{**}P < 0.01$, $^{****}P < 0.0001$ as determined by Student's *t* test.

Finally, we tested whether the $CoCl_2$-induced metabolic shift was sufficient to trigger mtDNA release. Indeed, high-throughput imaging revealed elevated cytosolic mtDNA levels in treated SH-SY5Y cells (Fig. 4I,J). These data indicate that metabolic impairments can interfere with mtDNA dynamics.

Mutagenic Stress Exacerbates Parkin-Mediated Mitochondrial Biogenesis and mtDNA Transcription Deficits

Next, we further explored the downstream effects of parkin deficiency–induced mtDNA dyshomeostasis. Although we observed an increase of cytosolic mtDNA in parkin-mutant neurons, this mtDNA release from the mitochondria was not accompanied by an upregulation of extracellular mtDNA or immune-related factors (Fig. S2C,D), which may be explained by the inability of iPSC-derived cultures to model age-associated phenotypes such as inflammation.[35] To overcome the rejuvenation-associated limitations of iPSC-derived neurons, we adapted a mitochondrial aging strategy from mice. Recently, an innovative mouse strain was generated that, contrary to most established rodent PD models, recapitulates motor phenotypes during the short lifetime of the animals.[10] To simulate mitochondrial aging, parkin-KO mice were crossed with animals harboring an error-prone version of POLG, which causes mtDNA mutagenic stress. The resulting parkin-KO "mutator" mice showed increased serum levels of ccf-mtDNA and inflammatory cytokines mediated by cGAS-STING signaling.[9] Inspired by this work, we differentiated iPSCs from a patient with compound-heterozygous mutations in *POLG* and subjected the resulting neurons to shRNA to reduce parkin expression (Fig. S3A).

Compared with *POLG*-mutant cells transduced with scrambled shRNA, parkin shRNA reduced 7S DNA:*MT-ND1* ratios (Fig. S3B) and showed significantly lower levels of mitochondrial biogenesis factors PGC1-α and NRF1 (Fig. S3A,C,D), strengthening our findings in *PRKN*-mutant neurons. Next, we quantified ccf-mtDNA in the extracellular medium and found a

significant upregulation, suggesting that parkin reduction in the presence of mtDNA stress elevated the release of mtDNA from mitochondria into the extracellular space (Fig. 3G). Furthermore, we found an increase in protein abundance of the cytosolic DNA sensor cGAS (Fig. 3H). Finally, we assessed the expression of key cytokines that were previously shown to be upregulated in serum from parkin-KO "mutator" mice and patients with *PRKN* mutations in response to cGas/STING signaling.[9] By contrast, RT-PCR analyses still revealed very low levels of interleukin 6 (*IL6*) and interleukin-1-beta (*IL1B*) in any of the investigated neurons (Fig. S3E), likely attributed to the absence of microglia in the cultures.

mtDNA Maintenance Impairments Propagate Neuroinflammation in *PRKN*-PD Tissue

Although iPSC-derived neurons allow the study of parkin-related mitochondrial functions, the cultures do not reflect the cellular diversity of the midbrain. Recent publications implicate glia-mediated inflammation in the pathogenesis of *PRKN*-associated PD.[9,34] In light of these findings, we next used postmortem tissue from a patient with PD with compound-heterozygous *PRKN* mutations and two healthy controls to assess the extent and possible consequences of mtDNA disintegration in a more comprehensive environment (Fig. 5A).

We first sought to validate our findings concerning mtDNA maintenance in human brain tissue. We

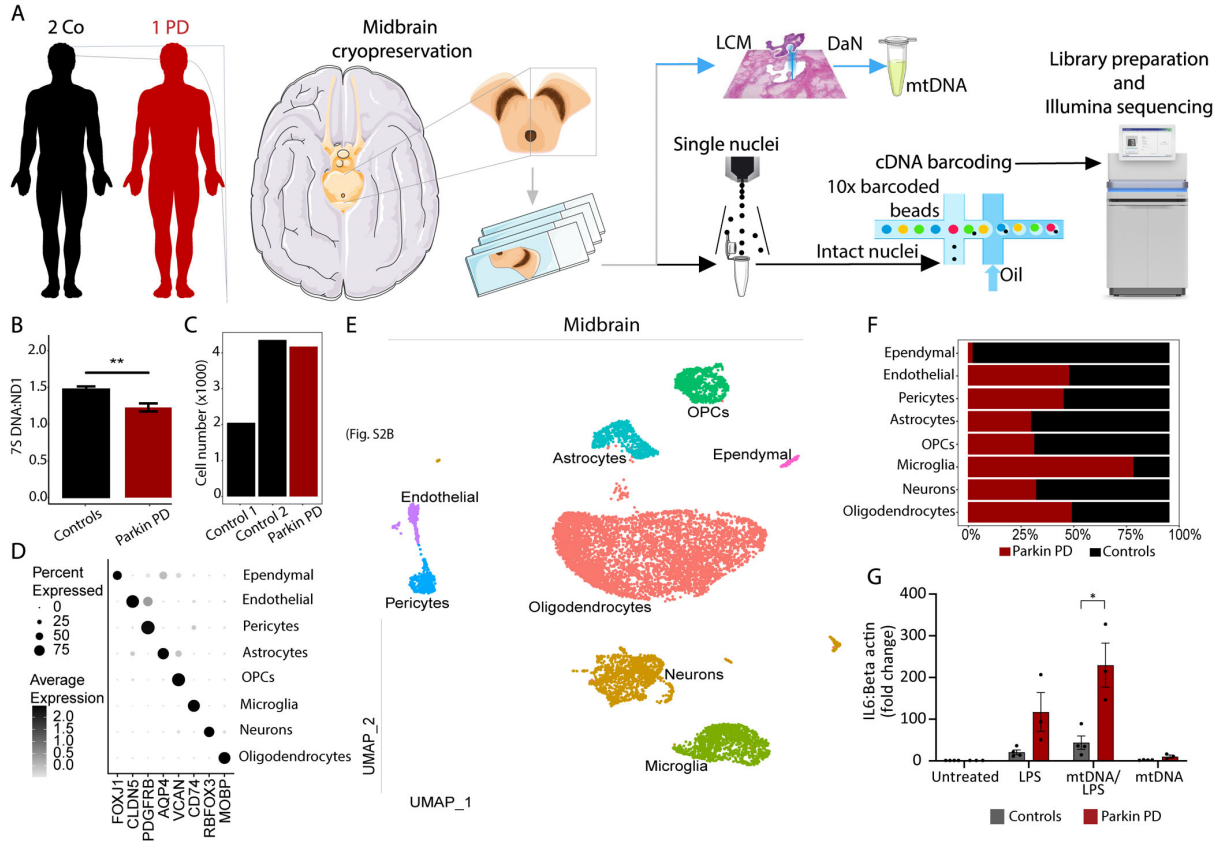

FIG. 5. Cell-type differences in human *PRKN*-mutant and control midbrains. (**A**) Handling of the midbrain tissue for single-cell studies. Midbrain sections were used for (1) laser capture microdissection (LCM) of dopaminergic neurons (DAN) and (2) nuclei isolation, 10X Genomics platform processing, and Illumina sequencing. (**B**) 7S DNA:mitochondrially encoded NADH:ubiquinone oxidoreductase core subunit 1 (7SDNA:*MT-ND1*) ratios quantified via multiplex real-time polymerase chain reaction from single postmortem DANs of the substantia nigra pars compacta. (**C**) Number of nuclei per sample. The analyzed population is composed of 4173 *PRKN*-mutant nuclei and 6405 control nuclei, making a population of 10,578 nuclei. (**D**) Representative cell-type specific marker genes. (**E**) The population of 10,578 nuclei projected onto a uniform manifold approximation and projection (UMAP) space. (**F**) Percentage of *PRKN*-mutant and control cell-type specific nuclei. (**G**) Fold change of interleukin 6 (*IL6*) expression at baseline (NT = nontreated) or after treatment with mitochondrial DNA (mtDNA), lipopolysaccharides (LPS), or both. n = 3 patients and n = 4 controls; data are presented as the mean ± SEM; SEM = standard error of the mean, *P < 0.05, **$P < 0.01$, ns = not significant as determined by two-way analysis of variance and Sidak's multiple comparisons test. Co = healty control subjects, PD/Parkin PD = Parkinson's disease patient with mutations in parkin, OPCs = oligodendrocyte precursor cells, *FOXj1* = forkhead box J1, *CLDN5* = claudin 5, *PDGFRB* = platelet derived growth factor receptor beta, *AQP4* = aquaporin 4, *VCAN* = versican, *RBFOX3* = RNA binding fox-1 homolog 3, *MOBP* = myelin associated oligodendrocyte basic protein.

applied LCM to midbrain tissue to isolate single neuromelanin- and TH-positive neurons (n = 10 per sample) from the SNpc, which were then subjected to RT-PCR. In line with our previous results, we found significantly reduced 7S DNA:*MT-ND1* ratios in postmortem patient DANs (Fig. 5B). However, we did not detect any differences in mtDNA deletion levels or in mtDNA copy number (data not shown).

Next, to determine whether *PRKN* mutation carriers suffer from neuroinflammation, we performed snRNAseq from postmortem ventral midbrain sections (Fig. 5A). A total of 10,578 high-quality nuclei (patient = 4173, controls = 2047 and 4358) were projected into two dimensions with the uniform manifold approximation and projection (UMAP) algorithm (Fig. 5C,E). We found eight major cell types including neurons and glial cells (Fig. 5D,E). Each cell cluster was annotated based on the expression of marker genes (Fig. 5D, Table S1). The most abundant cell type making ≈52.5% of the midbrain population are oligodendrocytes, followed by neurons (≈14.6%), microglia (≈11.6%), oligodendrocyte precursor cells (≈7.3%), and astrocytes (≈6.6%). Residual abundances were detected for other cell types. To assess neuroinflammation, we first compared cell density distributions in UMAP and observed a large increase in the microglial population and a decreased fraction of neurons and astrocytes (Fig. 5F) in the *PRKN*-mutant midbrain. Our results confirm the alteration in glial cell populations in the *PRKN* mutation carriers reported previously.[36] This shift infers an incorrect immune response, which likely leads to neuroinflammation. The resulting decrease of the *PRKN* midbrain neuronal population (Fig. 5F) compared with controls may be a trigger or downstream effect of the aforementioned immune response. Furthermore, the proinflammatory cytokines *IL1B* and tumor necrosis factor (*TNF)* were differentially expressed and upregulated in *PRKN*-mutant microglia compared with controls (Table S2). Accordingly, the immune response pathways, primarily the interleukin signaling pathways, were most perturbed in microglia from the *PRKN* mutation carrier (Tables S3 and S4).

Finally, to assess the causal link between mtDNA dyshomeostasis and neuroinflammation in *PRKN*-associated PD, we generated iPSC-derived neuron–microglia co-cultures from controls and patients with *PRKN* mutations and exposed them to LPS, mtDNA isolated from patients with *PRKN*-PD, or both. The composition of the co-cultures with regard to DANs and microglia was not affected by the different treatments (Fig. S4A,B). Moreover, stimulation by mtDNA or LPS alone did not reveal any differences in the expression of cytokines in cells lacking parkin. However, when mtDNA was added as a secondary trigger after LPS priming, we observed that patient-derived co-cultures showed a greater response in the expression of *IL6* (Fig. 5G). Although *IL1B* was equally upregulated after LPS/mtDNA treatment, the difference between *PRKN*-PD and control co-cultures was not significant (Fig. S4C).

Discussion

Using a multimodal approach, we explored novel mechanisms of mitochondrial quality control exerted by parkin. Although most parkin studies focused on its role in mitochondrial clearance, the wide range of parkin substrates suggests that the protein functions in cellular processes beyond mitophagy.[24] Thus, we decided to investigate the mitochondrial biogenesis and mtDNA maintenance pathways in parkin-deficient cells.

Mitochondrial biogenesis is synchronized in the nucleus, with PGC1-α acting as the master regulator.[27] Studies found a direct interaction between parkin and PGC1-α,[27] whereas others have shown an interaction with PARIS—a PGC1-α transcriptional repressor.[6] In the current study, parkin-depleted cells showed reduced PGC1-α protein levels while the abundance of PARIS remained unchanged, insinuating an alternative mechanism of PGC1-α reduction. We looked upstream and found that the SIRT1 protein was reduced in parkin-deficient cells. *PGC1-α* gene expression and protein deacetylation is regulated by the NAD^+-dependent energy sensor SIRT1.[28,29] Moreover, our and a published metabolic study in parkin-deficient neurons revealed increased lactate:pyruvate ratios, suggesting lower levels of freely accessible NAD^+ as a result of metabolic remodeling from oxidative phosphorylation to glycolysis.[30,37]

PGC1-α can activate the NRFs, which control the expression of the mitochondrial transcription factors *TFAM* and *TFB2M*.[31] Our gene expression and protein analyses confirmed disruptions of this pathway at each level in cells lacking parkin. The sole semiautonomous organelle of human cells, mitochondria, encompass their own system to coordinate mtDNA transcription, replication, translation, and repair. Because of its dynamic nature and proximity to the ETC, mtDNA maintenance is exceptionally important for ensuring homogeneity and preventing the expansion of aberrant mtDNA molecules. Studies in mitotically active parkin-overexpressing cells have shown a direct interaction of parkin with TFAM and an association with the mitochondrial genome.[26,38]

Focusing on mtDNA integrity, we found significantly less 7S DNA per mtDNA molecule in iPSC-derived neurons, SH-SY5Y cells, and postmortem DANs lacking parkin. This is in agreement with previous findings in postmortem DANs isolated from patients with idiopathic PD (IPD).[20] The D-loop region of the

mitochondrial genome serves as the initiation site for its replication and transcription. The synthesis of 7S DNA in the D-loop is stimulated by TFAM, consistent with evidence showing that elevated TFAM matrix levels increase the rate of 7S DNA synthesis.[39] Indeed, calculating TFAM:mtDNA ratios, parkin-deficient neurons exhibited a significant reduction. Moreover, we observed decreased mtDNA gene expression that coincided with diminished ETC CI activity in parkin-KO SH-SY5Y cells. Of note, we previously reported ETC CI impairments in iPSC-derived neurons from our *PRKN*-mutant samples.[40] Interestingly, experiments in purified TH-positive neurons from patients with *PRKN* mutations highlighted that the 7S DNA phenotype is more pronounced in DANs, suggesting a link between mtDNA homeostasis and dopamine signaling. Because of their high energy requirements and the autoxidation properties of the neurotransmitter, DANs are particularly vulnerable to metabolic changes.[41,42] Interestingly, hypoxic conditions mimicked the mtDNA phenotypes observed in parkin-deficient cells. These findings further strengthened our hypothesis that a shift from oxidative phosphorylation to glycolysis triggers mtDNA dyshomeostasis in the absence of parkin.

Beyond alterations in the mitochondrial biogenesis pathway, we detected elevated mtDNA copy numbers but diminished TFAM abundance per mitochondrial genome in parkin-deficient neurons. TFAM reduction has previously been shown to allow mtDNA to escape from mitochondria into the cytosol, where it is recognized by the cytosolic DNA sensor cGAS, provoking activation of an innate immune response.[8] Indeed, we observed that neurons from patients with PD and parkin-KO SH-SY5Y cells incur higher levels of mtDNA in the cytosolic compartment compared with controls. We also quantified mtDNA molecules in the extracellular medium of our cellular samples, yet we did not detect any differences compared with controls or increases in inflammatory cytokines.

However, keeping in mind that reprogramming of postnatal cells can cause artificial rejuvenation,[35] we burdened parkin-deficient cells with mitochondrial mutagenic stress—a normal aging phenomenon[43]—to investigate mtDNA release and inflammation. To create a neuronal aging model of *PRKN*-PD, we adopted an approach by Pickrell and colleagues who crossed parkin-KO with *POLG*-mutant mice.[10] These animals exhibited levodopa-reversible motor deficits, a selective loss of nigral DANs, impaired mtDNA dynamics, and cGas/STING-mediated inflammation.[9,10] Accordingly, we generated iPSC-derived midbrain neurons from a patient with Alper's disease with compound-heterozygous *POLG* mutations and subjected the cultures to either scramble or parkin shRNA. Parkin knockdown in *POLG*-mutant neurons replicated the 7S DNA phenotype as well as disruptions of the mitochondrial biogenesis pathway. In addition, we detected elevated ccf-mtDNA levels in the cellular medium and an increase in cGAS protein abundance. In agreement with previous results in parkin-KO "mutator" mice, this suggests that parkin depletion combined with mitochondrial mutagenic stress triggers the release of mtDNA into the cytosol and extracellular space in patient neurons.

Microglia are considered the resident innate immune cells in the brain, which can be activated by various DAMPs. The lack of microglial cells in our neuronal cultures may explain the inability to detect inflammation in our samples. We therefore decided to use postmortem tissue from a patient with compound-heterozygous *PRKN*-PD and controls to investigate a potential link between parkin dysfunction and neuroinflammation using snRNAseq. Our results showed a strong infiltration of microglia in the *PRKN*-mutant midbrain and an upregulation of the proinflammatory cytokines *IL1B* and *TNF*. This dysregulation resulted in the perturbation of immune and oxidative stress response pathways.

To additionally evaluate the extent of the microglia phenotype in *PRKN*-PD, we made use of our recently published single-cell data set of five patients with IPD and six controls.[23] Comparing the cell-type distribution across the three groups (Fig. S5A-D), the *PRKN*-mutant midbrain showed an even larger percentage of microglia than the IPD tissue samples (Fig. S5D). Moreover, the expression of microglia activation markers heat shock protein 90 alpha family class A member 1 (*HSP90AA1*) and *IL1B* was the highest in the *PRKN*-mutant cell population (Fig. S5E). Thus, despite the limitation of examining brain tissue from a single mutant case, this cross-comparison further supports a role for microglia in the pathogenesis of *PRKN*-PD.

With regard to the distribution of other glial cells, we detected a reduction in astrocytes in *PRKN*-PD (Fig. S4D), which is in line with previous observations in the *PRKN*-mutant midbrain.[36] The resulting lack of astroglial neuron support likely perpetuates the inflammatory phenotypes in *PRKN*-PD as indicated by elevated expression of the astrocyte activation marker cluster of differentiation 44 (*CD44*) (Fig. S5F). Interestingly, despite lower overall astrocyte numbers, *CD44* levels in *PRKN*-PD astrocytes were even higher than in IPD astrocytes (Fig. S5F). Although additional rare *PRKN*-mutant midbrain samples need to be studied in the future, our snRNAseq analysis, which also considered our published results from IPD cases, provides valuable insights into the cell-type composition and transcriptomic landscape of the *PRKN*-PD midbrain.

Finally, to assess whether mtDNA dyshomeostasis and inflammation are causally linked in *PRKN*-PD, we generated iPSC-derived neuron–microglia co-cultures from controls and patients with *PRKN* mutations, which were treated with mtDNA isolated from *PRKN*-mutant cells. Our results showed that, when added as a secondary stimulus to LPS priming, mtDNA caused *IL6* overexpression

in cells lacking parkin, suggesting that parkin deficiency renders cells more responsive to proinflammatory stimuli.

Taken together, our study highlights parkin's involvement in mtDNA maintenance and supports a link between mtDNA dyshomeostasis and inflammation in human cellular models of PD. In iPSC-derived cultures from patients with *PRKN* mutations, we observed that mtDNA transcription-associated 7S DNA is preferentially depleted in DANs. This TFAM deficiency-mediated phenotype is likely the consequence of SIRT1 depletion and inactivation in response to a lack of free NAD^+ in the absence of parkin. However, the origin of the mitochondrial energy deficit in *PRKN*-mutant neurons currently remains elusive. Interestingly, recent studies suggest that parkin deficiency can be a driver of altered mitochondrial metabolism. Either via its function in mitochondrial clearance or through translational control of nuclear-encoded ETC mRNAs,[5,26] the mutant protein could trigger the respiratory complex impairments detected in patient neurons. With SIRT1 acting as a connector between cell metabolism, mitophagy, and biogenesis pathways, further research will be needed to determine the exact sequence of events triggering mitochondrial dysfunction in parkin-deficient DANs.[44] Moreover, additional analyses in iPSC-derived co-culture systems should aim at the identification of the immune signaling pathways activated in microglia in response to neuronal release of mitochondrial DAMPs, including mtDNA. Such investigations will pave the way for innovative anti-inflammatory treatment approaches in PD.

Acknowledgments: We express our gratitude to the tissue donors and their families for their generous participation. Postmortem tissue for this study was provided by the Newcastle Brain Tissue Resource and Juntendo University. Moreover, Prof. Dr. Doug Turnbull (Wellcome Trust Centre for Mitochondrial Research, Newcastle University) kindly provided fibroblasts for the study from a patient with Alper's disease. We are grateful to Thea Maria Van Wüllen (Luxembourg Centre for Systems Biomedicine) and Carola Dietrich (Max-Planck-Institute for Human Molecular Genetics, Berlin) for their assistance in postmortem sample preparation for single-cell RNA sequencing. We thank Nassima Ouzren and Ursula Heins-Marroquin for optimizing protocols for experiments used in the study. In addition, the authors thank Dr. Christian Jäger and Xiangyi Dong from the Luxembourg Centre for Systems Biomedicine Metabolomics Platform for the generation of metabolomics data. Finally, this project was supported by the Imaging Facility and the Disease Modelling and Screening Platform, Luxembourg Centre for Systems Biomedicine, University of Luxembourg, and Luxembourg Institute of Health, Luxembourg. Open access funding enabled and organized by Projekt DEAL.

Data Availability Statement

Raw data for the midbrain tissue sample from the *PRKN* mutation carrier is available in the GEO with accession number GSE166790. Raw data for the two control samples were previously sequenced used in this study are available in the GEO with the accession number GSE157783 (data sets: C2-GSM4774937, C3-GSM4774938). Other data are available upon request.

References

1. Panigrahi B, Martin KA, Li Y, et al. Dopamine Is Required for the Neural Representation and Control of Movement Vigor. Cell 2015; 162(6):1418–1430. https://doi.org/10.1016/j.cell.2015.08.014
2. Lücking CB, Dürr A, Bonifati V, et al. Association between early-onset Parkinson's disease and mutations in the parkin gene. N Engl J Med 2000;342(21):1560–1567. https://doi.org/10.1056/NEJM200005253422103
3. Grünewald A, Kumar KR, Sue CM. New insights into the complex role of mitochondria in Parkinson's disease. Prog Neurobiol 2019; 177:73–93. https://doi.org/10.1016/j.pneurobio.2018.09.003
4. Kitada T, Asakawa S, Hattori N, et al. Mutations in the parkin gene cause autosomal recessive juvenile parkinsonism. Nature 1998; 392(6676):605–608. https://doi.org/10.1038/33416
5. Narendra D, Tanaka A, Suen DF, Youle RJ. Parkin is recruited selectively to impaired mitochondria and promotes their autophagy. J Cell Biol 2008;183(5):795–803. https://doi.org/10.1083/jcb.200809125
6. Shin JH, Ko HS, Kang H, et al. PARIS (ZNF746) repression of PGC-1α contributes to neurodegeneration in Parkinson's disease. Cell 2011;144(5):689–702. https://doi.org/10.1016/j.cell.2011.02.010
7. Chocron ES, Munkácsy E, Pickering AM. Cause or casualty: The role of mitochondrial DNA in aging and age-associated disease. Biochim Biophys Acta Mol Basis Dis 2019;1865(2):285–297. https://doi.org/10.1016/j.bbadis.2018.09.035
8. West AP, Khoury-Hanold W, Staron M, et al. Mitochondrial DNA stress primes the antiviral innate immune response. Nature 2015; 520(7548):553–557. https://doi.org/10.1038/nature14156
9. Sliter DA, Martinez J, Hao L, et al. Parkin and PINK1 mitigate STING-induced inflammation. Nature 2018;561(7722):258–262. https://doi.org/10.1038/s41586-018-0448-9
10. Pickrell AM, Huang CH, Kennedy SR, et al. Endogenous Parkin Preserves Dopaminergic Substantia Nigral Neurons following Mitochondrial DNA Mutagenic Stress. Neuron 2015;87(2):371–381. https://doi.org/10.1016/j.neuron.2015.06.034
11. Seibler P, Graziotto J, Jeong H, Simunovic F, Klein C, Krainc D. Mitochondrial Parkin recruitment is impaired in neurons derived from mutant PINK1 induced pluripotent stem cells. J Neurosci Off J Soc Neurosci. 2011;31(16):5970–5976. https://doi.org/10.1523/JNEUROSCI.4441-10.2011
12. Kriks S, Shim JW, Piao J, et al. Dopamine neurons derived from human ES cells efficiently engraft in animal models of Parkinson's disease. Nature 2011;480(7378):547–551. https://doi.org/10.1038/nature10648
13. Haenseler W, Sansom SN, Buchrieser J, et al. A Highly Efficient Human Pluripotent Stem Cell Microglia Model Displays a Neuronal-Co-culture-Specific Expression Profile and Inflammatory Response. Stem Cell Rep 2017;8(6):1727–1742. https://doi.org/10.1016/j.stemcr.2017.05.017
14. Reinhardt P, Glatza M, Hemmer K, et al. Derivation and expansion using only small molecules of human neural progenitors for neurodegenerative disease modeling. PloS One 2013;8(3):e59252. https://doi.org/10.1371/journal.pone.0059252
15. Sandor C, Robertson P, Lang C, et al. Transcriptomic profiling of purified patient-derived dopamine neurons identifies convergent perturbations and therapeutics for Parkinson's disease. Hum Mol Genet 2017;26(3):552–566. https://doi.org/10.1093/hmg/ddw412
16. Arena G, Cissé MY, Pyrdziak S, et al. Mitochondrial MDM2 Regulates Respiratory Complex I Activity Independently of p53. Mol Cell 2018;69(4):594–609.e8. https://doi.org/10.1016/j.molcel.2018.01.023
17. Vengellur A, LaPres JJ. The role of hypoxia inducible factor 1alpha in cobalt chloride induced cell death in mouse embryonic fibroblasts. Toxicol Sci Off J Soc Toxicol 2004;82(2):638–646. https://doi.org/10.1093/toxsci/kfh278
18. McCormack JG. Mitochondria. A practical approach; Edited by V M Darley-Usmar, D Rickwood and M T Wilson. pp 340. IRL Press, Oxford. 1987. £29 or £18 (pbk) ISBN 1-85221-034-6 or 033-8 (pbk). Biochem Educ 1988;16(2):118. https://doi.org/10.1016/0307-4412(88)90107-0

19. Delcambre S, Ghelfi J, Ouzren N, et al. Mitochondrial Mechanisms of LRRK2 G2019S Penetrance. Front Neurol 2020;11:881. https://doi.org/10.3389/fneur.2020.00881
20. Grünewald A, Rygiel KA, Hepplewhite PD, Morris CM, Picard M, Turnbull DM. Mitochondrial DNA Depletion in Respiratory Chain-Deficient Parkinson Disease Neurons. Ann Neurol 2016;79(3):366–378. https://doi.org/10.1002/ana.24571
21. Rygiel KA, Grady JP, Taylor RW, Tuppen HAL, Turnbull DM. Triplex real-time PCR--an improved method to detect a wide spectrum of mitochondrial DNA deletions in single cells. Sci Rep 2015;5:9906. https://doi.org/10.1038/srep09906
22. Meiser J, Delcambre S, Wegner A, et al. Loss of DJ-1 impairs antioxidant response by altered glutamine and serine metabolism. Neurobiol Dis 2016;89:112–125. https://doi.org/10.1016/j.nbd.2016.01.019
23. Smajić S, Prada-Medina CA, Landoulsi Z, et al. Single-cell sequencing of human midbrain reveals glial activation and a Parkinson-specific neuronal state. Brain J Neurol. Published online December 17 2021;awab446. https://doi.org/10.1093/brain/awab446
24. Sarraf SA, Raman M, Guarani-Pereira V, et al. Landscape of the PARKIN-dependent ubiquitylome in response to mitochondrial depolarization. Nature 2013;496(7445):372–376. https://doi.org/10.1038/nature12043
25. Palikaras K, Lionaki E, Tavernarakis N. Balancing mitochondrial biogenesis and mitophagy to maintain energy metabolism homeostasis. Cell Death Differ 2015;22(9):1399–1401. https://doi.org/10.1038/cdd.2015.86
26. Kuroda Y, Mitsui T, Kunishige M, et al. Parkin enhances mitochondrial biogenesis in proliferating cells. Hum Mol Genet 2006;15(6):883–895. https://doi.org/10.1093/hmg/ddl006
27. Zheng L, Bernard-Marissal N, Moullan N, et al. Parkin functionally interacts with PGC-1α to preserve mitochondria and protect dopaminergic neurons. Hum Mol Genet 2017;26(3):582–598. https://doi.org/10.1093/hmg/ddw418
28. Cantó C, Auwerx J. PGC-1alpha, SIRT1 and AMPK, an energy sensing network that controls energy expenditure. Curr Opin Lipidol 2009;20(2):98–105. https://doi.org/10.1097/MOL.0b013e328328d0a4
29. Amat R, Planavila A, Chen SL, Iglesias R, Giralt M, Villarroya F. SIRT1 controls the transcription of the peroxisome proliferator-activated receptor-gamma Co-activator-1alpha (PGC-1alpha) gene in skeletal muscle through the PGC-1alpha autoregulatory loop and interaction with MyoD. J Biol Chem 2009;284(33):21872–21880. https://doi.org/10.1074/jbc.M109.022749
30. Williamson DH, Lund P, Krebs HA. The redox state of free nicotinamide-adenine dinucleotide in the cytoplasm and mitochondria of rat liver. Biochem J 1967;103(2):514–527. https://doi.org/10.1042/bj1030514
31. Gleyzer N, Vercauteren K, Scarpulla RC. Control of mitochondrial transcription specificity factors (TFB1M and TFB2M) by nuclear respiratory factors (NRF-1 and NRF-2) and PGC-1 family coactivators. Mol Cell Biol 2005;25(4):1354–1366. https://doi.org/10.1128/MCB.25.4.1354-1366.2005
32. Jornayvaz FR, Shulman GI. Regulation of mitochondrial biogenesis. Essays Biochem 2010;47:69–84. https://doi.org/10.1042/bse0470069
33. Suen DF, Narendra DP, Tanaka A, Manfredi G, Youle RJ. Parkin overexpression selects against a deleterious mtDNA mutation in heteroplasmic cybrid cells. Proc Natl Acad Sci U S A 2010;107(26):11835–11840. https://doi.org/10.1073/pnas.0914569107
34. Borsche M, König IR, Delcambre S, et al. Mitochondrial damage-associated inflammation highlights biomarkers in PRKN/PINK1 parkinsonism. Brain J Neurol 2020;143(10):3041–3051. https://doi.org/10.1093/brain/awaa246
35. Mertens J, Paquola ACM, Ku M, et al. Directly Reprogrammed Human Neurons Retain Aging-Associated Transcriptomic Signatures and Reveal Age-Related Nucleocytoplasmic Defects. Cell Stem Cell 2015;17(6):705–718. https://doi.org/10.1016/j.stem.2015.09.001
36. Kano M, Takanashi M, Oyama G, et al. Reduced astrocytic reactivity in human brains and midbrain organoids with PRKN mutations. NPJ Park Dis 2020;6(1):33. https://doi.org/10.1038/s41531-020-00137-8
37. Okarmus J, Havelund JF, Ryding M, et al. Identification of bioactive metabolites in human iPSC-derived dopaminergic neurons with PARK2 mutation: Altered mitochondrial and energy metabolism. Stem Cell Rep. 2021;16(6):1510–1526. https://doi.org/10.1016/j.stemcr.2021.04.022
38. Rothfuss O, Fischer H, Hasegawa T, et al. Parkin protects mitochondrial genome integrity and supports mitochondrial DNA repair. Hum Mol Genet 2009;18(20):3832–3850. https://doi.org/10.1093/hmg/ddp327
39. Gensler S, Weber K, Schmitt WE, et al. Mechanism of mammalian mitochondrial DNA replication: import of mitochondrial transcription factor A into isolated mitochondria stimulates 7S DNA synthesis. Nucleic Acids Res 2001;29(17):3657–3663. https://doi.org/10.1093/nar/29.17.3657
40. Zanon A, Kalvakuri S, Rakovic A, et al. SLP-2 interacts with Parkin in mitochondria and prevents mitochondrial dysfunction in Parkin-deficient human iPSC-derived neurons and Drosophila. Hum Mol Genet 2017;26(13):2412–2425. https://doi.org/10.1093/hmg/ddx132
41. LaVoie MJ, Hastings TG. Dopamine quinone formation and protein modification associated with the striatal neurotoxicity of methamphetamine: evidence against a role for extracellular dopamine. J Neurosci Off J Soc Neurosci 1999;19(4):1484–1491.
42. Graves SM, Xie Z, Stout KA, et al. Dopamine metabolism by a monoamine oxidase mitochondrial shuttle activates the electron transport chain. Nat Neurosci 2020;23(1):15–20. https://doi.org/10.1038/s41593-019-0556-3
43. Reeve A, Simcox E, Turnbull D. Ageing and Parkinson's disease: why is advancing age the biggest risk factor? Ageing Res Rev 2014;14:19–30. https://doi.org/10.1016/j.arr.2014.01.004
44. Agarwal E, Goldman AR, Tang HY, et al. A cancer ubiquitome landscape identifies metabolic reprogramming as target of Parkin tumor suppression. Sci Adv 2021;7(35):eabg7287. https://doi.org/10.1126/sciadv.abg7287

Supporting Data

Additional Supporting Information may be found in the online version of this article at the publisher's web-site.

Parkin deficiency impairs mitochondrial DNA dynamics and propagates inflammation

Kobi Wasner, PhD[1], Semra Smajic, MSc[1]*, Jenny Ghelfi, BSc[1]*, Sylvie Delcambre, PhD[1], Cesar A. Prada-Medina, PhD[2], Evelyn Knappe, MSc[3], Giuseppe Arena, PhD[1], Patrycja Mulica, MSc[1], Gideon Agyeah, MSc[1], Aleksandar Rakovic, PhD[3], Ibrahim Boussaad, PhD[1,9], Katja Badanjak, MSc[1], Jochen Ohnmacht, PhD[1,8], Jean-Jacques Gérardy, BSc[5], Masashi Takanashi, MD[4], Joanne Trinh, PhD[3], Michel Mittelbronn, MD,[1,5-8], Nobutaka Hattori, MD, PhD[4], Christine Klein, MD[3], Paul Antony, PhD[1,9], Philip Seibler, PhD[3], Malte Spielmann, MD[2,10], Sandro L. Pereira, PhD[1,7], and Anne Grünewald, PhD[1,3]

*These authors contributed equally.

1 Luxembourg Centre for Systems Biomedicine, University of Luxembourg, Esch-sur-Alzette, Luxembourg

2 Max Planck Institute for Molecular Genetics, Berlin, Germany

3 Institute of Neurogenetics, University of Lübeck, Lübeck, Germany

4 Department of Neurology, Juntendo University, Tokyo, Japan

5 National Center of Pathology, Laboratoire National de Santé, Dudelange, Luxembourg

6 Luxembourg Center of Neuropathology, Dudelange, Luxembourg

7 Department of Oncology, Luxembourg Institute of Health, Luxembourg, Luxembourg

8 Department of Life Science and Medicine, University of Luxembourg, Esch-sur-Alzette, Luxembourg

9 Disease Modelling and Screening Platform, Luxembourg Centre of Systems Biomedicine, University of Luxembourg & Luxembourg Institute of Health, Luxembourg

10 Institute of Human Genetics, University of Lübeck, Lübeck, Germany

Corresponding author:

Anne Grünewald, Ph.D., Luxembourg Centre for Systems Biomedicine, University of Luxembourg, 6 avenue du Swing, L-4367 Belvaux, Luxembourg, phone: (+352) 46 66 44 9793, e-mail: anne.gruenewald@uni.lu

List of content

1. Supplementary methods

1.1. Cell culture

1.1.1. Generation of small molecule neural precursor cells (smNPCs)

smNPCs were cultured and expanded in N2B27 medium - Neurobasal (Gibco)/DMEM-F12 (Gibco) 50:50 with 1% B27 lacking vitamin A (ThermoFisher), 0.5% N2 (Life Technologies), 1% penicillin-streptomycin (ThermoFisher) and 1% 200 mM glutamine (Westburg) - supplemented with 3 µM CHIR 99021 (Sigma), 150 µM ascorbic acid (AA) (Sigma) and 0.5 µM purmorphamine (Sigma). The medium was changed every second day.

1.1.2. Generation of midbrain neurons

To initiate neuronal differentiation, smNPCs were counted using the Countess II FL Automated Cell Counter (ThermoFisher) and seeded onto Matrigel-coated (Corning) 6-well plates in N2/B27 medium supplemented with 1 µM purmorphamine, 200 µM ascorbic acid (AA) and 100 ng FGF8 (PeproTech) for 8 days. For the next 2 days, cells were cultured in N2/B27 medium with 0.5 µM purmorphamine and 200 µM AA. For the remainder of the differentiation (22 days), cells were maintained in Maturation medium: N2/B27 supplemented with 200 µM AA, 500 µM dibutyryl-cAMP (Applichem), 1 ng/mL TGF-β3 (Peprotech), 10 ng/mL GDNF (Peprotech) and 20 ng/mL BDNF (PeproTech). The medium was changed every second day.

1.1.3. Generation of induced pluripotent stem cells (iPSCs)

Skin fibroblasts obtained from an Alper's disease patient with *POLG* mutations (Fig. S1A) were reprogrammed into iPSCs using the Epi5^{TM} Episomal iPSC Reprogramming Kit (ThermoFisher) according to the manufacturer's instructions. Briefly, fibroblasts were maintained in DMEM supplemented with 10% FBS and 1% Penicillin-Streptomycin. Once 75-90% confluent, fibroblasts were washed with PBS (Gibco) and detached by adding 0.05% Trypsin/EDTA (ThermoFisher) for 5 min at 37°C. Cells were then collected and counted using the Countess II FL Automated Cell Counter. Next, 1 x 10^7 cells were removed, centrifuged at 200 x g for 5 min and transduced with Epi5™ Reprogramming Vectors and Epi5™ p53 & EBNA Vectors using the Amaxa Nucleofector I (Lonza) with 3 pulses at 1650 V for 10 ms. After transfection, cells were seeded onto irritated mouse embryonic fibroblasts and cultured

in mTeSR™ 1 complete medium (STEMCELL Technologies). The medium was changed every day. After ~1 month, iPSC colonies were picked based on their stem-cell-like morphology and expanded on Matrigel-coated plates. The generation of smNPCs and midbrain neurons was performed identically as described for iPSCs from Parkin mutation carriers.

1.1.4. Generation of isogenic Parkin-knockout neuroblastoma cells

Parkin knockout neuroblastoma (SH-SY5Y) cells were generated using an RNA-guided CRISPR/Cas9 endonuclease. For this, SH-SY5Y cells were transiently cotransfected with plasmids expressing either a human codon-optimized Cas9 (hCas9 was a gift from George Church [Addgene plasmid # 41815]) and a guide RNA (gRNA_Cloning Vector was a gift from George Church [Addgene plasmid # 41824]) containing a 19-base long sequence that matches the human *PRKN* target sequence 5'- GTGGTTGCTAAGCGACAGG -3'. Upon transfection, cells were re-suspended in growth medium, counted and plated onto Petri dishes at a density of 1 cell/cm2. Cells were grown until they formed distinct, monoclonal colonies. The colonies were scraped off, transferred into different wells of a 6-well plate, and propagated to obtain enough material for the DNA extraction for Sanger sequencing. We identified one clonal cell line carrying a homozygous mutation c.100_101insC (p.Q34PfsX5) in the *PRKN* gene resulting in a premature stop codon, further leading to nonsense-mediated decay. To induce hypoxia, SH-SY5Y cells were plated onto a 6-well plate at a density of 1.1 million cells/well and, the following day, treated for 24h with 200 µM $CoCl_2$ (Merck, C8661) in MOPS (ROTH, 6979.2) buffer.

1.2. Parkin silencing

For Parkin knockdown, the lentiviral pLKO.1 vector (Addgene) was used to express short hairpin RNA (shRNA) against human Parkin (Sense: ccggCCAGTAGCTTTGCACCTGATTctcgagAATCAGGTGCAAAGCTACTGGtttttg).[1] The MISSION pLKO.1-puro Non-Mammalian shRNA control Plasmid DNA (Sigma), targeting no known mammalian genes, was used as negative control for lentiviral transduction (Sense: CCGGCAACAAGATGAAGAGCACCAACTC-GAGTTGGTGCTCTTCATCTTGTTGTTTTT). Lentiviral constructs, as well as 2nd generation packaging plasmids (psPAX2, pMD2G), were transfected in HEK293T cells by calcium phosphate precipitation in the presence of 25 µM

chloroquine. HEK293T cell culture medium, containing the respective lentiviral particles, were harvested 48 hrs post-transfection, passed through 0.45 µM filters and used to transduce target cells overnight, in presence of 8 µg/mL Polybrene.

1.3. Generation and treatment of iPSC-derived neuron-microglia co-cultures

DANs and microglia cells were generated according to previously described protocols.[2-4] At day 92 of neuronal differentiation, $4x10^5$ microglia precursor cells were plated onto corresponding cell lines of neurons leading to their maturation. Equal amounts of both cell types were co-cultured for 35 days before treatment with LPS (100 ng/mL) for 3 hours and mtDNA (300 ng) for 1 hour. A mixture of mtDNA extracted from all *PRKN*-mutant patients was used.

1.4. Immunocytochemistry

SH-SY5Y cells, iPSC-derived smNPCs and midbrains neurons were fixed in 4% paraformaldehyde for 15 min at room temperature and then washed three times in PBS (Gibco). Cells were then permeabilized in the blocking buffer (1% bovine serum albumin [Sigma], 0.25% Triton-X 100 [Sigma] in PBS) for 1 hr at room temperature. Cells were then stained overnight at 4°C with primary antibodies in blocking buffer. For smNPCs, cells received antibodies against Nestin (R&D Systems, MAB1259), Pax6 (BioLegend, 901301) and Musashi (Abcam, ab21628). For neurons, cells were subjected to several combinations of antibodies (depending upon the experiment) against TUBB3 (BioLegend, 801202), tyrosine hydroxylase (Sigma T8700), DNA (Progen AC-30-10), TOM20 (Santa Cruz SC-17764). The next day, cells were washed three times in PBS and then stained with fluorescent secondary antibodies in blocking buffer for 1h at room temperature. Cells were then washed three times in PBS, and incubated with Hoechst 33342 (ThermoFisher) for 10 min. For the assessment of mtDNA release into the cytosol, cells were incubated for 30 minutes at room temperature with HCS CellMask™ Orange stain (ThermoFisher) prior to the nuclear staining and following the manufacturer's indications. Images were taken using a 20X objective (for smNPCs) or 40X objective (for neurons) using the Zeiss Axio Imager 2 microscope, or 60X objective for neurons and SH-SY5Y cells on the Cell Voyager CV8000 high-content screening confocal microscope (Yokogawa Electric Corporation).

1.5. Western blotting

Antibodies used in the study: Parkin (Santa Cruz sc-32282), SIRT1 (Abcam ab32441), PGC1-α (Novus Biologicals NBP1-04676), NRF1 (Abcam ab175932), NRF2 (Cell Signaling abe1047), VDAC (Abcam ab14734), LC3A/B (Cell Signaling, 4108), TFAM (Abcam ab47517), TUBB3 (Tuj1) (BioLegend 801202), tyrosine hydroxylase (Sigma T8700), cGAS (Santa Cruz sc-515777) and beta-actin (Sigma A1978).

1.6. Metabolite extraction and metabolomics analysis

Metabolites from 35d-old neurons were extracted using a Methanol/Water-Chloroform mix. Neurons were seeded in 12-well plates at day 25 of differentiation and then maintained for 5 days. Cells were washed once with 0.9% NaCl (Sigma). Metabolism was quenched with 200 µL ice-cold methanol (Roth). 80 µL of 4°C water was added and the plate was placed on an orbital shaker for 10 min at 4°C. The mixture was transferred to a tube containing 100 µL of ice-cold chloroform (Roth) and then shaken on a thermomixer at 4°C for 5 min. An additional 100 µL of ice-cold chloroform and 4°C water were added. The samples were then vortexed and centrifuged for 5 min at 21000 x g, 4°C. 125 µL of the upper phase were transferred to a glass vial and dried in a vacuum centrifuge. Samples were capped and kept at -80°C until measurement.

Polar metabolites were derivatized and measured by GC-MS using an Agilent 7890B GC coupled to an Agilent 5977A Mass Selective Detector (Agilent Technologies) following an established method. The MetaboliteDetector software package (Version 3.220180913) was used for mass spectrometry (MS) data post processing and quantification. NAD^+:NADH ratios were determined using the colorimetric NAD/NADH Quantification Kit from Sigma following the manufacturer's instructions.

1.7. Mitochondrial extraction

SH-SY5Y cells were resuspended and washed in homogenization buffer (HB) (10 mM Tris, pH 7.4, 1 mM EDTA, 250 mM Sucrose) with protease and phosphatase inhibitors (Halt Protease & Phosphatase inhibitor cocktail). After washing the pellet at 4000 x g for 5 min at 4°C, fresh HB was added and the pellet was homogenized for 1 min on ice

using a pellet pestle (Sigma). Homogenates were then centrifuged at 1500 x g for 10 min at 4°C and the supernatant was removed. After two washing steps in HB, mitochondria were pelleted by centrifugation at 8000 x g for 10 min.

1.8. NADH-COQ1 reductase assay

To measure complex I activity, mitochondrial homogenates were subjected to three freeze/thaw cycles in HB buffer and then placed in buffer containing 20 mM K^+Phosphate buffer (sodium phosphate (VWR), magnesium chloride (Sigma), 150 µM NADH (Sigma), 1 mM potassium cyanide (Sigma), and bovine serum albumin (BSA) (Sigma)) followed by an additional three freeze/thaw cycles. Samples were then placed into a 96-well plate (Greiner Bio-One) and kinetic measurement was evaluated at 340 nm using the Biotek Cytation 5 plate reader (Biotek). We first measured baseline activity for 3 min, then added 50 µM ubiquinone (Sigma) and measured kinetics for 10 min, and finally added 10 µM rotenone (Abcam) and measured for 10 min.

1.9. Citrate synthase assay

The citrate synthase assay was performed on the same mitochondrial extracts as in the NADH-COQ1 assay. Here, we followed a modified protocol based on Coore *et al.*[5] First, we subjected mitochondria to three freeze/thaw cycles in HB buffer and then added a buffer containing 100 mM Tris (Sigma), 100 µM acetyl CoA (Sigma), 100 µM DTNB (Sigma) and 0.1% Triton X (Sigma), followed by three more freeze/thaw cycles. The samples were then added to a 96-well plate (Greiner Bio-One) and kinetic measurement was performed at 412 nm in the BioTek Cytation 5 plate reader (BioTek) at baseline for 3.5 min. We then added 100 µM oxaloacetic acid (Sigma) and measured for an additional 10 min.

1.10. Quantitative PCR analyses

1.10.1. MtDNA integrity and copy number analyses

DNA was extracted using the QIAmp DNA Mini Kit (Qiagen) following the manufacturer's instructions. Transcription and copy number were measured using a real-time polymerase chain reaction (RT-PCR) method on the LightCycler

480 (Roche) with TaqMan probes for *D-loop, MT-ND1*, *MT-ND4,* and the nuclear single copy gene *B2M* as described.[6,7]

1.10.2. Digital PCR

DNA was quantified using a digital PCR (dPCR) assay with TaqMan probes specific for *MT-ND1* and *B2M*. dPCR was executed using the QuantStudio 3D Digital PCR System (Applied Biosystems) as published.[6, 7]

1.10.3. RNA extraction and quantitative PCR

RNA was prepared by using the RNeasy Mini Kit (Qiagen). RNA was then reverse-transcribed into cDNA using SuperScript III Reverse Transcriptase (ThermoFisher) and measured via RT-PCR using iQ SYBR Green Supermix (Biorad) on the LightCycler 480. Primer sequences are summarized in Table S5.

1.11. Laser capture microdissection

Frozen sections were fixed with 4% paraformaldehyde for 10 min and then washed in distilled water for 10 min. After three 5 min washes in TBST buffer, a TH primary antibody (Merck) was applied for 1 hr at room temperature. After three more washes, a secondary antibody (Santa Cruz) was applied for 30 min at room temperature. Following more washing, sections were incubated with DAB (Millipore) and 3% H2O2 for 4 min at room temperature and then washed in distilled water for 5 min. Single TH-positive neurons were isolated through laser capture microdissection (LCM) using the PALM MicroBeam (Zeiss) and captured in 15 µL of lysis buffer (50 mM Tris-HCl, pH 8.5, 1 mM EDTA, 0.5% Tween-20, 200 ng/mL proteinase K), centrifuged for 10 min at 20,000 x g at 4°C and then incubated for 3 hr at 55°C and 10 min at 95°C.

1.12. Single-nuclei RNA sequencing (snRNAseq) and data analysis

1.12.1. Tissue processing

Eight sections of the *PRKN*-mutant brain were pooled together for nuclei isolation. Tissue was collected in cold lysis buffer (10 mM Tris-HCl, 10 mM NaCl, 3 mM MgCl2, 0.1% NonidetTM P40). The resulting tissue suspension was

filtered and pelleted by centrifugation. Pellets were washed with 'nuclei wash and resuspension buffer' (1xPBS, 1% BSA, 0.2 U/µL RNase inhibitor) and then filtered and re-pelleted. Next, pelleted nuclei were incubated in DAPI solution (1.5 µM DAPI in 1x PBS) for 5 min prior to FACS-sorting. After dissociation, the nuclei suspension was subjected to FACS-sorting with FACSDiva Cell Sorter (BD Biosciences). Single DAPI-positive nuclei were sorted. To sequence harvested nuclei and prepare cDNA libraries, the Chromium Next GEM Single Cell 3'Kit v3.1 was used. The quality of resulting cDNA was assessed with the Agilent 2100 Bioanalyzer System.

1.12.2. Sequencing and data analysis

Sequencing was performed via Illumina NovaSeq 600-S2. Resulting data was processed identically to controls.[8] Briefly, after sequencing, the quantification of transcripts and filtering FASTQ files were produced from raw base call outputs with the Cell Ranger (10X Genomics) *mkfastq* pipeline v.3.0. Further, with the Cell Ranger (10X Genomics) count pipeline v.3.0 with default parameters, we obtained a gene-barcode UMI count matrix per sample. Considering that nuclei rather than cells were sequenced, we utilized the Cell Ranger recommended variation of the human reference transcriptome (hg38), which also annotates introns as exons. Only barcodes with more than 1500 UMIs and 1000 genes were included. Moreover, only those with less than 10% of mitochondrial-encoded and 10% ribosomal encoded genes were kept. Only genes detected in more than three barcodes were retained and ribosomal and mitochondrial-encoded genes were removed. With Scrubblet57, possible multiplet barcodes were identified, and such were kept with an estimated duplet score smaller than 0.15.

To determine the cell types comprising human midbrain tissue samples, we pooled the samples in a single embedding following the Seurat v3 integration workflow.[9] The top 4000 most variable genes were identified with *SelectIntegrationFeatures*, and used to determine the between-sample cell-anchors with *FindIntegrationAnchors*. The *IntegrateData* function was used to build a centered expression matrix, which was further used for principal component analysis. After, the Shared Nearest Neighbor (SNN) cell graph was built with the top 25 principal components and then clustered using the Louvain algorithm (resolution = 1.5) with the *FindClusters* function. With the FindAllMarkers function we detected the marker genes (expressed in minimally 25% of the cluster) for each cluster by using the default 'wilcox' test. With such top marker genes, each cell cluster was cell-type annotated. To

identify the differentially expressed genes in microglia, *FindMarkers* function with *logfc.threshold=0.25* and *min.pct=0.05* was used to compare microglia clusters between control and Parkin conditions. This list of differentially expressed genes was further utilized in pathway enrichment analysis with MetaCore software.

2. Supplementary figures

A

Disease Status	Sample	Sex	Age of Sampling	AAO	Gene	Mutation
Healthy	Control 1	M	39	N/A	N/A	N/A
Healthy	Control 2	F	37	N/A	N/A	N/A
Healthy	Control 3	M	40	N/A	N/A	N/A
Parkinson's disease	Parkin-PD 1	M	58	43	*PRKN*	c.1072Tdel (hom)
Parkinson's disease	Parkin-PD 2	M	57	15	*PRKN*	delEx4; + c.924C>T
Parkinson's disease	Parkin-PD 3	F	41	37	*PRKN*	del Ex1;c.924C>T
Alpers' disease	POLG	M	1 month	Birth	*POLG*	c.1399G>A; c.2740A>C

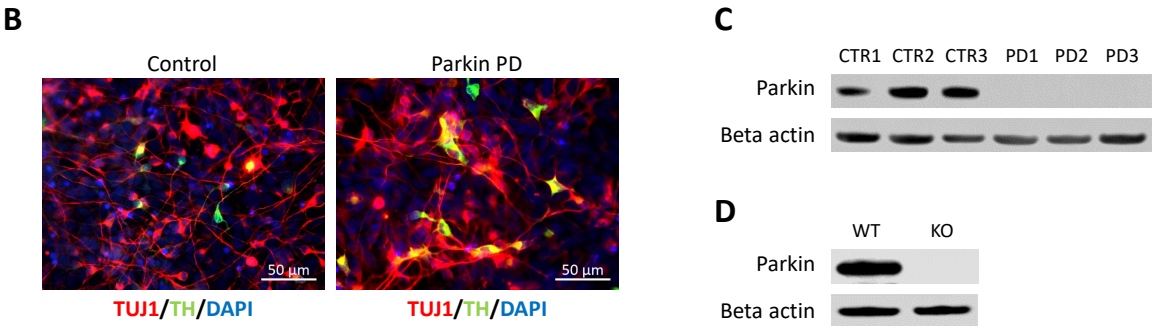

Figure S1 Derivation and characterization of iPSC-derived midbrain neurons and SH-SY5Y cells. (A) Overview of patients and controls included in the *in vitro* part of the study. **(B)** iPSC-derived neurons were stained for the neuronal marker TUJ1 and the catecholamine rate limiting enzyme tyrosine hydroxylase (TH). Images were taken using a 40x objective. **(C)** Parkin protein abundance in iPSC-derived patient and control neurons. Protein was extracted and subjected to Western blotting analysis using anti-Parkin and anti-beta-actin antibodies. Representative cropped images are shown. **(D)** Parkin protein abundance in control and isogenic Parkin-knockout SH-SY5Y cells. Representative cropped images are shown.

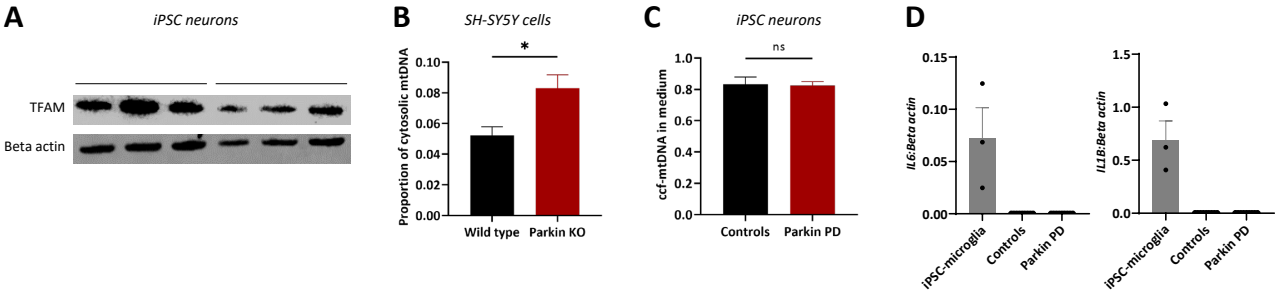

Figure S2 MtDNA dynamics and inflammation in PRKN-mutant and control iPSC-derived neurons. (A) Representative cropped Western blot images of TFAM and beta-actin. **(B)** Quantification of mtDNA in cytosolic and mitochondrial fractions from Parkin-PD and control iPSC-derived neurons. mtDNA levels were quantified by means of real-time PCR targeting the mtDNA fragment *ND1* and the nuclear single copy gene *B2M*. The proportion of cytosolic mtDNA normalized to cytosolic *B2M* copies was calculated relative to the total amount of cellular mtDNA copies. **(C)** Extracellular ccf-mtDNA in medium from Parkin-PD and control iPSC-derived neurons. Quantification by means of multiplex dPCR with probes against *ND1* and *B2M.* The proportion of extracellular *ND1* normalized to extracellular *B2M* copies was calculated relative to the total amount of mtDNA copies present in the medium and cells. **(D)** *IL6* and *IL1B* gene expression. *IL6* and *IL1B* levels were measured relative to the house-keeping gene *Beta-actin*. *IL6* and *IL1B* expression in iPSC-derived control microglia served as a positive control. n = 3 or 5 biological replicates, data are presented as the mean ± SEM; **P* < 0.05, ***P* < 0.01, ns = not significant as determined by student's t-test.

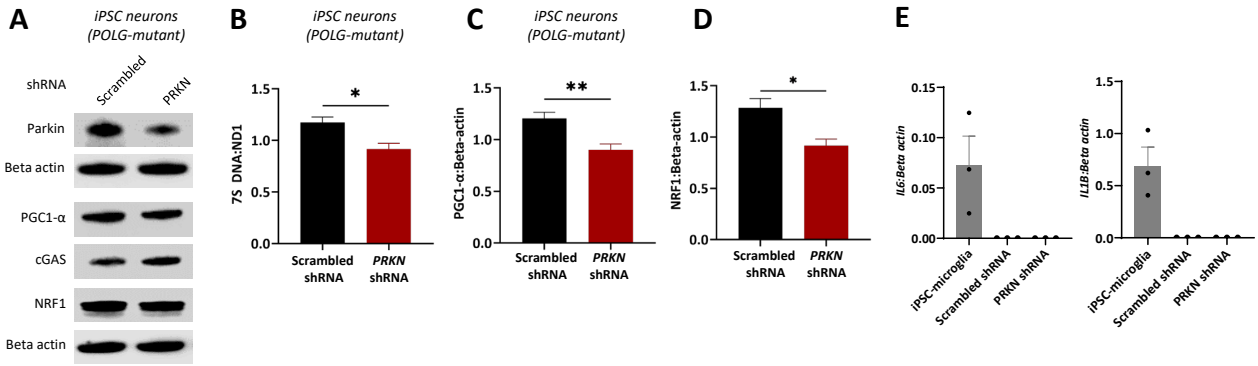

Figure S3 MtDNA dynamics and inflammation in iPSC-derived neurons from a compound-heterozygous POLG mutation carrier transduced with scrambled or PRKN shRNA. (A) Representative cropped images of Western blot membranes of whole cell lysates. Cells were harvested 5 days post transduction and subjected to Western blot analysis. **(B)** Quantification of 7S-associated transcription via multiplex RT-PCR. mtDNA transcription initiation events were determined by calculating the 7S DNA:ND1 ratios. **(C)** Quantification of PGC1-α protein levels relative to Beta-actin from (A). **(D)** Quantification of NRF1 protein levels relative to Beta-actin from (A). **(E)** *IL6* and *IL1B* gene expression in *POLG*-mutant iPSC-derived neurons transduced with scrambled or *RRKN* shRNA. *IL6* and *IL1B* levels were measured relative to *Beta-actin*. *IL6* and *IL1B* expression in iPSC-derived control microglia served as a positive control. n = 3 or 5 biological replicates, data are presented as the mean ± SEM; **P* < 0.05, ***P* < 0.01, as determined by student's t-test.

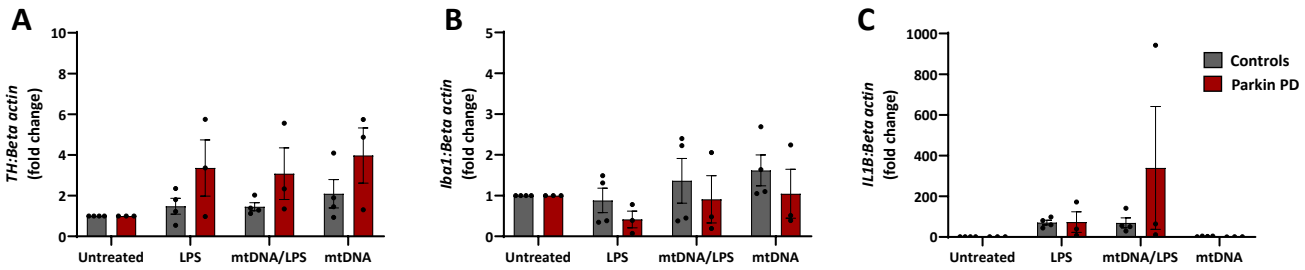

Figure S4 Expression of neuronal, microglial and inflammatory marker genes in PRKN-PD and control neuron-microglia co-cultures. (A) Dopaminergic neuron abundances in co-cultures. Expression of *TH* was measured relative to *Beta-actin* by means of qPCR. This assessment did not reveal significant differences between lines and treatments. **(B)** Microglia abundance in co-cultures. Quantifying the expression of the microglial marker gene *Iba1* relative to the house-keeping gene *Beta-actin* by qPCR did not show differences between investigated lines and treatments. **(C)** Pro-inflammatory cytokine analysis. Quantitative gene expression analysis of *IL1B* relative to *Beta-actin* revealed a non-significant upregulation in *PRKN*-PD co-cultures after co-treatment with LPS and mtDNA.

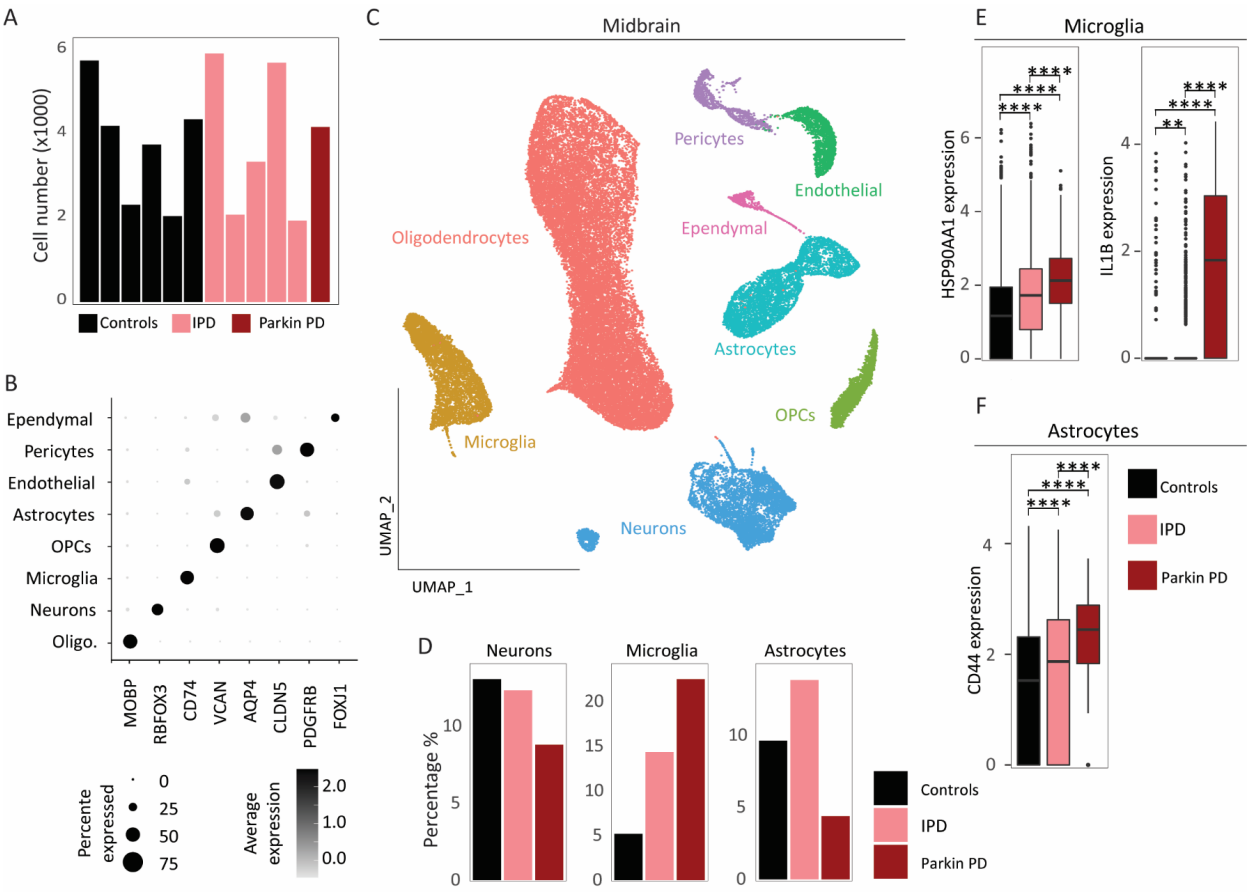

Figure S5 PRKN-mutant midbrain single-nuclei transcriptome comparison with six healthy controls and five idiopathic Parkinson's disease (IPD) cases. (A) Number of nuclei per sample. **(B)** Cell-type specific marker genes. **(C)** UMAP representation of 45.608 nuclei from *PRKN*-mutant, control and IPD midbrain samples. **(D)** Percentage of *PRKN*-mutant, control and IPD neuronal, astrocytic and microglia nuclei. **(E)** *CD44* gene expression in astrocytes in *PRKN*-mutant, control and IPD samples. **(F)** *HSP90AA1* and *IL1B* gene expression in microglia in *PRKN*-mutant, control and IPD samples.

3. Supplementary tables

Table S1 Marker genes for cell clusters

Table S2 Differentially expressed genes in *PRKN*-mutant midbrain microglia

Table S3 *PRKN*-mutant midbrain microglia; upregulated pathways

Table S4 *PRKN*-mutant midbrain microglia; downregulated pathways

(Tables S2-4 were submitted as csv files)

Table S5 Sequences of primers used in the study

Gene	Forward	Reverse
Beta-actin	5’ - CGAGGACTTTGATTGCACATTGTT	5’ - TGGGGTGGCTTTTAGGATGG
MT-ND1	5’- ATACCCACACCCACCCAAGAAC	5’- GGTTTGAGGGGGAATGCTGGA
MT-CYTB	5’- CTGATCCTCCAAATCACCACAG	5’- GCGCCATTGGCGTGAAGGTA
MT-COX1	5’-GGAGCAGGAACAGGTTGAACAG	5’-GTTGTGATGAAATTGATGGC
TFAM	5’-AAGATTCCAAGAAGCTAAGGGTGA	5’-CAGAGTCAGACAGATTTTTCCAGT
TFB2M	5’-TCTGGCAATTAGCTTGTGAG	5’-CTTACGCTTTGGGTTTTCCA
Twinkle	5’-ATTGTAGAAGGACGTGGACG	5’-TGCAGAGCTCACTCTAGGTG

4. References

1. Arena G, Cissé MY, Pyrdziak S, et al. Mitochondrial MDM2 Regulates Respiratory Complex I Activity Independently of p53. *Mol Cell*. 2018;69(4):594-609.e8. doi:10.1016/j.molcel.2018.01.023

1. Kriks S, Shim JW, Piao J, et al. Dopamine neurons derived from human ES cells efficiently engraft in animal models of Parkinson's disease. *Nature*. 2011;480(7378):547-551. doi:10.1038/nature10648

2. Haenseler W, Sansom SN, Buchrieser J, et al. A Highly Efficient Human Pluripotent Stem Cell Microglia Model Displays a Neuronal-Co-culture-Specific Expression Profile and Inflammatory Response. *Stem Cell Rep*. 2017;8(6):1727-1742. doi:10.1016/j.stemcr.2017.05.017

3. Reinhardt P, Glatza M, Hemmer K, et al. Derivation and expansion using only small molecules of human neural progenitors for neurodegenerative disease modeling. *PloS One*. 2013;8(3):e59252. doi:10.1371/journal.pone.0059252

4. Coore HG, Denton RM, Martin BR, Randle PJ. Regulation of adipose-tissue pyruvate dehydrogenase by insulin and other hormones. *Biochem J*. 1971;125(1):115-127

5. Grünewald A, Rygiel KA, Hepplewhite PD, Morris CM, Picard M, Turnbull DM. Mitochondrial DNA Depletion in Respiratory Chain-Deficient Parkinson Disease Neurons. *Ann Neurol*. 2016;79(3):366-378. doi:10.1002/ana.24571

6. Rygiel KA, Grady JP, Taylor RW, Tuppen HAL, Turnbull DM. Triplex real-time PCR--an improved method to detect a wide spectrum of mitochondrial DNA deletions in single cells. *Sci Rep*. 2015;5:9906. doi:10.1038/srep09906

7. Smajić S, Prada-Medina CA, Landoulsi Z, et al. Single-cell sequencing of human midbrain reveals glial activation and a Parkinson-specific neuronal state. *Brain*. Published online December 17, 2021:awab446. doi:10.1093/brain/awab446

8. Stuart T, Butler A, Hoffman P, et al. Comprehensive Integration of Single-Cell Data. *Cell*. 2019;177(7):1888-1902.e21. doi:10.1016/j.cell.2019.05.031